(1)

# LASER DIODE PUMPED SOLID STATE LASERS

FINAL REPORT

SAIC 168-352-040

Science Applications International Corporation



January 1987

Approved for public release: Distribution is unlimited.





Post Office Box 1303, 1710 Goodridge Drive, McLean, Virginia 22102, (703) 821-4300

LASER DIODE PUMPED

SOLID STATE LASERS

FINAL REPORT

SAIC 168-352-040

SAIC

Science Applications International Corporation

January 1987



Post Office Box 1303, 1710 Goodridge Drive, McLean, Virginia 22102, (703) 821-4300

TABLE OF CONTENTS

TABLE OF CONTENTS (Continued)

TABLE OF CONTENTS (Continued)

## FOREWORD

This report summarizes the work performed under a program sponsored by NOSC (Contract No. N00014-85-C-0174), which FIBERTEK, Inc. carried out as a subcontractor to Science Applications International Corporation. The study provides an assessment of the technical and economic issues surrounding the practical application of laser diode arrays for pumping solid state lasers.

The general objective of the study was an evaluation of the state-of-the-art of diode array fabrication; identification of potential solid state laser candidates suitable for diode pumping; evaluation of different pump configurations; investigation of different cooling techniques and resonator designs; and a conceptual design of a cost-effective laser system.

The study motivation stems from the need to classify some of these issues in view of the rather dramatic developments which have taken place in the area of diode pumped laser systems. Most notable are the impressive improvements made in laser diode array performance and fabrication technology, the emergence of several military and commercial lasers pumped by laser diode arrays, and the cost projections made by several leading manufacturers which seem to indicate that widespread applications of laser diode arrays as part of all solid state lasers could become a reality.

# 1. INTRODUCTION AND SUMMARY

The most promising alternative to flashlamp pumping of solid state lasers has always been the diode laser. Throughout the last twenty years numerous laboratory devices have been assembled which incorporated single diode lasers, small laser diode arrays or LED's for pumping of Nd:YAG, Nd:glass and a host of other Nd lasers. The low power output, low packaging density, and extremely high cost of diode lasers prevented any serious applications for laser pumping in the past.

The reason for the continued interest in this area stems from the potential dramatic increase in system efficiency and component lifetime, and reduction of thermal load of the solid-state laser material. The latter not only will reduce thermo-optic effects and therefore lead to better beam quality but also will enable an increase in pulse repetition frequency. The attractive operating parameters combined with low voltage operation and the compactness of an all solid-state laser system have a potential high payoff.

The high pumping efficiency compared to flashlamps stems from the good spectral match between the laser diode emission and the Nd absorption bands. Actually, flashlamps have a higher radiation output to electrical input efficiency (70 percent) than laser diodes (25-50 percent); however, only a very small fraction of the blackbody spectrum is usefully absorbed by the various Nd bands.

A concomitant advantage derived from the spectral match between the diode laser emission and the long wavelength Nd absorption band, is a reduction in the amount of heat which is deposited in the laser material.

An overwhelming advantage of laser diode pumping compared to arc lamps is system lifetime and reliability. Laser diode arrays have exhibited lifetimes on the order of 10,000 hours in cw operation and $10^9$ shots in the pulsed mode. Flashlamp life is on the order of $10^7$ shots, and about 200 hours for cw

operation. In addition, the high pump flux combined with a substantial U content in lamp pumped systems causes material degradation in the pump ca and in the coolant, which leads to systems degradation and contributes to maintenance requirements. Such problems are virtually eliminated with la diode pump sources.

The absence of high voltage pulses, high temperatures and UV radiati encountered with arc lamps leads to much more benign operating features o laser diode pumped systems. Laser diode technology dates back to 1962 wh laser action in GaAs diodes was first demonstrated. However, it took a d to transform a fragile device requiring cryogenic coolant into one capabl emitting a continuous beam at room temperature. The pace of development accelerated greatly over the past decade making diode lasers one of the fastest-moving laser technologies. In particular device improvements suc double heterostructures, multiple quantum well structures, gradient index single quantum well structures, monolithic phased arrays, multiple stripe lasers which were made possible by improved manufacturing technologies su LPE and particular MOCVD have lead to a dramatic reduction of threshold current and increases of slope efficiency, lifetime and output power.

At present, the most important application for single diode lasers i optical disk recording. Fueled by strong consumer acceptance of compact players, sales of 780 nanometer AlGaAs diode lasers grew to several milli per year and prices dropped below $10.00 for a single device. Developed manufactured almost exclusively by Japanese companies, these diodes are causing a "low cost spillover" into such areas as printers, copiers, CD-R and other similar applications in the reprographics area.

The longer wavelength diode lasers, based on the InGaAsP Compound, w are used in fiberoptic telecommunications, have less than 1 percent of th total market for diode lasers.

The application of laser diodes may soon also include bar code reade optical alignment instruments, etc., if researchers at NEC, Sony and Tosc

succeed in developing a red-emitting diode laser which will directly compete with He-Ne lasers.

Single diode lasers utilized in these commercial applications are not practical for solid state laser pumping due to the low power outputs. However, in parallel with the mass production of single laser diodes in Japan, went a development in the U.S. which is aimed at the fabrication of powerful monolithic arrays. The development of these multistripe lasers was originally pioneered by Xerox and Spectra Diode Laboratories, and now RCA, McDonnell Douglas, TRW and GE in addition to several foreign companies, notably Siemens, are working on diode arrays. The development of diode arrays follows two different pathways. By fabricating multiple stripes on a single GaAs substrate with small enough stripe-to-stripe spacing, one can produce an array which "inherently" phase locks.

The output from a phase-locked array can be focused on an almost diffraction limited spot. Industry motivation to develop phased arrays stems from the potential applications in read/write optical memories and laser printers. Since coherent arrays produce more power than single diode, they can increase throughput or bit rate of these systems. Considerable interest for phased arrays has also centered on laser transmitters for ground based, point-to-point communication links, and for certain classified military programs.

A technological spill-over of phase locked arrays is the development of incoherent arrays. Higher power levels and more stripes on a single chip can be obtained if the concept of phase-locking is abandoned.

Significant progress has been made recently in developing the monolithic, linear laser diode array. Output power, slope efficiency, laser threshold and wavelength control have all been dramatically improved due to a combination of new structures and MOCVD growth techniques.

These incoherent arrays could become the building blocks for solid state laser pumps. In contrast to applications for data storage or printing, laser

pumping does not require small focusable spot size, spectral purity, and l
noise. Incoherent arrays are lacking in these respects and their main application is for laser pumping. State-of-the-art performance of linear arrays is up to 40 W per cm. Commercially, devices with 5 W to 10 W per c are available. Performance of planar arrays, produced by stacking linear arrays, has reached the impressive level of 1 kW/$cm^2$. Efficiencies for th devices range from 25 to 50 percent. These performance levels are not ju: achieved in a few singular laboratory devices. Several manufacturers are capable of producing linear and planar arrays in large quantities to these specifications. However, these devices are very expensive at present, and cost is the major obstacle which prevents the construction of practical solid-state lasers based on diode pumping.

The prototype linear and planar arrays built to date, and the laser performance which has been achieved, have clearly demonstrated that diode pumping is no longer a question of technical feasibi ity, but rather a question of economic viability.

Despite the prospect for more compact and efficient solid state lase: afforded by diode laser pumping, and several potential applications inclu( free space optical communications, medical lasers, remote sensing and 0.5: illuminators, no market driver has been clearly identified yet, which wou' lead to a major cost reduction of diode laser arrays.

Industrial applications could eventually become extensive enough to sustain a large production rate, but in order to open the commercial mark( the cost has to come down one to two orders of magnitude. This is turn requires a large front end investment.

At the present time the development of laser diode pumped solid stat( lasers is mainly pursued in two areas. The major effort for the design a: fabrication of 2-D diode arrays is directed towards the development of a ' source for blue-green lasers for submarine communications. A solid state

laser pumped by laser diode arrays has many attractive features for a satellite based system.

High pulse energies are required for this application, and the configuration best suited is the side pumped slab laser. McDonnell Douglas has demonstrated the technical feasibility of such a device. Their Nd:YaG slab laser pumped by 3.86 $cm^2$ of planar arrays produces 100 mJ in a Q-switched pulse.

On the other side of the power spectrum are very small, end pumped Nd:YAG lasers produced by several commercial firms. Careful matching of the pumps profile and the resonator mode results in very efficient designs, up to 8 percent overall efficiency has been achieved. These devices which produce a fraction of a watt of output power have also been Q-switched and frequency doubled. Overall efficiencies of up to 10 percent are considered to be feasible in diode-pumped Nd:YAG lasers.

In view of the rapidly growing interest in diode laser pumping of solid state lasers, the work performed under this contract reviews the major issues related to this exciting and potentially far reaching technology.

Chapter 2 of this report describes the state-of-the-art of linear and two dimensional laser diode arrays designed for pumping solid state lasers. The newest device fabrication technologies, current and projected performance of linear and planar arrays will be discussed.

Feasibility of producing arrays and employing them as pump sources for Nd:YAG lasers has now been demonstrated. There are no technological barriers preventing the use of laser diode arrays for pumping of solid state lasers. There is, however, currently an economic barrier. Due to the low production volume manufacturing, costs are very high and must be reduced sharply before widespread applications will emerge.

There are several U.S. and foreign firms which have the capability t implement a high volume array fabrication production facility provided a market can be developed to warrant the investment associated with such a facility (Spectra Diode Lab, McDonnell Douglas, TRW, G.E., Siemens, RCA).

In Chapter 3 the properties and performance of solid state lasers wh have been pumped with diode laser arrays are summarized, and several new potential candidate materials are discussed.

Due to its high gain and reasonable absorption coefficient, Nd:YAG i most widely used material for diode pumping. Desirable properties of new solid state lasers include a longer fluorescence lifetime, a broader abso tion band and a higher absorption coefficient as compared to Nd:YAG. In addition new laser materials could open up new wavelength regimes.

A long fluorescence lifetime of the lasing material reduces the peak power requirements, and therefore the number of diodes needed to produce given outpu' energy. This is because laser diodes are low-energy devices i.e. they are peak power limited. A broader absorption band as compared Nd:YAG, allows operation of the diode array over a wider temperature regi

Particularly for military systems, a less stringent temperature cont ler for the array, as is needed for Nd:YAG lasers, would be highly desira A higher absorption coefficient than that obtained for the 808 nm line ir Nd:YAG would lead to a higher pump efficiency in small, side-pumped laser

Potential solid state laser candidates include Nd:YLF, Ho:YLF, Nd:La Nd:LNA. Properties of these materials will be discussed.

In Chapter 4 important crystal geometrics and diode array pump confi ations are discussed. The geometry of the laser must be chosen to achiev pump intensities required for efficient operation as well as efficient e› tion over the entire pump volume.

At low powers, the focused end pump configuration meets these criteria. At high energy per pulse applications, planar arrays and slab configuration appear to be optimum because high packaging densities can be achieved. If a high repetition rate is also required, the heat dissipation from the arrays rather than pump flux will become the limiting factor.

With the introduction of high-power laser diode bars having emission lengths of over 1 cm, new pump geometries must be conceived which provide the required pump intensities and for extracting energy over the entire pump volume.

One possible configuration has been thoroughly analyzed by FIBERTEK, Inc. It is a cylindrical laser rod surrounded by linear arrays. The arrays are mounted on long heat sink structures and contain cylindrical optics. The optics allows the arrays to stand off from the laser crystal, which is important for cooling of the laser crystal and the arrays. In addition, with a properly designed optical system, distribution of pump radiation can be adjusted to match the cavity mode volume. A detailed ray trace program was developed for this geometry which permits optimization of the system. The laser arrays can be either arranged symetrically around the laser crystal, or distributed in a half cylinder. In this case, the laser crystal is mounted in a heat sink containing a back reflector.

In FIBERTEK, Inc.'s opinion, this geometry is very promising in bridging the gap between high power applications met with slab designs, and low power lasers based on end pumping.

In Chapter 5 advanced heat exchanger designs are evaluated for cooling of high density planar arrays. Currently developed arrays are capable of 1 $kW/cm^2$ peak power. However, heat extraction is on the order of 10 $W/cm^2$. Advanced designs discussed in this report can increase the heat extraction capability to about 100 $W/cm^2$.

Unstable and stable resonator designs suitable for diode pumped laser will be discussed in Chapter 6. The laser medium of a diode pumped system thermally less strained as compared to an arc lamp system. Thermal lensir and birefringence are less severe, therefore one can expect that a larger fraction of the multi-mode output can be obtained in $TEM_{00}$ mode. Resonatc of particular interest are the stable, telescopic resonator, the confocal negative branch resonator with aperture stop, and the confocal positive b resonator with apodized aperture.

In Chapter 7 a detailed design of a cw pumped laser is provided whicl produces 3 W of output power at 0.532 $\mu$m. Such a laser may find applicat for underwater illuminators. The pump configuration selected is a sidepur Nd:YAG rod pumped by a semicylindrical arrangement of linear laser diode arrays. A trade-off among cw intracavity doubling, mode-locking, or Q-switching led to the selection of a cw pumped, repetitively Q-switched, intracavity doubled laser.

Chapter 8 contains the conclusion of this work, and the Appendices include a complete listing of the computer program written for a sidepump rod system and a floppy disk containing the menu driver design program. addition several memos generated during the course of this program are included.

## 2. DIODE ARRAY FABRICATION (Task 1)

In this section we will discuss diode fabrication technology, performance and cost as related to devices useful for solid state laser pumping.

### 2.1 DEVICE FABRICATION TECHNOLOGY

New device structures and fabrication methods have resulted in improvements of efficiency, power output, packaging density and reliability of diode lasers. These improvements which have a direct impact on the performance of laser diodes as pump sources for solid state lasers will be discussed below.

Other developments such as improvements in spatial mode and beam pattern stability, spectral purity, single logitudinal mode, and operation at very high modulation frequencies (several GHz) are primarily important for imaging and communications applications and will not be further considered here.

#### 2.1.1 Single Diodes

The structure of the first diode lasers was a homojunction (see Figure 2-1a). These diodes typically had threshold current densities of 40000 A/cm$^2$ and quantum efficiencies of 20 percent. Homojunction diode lasers are made entirely of a single semiconductor compound, typically gallium arsenide, with different portions of the device having different dopings. The junction layer is the interface between n- and p-doped regions of the same material.

The development of GaAlAs-GaAs single heterojunction laser diodes was a very significant improvement. Threshold current density decreased to 8000 A/cm$^2$ and quantum efficiency increased to 40 percent. In a single heterojunction diode, the active layer is sandwiched between two layers of different chemical compositions, typically GaAs and GaAlAs, which have different band gaps (see Figure 2-1b).

In the single heterojunction laser, the narrow layer serves as both the recombination region and the optical cavity. Good optical confinement is

Figure 2.1 Different diode laser structures:
(Ref. J.Hecht, Laser & Applications, Jan. 1984
a) Homojunction
b) Single heterojunction
c) Double heterojunction

More details of the important double heterojunc
is shown in d).
Ref. D. Botez, IEEE Spectrum June 1985, P. 43

a)

b)

c)

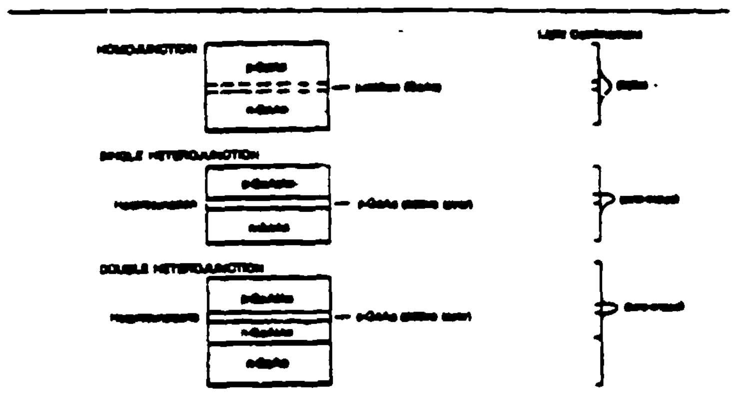


d)

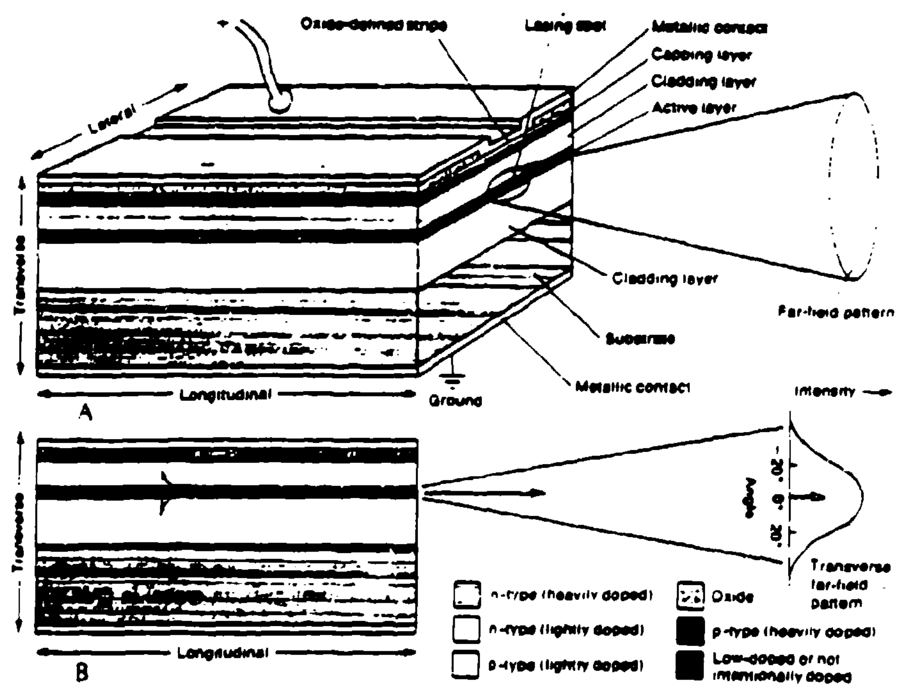

achieved by maintaining a relatively large difference between the indices of refraction of the p and p+ regions. Thus, the recombination region and the region of mode-guiding overlap to a large extent.

A further reduction in threshold current density (1000-3000 A/cm$^2$) was achieved with a double-heterojunction structure. The double-heterojunction lasers have an active layer bound by two layers of different material. Usually the double-heterojunction laser is formed by a multiple-layer epitaxial process and consists of a GaAlAs-GaAs-GaAlAs structure, with a thin (about 0.5 $\mu$) GaAs active region. (See Figure 2-1c). Because the double-heterojunction laser diode provides improved confinement to a narrower region, low threshold current densities are obtained. A detailed view of the double heterostructure is shown in Figure 2-1d. These laser diodes have threshold current densities low enough to operate continuously at room temperature. Because the active region is thinner than those of the single-heterojunction lasers the damage level is lower too. Therefore, these lasers have proven the most suitable for continuous operation. They cannot produce pulses with high peak power, but they can operate continuously or with high duty cycle at moderate powers (milliwatts) at room temperature.

High peak powers in pulses less than 1 $\mu$sec and with low duty cycles are obtained with single heterojunction devices.

Pumping of solid state lasers such as Nd:YAG or Nd:YLF requires either a cw source or a pulsed source with a pulse duration of 200-300 $\mu$sec. Due to the small heat capacity of the pn-junction of the laser diode, the latter pulse width represents quasi-cw operation.

Therefore laser diodes with double-heterojunction structure are most suitable for pumping either cw or Q-switched solid state lasers.

The most recent developments in high efficiency CW pumped laser diodes are the multiple quantum well (MQW) structures and the graded index single quantum well (GRIN) structures.

In a MQW structure the active layer is divided into a number of extr[e]
thin sublayers with different band gaps. The potential wells thus formed
to improve the optical coupling between neighboring laser channels.

Multiple quantum well structures require the ability to prepare ultr[a]
thin GaAs and $Al_xGa_{1-x}As$-layers. Wafers with different numbers of wells,
different well and barrier thicknesses are prepared by several companies.
Commercial devices offered by Spectra Diode Labs contain as many as 15 la[yers].
The semi-conductor layer structure consists of the substrate, cladding la[yers],
quantum well layers, barrier layers, etc. The active zone typically cons[ists]
of four 130 Å thick GaAlAs wells and three 40 Å thick barrier layers.

The ability to profile the GaAs composition of the epilayers by MBE
MOCVD techniques also made possible the preparation of a laser with grade[d]
index waveguide and separate carrier and optical confinements (GRIN-SCH).

Such structures provide not only separate confinement of light and
carriers to provide further optimization possibilities for the threshold
current, but also an arbitrarily graded index profile outside the carrier
confinement region.

Instead of trapping electrons in a multiple well structure the GRIN
technology is based on a graded index structure to collect electrons and
funnel them into a single quantum well. The graded index region provides
the waveguide structure for the laser action.

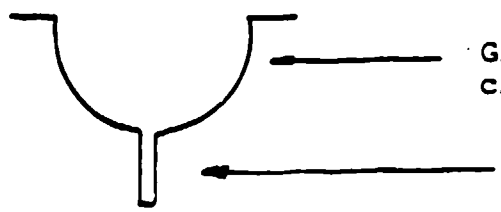

This technology, which is only about 12 months old, represents the state-of-the-art in CW laser diode production. In order to produce single quantum well structures, one needs special MOCVD equipment, which is capable of making very sharp transitions. The quantum well structure essentially represents a monatomic layer embedded in thick layers of different compositions. Companies and organizations which have started to make graded index, single quantum well structures include: McDonnell Douglas, TRW, General Electric, and the University of Illinois.

The performance of laser diodes based on the graded index, single quantum well structure is about a factor two better than multiple quantum well designs. For example quantum efficiencies at room temperature of 50 to 60 percent are routinely achieved. The output from a 6 $\mu$m stripe is as high as 1.5 watts. For double heterostructures the output is typically 10 mW/$\mu$m. For single quantum well structures the output is 20-25 mW/$\mu$m. The damage threshold is considerably higher in single quantum well structures due to a lower current density than multiple, quantum well structures. At the McDonnell Douglas R&D facility at Elmsford, New York, linear arrays yielding 20 watts per cm have been fabricated.

These devices consist of 60 $\mu$m wide stripes spaced at 400 $\mu$m centers. (25 units with 0.8 W output each.)

The GRIN structure is the latest development in the evolution of laser diodes which started with homojunction, single and double heterojunction and led to multiple and single quantum well structures. During this evolutionary process quantum efficiency has been increased from a few percent to over 70 percent.

## Devices with High Output Power

For solid state laser pumping, the maximum power during a 200 $\mu$sec pulse and the maximum repetition rate capability are of interest. (See References 2.1 to 2.6)

The first limitation relates to the power density at the emitting su and the limit imposed by facet damage. The maximum repetition rate relat the average power capability of the device and is determined by the desig cooling of the heat sink.

The output powers of conventional gallium aluminum arsenide diode la are limited by catastrophic optical damage. The destruction of the laser facet is caused by absorption of laser radiation, which can reach intensi of several megawatts per square centimeter at the facet. The active laye a semiconductor laser is made of material which is highly absorptive at t laser wavelength when current is not flowing through the p-n junction. U bias, however, minority carriers are injected into the active layer, crea a population inversion and thereby reversing its characteristics from absorbing to gain-providing.

At the interface of the active layer with the external ambient, howe electronic surface states provide highly efficient centers for nonradiati recombination and deplete this inversion. This causes the active-layer material in those regions of the facets to become absorbing. The heating occurs because of this absorbed radiation causes the material's band gap shrink, making the active layer even more strongly absorbing. The subseq thermal runaway results in damage to the facet by localized melting.

Because catastrophic optical damage is determined by power density, can increase the total power of a laser by spreading the beam over a larg area of the output facet, or by increasing the damage threshold of the fa

A larger emitting surface can be achieved by either increasing the thickness or the width of the lasing region.

Increase of the Thickness of the Emitting Surface

Structures which widen the optical mode perpendicular to the plane o junction, include the large optical cavity, the thin active layer and the single quantum well/separate confinement heterostructure. In all these

structures the optical wave is weakly guided by a thin active layer, causing the mode to spread into the cladding layers.

For example, in the large optical cavity design the two regions of a double-heterojunction laser diode are separated by a waveguide region. This layer is a lightly n-type doped material with a very low absorption coefficient at the lasing photon energy. As a result the thickness of that region can be increased to reduce the optical flux density in the active region without reducing external quantum efficiency.

Increase of the Width of the Emitting Surface

The available output power from laser diodes can be increased to some extent by using multilayer waveguide structures as described above. However, in order to effect order-of-magnitude improvements the beam must be expanded laterally within the active region. In principle, the power can be spread out parallel to the junction simply by increasing the active stripe width.

While the light is tightly confined in the transverse direction, that is not the case in the lateral direction. At first look, it might appear that light generated under the metallic contact will spread through the entire plane of the active layer. However, the injection of carriers into the active layer alters the refractive index of the active layer directly beneath the electric contact. If the electric contact is shaped into a narrow stripe (less than 8 micrometers wide) running the length of the diode, the profile of the injected carriers provides a weak complex waveguide that confines the light laterally--a mechanism commonly referred to as gain guiding. (See Figure 2-2a and 2-2c.)

In the index-guided laser, in addition to confining the current via a stripe, the light is also confined or guided in the lateral plane by a region of a higher refractive index than the outer regions. (See Figure 2-2b.) Since the light in these structures is guided by variations in the real refractive index of the various materials, the corresponding devices are known as index-guided lasers. Index-guided lasers supporting only the fundamental

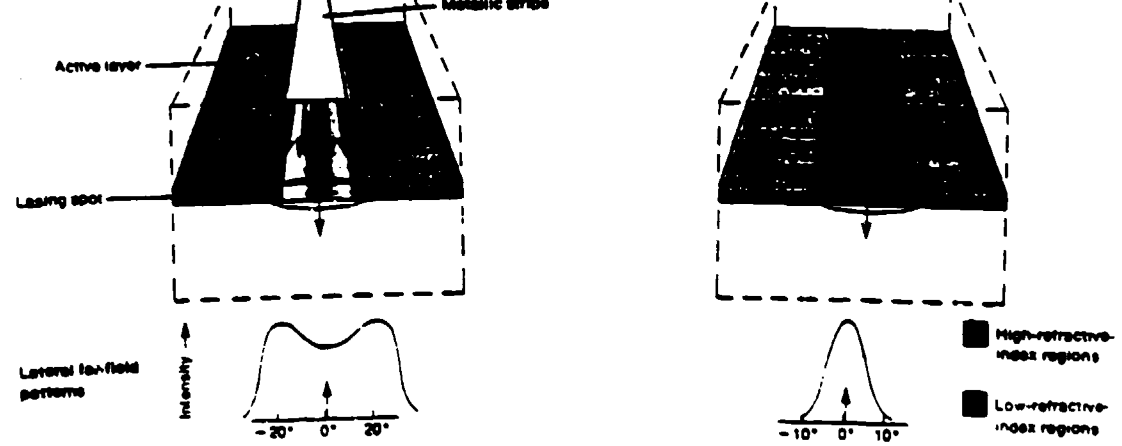


Figure 2.2 Wave-confining structure

a) Gain-guided structure (Ref. Dan Botez, IEEE Spect
June 1985, P. 43)

b) Index guided structure

c) Detail of gain guided single-stripe laser
(Ref. P.S. Cross et al, Photinics Spectra 1984, F

c)

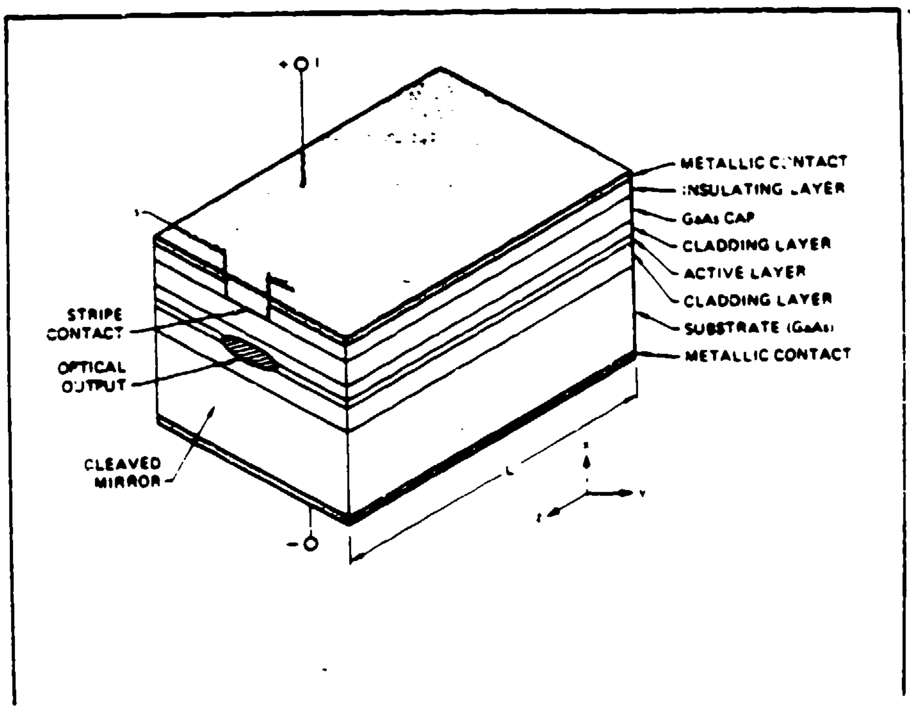

transverse mode therefore, they emit a single, well-collimated beam of light whose intensity profile is a bell-shaped Guassian curve.

Although index guiding is considered more desirable for many applications, it is also a more difficult process to implement in semiconductor production. Gain guiding does not put such serious demands on manufacturing processes, leading to much lower costs. Today, gain guiding is the dominant technique in commercial lasers.

Since the application of laser diodes for solid state laser pumping does not make any stringent demands on beam quality gain guided lasers will most likely be the choice for a cost efficient design.

In a gain guided laser we could expect output power to increase linearly with stripe width. Therefore one could consider preparing a wide-stripe laser with a width of several hundred micrometers. Such broad-area lasers do emit substantial power, but as a result of optical-field/injected charge interactions, they often lase in a multitude of incoherent filaments. Also, the large waveguide can support several transverse modes which generally change as the driving current is increased.

The relatively poor optical quality of these wide stripe devices is not a hinderance to their use as pump sources. However, the device susceptibility to uncontrollable filamentary operation can lead to localized damage of the faces and substantially reduce the life of the diodes.

In order to achieve more stable laser operation, a broad active stripe can be divided into several nominally single-mode stripes. Multistripe structures or linear arrays will be discussed in the next section.

### 2.1.2 Linear Arrays

The high structural and compositional uniformity of epitaxial layers grown by recently developed methods allows the integration on one and the same substrate of a large number of semiconductor lasers arranged side by side.

The original objective of this effort was to obtain higher power levels ir stable radiation pattern than those available from a single laser. The lateral optical coupling of closely spaced laser resonators provides, howe certain additional features such as the phase-locked operation.

Crystal growth of (GaAl)As is currently carried out in one of three liquid-phase epitaxy (LPE); metal-organic chemical vapor deposition (MO-C' or molecular-beam epitaxy (MBE). The first of these methods is the tradi- tional technique, while the latter two have only become available more recently. Although both MO-CVD and MBE are perhaps more difficult and co to implement than LPE, they are capable of the much finer compositional a dimensional control required for successful, reproducible growth of large array diode lasers.

Furthermore, MOCVD and MBE are better suited to economical high-yiel mass production of conventional lasers, and should supplant LPE in the ve near future.

After growth, various processing steps including photolithography, p implantation, metallization, crystal cleaving, sawing, soldering, and lea bonding are implemented to produce approximately 1000 lasers from each sq centimeter.

The stripes are formed by a spatial variation of injected current or material composition (index-guided). The main attraction of stripe-geome lasers is their ability to limit the number of modes in which the laser c oscillate, with the general goal being a single spatial mode and better o quality than the multimode beams produced by wide stripe diode lasers.

Multistripe systems can be fabricated as coherent or incoherent arra In the coherent design each stripe operates in the fundamental transverse and is evanescently coupled to the adjacent stripes. Since the stripes a close proximity to each other and since the gain-guides do not tightly co the light laterally, the optical mode beneath each stripe couples via

evanescent waves to its neighbors. Thus the array of optical fields becomes locked in phase, and, if the phase difference between adjacent stripes is zero, the lateral radiation pattern consists of a single narrow lobe.

At higher power levels, neighboring array elements generally lase $180^{\circ}$ out of phase to each other. This phenomenon produces a two-lobed "rabbit-ear" far-field pattern, which cannot be focused to a single spot.

At output power levels of 100 to 500 mW phased arrays generate well collimated output beams.

For side pumping of laser slabs or cylindrical crystals, phase coherence of the output beam is not required because the radiation pattern does not have to be tightly imaged into a small spot. Therefore incoherent linear arrays are employed for solid state laser pumping. Incoherent arrays have an optically insulating layer between the active stripes. Therefore, each stripe represents an independent layer. This has the advantage that a very large number of stripes can be built on a monolithic substrate. For example, a 25 W device produced by Spectra Diode Lab has 1000 stripes. In coherent arrays, the total width cannot exceed a certain limit, otherwise spontaneous emission and lateral lasing will occur.

Incoherent arrays can be stacked in length to any practical size. Typically, linear arrays are made from modules containing for example, in the case of a 1W Siemens laser, 36 stripes. Up to five modules can be mounted on a common heat sink to produce a 5 W incoherent array.

Figure 2-3 shows schematic diagrams of phase-locked and incoherent linear arrays.

The catastrophic optical damage mechanism, described earlier, which results from absorption of the active region at the facet, can be avoided in a new class of structures: they are the nonabsorbing facet or "window" lasers. In these devices the active layer does not extend to the facet. Since the

Figure 2.3 Phase-locked and incoherent linear arrays (6, 5,
(Ref. P.S. Cross, Photonics Spectra, Sept. 1984
P. 79 and D.R. Scifres et al, sppl. Lett. vol.
Feb. 1979, P. 259)

a)

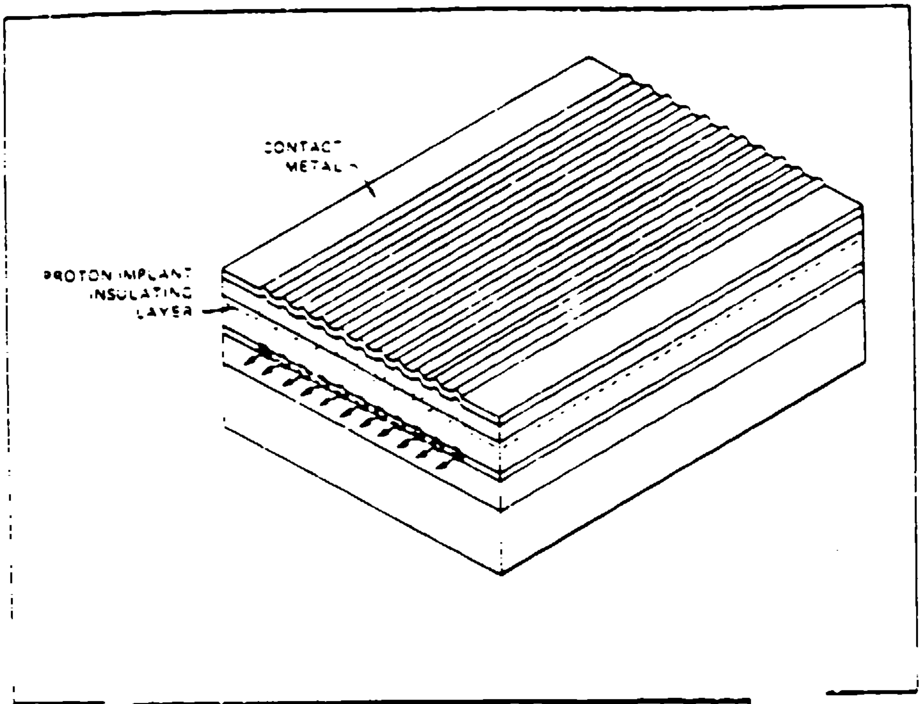


b)

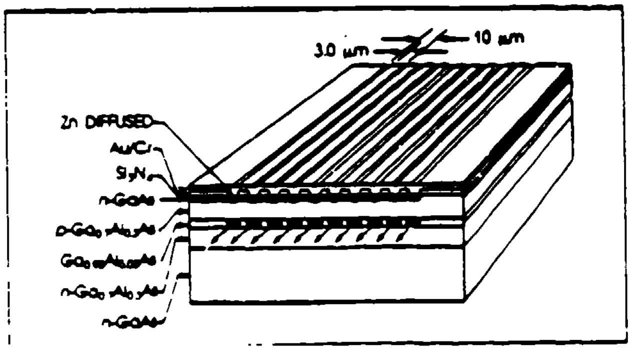


(Ref. G.L. Harnagel et al, Electronics
Letters, Feb. 1986, Vol. 22, P. 231

c)

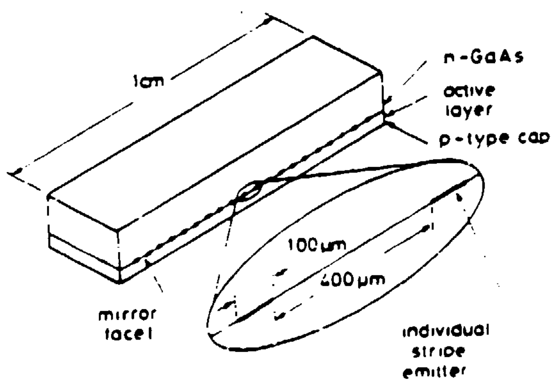

active layer is isolated from the surface, no absorbing regions exist and catastrophic optical damage is avoided.

Figure 2-4 is a diagram of one such geometry. The interior of this structure is identical to that of a nonwindow heterostructure laser and consists of a thin (approximately 100 nanometers) n-type AgAlAs layer sandwiched between upper and lower cladding layers of p- and n-type GaAlAs, respectively. The aluminum content of each of the cladding layers is higher than that of the active layer. This double heterostructure is embedded in a current-blocking structure consisting of an n-GaAlAs layer overlying one of p-GaAlAs, forming a reverse biased p-n junction. The aluminum concentrations of the blocking layers are similar to those of the cladding layers. The lower aluminum fraction of the active layer gives it a higher refractive index than its neighboring layers, resulting in transverse confinement for light traveling along the laser cavity. The window laser differs from the conventional buried heterostructure (BH) laser in the facet region, where the double heterostructure is replaced by AsAlAs of the same aluminum concentration as the blocking layers. At the laser's output wavelength, the absorption coefficient of this material is smaller than that of unpumped active-layer GaAlAs by several orders of magnitude. The facet can therefore be considered for all practical purposes to be transparent, and optical damage is eliminated.

The combination of monolithic multistripe laser diodes with a window structure may be the optimum configuration for solid state laser pumping. This way the emitting surface is increased and the damage threshold is raised.

### 2.1.3 Two-Dimensional Arrays

#### a) Stacked 2-D Arrays

The only viable approach so far, demonstrated for fabricating high power 2-D arrays of diode lasers, begins by subassembling extended linear arrays or "bars" (up to about 1 cm) of individual stripe lasers, and then stacking these linear arrays to form a 2-D array. The major process steps required to

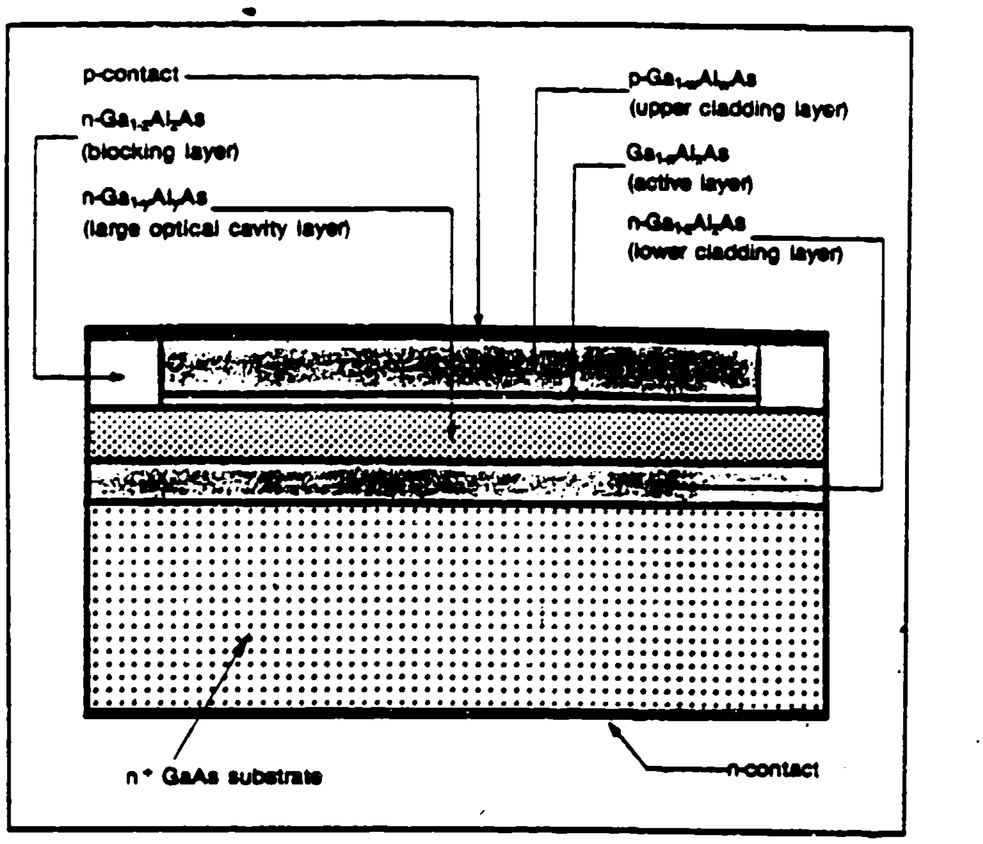


Figure 2.4 Side view of the window large optical cavity-b· heterostructure (LOC-BH) laser

(Ref. 7. Ungar et al, Lasers & Application September 1985, P. 111)

fabricate the 2-D structure are shown schematically in Figure 2-5. The process starts by growing a sequence of layers of AlGaAs on a GaAs substrate (typically "D" shaped about 2" in diameter) using Metallorganic Chemical Vapor Deposition (MOCVD). These layers serve to provide carrier and optical confinement to achieve good lasing efficiency. Next the stripe laser patterns are produced photolithographically and the contact metallizations are deposited. The wafer is then separated into one cm long, linear arrays by cleaving along crystal planes to form the laser cavity mirrors. Dielectric coatings are applied to the facets as soon as possible to inhibit degradation and to prevent light from being lost out the back facet.

The laser bars are next soldered onto mounting plates made of a material with high termal conductivity and with a coefficient of expansion that matches GaAs. Examples of such materials are BeO and Cu/W composites. A spacer plate is then attached to the mounting plate to provide adequate clearance between layers in the 2-D stack. The spacers can also serve as wirebonding pads and as additional thermal conduction paths to remove heat dissipated in the laser bars. Finally, the linear subassemblies are stacked to form the 2-D array.

b) Monolithic Two-Dimensional Arrays

The basic method of stacking up linear arrays to create 2-D arrays requires a large number of fabrication processes. An intuitively appealing alternative approach is to fabricate two-dimensional arrays directly at the wafer stage, thereby substantially reducing the manufacturing complexity. At present, there is only limited research being conducted on such "surface emitting" laser structures, and the results to date have been relatively poor. For example, cw room temperature operation has only been possible at very low power density using InGaAsP material and has not been achieved at all with AlGaAs. Nevertheless, the potential for emulating the silicon VLSI revolution makes this "high risk-high potential" approach attractive, especially for very high volume applications.

Two potential configurations for achieving surface emission are shown in Figure 2-6. The first (Figure 2-6a) is a "horizontal" distributed Bragg

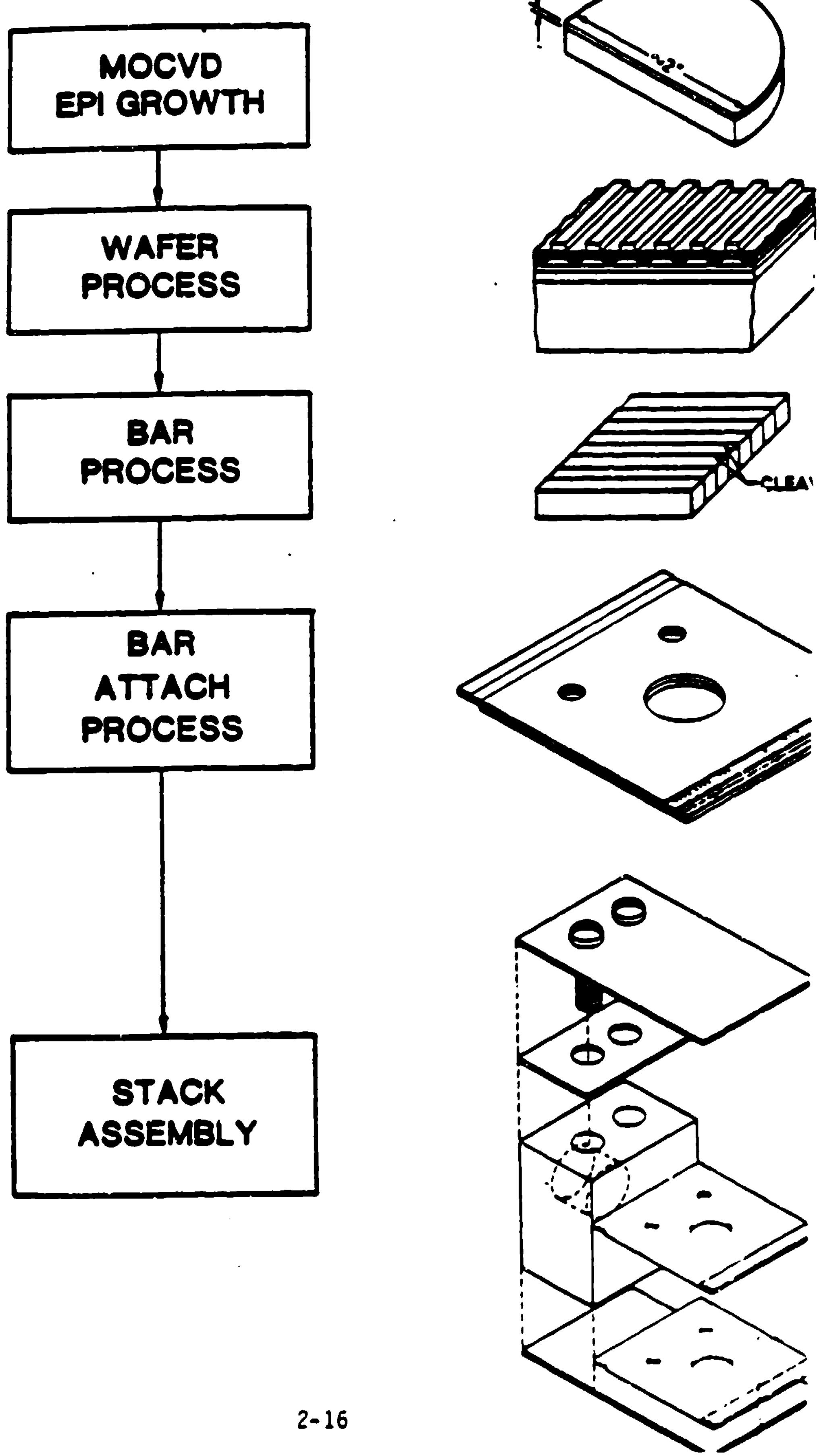
MOCVD
EPI GROWTH
WAFER
PROCESS
BAR
PROCESS
BAR
ATTACH
PROCESS
STACK
ASSEMBLY

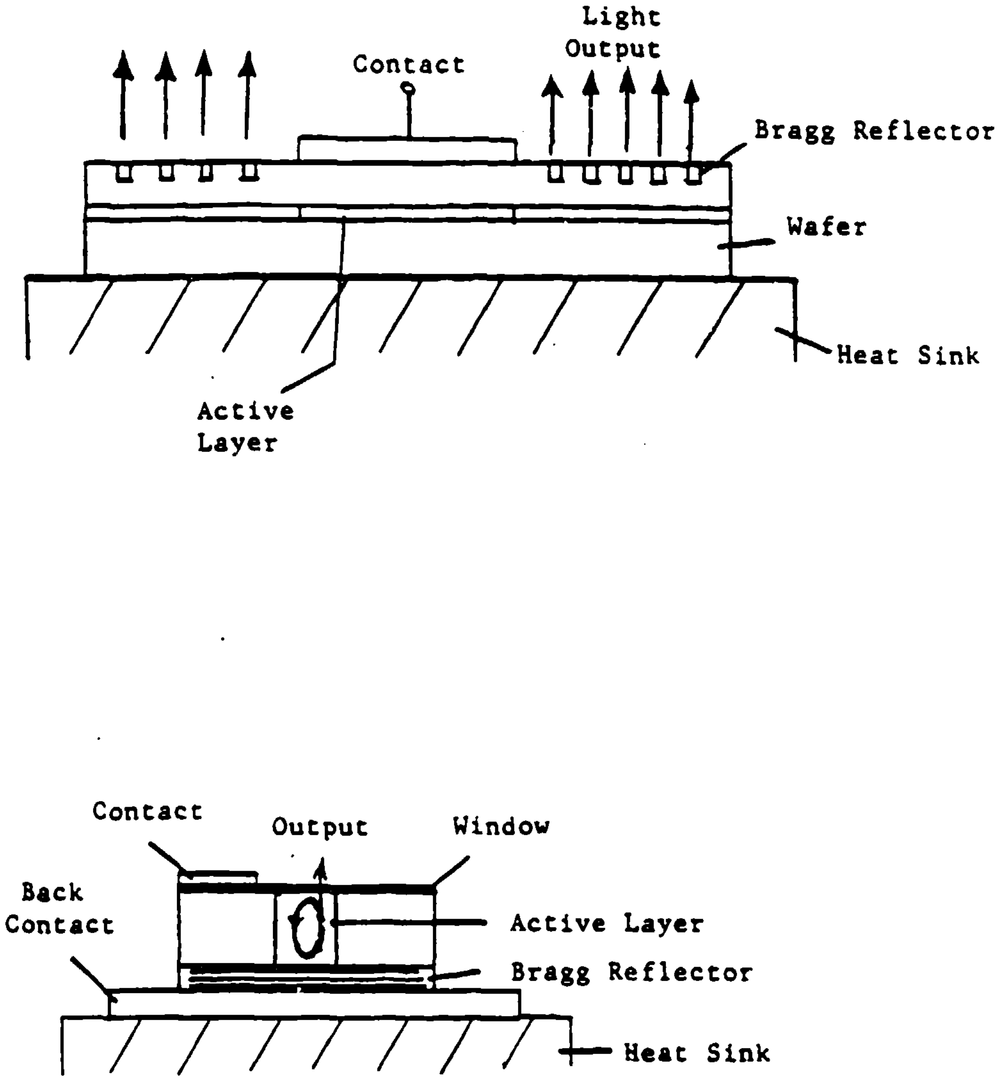


Figure 2.6 Monolithic 2-Darray with horizontal (a) and vertical (b) distributed Bragg reflector.

reflector (DBR) structure that employs a second order grating (period is 200 nm) in or near the active layer to provide the feedback necessary foı laser operation and tc couple light out of the active region as shown. current is injected into the center of the structure (where there is no grating) to create optical gain, and the light is coupled out in the "wi regions over the gratings where the metallization has been removed. In to efficiently remove the waste heat, the structure must be bonded epi-s down to a heatsink that is probably metallic and optically opaque. As a result, the light must couple out through the substrate side of the wafe which in turn must consist, for example, of AlGaAs with high Al content minimize absorption of the light as it passes through.

A second configuration (Figure 2-6b) is a "vertical" DBR structure which the periodic reflectors are grown during the MOCVD epitaxial layer growth. The injected current will now ideally flow horizontally through active region as shown and then out through the substrate. As with the horizontal DBR, the vertical structure must be bonded epi-side down and transparent substrate.

In any planar 2-D configuration, the individual active elements wil arrayed across the surface of an entire wafer. As an example, a plan vi a wafer section containing horizontal DBR lasers is shown in Figure 2-7. grating regions can be seen arranged in rows separated by the active reg The top surface is largely covered with metal to carry the current to th active regions, but there are openings in the metal to allow the light t escape. The typical size of each active element might be about 10 $\mu$m by 250 $\mu$m, with 10 $\mu$m separations between rows of elements. Assuming that 50 percent of the total surface can be covered with active elements and each element emits 50 mW (consistent with power densities in conventiona laser diodes), the 2-D structure has a power density of about 1 kW/cm$^2$. value is essentially the same as that obtained with the stacked 2-D arra structure and therefore can be considered as an interchangeable approach

Figure 2.7
Wafer section containing horizontal distributed Bragg reflectors
(Ref. D. Scifres, Spectra Diode Lab, White paper prepared for LLNL, June 1986)

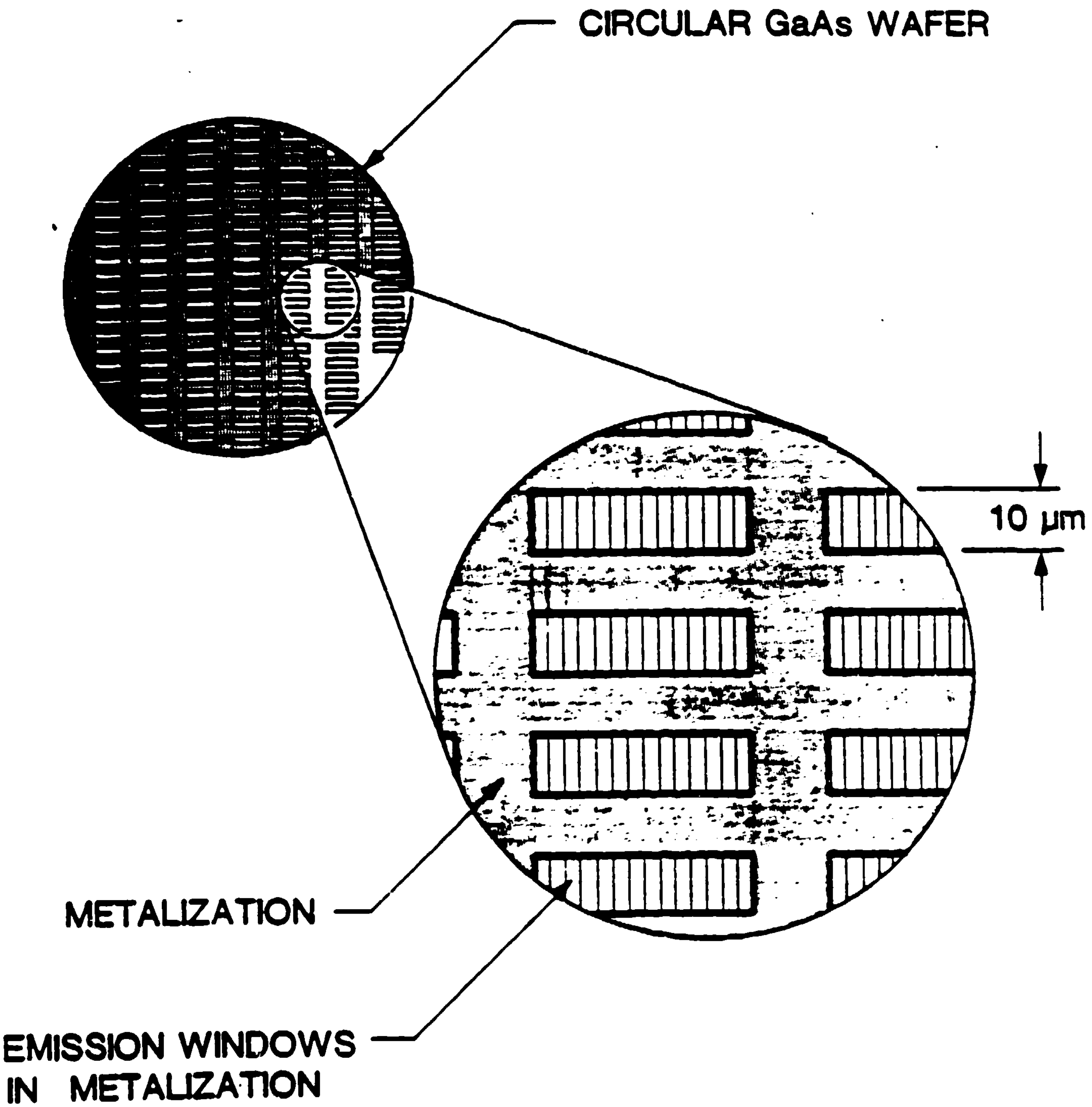

Some of the technical challenges that must be overcome in order to utilize a monolithic 2-D array include:

- Reducing the electrical resistance of the top metallization to an acceptable value which may require thicknesses up to 1 mm
- Achieving low thermal resistance to the heat sink over extended a
- Developing a transparent substrate technology in the AlGaAs mater system, and
- Geting high yield through wafer fabrication which would require v low defect densities and redundant designs.

## 2.2 PERFORMANCE OF LINEAR AND 2-D ARRAYS

In this section we will briefly discuss currently realized, as well near term projected, performance levels of laser diode arrays suitable fc solid state laser pumping. Parameters of particular interest are power output, efficiency, wavelength and lifetime.

### 2.2.1 Output Power

Through a combination of improved device technology, and integratior an increasing number of devices into arrays, laser diodes have achieved e higher optical output levels in recent years. A number of companies suct Spectra Diode Laboratories, Ortel, Siemens and Mitsubishi offer coherent incoherent linear diode arrays for the commercial market. In addition, a number of companies such as McDonnell Douglas, TRW, RCA and GE are involv the fabrication of arrays for military applications.

The power levels of laser diode arrays mentioned below are for quas laser diodes, i.e. for pulsewidth longer than a few microseconds. Since pumping of a Nd:YAG laser requires pulselength on the order of 200 $\mu$sec potential diode pump sources for Nd lasers operate in the quasi-cw mode.

Diode lasers capable of very high peak power have been in existance many years, but these devices typically operate only under short pulse (: 100 nanoseconds) and low-duty-cycle conditions.

As the pulse width of a typical aluminum gallium arsenide diode laser is increased, its maximum peak power capability decreases, as shown in Figure 2-8. The cause of this limitation is catastrophic facet degradation, a process whereby optical energy is absorbed near the facet, initiating a thermal runaway condition that raises the local temperature of the facet to the melting point. Because of the small volume of material involvd in this process, catastrophic facet damage can occur in less than one microsecond. For pulses longer than a few microseconds, the heat generated by optical absorption diffuses out of the laser material, and the catastrophic damage limit for diode lasers operated in long-pulse mode approaches the cw damage limit. Thus, long-pulse operation ($>> 1\ \mu s$) is also called quasi-cw operation.

Figure 2-9 shows the peak power pulse width relationship of a commercial diode array (SDL-2410-C).

We also note that the structures discussed below have incoherent outputs, because the stripes are separated by isolation regions, which prevent phase-locking. By forming these laterally isolated regions high power laser diode arrays can be fabricated by merely adding more stripes. Otherwise, as the width of the laser approaches and exceeds the cavity length, transverse lasing and amplified spontaneous emission compete for carriers, and the desired laser action is diminished.

Linear Arrays

As examples of state-of-the-art linear arrays suitable for Nd:laser pumping, we will consider arrays made by Spectra Diode Laboratories, McDonnell Douglas and Siemens. SDL is clearly the leader in the fabrication of coherent and noncoherent laser diode arrays for commercial use. A state-of-the-art array is a 1,000 stripe device with a 25 watt output in a 200 $\mu$sec pulse across a one centimeter bar. In this design the individual stripe produces 25 mW, which is low enough to guarantee good lifetime. Another design having a lower packaging density (20 percent of the bar length) produces 11 watts. This power level is generated by twenty, 10-stripe lasers. Each stripe

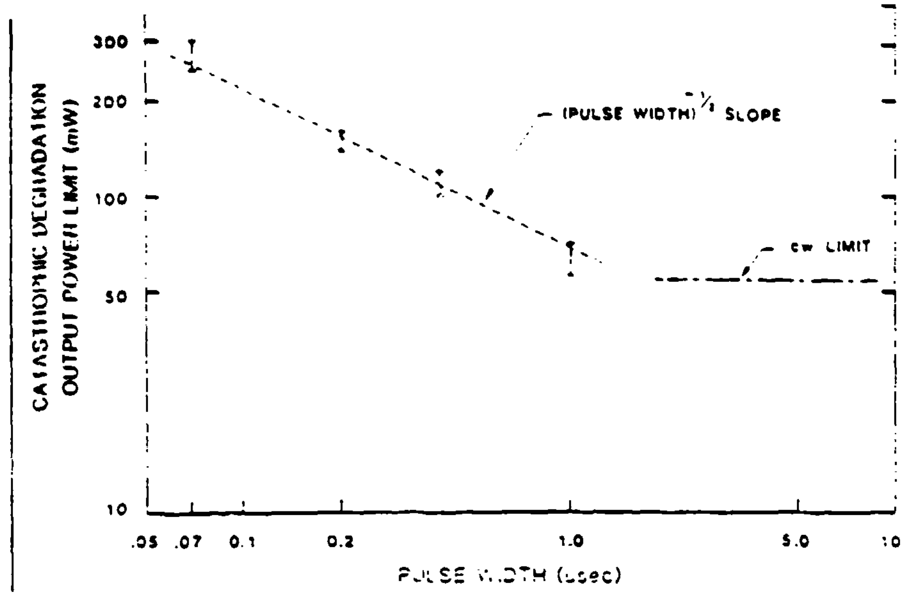


Figure 2.8 Catastrophic degradation power versus pulse wi
for 6 μm wide single-stripe AlGaAs lasers.
(Ref. G. Harnagel et al, Lasers & Applications
June 1986, P. 135)

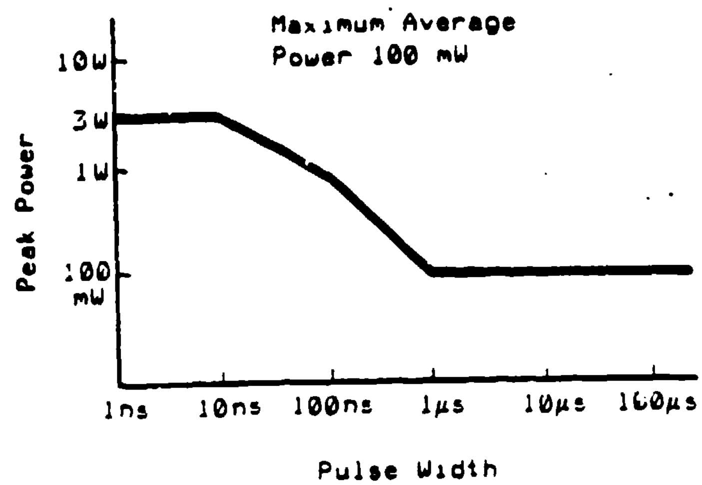


Figure 2.9 Peake power vs pulse width for commercial di
arrays (spectra Diode Lab SDL-2410)

occupies 100 $\mu$m of facet length, and the stripes are spaced on 500-$\mu$m centers. The device was operated at a repetition rate of 50 Hz by applying current pulses 150 $\mu$sec long. Figure 2-10 shows a plot of output power versus diode current. The maximum peak current was 11 W at 17.3 A and the best slope efficiency was 0.96 W/A. This corresponds of a 61 percent quantum efficiency. The maximum conversion efficiency of optical power output to electrical power input was 27 percent.

At McDonnell Douglas a large number of bars are fabricated from wafers received from Siemens and Hewlett Packard. The bars are assembled into 2-D arrays. Typical output per bar is 25 W. In some cases as much as 60 W/cm has been achieved.

The latter performance is the result of the graded index, single quantum well design of diodes fabricated either with MOCVD or MBE techniques.

In order to illustrate the progress made with multistripe laser diodes we have listed the progression of output powers achieved from devices made by SDL over the last two years.

| Number of Stripes | Aperture Width mm | Output Power W |
|---|---|---|
| 40 | 0.4 | 2.5 |
| 140 | 0.8 | 4.0 |
| 100 | 1.0 | 5.4 |
| 200 | 10.0 | 11.0 |
| 1000 | 10.0 | 25.0 |

A ten-fold improvement in power was achieved within two years.

From the data shown above, we see that the power output per stripe ranges from 25 mW to 60 mW. As was discussed before, facet damage sets the upper limit for the power emitted from one stripe.

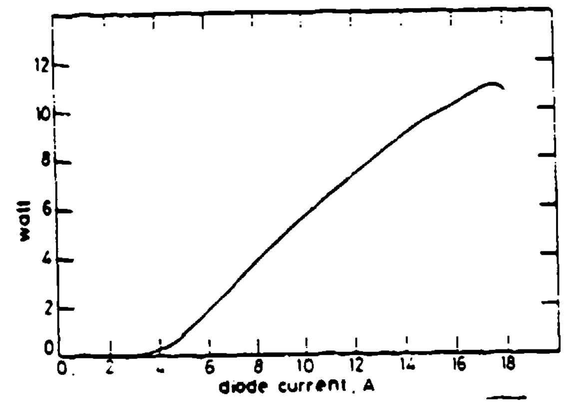


Figure 2.10 Optical output power vs. diode current for a 2
stripe monolithic array.

(Ref. D.R. Scifers, Appl. Phys. Lett. vol. 41, Dec. 1982, P. 1030)

However, if the gain guided, double-heterojunction multiple "stripe" geometry is combined with the window-laser approach, 100 mW per stripe seems quite achievable. This will lead to one cm bars capable of 100 W output in a 200 μsec pulse.

Similarly high output powers are projected for gradient index, single quantum well structures which have a higher damage threshold compared to double heterostructure devices.

Standard commercial devices offered by SDL and Siemens have an output of 5 W "quasi-CW" and consist of 140 and 180 stripes respectively. In the Siemens design, each stripe is 15 μm wide and 300 μm long. The average power or duty cycle of these devices is determined by the heat dissipation capability of the mounting structure.

<u>2-D Arrays</u>

Only one company, McDonnell Douglas, has currently the fabrication capability to produce stacked 2-D arrays. The company has developed the technology to produce arrays with an output power of one $kW/cm^2$ for 200 μm long pulses. (See Figure 2-11.)

For example, one 0.5 $cm^2$ array produced 475 W peak power in a 200 μsec long pulse. The array is made up by stacking 20 bars each one cm long. Each bar produces 24 W and is fabricated from 120 μm wide, 10 stripe modules. About 80 modules are mounted on a one cm bar.

McDonnell Douglas has fabricated a number of 2-D arrays ranging from 0.5 $cm^2$ to several $cm^2$ in area.

The largest 2-D stacked array built to date is comprised of seven subarrays each having an area of 0.55 $cm^2$. Each subarray produces a peak power of 413 W in a 216 μsec long pulse, therefore a total energy per pulse of 620 mJ is achieved from the 3.85 $cm^2$ array. The electrical input into each subarray is 58A at 30 V which results in an optical output to input efficiency

Laser Diode Bar On Heat Sink Plate

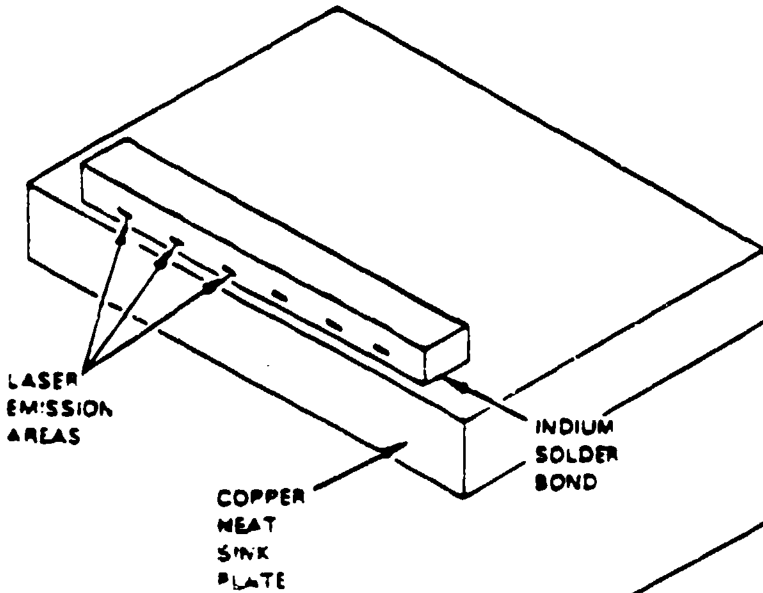


Mounted Laser D.

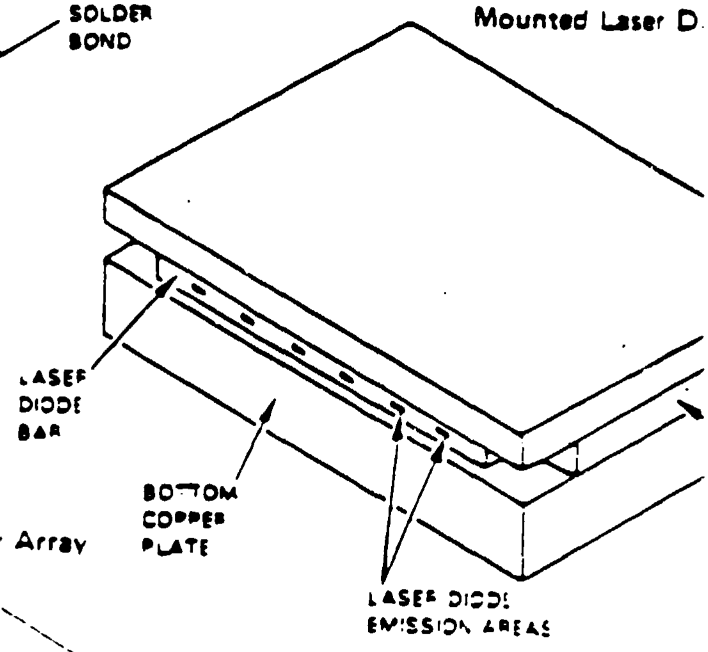


Laser Diode Bar Array

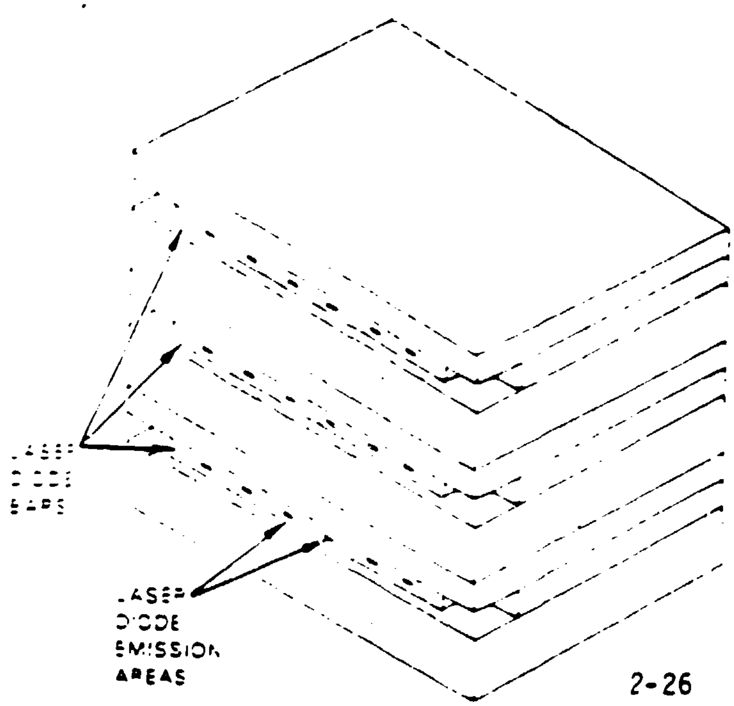

of 24 percent. The array was employed to pump a Q-switched Nd:YaG slab laser. Details of the performance of the laser will be given in Section 4.3.

The power density of about one $kW/cm^2$ which can be achieved from these arrays is limited by the laser diode fabrication technology. The achievable average power is determined by the heat sink. The arrays mentioned above are typically pulsed at 50 Hz, i.e. the duty cycle is around 1 percent. Therefore the average power from an array is typically 10 $W/cm^2$.

Utilizing advanced heat sink designs (see Section 5) it is expected that this limit can be raised to (100 to 200) $W/cm^2$.

The output levels mentioned above have been achieved with arrays operating at (20-25 percent) overall efficiency. Clearly if the efficiency can be increased (i.e. window laser, GRIN structures, etc.) the heat loading will decrease accordingly and higher average powers can be achieved.

### 2.2.2 Efficiency

The energy conversion efficiency of a laser diode depends on:

a) Internal quantum efficiency
b) Electrical series resistance
c) Threshold current
d) Operating point of the laser relative to the threshold current.

Improvements of the items a to c can be achieved by optimizing the internal structure of the laser through parameters such as layer thickness, composition and doping concentrations. Item d requires that the laser be operated at very high output power densities. This is illustrated in Figure 2-12, with plots of the light versus current and power conversion efficiency versus current for a 10 stripe laser operation in quasi-cw (150 μsec pulse) mode. Up to threshold (200 MA), the conversion efficiency is nearly zero because little power is emitted below threshold. However, the efficiency rises rapidly above threshold to about 35 percent at 800 MW output. This peak value of efficiency

of current (Spectra Diode Lab, Model SDL-10)

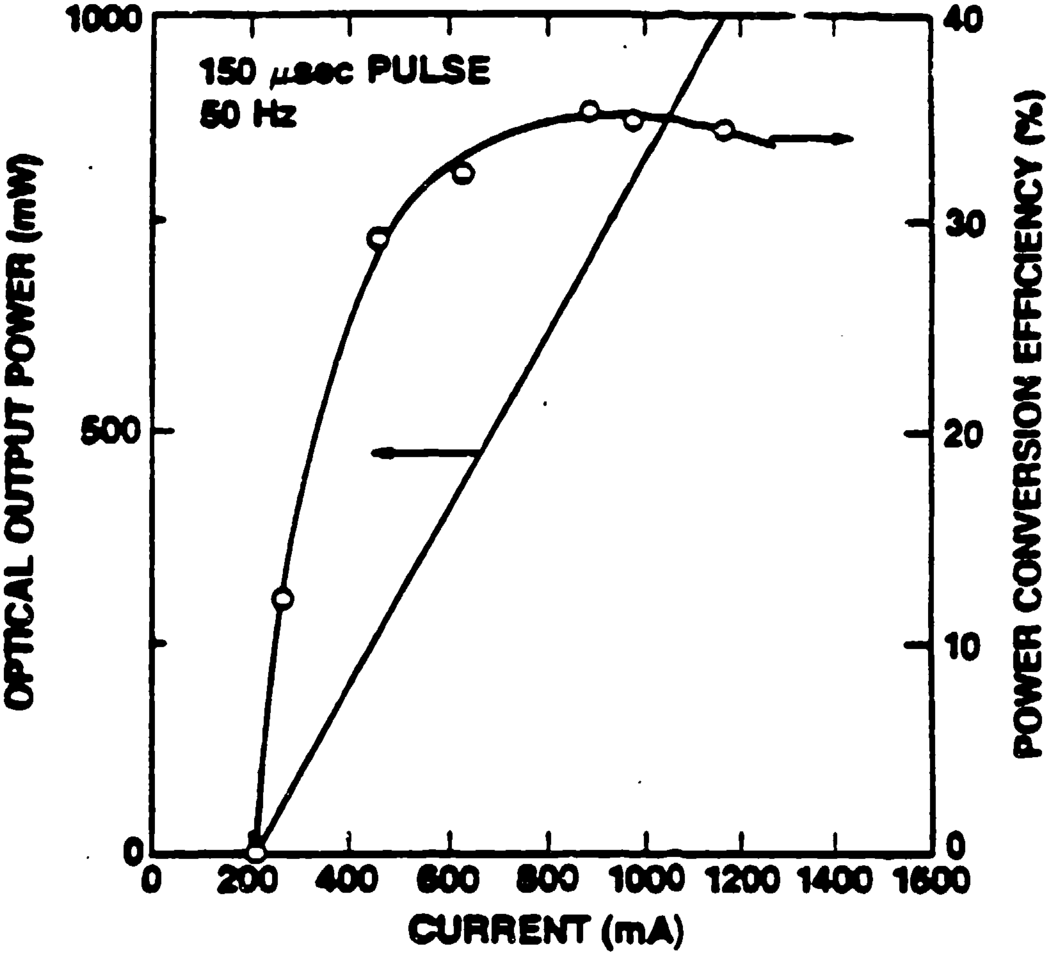


(Ref. White paper prepared by Spectra Diode Laboratories entitled, "The development and production of ultra-high power/two dimensional diode laser arrays, June 4, 1986)

is set primarily by the differential quantum efficiency and electrical series resistance. Since the maximum efficiency occurs at very high power (near the catastrophic damage limit, in fact), the output facet will degrade rapidly. Therefore, in order to achieve the highest possible power conversion efficiency, it will be necessary to minimize the facet degradation associated with high power density.

The performance of commercially available laser diodes and arrays is usually expressed in terms of slope efficiency. This eliminates the need for stating specific operating points at which a particular overall efficiency is achieved. With the threshold current and slope efficiency given, the overall efficiency for a particular operating point can be calculated.

Commercially available devices have slope efficiencies on the order of 25 percent. Index guided, single quantum wells structures achieve slope efficiency 40-50 percent on the average. Individual bars can be higher than that. Also in the window laser, a slope efficiency well over 50 percent has been achieved.

Projections from several researchers indicate that slope efficiencies of 60 of 70 percent will be achieved for laser diodes within the next five years.

The conversion efficiency of a diode array not only has a direct influence on the overall efficiency of the solid state laser but also is one of the key parameters determining the design of 2-D arrays. As will be discussed in more detail in Section 5, heat dissipation in a 2-D array is the limiting factor with regard to average power from the laser. The average power of the laser can be increased by increasing the efficiency of the laser arrays. At present, the projected, reproducible conversion efficiency of the 2-D arrays is about 20 percent. Therefore, for every watt emitted, 4 watts are dissipated. On the other hand, graded index, single quantum well structures have consistently exhibited conversion efficiencies of 40 percent and higher. In this case, only 1.5 watts are dissipated for every watt emitted--a reduction of over 60 percent. Thus, the average emitted power could be

increased a factor of 2.6 without increasing the total dissipated power ( array. It is readily apparent that tremendous gains in average output pc can be made by increasing the diode efficiency above 20 percent. Such improvements would be crucial in applications requiring high repetition high power density or where high conversion efficiency itself is a primar parameter.

### 2.2.3 Lifetime Considerations

One of the several attractions of diode lasers is their long lifeti Room-temperature values now approach $10^5$ hours at cw output powers of a milliwatts per stripe.

Operating lifetimes generally range in the tens of thousands of hou double-heterojunction GaAlAs lasers emitting about 10 to 20 milliwatts a temperature.

Lifetime was a serious problem with early diode lasers, but fabrica technologies have addressed reliability issues, and as a result diode la have achieved the impressive operating lifetimes mentioned above. In ge lifetime is longer for diode lasers with lower threshold currents, refle a general tendency for degradation to increase with operating current. low-threshold laser structures come into commercial use, laser lifetimes should continue to increase. Individual diodes in an array can fail for variety of reasons, and laser diode degradation can be broadly attribute three major causes:

- Damage to the laser mirrors (facets) which reduces their reflect or increases the nonradiative carrier recombination at the facet
- Ohmic contact degradation which increases the electrical and the resistance of the laser, and
- Internal damage, which results from the formation or movement of lattice defects into the active region of the laser, decreases t internal quantum efficiency and increases the optical absorption

The degradation modes of facet mirror damage, contact degradation and internal damage have been extensively studied by laser diode manufacturers.

For this study, data have been made available from McDonnell Douglas, Siemens and Spectra Diode Laboratories. Some indications of laser lifetime come from accelerated aging tests, in which the laser runs well above room temperature (e.g. above 70°C) for long intervals. Extrapolation of high-temperature degradation rates can indicate room-temperature lifetime.

As an example, Figure 2-13 shows the results of extensive life tests performed at SDL on a multistripe laser.

Specifically, 10-stripe MQW lasers in the 810-nanometer region were operated at 100-mW cw output, and the drive currents were monitored as a function of time for heatsink temperatures of 30°C, 70°C, and 100°C.

After screening for infant mortalities at 70°C, two laser lifetimes were determined for each temperature. The lifetime for gradual degradation was obtained by extrapolating the operating current to twice its initial value, using the measured degradation rate. The lifetime for catastrophic failure was the actual elapsed time before sudden failure occurred. Figure 2-13 shows plots of the cumulative failures as a function of time for both lifetimes at 70°C and 100°C. At 30°C only the extrapolated failures due to gradual degradation are shown, because only one abrupt failure occurred at this temperature.

From this investigation, three failure modes were identified: 1) sudden failure during burn-in (screening), which is related to the formation of dark line defects; 2) gradual degradation, which is observed at all temperatures; and 3) sudden failure related to increases in thermal resistance (attributable to failure of the bonding metallizations) at the higher temperatures. The best lasers exhibited degradation rates of 5 to 10 percent per thousand hours at 70°C. Below 30°C the gradual degradation mechanism is the primary method of failure. At 30°C the estimated mean time to failure for the 100-mW cw 10-stripe diode laser is more than 31,000 hours (median lifetime is more than 22,000 hours).

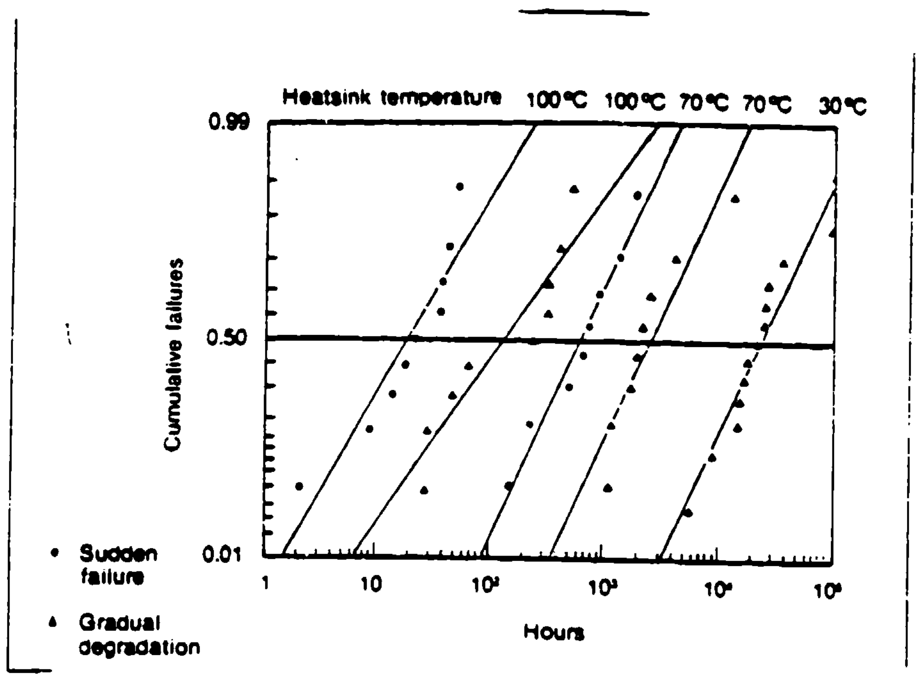


Figure 2.13 Plot of 10-stripe diode laser array lifetimes at 30°C, 70°C, and 100°C. At 30°C, the estim mean time to failure is more than 31,000 hour (median lifetime is more than 22,000 hours)

(Ref. P. Cross et al, Lasers & Applications April 1 P. 89)

McDonnell Douglas reports that accelerated life tests indicate mean time to failure up to $10^5$ hours. It has been observed that failure of an individual diode does not short out an entire array, because the bulk resistance is sufficiently high to cause a redistribution of the current. Lifetime estimates for arrays which are operated within their proper temperature limits are on the order of five to ten years continuous operation.

Figure 2-14 shows the result of a still continuing lifetest. After an initial drop in power during the burn-in phase, the output did not decrease noticeably during the next 3000 hours. This time is equivalent to $4 \times 10^{10}$ shots at a pulse width of 200 $\mu$sec. The projected long lifetime of these arrays compared to flashlamps for example, is one of the major reasons for DARPA's interest in these devices for space-based solid state lasers.

Figure 2-15 shows the optical output history of a 0.45 $cm^2$ array fabricated from sixteen 9 mm bars. The measured electrical conversion efficiency was 26.4 percent. A pulse repetition rate of 50 Hz was selected to accelerate the test. Figure 2-16 shows the power output versus current for the array at the beginning and at $10^9$ shots. As can be seen from these curves, the output power of the array was about 70 percent of the initial value after $10^9$ shots.

Another data point regarding lifetime can be obtained from a commercial manufacturer of laser diodes. Siemens is offering one cm long linear arrays made from 180 stripes with an output power of 5 W. The company guarantees 10,000 hours lifetime for these devices.

### 2.2.4 Spectral Properties

The spectral properties of laser diode arrays which are most critical for the pumping of solid state lasers are the center wavelength of the emission, the spectral with of the array and the wavelength shift with temperature.

Wavelength of a diode laser depends primarily on the bandgap of the material in which the electrons and holes recombine. In a binary compound

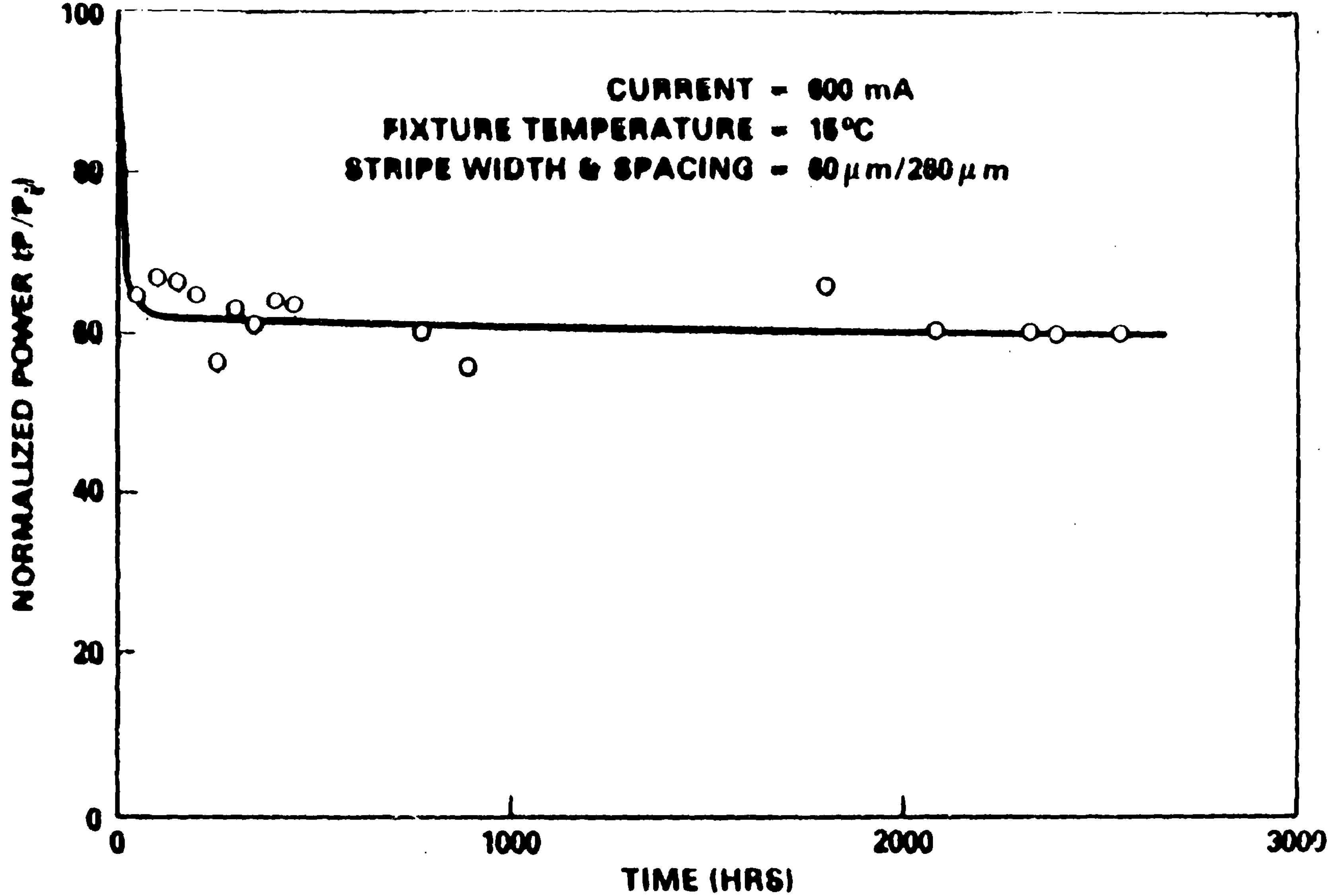

CURRENT = 600 mA
FIXTURE TEMPERATURE = 15°C
STRIPE WIDTH & SPACING = 80 μm/280 μm
NORMALIZED POWER (P/P$_i$)
100
80
60
40
20
0
0
1000
2000
3000
TIME (HRS)

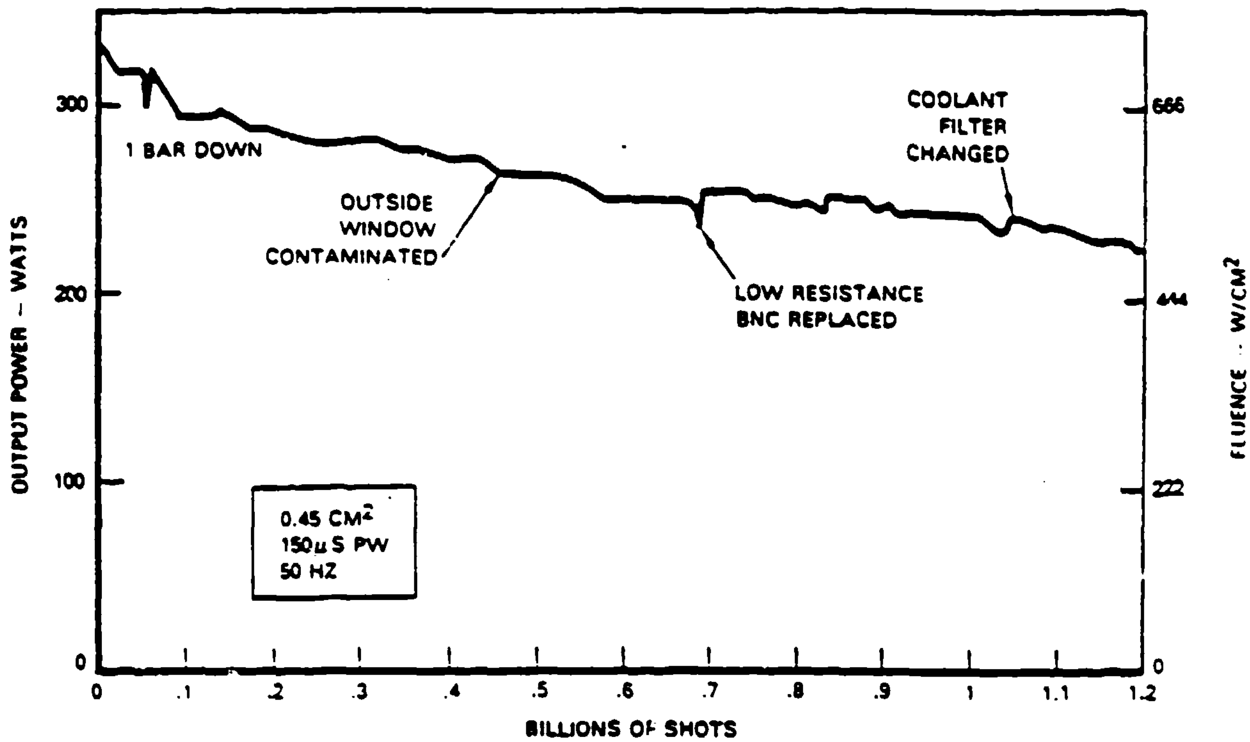


Figure 2.15 Array Durability Tests
(Ref. McDonnell Douglas, Report N66001-83-C-0072)

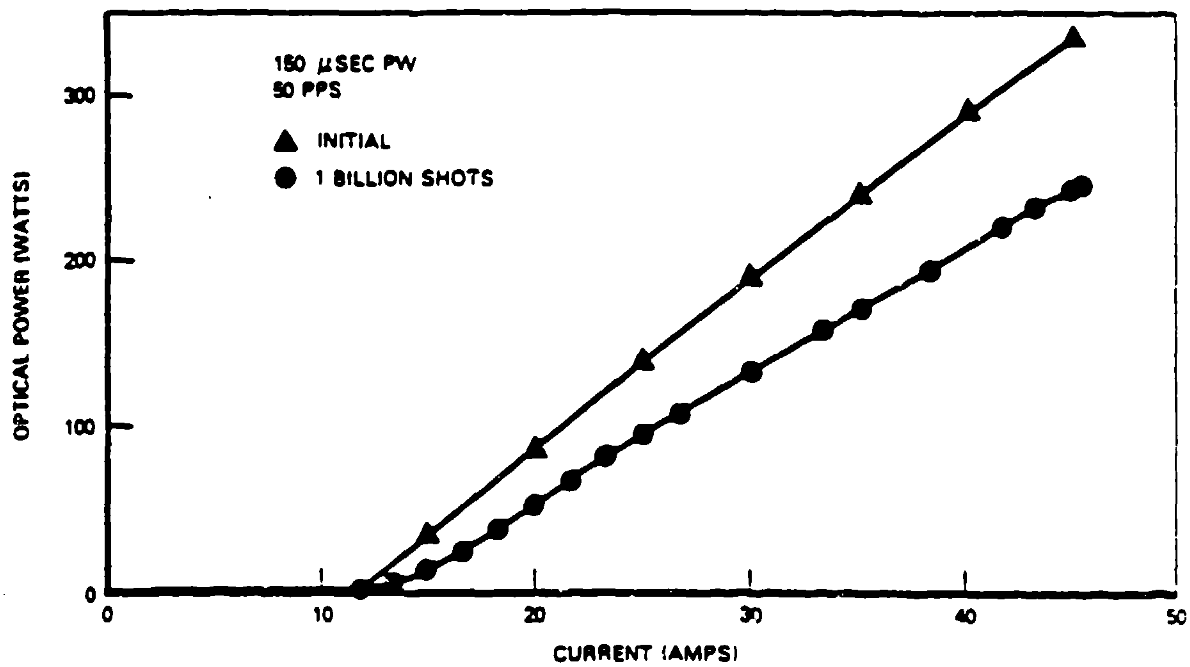


Figure 2.16 Optical Power vs. Current

(Ref. McDonnell Douglas, Report N66001-83-C-0072 April 1986)

like gallium arsenide the bandgap has only one possible value. Where the relative proportions of different elements can vary, including ternary compounds like GaAlAs and quaternary compounds such as InGaAsP, a range o possible wavelengths can be obtained as shown.

Nd ions in a number of hosts such as YAG, YLF and glass have substan absorption in the vicinity of 0.807 $\mu$m, which is the emission wavelength diode lasers with $Ga_{0.91}Al_{0.09}As$ active regions. As far as pumping of Nd lasers is concerned the output wavelength can be tailored to the peak absorption by adjustments of the Al concentrations. Typically a change i concentration of 1 percent, results in a 10Å change in wavelength.

More difficult to achieve is a narrow spectral width in an array. T bandwidth of the Nd:YAG absorption line at 808 nm is 20 Å for an absorpti coefficient larger than 3.8 $cm^{-1}$. Individual laser diodes have a spectra width of 20 to 40 Å full width, half maximum.

Compositional changes and temperature gradients within an array lead much broader spectral output for the whole array as compared to a single device.

In a GaAlAs structure the peak emission changes 3Å/C. Therefore, in order to keep the spectral output from an array within the peak absorptic region of Nd:YAG, the compositional variation has to be controlled within fraction of 1 percent Al, and the temperature variation across the array to be kept below 20°C.

The question arises, what other solid state lasers, besides Nd, can pumped with laser diodes?

By varying the composition of $Ga_{1-x}Al_xAl$ laser diodes, the band gaps be tuned, and output wavelength between 770 and 900 nm can be achieved. long as the potential lasing material has good absorption between 770 nm 900 nm GaAlAs laser diodes are the obvious choice.

There are two necessary material-related requirements for the creation of a room temperature CW diode laser: a direct bandgap III-V compound that emits light efficiently, and availability of a binary III-V compound substrate material with lattice-constant-matching-alloy compounds so that heterojunction can be created.

In ternary and quaternary compounds a range of possible wavelength can be obtained, as shown in Figure 2-17. But not all wavelengths depicted in Figure 2-17 are attainable. Some compounds lack the direct bandgap energy-level structure needed for efficient production of light; these indirect bandgap materials are not suitable for use as diode lasers. Another difficulty is that ternary or quaternary compounds are grown on substrates of binary compounds for the growth to proceed properly, the spacing of atoms in the substrate must be close to that in the compounds being grown. The development of strained-layer superlattice structures may enhance the range of compounds that can be grown, but at present, only a limited range of diode-laser materials are used commercially as shown in Table 2-1.

While pulsed lasers are made in the wavelength range between 0.9 and 1.2 $\mu m$, the difference in bandgap energy and index of refraction between InGaAsP and InP is not large enough to confine the injected electrons and holes or the light, and hence, low threshold lasers cannot be achieved. Through materials research efforts to reduce defects propagating from the substrate/epitaxial layer interface, the lattice match requirement may be relaxed in the future such that reliable, low threshold InGaP/InGaAs lasers could be made reproducibly.

Laser diodes with emission wavelength shorter than 700 nm are in demand as light sources of data processing equipment, bar code readers in supermarkets, and as a replacements for HeNe lasers. In particular several Japanese companies such as Toshiba, NEC and Sony are very active in the development of short wavelength laser diodes. These companies have all developed new experimental diode lasers made from InGaAlP. Continuous wave visible wavelength operation has been achieved at room temperature with

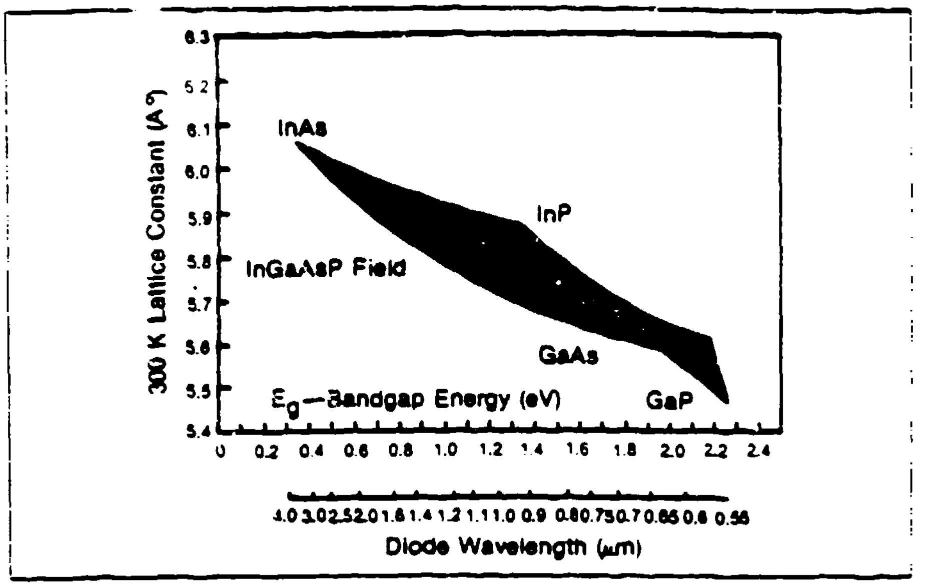


Figure 2.17 Plot of lattice constant versus bandgap energ

(Ref. J. Hecht, Lasers & Applications, Jan. 1984, P. 61)

| Material | Commercially Available Wavelengths (nm) |
|---|---|
| GaAs | 904 |
| GaAlAs | 770 to 900 |
| InGaAs | 1060 |
| InGaAsP | 1300 to 1550 |

Table 2.1 Wavelengths of Commercial III-VI Diode Lasers

(Ref. J. Hecht, Lasers & Applications, Jan. 1984, P. 61)

wavelength ranging from 670-690 nm. Maximum cw output is 20 mW. The device was produced by MOCVD, thin layers of InGaAlAs and InGaP could be grown on a GaAs substrate.

The technology of these new compounds will have to be developed further in order to overcome reliability problems.

Device-material changes require the longest development cycle, and diode lasers with good CW properties between 0.65 and 0.78 $\mu$m are still three to five years away. Emission wavelength shorter than about 0.6 $\mu$m is not technologically straightforward based on what we now know. There are at present no efficient (greater than 25 percent internal efficiency) LED's or direct bandgap materials with emission wavelengths much shorter than 0.65 $\mu$m, and even n- and p-type doping in such high-bandgap materials is difficult due to self-compensation.

Even if such lasers were developed, the high density of electron hole recombination and the high energies released during nonradiative transitions in these high bandgap materials will probably lead to fast degradation. Yellow, green, and blue diode lasers will probably not be available within the next ten years.

## 2.3 COST PROJECTIONS

In this section an attempt will be made to relate the price of laser diode arrays to performance and production quantities.

The cost of laser diode arrays is the biggest hinderance to their use for laser diode pumping. Therefore a good understanding of the relationship between cost and production quantities is very important in projecting the

potential of these pump sources for solid state lasers. Our projections ar based on the following inputs:

- Current prices:
  Linear and 2-D arrays are currently fabricated in small quantities which can best be described as pilot production runs. Linear array up to the 5W output level are commercially available, whereas more powerful linear arrays and all 2-D arrays are built essentially on single unit basis, under Government sponsorship. The current cost these devices will therefore establish an upper limit. On the othe hand, since laser diodes for use in disk players are manufactured i the millions, the cost of these devices will therefore establish a lower bound.

- Quotations for Limited Production Runs
  FIBERTEK, Inc. did approach several major manufacturers of linear arrays for quotations of laser quantities of their existing device: Quotations for production runs of up to 10,000 units have been received.

- Projections by Laser Diode Manufacturers
  As a result of visits and discussions with personnel from Spectra Diode Laboratories, RCA, McDonnell Douglas, Siemens, SPIRE and Nigh Vision Laboratory, valuable insight and information was gained regarding the cost drivers in the cost-quantity relationship. In particular, Spectra Diode Laboratory made available to us a cost analysis they performed for Lawrence Livermore National Laboratory regarding large scale fabrication of 2-D arrays.

It is also worth mentioning, that this particular technology is chang very rapidly. For example, projection regarding performance and cost of l diode arrays which would have been purely speculative about a year ago, manufacturers are now willing to submit firm quotations.

The activity in laser diode array fabrication is mainly due to a potentially large market of coherent arrays for laser printers and related applications requiring high power. Incoherent arrays are a spin-off of th activity and the prime motivation for companies to invest in this area ster from several large military programs. Also a contribution to this activit the realization by several manufacturers that industrial applications coul eventually become large enough to absorb a large production quantity of la: diode arrays. However, a market driver for cost reduction of incoherent drivers has not been clearly identified yet.

Laser diode pumped solid state lasers could replace lamp pumped systems in applications where the size of the system, efficiency, or maintenance time and expenses are important enough to outweigh the higher investment cost.

The history of the semiconductor industry gives some reason to hope that prices will drop even more rapidly than projected. There is a certain analogy between the transistor and integrated circuits and single laser diodes and multistripe arrays. In the past, individual diodes were mounted on a heat sink and connected electrically. Now up to several hundred stripes can be produced on one bar. Each stripe is more powerful than an individual diode about 10 years ago. The ultimate limit is about 1000 stripes per bar. For example Spectra Diode Laboratory producd a 1000 stripe linear array with an output of 25 watts. The power increased about 1000 fold, and the cost came down by about the same factor over a 10 year span.

### 2.3.1 Single Devices

Single laser diodes employed in compact disk players, printers and memories are mass produced at a rate of approximately six million units a year by Japanese manufacturers such as Sharp Electric Company, Mitsubishi and Sony Corporation. These AlGaAs laser diodes emit at 780 nanometers and have output powers between five and ten nW. The devices have been made by the liquid-phase epitaxial method so far, but the Japanese industry is switching over to MOCVD in order to get higher yield and better quality control.

The price for these diodes is about $8.00 per unit. This price clearly demonstrates the economy of scale which can be achieved at large production runs.

In contrast to these mass produced units are long wavelength emitters for telecommunications which lase at 1300 nm. Production quantities are in the few thousands and the price is $800.00. Industry sources indicated that if the demand for communication devices equaled that of compact disk players, the price would become similar to that of the AlGaAs diodes.

Two companies, Spectra Diode Laboratories and Siemens, provided cost and quotations for production runs up to 10,000 units. Also both companie gave preliminary cost figures for larger production quantities.

Spectra Diode Lab/25W Array

This array is mounted on a one cm long bar. Output peak power is 25 for a pulse width of 150 $\mu$sec. The maximum repetition rate, limited by thermal dissipation, is 50 Hz. Therefore the device has an average power capability of 200 mW. As a result of an individual contract, SDL built on device at an original cost of $50,000. The device is offered for sale now $12,000 in quantities of at least 10 units. In production quantities of a least 10,000 units the cost will be around $500.00 and at production rates 100,000 units the cost is expected to decrease to $200.00. Produced in th millions the cost could become as low as $50.00. At that level, the total materials cost and the cost of the mount becomes a significant part of the final price. Personnel from SDL estimated that the breakdown is on the or of $20 for the mount and $30 for the device. The relatively high cost of mount stems from the material cost and high fabrication cost due to the toxicity of the materials. In order to match the thermal expansion coeffi cient, the bars are mounted on one cm by one cm and 250 $\mu$m thick BeO heat sinks.

Siemens

The company is offering on a commercial basis a 5W linear array made from 180 stripes. Each stripe is 300 $\mu$m long and 15 $\mu$m wide. The stripes grouped in modules of 36 stripes. Five modules comprise a one cm long bar The linear array sells for approximately $3,000 in quantities up to 10 uni At a production quantity of 10,000 units, this price drops to $300. Above that number, Siemens personnel indicated that for every 10 fold increase production the price will drop a factor of two.

### 2.3.3 Two-Dimensional Arrays

Two-dimensional arrays are currently fabricated only by McDonnell Douglas. Their standard module is 0.5 $cm^2$ made from one cm wide bars. Output power from one array is between 450 W and 475 W. Several arrays were made available to a number of Government Laboratories at a single unit cost of about $250,000.

Spectra Diode Laboratory is very much interested in entering the field of 2-D stacked array production. The company performed a cost analysis which relates the selling price of these units to the quantities produced. The cost analysis was derived by a careful evaluation of all the steps necessary to make these arrays. A large number of steps is involved in the manufacturing process of 2-D arrays. These steps include wafer fabrication, generation of stripe patterns, metallization of contacts, wafer separation, application of dielectric coatings, soldering of bars to mounting plates and stacking of the arrays.

The result of SDL's cost projections show, that a one $cm^2$ array producing one kW of peak power in a 200 $\mu$sec pulse can be built for $125,000, at a production quantity of 25 units. For 100 and 500 units, the price drops to $62,000 and $22,000, respectively.

The most labor intensive processes are bar fabrication and linear array assembly. Cost reduction through manufacturing engineering to improve productivity and yield, it was felt by SDL personnel, could drop the price to $13,500.

After having made these improvements in yield, productivity and materials savings, economies of scale will decrease the price to $7,500 if the production is increased to 5,000 units.

A larger production quantity than that would require an automated, high volume production. This would require a MOCVD growth station with large reactors, large wafer (3-4" diameter) fabrication and photolithography

kW array at very high volumes (around one million) could be as low as $1(

### 2.3.4 Conclusion

We can graphically present the data base discussed in the previous section. Figures 2-18 and 2-19 show the price-volume relationship for 1· and 2-D arrays, respectively.

Several general conclusions can be drawn from the data:

The cost of laser diodes is very sensitive to production quantities cost will come down dramatically with increased production. Current fab tion quantities of 5 W and 25 W linear arrays and 1 kW/cm$^2$ 2-D arrays ar even in the pilot production phase. Less than 10 units of each type hav fabricated to date. The current production rate of these units represen far left hand corner of Figure 2-18 and Figure 2-19. There are no immed identifiable market needs such as existed for single diodes, used in dis players, laser printers, etc., which would indicate that the devices wil produced in very large quantities in the foreseeable future. Therefore unlikely that we will see a production which will drive the price to the numbers shown on the right hand corner of the graphs. The low cost figu for these high production quantities are believable, in FIBERTEK, Inc.'s opinion if one takes as an example the cost of $8.00 for mass produced l diodes. The major cost elements of a laser diode are the fabrication an testing of the chip, and the cost of heat sinking and mounting. At the high production level the cost is almost shared between chip fabrication mounting cost.

Therefore, the $8.00 device, although of low power, has a substanti amount of fixed costs such as wafer fabrication, testing, heat sinking a mounting. There is no reason why a multi-stripe device should cost subs tially more than the single stripe device if built at the same quantitie

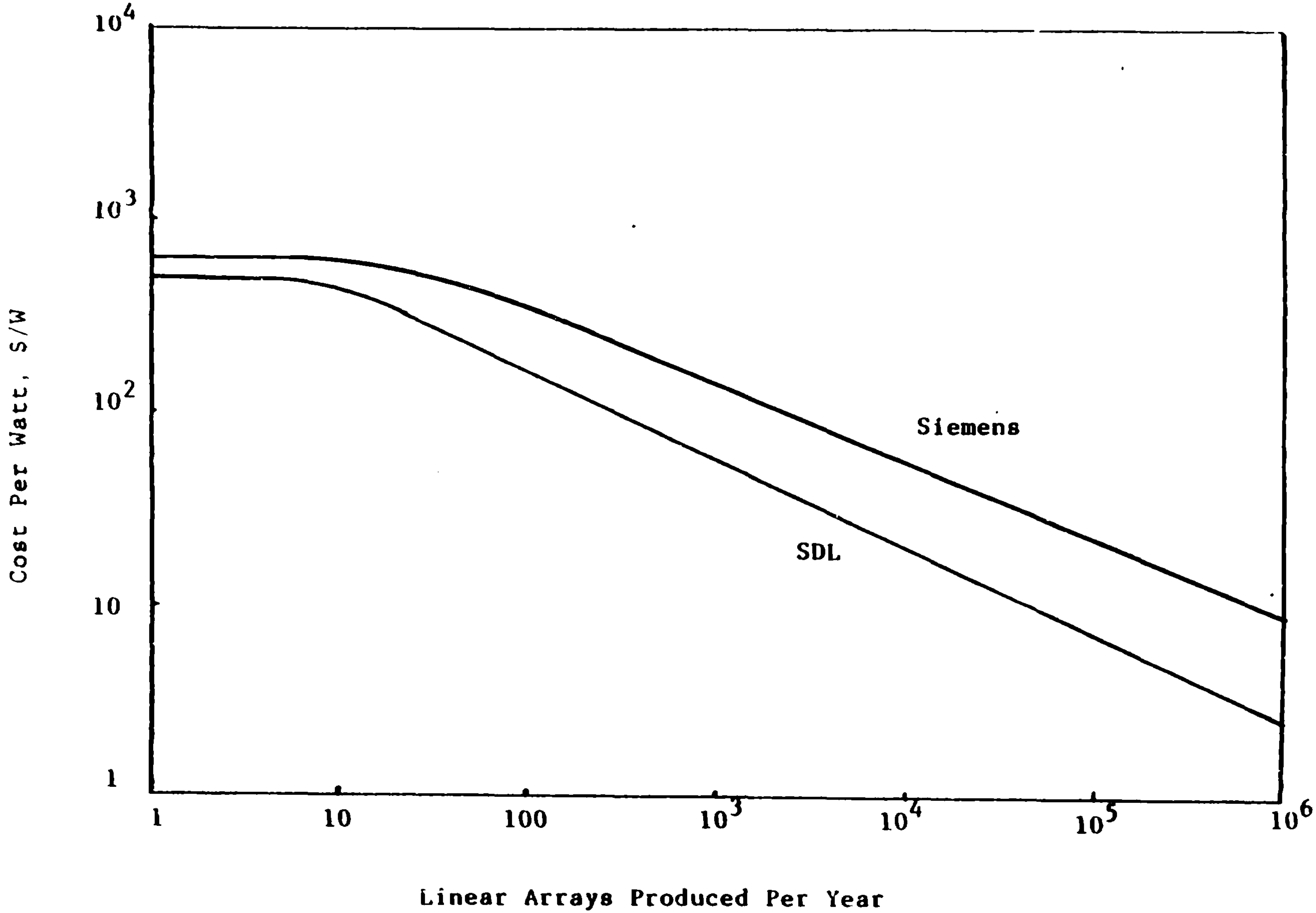


Figure 2.18 Projected relationship between price and production volume for linear arrays (data supplied by Siemens and SDL)

2-D arrays (Based on data supplied by SDL)

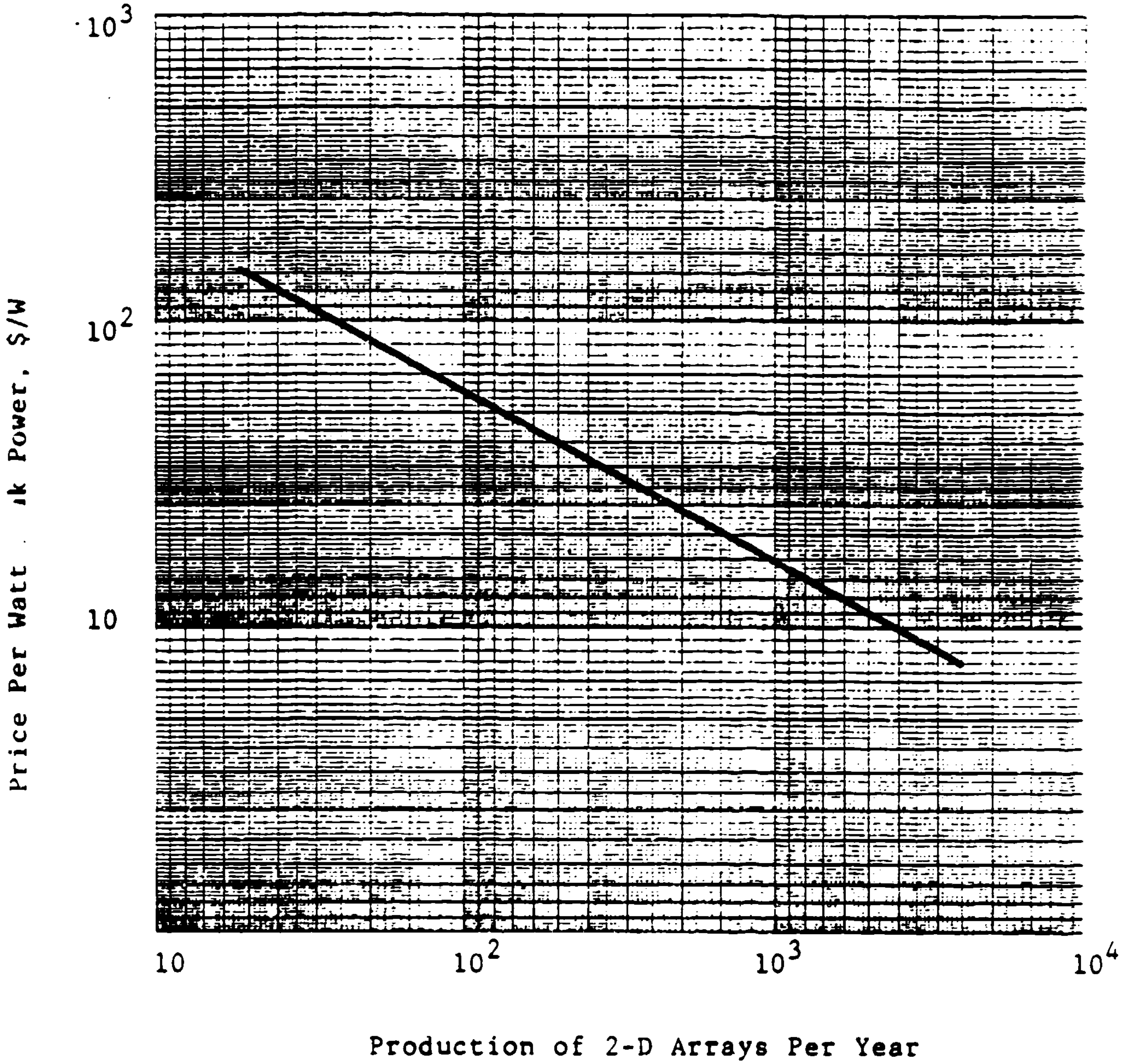

In a fully automated production facility, the cost of linear arrays should be only weakly dependent on the number of stripes. The labor to produce one unit and the material cost will be essentially the same, clearly the yield will be lower and have an impact on price. Therefore, the ultimate goal of producing devices with 1 watt output power for around $10.00 is not unrealistic, provided a market can be found to warrant such large quantities. If the pump source of solid state laser drivers for inertial confinement fusion, is switched from flashlamps to laser diode arrays, then such a market will be created. These pump devices would improve the performance of systems like NOVA in several ways: achievement of much higher overall efficiency; far less heating of the laser therefore high repetition rate operation would be possible, and due to the absence of high voltage lines the system would have much more benign operating parameters. Given the current funding situation for inertial confinement fusion, it is unlikely that such a project costing probably 200 MS could be launched.

Lacking a real need for mass production of linear or 2-D incoherent arrays, our predictions are as follows: As a result of Government funding and some interest from private industry, high power linear arrays and 2-D arrays will probably be built by the hundreds, or possibly on the order of few thousands as far as linear arrays are concerned. Military applications clearly include space applications such as submarine communications, space surveillance, etc., and also medium power lasers either airborne or ground based where size and power consumption are of prime concern.

In the near term, more commercial lasers will appear in the low to medium average power range pumped by laser diodes. Particularly for certain medical applications where overall size, benign operating features, and low maintenance of the laser are critical. For high average power lasers, more than 10 to 20 watts, the cost of the pump source will be prohibitive during the next three years.

In order to put the array cost in proper perspective as will calculate the cost of a complete pump system for two typical Nd:YAG lasers. The first

industry.

Target Designator

A typical system produces 150 mJ at a repetition rate of 20 ppsec. Flashlamp input is 12 Joules in a 200 μsec pulse. Average output power and the electrical input is about 300 W (if we account for power supply efficiency and cooler requirements).

For the laser diode array we will assume a conversion efficiency of Q-switched laser output to pump radiation 28 percent, consistent with da obtained from McDonnell Douglas. Therefore 150 mJ/0.28 = 535 mJ energy pulse is required from the array. This translates into 2.2 kW pump powe 200 μsec long pulse. At the price of arrays estimated, at the 500 unit year level, a laser diode array pump source for such a system would cost $22,000 x 2.7 = $59.400. Adding the cost for power supply and temperatu controller the complete pump system will be about $65,000. The cost of flashlamp system including the lamp, militarized power supply, and trigg unit is about one tenth of that amount.

In this application the advantage of a diode pumped Nd:YAG laser do outweigh the cost difference. Military lasers are operated only intermi tantly, therefore the long lifetime of the array is not of primary conce such as is for example in a space based laser. Flashlamps in target des tors have an operating life of approximately $10^7$ shots which is consider adequate for most situations. In our opinion, the production of 2-D arr would have to be much higher i.e. on the order of 10,000 units per year the price could come down to a level where the system can effectively co in the military rangefinder and target designator and target marker area

Commercial CW Pumped ND:YAG Laser

A medium power Nd:YAG laser, which is cw pumped and repetitively Q-switched will be considered. Such a laser, used extensively for resis

trimming, Si scribing, etching, drilling, cutting, etc., typically has 50 W multimode output and about 8 W $TEM_{00}$.

The system is pumped by a single krypton arc lamp with an input of 2 W. Overall plug efficiency in multimode operation is therefore 2.5 percent, and 0.4 percent for $TEM_{00}$ mode operation.

Now we replace the krypton arc lamp with a number of linear arrays. We select linear arrays rather than a 2-D array because one has to remove the heat from the pump source. A 2-D array is capable of high peak power but is very limited in average power.

We assume an output of 100 W from the arrays which should produce 28 W multimode output. This pump power can be generated by 20 linear arrays made by Siemens. Each array, if mounted to a proper heat sink is capable of 5 W CW output. Because of the drastically reduced thermal loading of the laser rod as a result of diode pumping, thermal lensing, and birefringence will be reduced also. Therefore we can expect a larger fraction of multimode beam power can be utilized in $TEM_{00}$ operations. According to our estimates this laser should produce 8 W $TEM_{00}$ power also. Assuming a 25 percent conversion efficiency of the diodes the system electrical input is 400 W.

The cost for the laser diode pump source is approximately $20,000 if we take a cost at the 500 unit per year production level. The price for a krypton arc lamp and power supply is about $2500. Despite this large difference in initial equipment cost, in this case the economics is much more favorable towards the diode system.

These Nd:YAG systems are used one or two shifts a day and operating and maintenance costs are an important consideration of the total investment. We assume a five year life of the system i.e. 10,000 hours. A krypton arc lamp cost $200 and needs replacement every 200 hours. Over the life of the system, lamp replacement costs will be $10,000. The cavity reflector needs to be refurbished every 1000 hours due to the heat and the UV content of the lamp,

is \$500. This adds another \$2500 to the maintenance cost.

In addition the system saves on electricity, 10,000 hours x 1.6 kW :
16,000 kW. At a price of 8 cents/kW this amounts to \$1280. Considering
time of the system and labor costs to perform these maintenance operatio
the higher investment of a diode pumped system are offset by lower opera
and maintenance costs. This calculation assumes that the laser diode ar
have a 10,000 hour lifetime. This number is guaranteed by Siemens for t
arrays. It is conceivable, that a diode pumped system, whose pump cavit
purged and sealed in a $N_2$ atmosphere to protect it from dust and dirt in
atmosphere could operate maintenance free for five years.

It should be pointed out, that in reality the cost figures are prob
even more favorable for the cw pumped system, than the ones shown above.
likelihood of a production rate of 500 linear arrays per year is so much
higher than a production of 500 planar arrays that one can reason as fol
It takes about 40 linear arrays to fabricate one 1 kW/cm$^2$ planar array,
therefore the cost of a planar array at the 500 unit per year level shou
compared with a 20,000 unit per year production of linear arrays. In th
case, we obtain from Figure 2-18 a cost of \$50 per watt for the linear a
or \$5,000 for the complete diode pump source of the cw laser. At this c
level, the diode pump can clearly compete cost wise with the krypton arc
system.

From the foregoing discussion we can conclude that with regard to d
pumping of Nd:YAG lasers no technological barriers exist. Fabrication
techniques--although on a very labor intensive basis--are on hand to des
and build linear and 2-D arrays suitable for pumping. There is also no
question that laser diode pumping, either cw or pulsed, is only advantag
from a performance point of view.

The use of laser diodes as pump sources is purely an economical question.

- Small end pump Nd:YAG lasers utilizing one or a few linear arrays are already on the market. They are economically viable because these very small lasers are technically unique due to their small size, and the cost of one or several small arrays is tolerable.

- For space applications of solid state lasers, 2-D laser diode arrays will clearly play a role. The cost of the arrays is of secondary importance in this case, due to the overall cost of satellite based systems. If the arrays have to produce high average powers (several hundred watts per $cm^2$) besides high peak power (1kW/$cm^2$) then the issue of heat extraction from densely packaged arrays will become a technical issue.

- In order to progress from the current level of demonstrated feasibility to high volume production a 30 to 40 million dollar Government program is needed to create the initial market. This would provide enough incentive for industry to implement cost reduction technologies, increase productivity in the wafer and fabrication and array assembly process. At the end of this Government program, the production would be at a sufficiently high level such that the price of these arrays could become a viable alternative to arc lamp pumped systems. At this point, the commercial market will sustain the production level and bring cost down even farther.

  The rationale for the size of the Government program follows from Figure 2-19. For example, at a cost of $7/watt probably enough commercial applications will open up to maintain a production level of 5,000 arrays a year. In order to get to this cost level, an initial market of 35 million dollars worth of arrays has to be created.

- There is an operating regime, such as 5-10 W cw pumped repetitively Q-switched Nd:YAG lasers, where the costs are at least within reach, even at a modest production rate of diode arrays. Therefore, in the absence of a large Government cost reduction program, several cw pumped Nd:YAG lasers utilizing linear arrays will probably appear on the market.

  There are several reasons for that: It is much more likely that a larger number of linear arrays will be fabricated as opposed to 2-D arrays. Linear arrays are not only less expensive per watt of output, they are also simpler to mount and cool. In addition several domestic as well as foreign supplies are working on the perfection of linear arrays, whereas 2-D arrays are only fabricated by McDonnell Douglas at present. In addition, for cw applications one does not need the high power density of 2-D arrays, since the performance is limited by the heat removal capability of the heat sink.

by SDL)

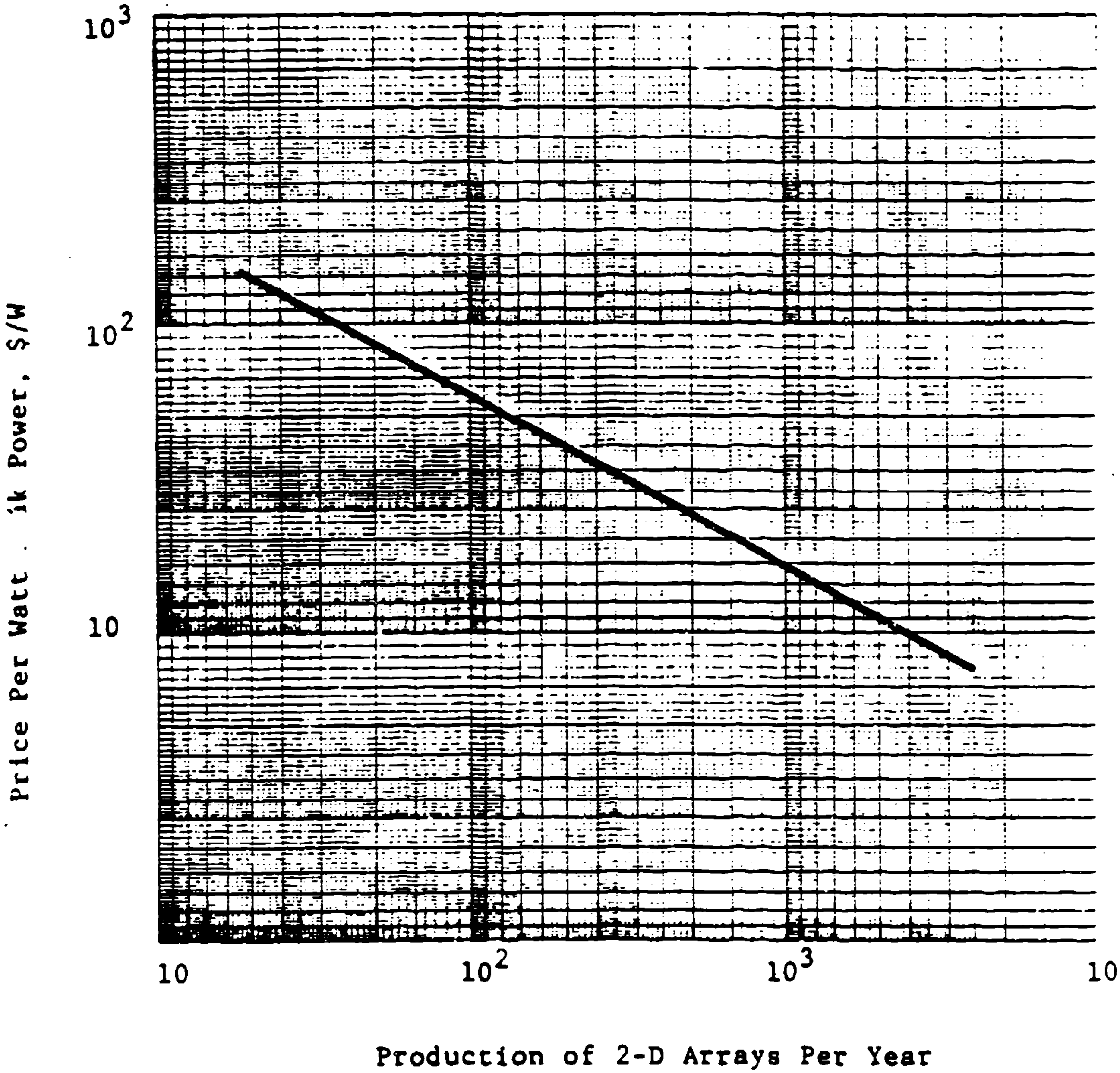

$10^3$
$10^2$
10
Price Per Watt . ık Power, $/W
10
$10^2$
$10^3$
10
Production of 2-D Arrays Per Year

Figure 2-20 illustrates the fact that diode arrays are most economically utilized in cw operation. We consider a laser with a given average output power of 100 W. Since laser diodes are power limited, pulsed operation requires many more diodes as compared to cw operations. The number of laser diode arrays required is proportional to the output energy per pulse. This is quite different from flashlamp pumped systems, whose costs are almost solely dependent on average power, and vary very little with repetition rate and energy power pulse.

Figure 2.20 Array Cost vs. Repetition Rate

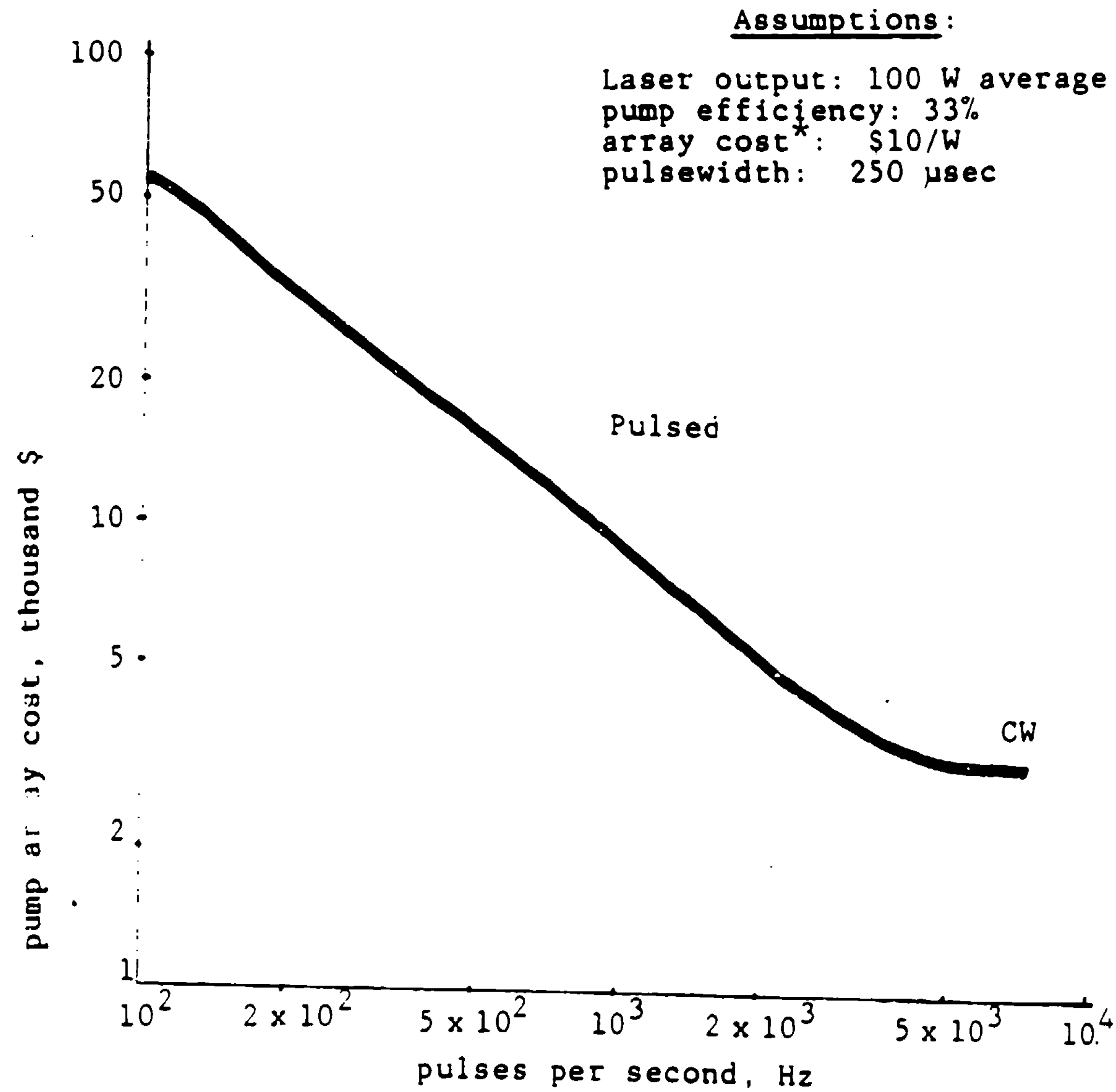


*Note: The cost of $10/W is based on a production qual of 50,000 linear arrays per year (see Fig. 2.. At low repetition rates (below 500 Hz) a cost o $5/W was assumed, because at a low duty cycle t! diodes can be operated at about twice their cw output.

## References

2.1 McDonnell Douglas, Diode pumped lab laser study--risk reduction phase. Technical Report N66001-83-C-0072.

2.2 P.S. Cross, D. Scifres, Spectra Diode Laboratories, White paper on: The development and production of ultra-high power, two dimensional diode laser arrays June 4, 1986.

2.3 P.S. Cross, R.R. Jacobs, D.R. Scifres. Photonics spectra 1984, September, P. 79.

2.4 D. Botez, IEEE Spectrum, June 1986, P. 43.

2.5 J. Hecht, Lasers & Applications, January 1984, P. 61.

2.6 Y. Suematsu, Physics Today, May 1985, P. 32.

# 3. LASER CANDIDATES (Task 2)

Laser diode pumping offers the possibility to use crystals other than Nd:YAG for the laser medium. For example, the laser medium could be selected for better energy storage, wavelength, or diode absorption and for more optimum system performance.

In Subsection 3.1 we will discuss laser materials for which laser diode pumping has already been demonstrated. A brief summary of the experimental results will be presented, as well as comments regarding future applications of these materials will be given.

In Subsection 3.2 we will discuss several solid state laser materials which hve spectroscopic properties which may make them suitable candidates for laser diode pumping.

In Subsection 3.3 a number of laser materials will be discussed which are currently the subject of great interest but are not likely to become candidates for diode pumping.

## 3.1 DEMONSTRATED PERFORMANCE

### 3.1.1 Nd:YAG

Most of the research on diode pumped solid state lasers has been concentrated on Nd:YAG. The popularity of this material stems from its excellent optical and physical properties combined with high gain, excellent crystal quality and a pump band which is conveniently located at the peak emission of GaAlAs laser diodes. Systems have been built recently, ranging from an endpumped Nd:YAG fiber with 50 $\mu m$ in diameter producing a few milliwatts of output power[1], to small endpumped Nd:YAG slabs generating a few hundred mW of power[2], all the way to a sidepumped Nd:YAG slab laser with 100 mJ Q-switched output[3].

Since this report deals mostly with Nd:YAG as the lasing medium no further elaboration will be provided in this section.

### 3.1.2 Nd:YLF

There are several potential advantages of using Nd:YLF as opposed t Nd:YAG in laser diode pumped systems. Nd:YLF has a fluorescence lifetim 440 $\mu$sec, almost twice as long as Nd:YAG. This means, that in pulsed sy to obtain equivalent pulse energy to Nd:YAG, only one half of the number laser diode arrays are required. Nd:YLF also naturally oscillates polar since YLF is uniaxial with the 1.047 $\mu$m line, the high gain transition. property is attractive for Q-Switching and second harmonic generation be it eliminates the need for polarizing elements in the cavity, which in t case of Nd:YAG, lead to optical losses as a result of thermally induced birefringence.

A spectral absorption curve of Nd:YLF for the region of interest is in Figure 3-1. As can be seen from this data, Nd:YLF is very compatible diode pumping due to an absorption peak at 792 nm.

Figure 3-2 shows the absorption spectrum for $\sigma$ and $\pi$-polarization o Nd:LiYF[4] over a wider spectral region. The strongest absorption occurs near infrared in the groups $^4I_{9/2}$ - $^4F_{5/2}$, $^4H_{9/2}$, and $^4I_{9/2}$ - $^4F_{\pi/2}$, $^4S_3$ which are responsible for over 50 percent of the total absorption. Nd:Y offers a reduction in thermal lensing and birefringence combined with im energy storage relative to Nd:YAG. However, gain is lower and the therm properties of YLF are not as good as YAG.

Laser diode pumping of Nd:YLF lasers has been demonstrated at 1.047 and 1.053 $\mu$m, with less than 1 mW threshold and internal quantum efficie approaching 70 percent[4]. Intracavity second-harmonic generation using MgO:LiNbO$_3$, has generated up to 145 $\mu$W output at 523.6 nm for 30.1 mW of laser pump power.

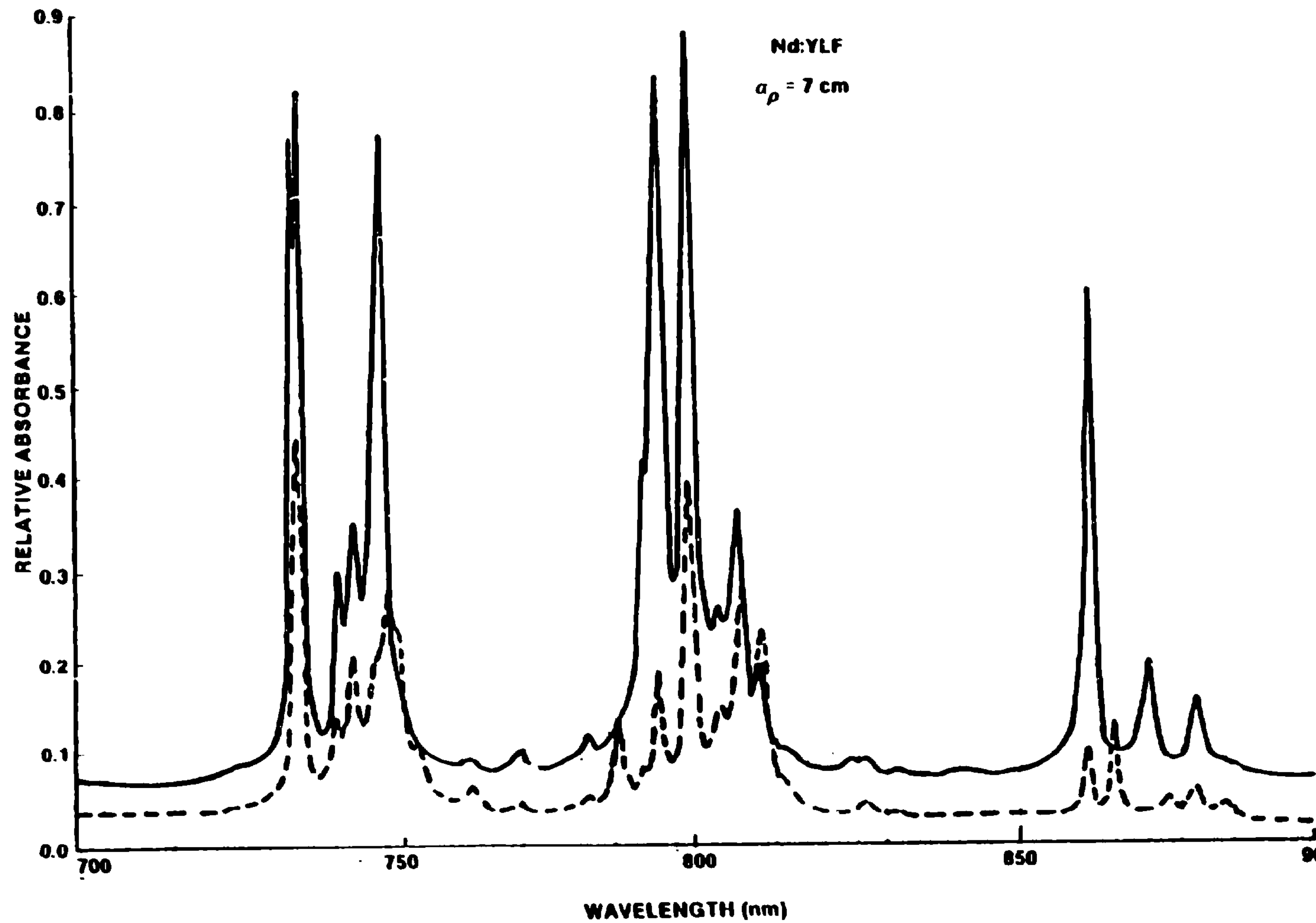


Figure 3.1 Nd:YLF Absorption

(Ref. Sanders, Assoc. Navy Blue, Program Review, March 12, 1985)

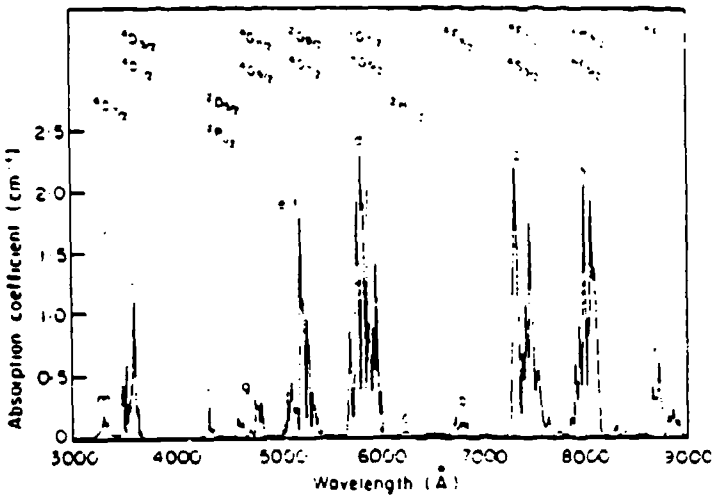


Γ - p

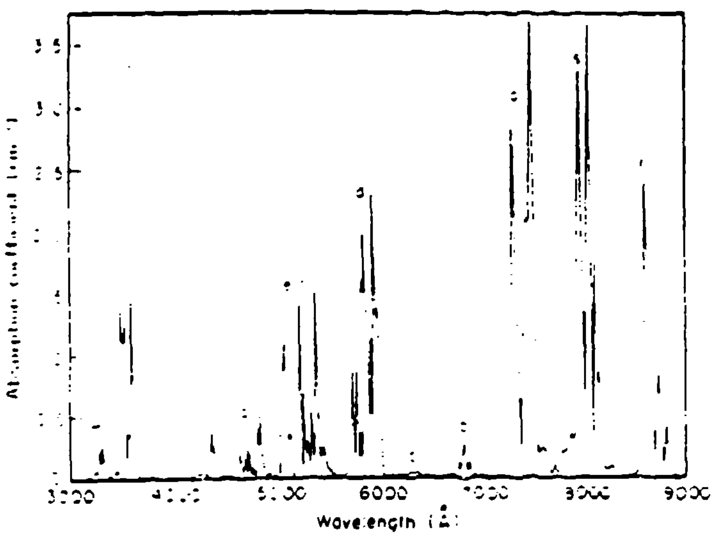


Π - pc

Figure 3.2   Absorption spectrum for Γ- and Π-polarisation
$LiYF_4$ with 2.2 at % Nd
(From A.L. Harmen et al. p. 1486)

The pump source was a single stripe diode laser with 30 mW of output power at 791 nm, which is the peak of the absorption in the $\pi$-polarization of Nd:YLF. The output from the diode laser was focused into the crystal in an end-pumped geometry with a microscope objective.

A typical Nd:YLF sample was 4 mm long and 3 mm in diameter with the end faces having 1.8 cm radii of curvature. One end face was a coated high reflector at 1.05 $\mu$m, and the other was 0.3 percent transmitting at 1.05 $\mu$m and high reflecing at 810 nm which is near the pump wavelength.

A laser diode pumped Nd:YLF laser is one of the prime contenders of the Navy Blue Program aimed at demonstrating 100 mJ output at 455.5 nm. This wavelength can be achieved by tripling one of the satellite laser lines located at 1.3665 $\mu$m. Figures 3-3 and 3-4 show the Nd:YLF emission spectrum and the stimulated emission cross-section, respectively.

### 3.1.3 Nd:Glass

With regard to laser diode pumping, Nd:glass has one desirable attribute, namely a broad absorption band. (See Figure 3-5). This makes the diode wavelength requirements less stringent. On the other hand, Nd:glass has a much lower gain than Nd:YAG, therefore, higher pump fluxes are required are efficient operation. This clearly represents a problem due to the power limitation of laser diode arrays. Although lasing action can be achieved in Nd:glass with laser diode pumping, as will be described below, we do not think, that the material is suitable for practical devices. With the modest pump fluxes available from laser diode arrays, the system cannot be pumped high enough above threshold, and as a result optical losses in the resonator will dominate and prevent high efficiency operation. Researchers at Stanford did build a small diode pumped Nd:glass laser recently[5]. The laser consisted of a 5 mm long piece of LHG-8 with 3 percent doping. To ensure low cavity losses, the coatings were applied to the polished piece of glass. One end was polished flat and coated with a HR at 1.06 $\mu$m and HT at 0.81 $\mu$m. The other end was polished to a 1.6 cm radius and coated 99 percent R at 1.06 $\mu$m.

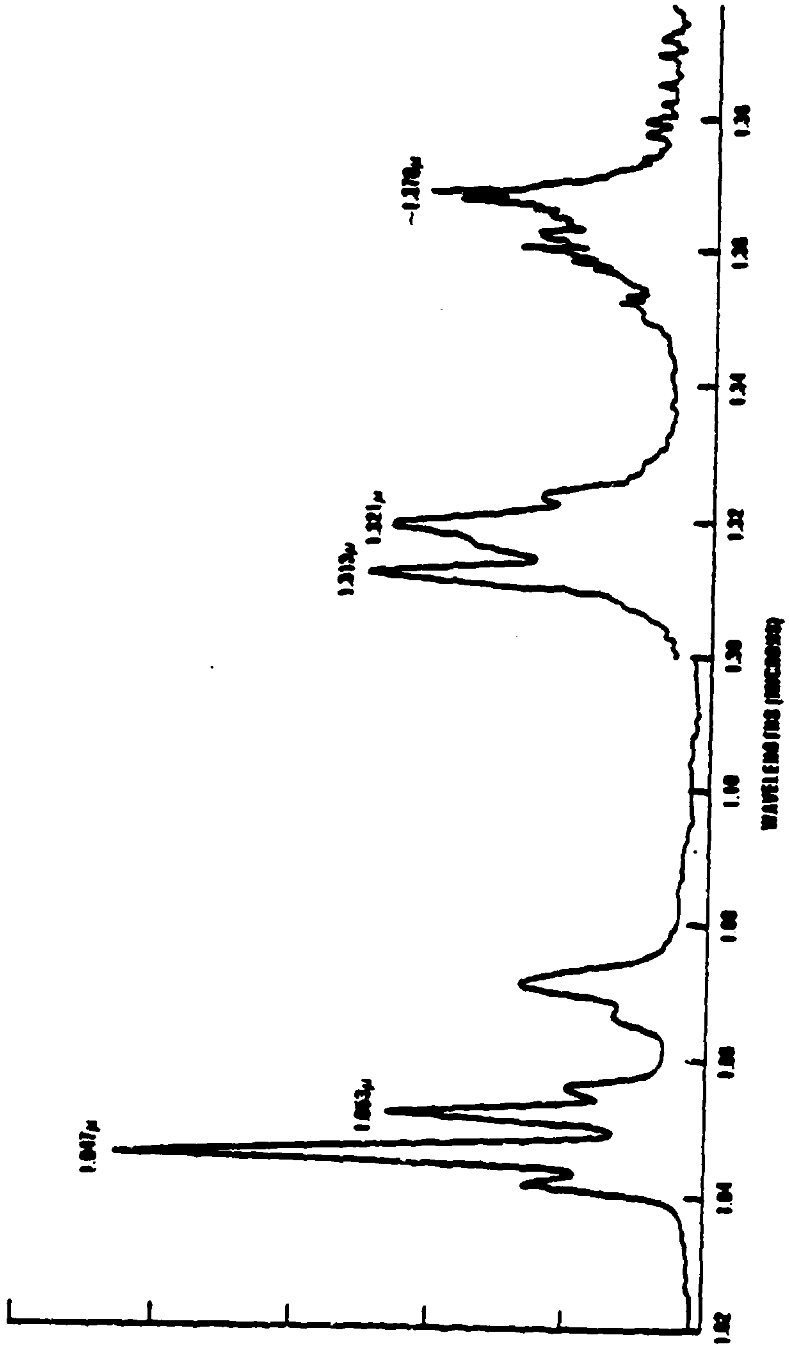

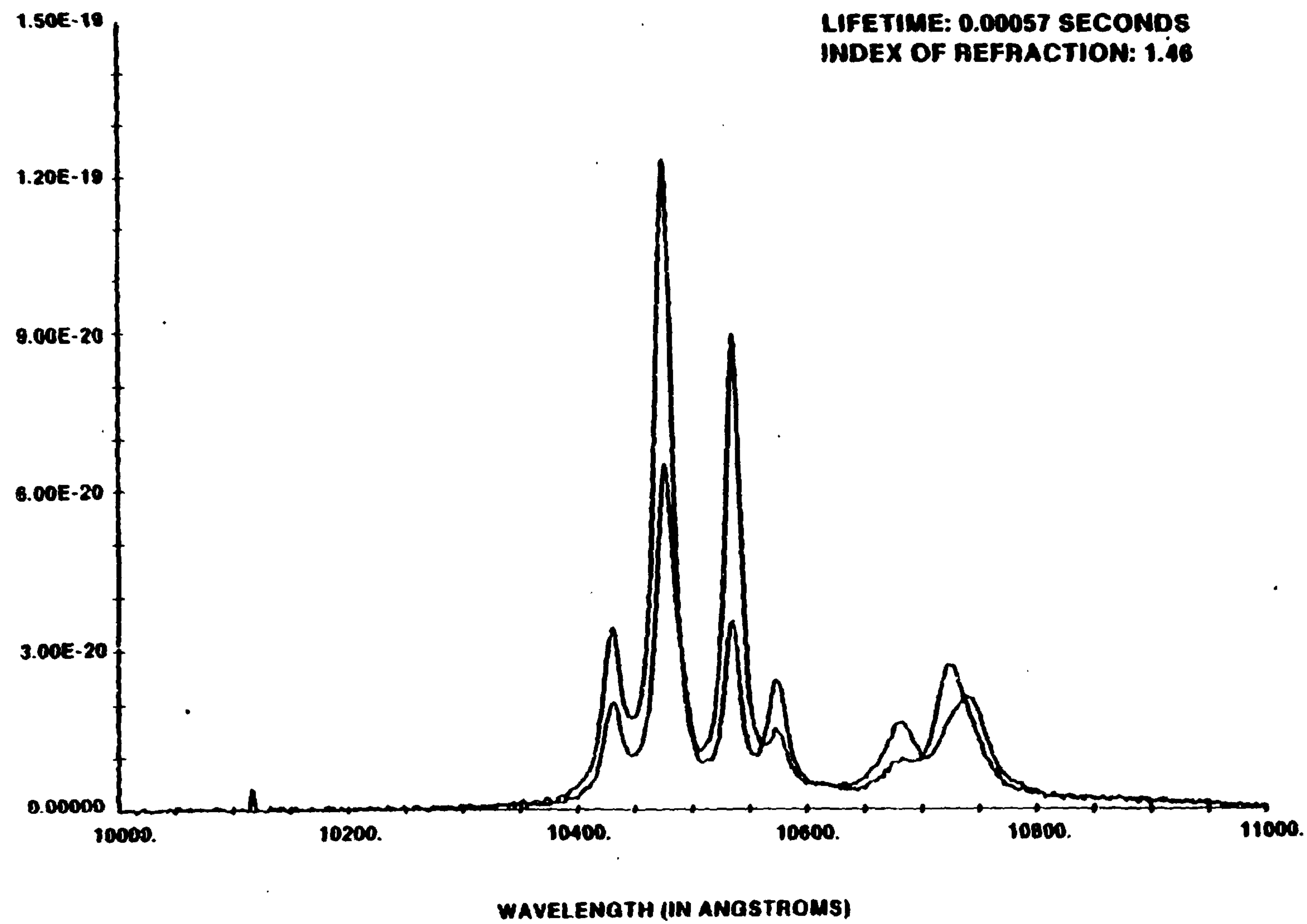


Figure 3.4a Stimulated emission cross section of Nd:YLF around 1.05 μm

(Ref. Sanders Assoc. Navy Blue, Program Review, March 12, 1985)

PI SPECTRUM, SIGMA SPECTRUM

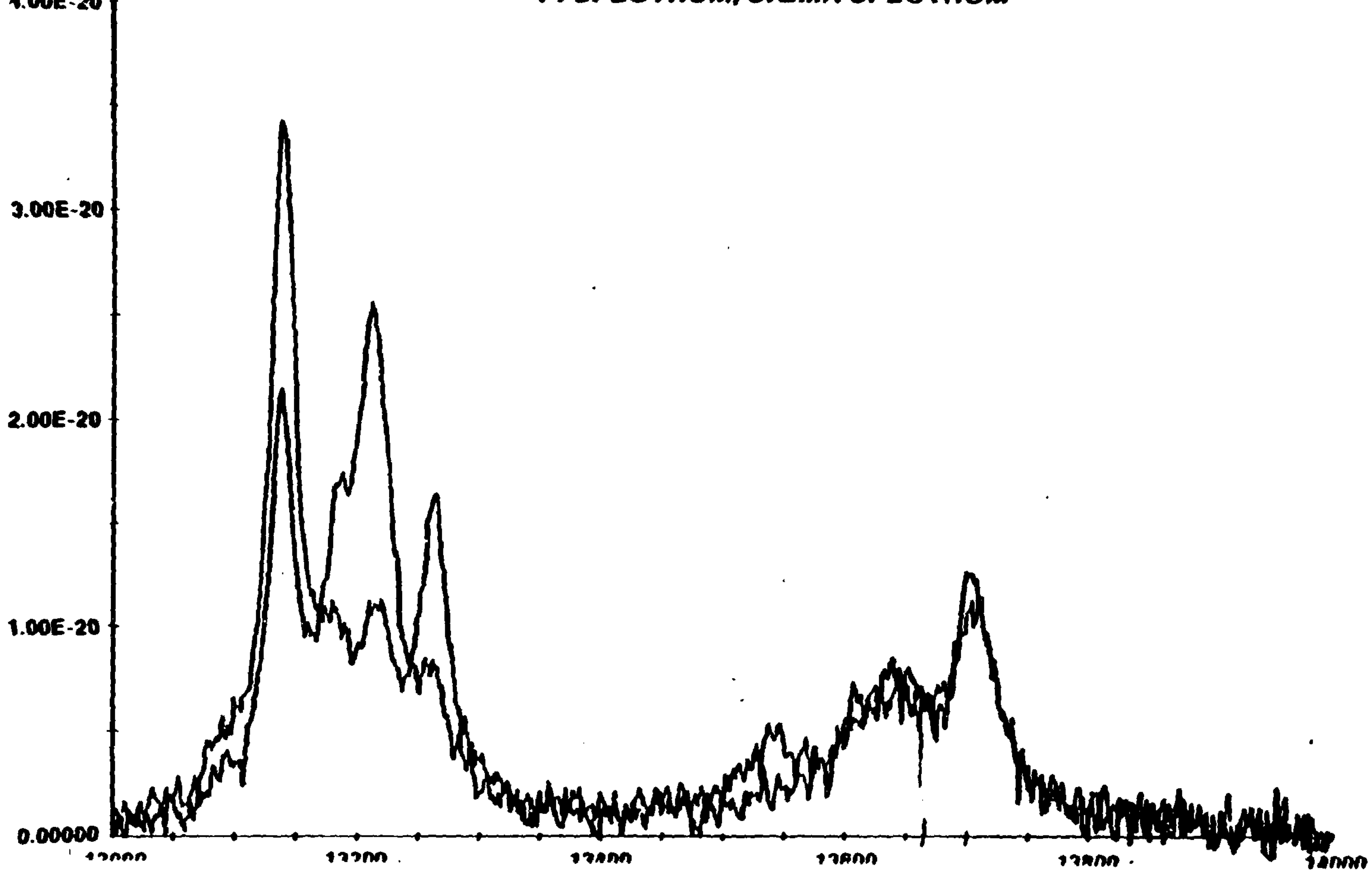

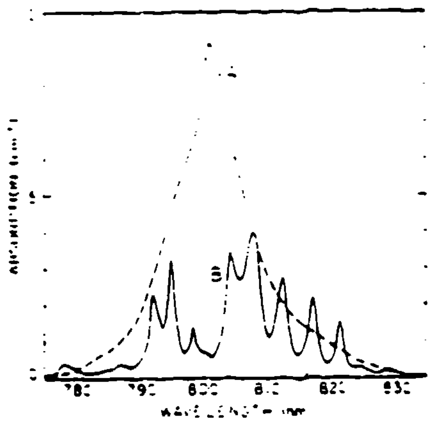

Figure 3.5 Absorption coefficient in LHG-8 3% Nd(A) and Nd:YAG(b)
(Kozlovsky et al., CLEO Conf. 1986, Paper WG4, P. 169 Technical Digest)

Diode pumping with a high-power multistripe diode laser showed a threshol the Nd:glass oscillator of 16 mW absorbed power and a slope efficiency of percent.

### 3.1.4 Ho:ErTmYAG

A holmium doped host has several interesting properties. The laser provides a different wavelength than those achievable with the Nd and the fluorescence lifetime is very long, on the order of 10 msec, which is ide time as far as pumping with diodes is concerned. Unfortunately Ho:ErTmYA to be cooled to liquid nitrogen temperature for laser action to occur. Researchers from NRC have recently demonstrated a diode array pumped holm laser.

Laser action was observed on the trivalent holmium $^5I_7$ to $^5I_8$, 2.1 $\mu$ transition. Laser action was achieved with a 10 mm length YAG rod sensit with 60 percent Er and 3 percent Tm in addition to the 2 percent Ho activ concentration. A 2.1 $\mu$m high reflectance coating transmitting at 785 nm placed on the flat surface and a 99.5 percent reflector at 2.0-2.1 $\mu$m was coated onto the curved surface of the rod. The sample was cooled to 77K end pumped with a 100 mW cw laser diode array (Figure 3-6). The temperat of the diode was adjusted so that the diode wavelength was centered at 785.5 nm.

The YAG resonator which is formed by the coated laser rod ends had a fundamental spatial mode beam waist diameter of 115 $\mu$m. The lasing thres occurred at 4.0 mW of incident pump power. With the diode operating at 1 a total of 34 mW was delivered to the sample. At this pump power 5.6 mW emission was obtained at 2.1 $\mu$m.

The gain of the $Ho^{3+}$ transition from $^5I_7$ to $^5I_8$ at 2.1 $\mu$m is high, a significantly enhanced by energy transfer from $Er^{3+}$ and $Tm^{3+}$.

The holmium laser holds the prospect of room temperature operation. Duczynski et al[7] reported on efficient energy transfer from Cr -> Tm with subsequent transfer of Tm -> Ho.

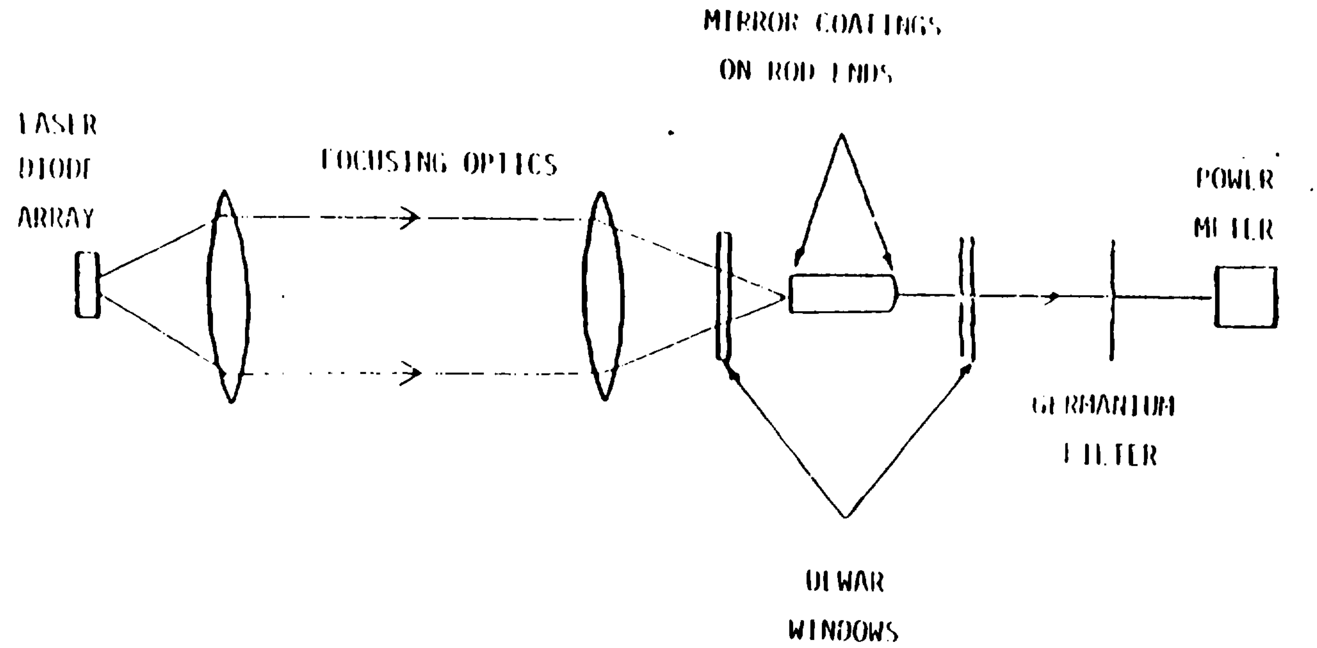


Figure 3.6 Schematic diagram of laser pumped Ho:YAG laser with end pumped geometry

Due to the broadband emission of $Cr^{3+}$, the sensitizer effect is not or restricted to $Nd^{3+}$; for example $Tm^{3+}$ can be pumped via $Cr^{3+}$ with a quantum efficiency near unity.

The excellent overlap between the $Cr^{3+}(^4Ti_2 \rightarrow {}^4A_2)$ emission and the $Tm^{3+}(^3H_6 \rightarrow {}^3F_4)$ absorption yields an efficient resonant Cr-Tm transfer system. At high $Tm^{3+}$ concentrations ($8 \times 10^{20} cm^{-3}$) the $Tm^{3+}$ ion converts energy down to the IR region with a quantum efficiency of nearly 2. The reason for this is the cross relaxation process $Tm^{3+}$ ($^3F_4 \rightarrow {}^3H_4$), $Tm^{3+}(^3H_{6}$ $^3H_4$) between adjacent ions.

Cr, Tm sensitized garnets were employed in these experiments, which demonstrated 2 $\mu$m cw laser action at room temperature.

Yttrium-scandium-gallium garnet (YSGG) and yttrium-scandium-aluminum garnet (YSAG) have been doped with $Cr^{3+}$($2.5 \times 10^{20} cm^{-3}$), $Tm^{3+}$ ($8 \times 10^{20} cm^{-3}$ and $Ho^{3+}$ ($5 \times 10^{19} cm^{-3}$), Scandium was chosen to create the low crystal fie strength for $Cr^{3+}$. Yttrium matches well for the ionic radii of $Tm^{3+}$ and H

The crystals were placed into a concentric cavity formed by two 5-cm radius mirrors having reflectivities of 98 percent at 2.08 $\mu$m. The crysta were pumped longitudinally with a krypton laser beam at 647.1 nm. For bot crystals Cr, Tm, Ho:YSGG and Cr, Tm, Ho:YSAG true cw operation was obtaine

Threshold was about 25 mW of absorbed pump power and the power slope efficiency is 13 percent. Since the lifetime of the upper $Ho^{3+}$ of the upp $Ho^{3+}$ laser state $^5I_7$ is approximately 10 ms, diode pumping should be possi

Unfortunately we did not have a detailed absorption spectrum to ascer that the absorption bands are in the wavelength regime suitable for diode pumping. Since the absorption spectrum will be dominated by $Cr^{3+}$, we can obtain a rough estimate from the data presented in Figure 3-7. It shows t transmission spectrum of $Cr^{3+}$:GdScGa garnet. From these data follows that pump wavelength would have to be rather short for GaAlAs, namely in the

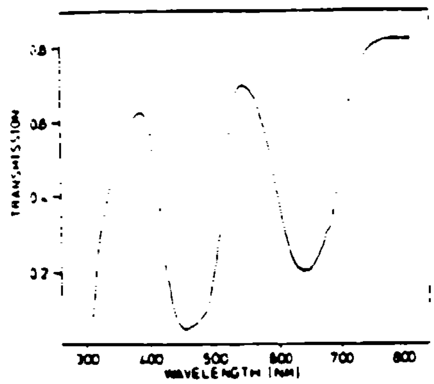


Figure 3.7 Transmission spectrum of the $Cr^{3+}$:GdScGa-garnet laser rod (l=7 mm)

neighborhood of 700 to 750 nm. Even at these wavelength absorption is not very strong, therefore only endpumped configurations with a long absorptic path are feasible.

## 3.2 POTENTIAL NEW MATERIALS

There are continuing efforts to find other laser materials which woul retain the advantages of Nd:YAG as to performance without showing some of disadvantages for diode pumping, such as a short upper state lifetime and weak and relatively narrow absorption line around 800 nm.

The requirements of the laser material employed for laser diode pump is somewhat different than with flashlamp excitation: First, the fluoresc lifetime of the upper laser level should be long in order to integrate the limited peak power from the laser diode.

Second, the laser material should have a strong absorption line betwe 780 and 900 nm, which is the emission range for GaAs diodes.

It will be at least five to ten years, before powerful laser diode a will become available at other wavelengths. Also, doubling of the GaAlAs diode output with KTP or organic nonlinear materials for the purpose of pumping solid state lasers is not practical either at the present time.

Third, in contrast to flashlamp pumped systems, the absorption band r only be a few hundred angstroms wide for diode pumped systems. Actually, line that wide would permit diode operation over a wide temperature range However, this would be totally inadequate for absorption of blackbody radiation.

In addition to finding materials with better properties than Nd:YAG, there is, of course, the desire to find materials which are not necessari better than Nd:YAG, but provide laser emission at different wavelengths.

The transfer lasers, dual-doped with chromium on the one hand and thulium, neodymium or holmium on the other, represent efforts to maximize pumping efficiency for flashlamp pumped lasers. Similar efforts could lead to a material optimized for laser diode pumping. Also it is our hope, that laser materials will be rediscovered which have been previously discarded because the pump bands were either too narrow or did not match flashlamp spectral outputs. As far as currently known candidates are concerned, the already mentioned Nd:YLF is in our opinion an excellent alternative which may even surpass Nd:YAD. Other promising materials which will be described here included Nd:NaYf, Ho:YLF, Nd:LuLAGG, and Nd:YALO.

### 3.2.1 Nd:NaYF

A potential candidate for laser diode pumping is $Nd^{3+}:Na_{0.4}Y_{0.6}F_{2.2}$ studied recently by Jenssen et al[8] at MIT. The crystal has an upper state lifetime of 900 $\mu$sec. In addition, the emission is relatively broad and the laser emission can therefore be tuned both in the 1.05 $\mu$m and the 1.30 $\mu$m regions. Laser action has previously been reported in this crystal by Kaminskii et al.[9]

Figure 3-8 shows the normalized emission spectrum of this material. The $^4F_{3/2} \rightarrow {}^4I_{11/2}$ transitions are broadened to a band between 1.035 $\mu$m and 1.075 $\mu$m. The $^4F_{3/2} \rightarrow {}^4I_{13/2}$ transition forms a band between 1.30 $\mu$m and 1.38 $\mu$m. These relatively broad emission bands indicate that the laser emissions may be tunable over a reasonably wide range.

The fluorescence lifetime of the $^4F_{3/2}$ level in this material is about 900 $\mu$s, which is considerably longer than in YAG (230 $\mu$s) and $LiYF_4$ (440 $\mu$sec). Thus, this host material is preferred in applications requiring high energy storage.

Room temperature cw laser emission in the 1.05 $\mu$m wavelength region was obtained by pumping with an argon laser (514.4 nm line). The pumped volume of the crystal was approximately 160 $\mu$m in diameter and 8 mm in length in a quasi concentric resonator of 20 cm length. (The absorption coefficient at the pump

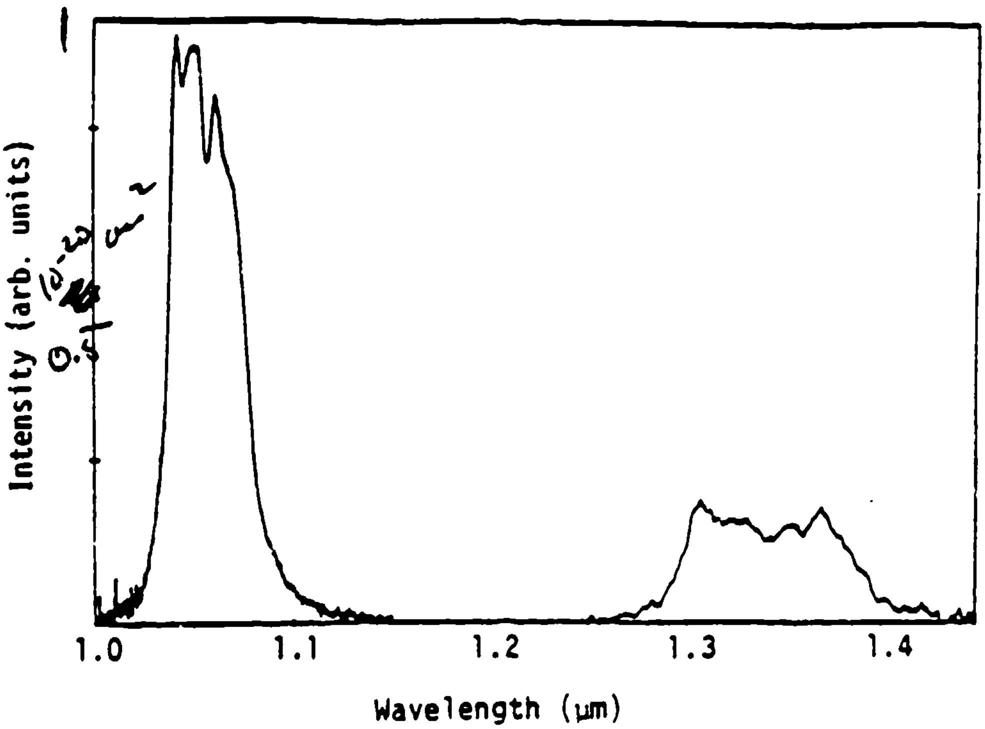


Figure 3.8 Emission spectrum of Nd: $Na_{0.4}Y_{0.6}F_{2.2}$.
Excitation wavelength is 514.5nm.
(Ref. M. Chou et al, Proceedings Tunable Solid State Zig Zag, Oregon, June 4-6, 1986, P. 158)

wavelength is 0.15 $cm^{-1}$). The output power in this free running mode with no tuning element is plotted in Figure 3-9 as a function of absorbed pump power.

Only a closer examination of the detailed spectroscopic data showing the Nd absorption line around 800 nm, and data on the stimulated emission cross-section, quantum efficiency etc., will reveal the full potential of this material.

### 3.2.2 Nd:LNA

The discovery of laser emission in hexagonal lanthanum neodymium hexa-aluminate ($La_{1-x}Nd_xMgAl_{11}O_{19}$) by a French group[10] has generated considerable interest for this material as a new, high power solid state laser.

Among the advantages of LNA is the ability to achieve a high neodymium content more than six time greater than Nd in YAG (7 x $10^{20}$ ions $cm^{-3}$) without severe concentration quenching of the fluorescence of strong segregation of the doping ion along the laser rod.

The earlier laser work demonstrated that an LNA laser has an efficiency and threshold comparable to Nd:YAG. The broad fluorescence spectrum from the $^4F_{3/2} \rightarrow {}^4I_{11/2}$ transitions of the Nd in LNA suggests the possibility of obtaining efficient CW tunable emission over a substantial wavelength range in a region of the spectrum that is generally devoid of tunable sources.

The fluorescence spectrum of Nd in LNA is shown in Figure 3-10a.

The fluorescence shows two broad, principal peaks centered at 1054 and 1082 nm. The full widths at half height of the two peaks are 44 and 74 Å, respectively. For the purposes of comparison, the fluorescence spectrum obtained under identical conditions from Nd in YAG is shown in Figure 3-10b. Fluorescence widths in YAG are typically 6Å. The broad width of the LNA curve, as compared to the YAG one, results from the fact that there are three different fluorescing sites in the LNA lattice, each of them is submitted to a

(Ref. M. Chou et al,
Proceedings Tunable
Solid State Lazers
Zig Zag, Oregon,
June 4-6, 1986, P. 158)

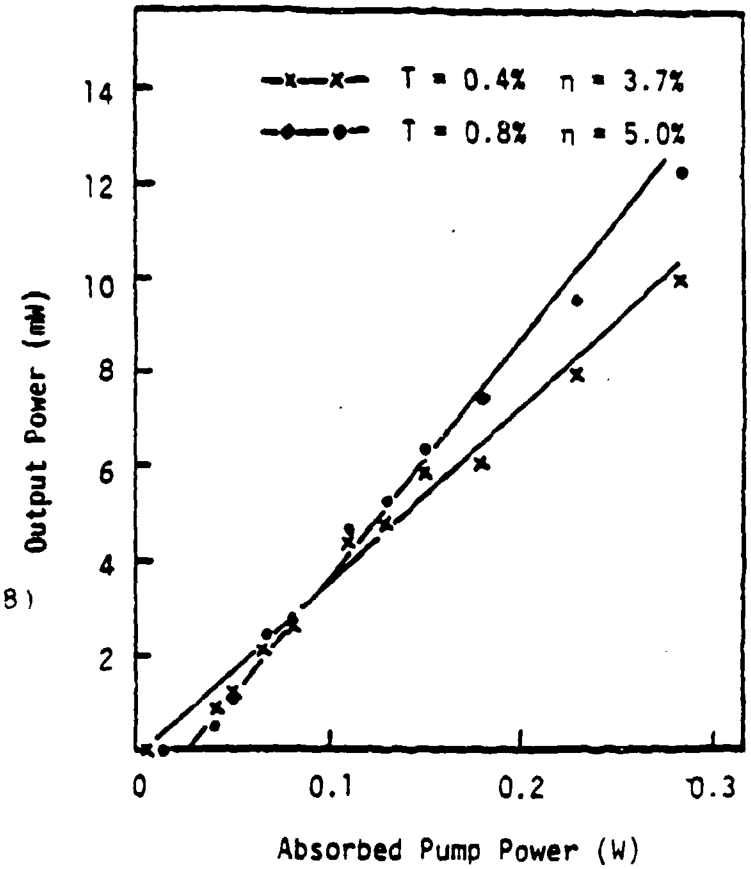


Figure 3.9 Output power as a function of absorbed pump power. T is the output mirror transmissivity, and n is the slope efficiency.

-3.17-

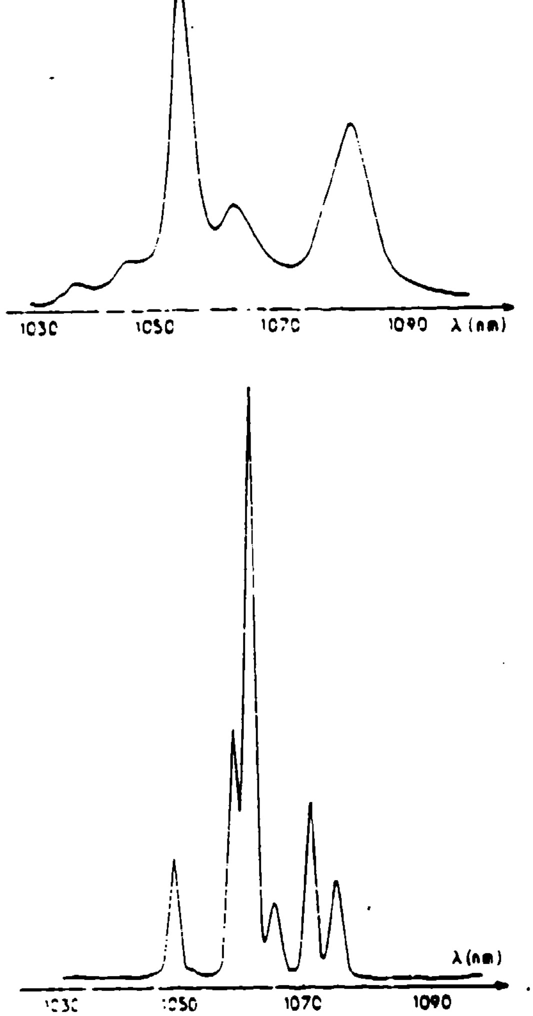


Figure 3.10(a) Fluorescence spectra of Nd in LNA (above) and YAG (below) excited at 752 nm.
(From Ref. 11)

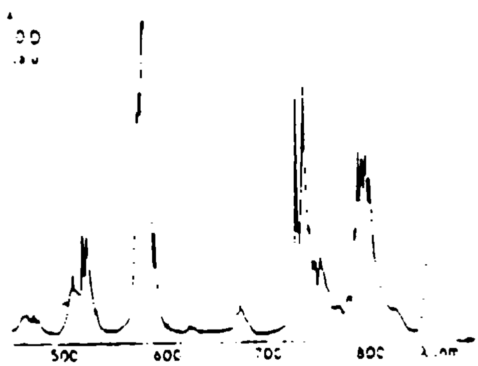


Figure 2.10(b)
Unpolarized absorption spectrum of LNA

(From Ref.

slightly different crystallographic field due to the different ion enviro ment. The relative widths of the two sets of fluorescence data illustrat wider tuning range one might expect from the Nd in LNA as compared to YAG

Lejus et al[11] have studied the laser performance of several LNA crys of 0.5 $\mu m$ diameter and AR coated on their two parallel, polished faces. samples were pumped with a Kr laser at 752 nm. About 0.4 W of output wer obtained for 1.9W input as shown in Figure 3-11. With very careful align 500 mW was achieved which corresponds to a conversion efficiency of 26 pe for the power or to a quantum efficiency of 36 percent. Tuning curves fo are shown in Figure 3-12.

LNA appears to be an excellent CW laser crystal with an efficiency comparable to that YAG when pumped by another laser. The large conversic efficiency (26 percent) with IR pumping in conjunction with its rather br tuning range in the 1 $\mu m$ region makes it an attractive material for laser diode pumping. The present results with IR pumping from a Kr laser are encouraging in that respect.

The optical properties of LaNdMg hexa-aluminate make it a promising material to be used as a diode pumped laser medium. Compared to Nd:YAG, has broader absorption bands around 800 nm, a longer fluorescent lifetime (320 $\mu$sec) higher Nd concentration, and about the same thermal conductivi and a gain which is about a factor 2 lower. Table 3-1 illustrates the re tionship between lifetime of the $^4F_{3/2}$ excited state and Nd concentratior

Clearly, for diode pumping the Nd: concentration cannot be higher 1 10 percent, otherwise the fluorescence lifetime becomes too short.

### 3.2.3 Nd:YALO

$YAlO_3$ and $Y_3Al_5O_{12}$ or YAG, are both derived from the $Y_2O_3$ - $Al_2O_3$ s the former is the 1:1 compound or perovskite phase, the latter is the 3:5 compound or garnet phase. Many of the physical properties of these two

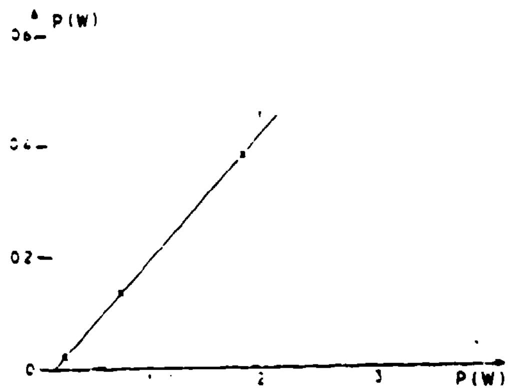


Figure 3.11

Output power of the LNA laser as a function of the Ar laser pump power.

(From Ref. 11)

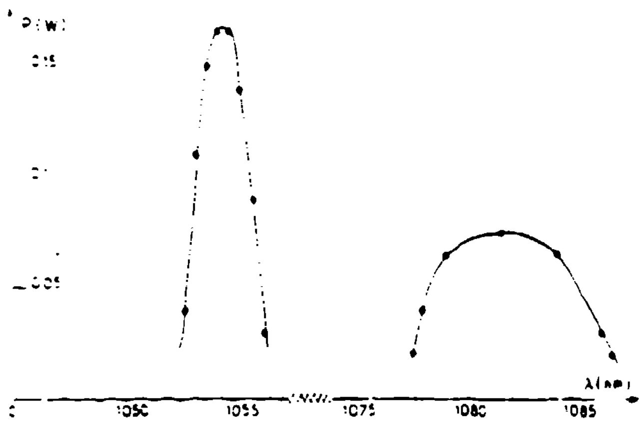


Figure 3.12

Turning curves of the LNA laser

(From Ref. 11)

Table 2.1 Fluorescence Lifetime as Function of Nd Concentration in $La_{1-x}Nd_xMgAl_{11}O_{19}$

| $x$ | 1 | 0.33 | 0.1 | 0.05 | 0.01 |
|---|---|---|---|---|---|
| $N$($10^{21}$ ions $cm^{-3}$) | 3.36 | 1.12 | 0.34 | 0.17 | 0.03 |
| $\tau/\mu s$ | 27 | 52 | 260 | 360 | 360 |

materials are similar. However, whereas YAG is cubic and optically isot
$YAlO_3$ is orthorhombic and anisoptropic.

In the early 1970's, the introduction of Nd:YALO was received with
enthusiasm because high average power in pulsed systems and high CW powe
output with thresholds and efficiencies comparable to YAG had been achie
Actually, Nd:$YAlO_3$ is the only solid state material other than Nd:YAG to
exhibit the high conductivity and hardness combined with low threshold
necessary to achieve high average power operation in the cw-pumped mode
room temperature.

Interest in this system was further motivated by the fact that the Perovskite structure results in an orthorhombic symmetry and consequentl yields polarized laser output. The YALO laser is then free from the depolarizing thermal birefringence which affects YAG performance when polarizing optics are inserted in the YAG cavity.

Late in 1970 large crystals of Nd:$YAlO_3$ with good optical quality be
commercially available. However, one difficulty that had prevented gene
acceptance for YALO as a substitute for YAG was the occurrence of discol
tion (browning) of the crystal after irradiation by flashlamps. This ef
was caused by crystal defects and was detrimental to an efficient excita
It could only be remedied by a careful heat treatment in a reducing
atmosphere.

Since crystals could not be grown that remained clear and transpare
after irradiation from pump radiation interest was eventually lost in th
material. Recently, however, W.C. Heraeus GmbH, West Germany, has been
to grow high optical quality YALO laser crystals in commercial quantitie
there is renewed interest in the material for applications in which a
polarized output is desirable. Since the discoloration in Nd:YALO is ca
by the UV content of the flashlamp, this effect does not show up in lase
diode pumped crystals.

One particularly interesting property of Nd:YALO is the fact, that due to its anisotropic properties, the gain and wavelength can be changed by selecting suitable orientations.

The laser properties of YALO are influenced by the optical anisotropy in two ways:

First, the emitted radiation is always linearly polarized in a direction depending on the rod orientation with respect to the crystal axes.

Second, the emission wave length depends on the rod orientation and on the polarization direction.

For example, a Nd-YALO rod cut along the a-axis, emits a wave length of 1.08 $\mu$ when the E-vector (polarization) is along the c-axis and at 1.065 $\mu$ for a b-axis polarization. A c-axis rod, on the other hand, always emits at 1.065 $\mu$ irrespective of the polarization direction of the radiation. The reason for this bahavior lies in the low symmetry of the crystal structure that leads to a complicated directional dependence of the gain in YAlO. This feature is an added advantage of YALO because it permits a tailoring of the gain and energy storage capabilities of the YALO to suit particular applications; e.g. Q-switching or cw-operation.

Massey et al[12] achieved up to 75 W of cw output linearly polarized in YALO about 15 years ago. They observed CW emission from two of the $^4F_{3/2}$-$^4F_{11/2}$ transitions (1.0645 and 1.0795 $\mu$m) and two of the $^4F_{3/2}$-$^4I_{11/2}$ transitions (1.3391 and 1.3411 $\mu$m). They also observed three additional $^4F_{3/2}$ - $^4I_{11/2}$ transitions (1.0729, 1.0909, and 1.0989 $\mu$m) when the system was flash-pumped with 20 J from a Kr flashlamp.

Recently Schearer et al[13] reported Cw laser emission from seven lines within the $^4F_{3/2}$-$^4I_{11/2}$ multiplet: 1.0645, 1.0729, 1.0795, 1.0845, 1.0909, 1.0921, and 1.0989 $\mu$m. Since Nd:YALO exhibits a fluorescence spectrum which is broader than Nd:YAP, they have also obtained some limited tuning for the 1.0795 and 1.0845 $\mu$m transitions.

The linearly polarized output of Nd:YALO, and the ırge number of la: lines which can be obtained, make Nd:YALO an interesting material for dio( pumped systems in military applications. One disadvantage of the materia compared to YAG is the shorter fluorescence lifetime. Figure 3-13 shows dependence of the lifetime with Nd concentration. Although $YAlO_3$ can be much higher with Nd compared to YAG, this property cannot be utilized to advantage in diode pumped systems because of fluorescence lifetime quench

### 3.2.4 Nd:LaLuGG

The co-doped garnet crystal $Gd_3(Se,Ga)_2Ga_3O_{12}$ or GSGG:Nd, Cr is the efficient flashlamp pumped solid state laser. The material is so efficie because of the wide absorption bands of $Cr^{3+}$ which overlap well with the emission of flashlamps, and the efficient transfer to $Nd^{3+}$ ions. The $Cr^{3}$ excitation in GSC? appears in the $^4T_2$ state, nonradiative transfer to $Nd^{3}$ ions can occur via the $^4T_2$-$^4A_2$ transition, which is spin allowed and has good spectral overlap with the $Nd^{3+}$ levels.

Rather than having broad absorption regions afforded by GSGG;NdCr, f laser diode pumping a stronger and wider absorption line around 800 nm is required. Both can be achieved in Nd:LaLuGG, or $(La,Lu)_3(Lu,Ga)_2$ $Ga_3O_{12}$. ionic radii of La and Lu are 1.05 Å and 0.86Å, respectively. Since they closely match the ionic radion of $Nd^{3+}$ which is 0.98Å, high doping levels be achieved. Huber et al[14] have grown LaLuGG with up to 3 percent Nd wit observing stray concentration quenching. Only at 10 percent $Nd^{3+}$ doping levels did quenching become a problem. Since Nd can substitute for Lu an the $Nd^{3+}$ ion will occupy different sites and experience different crystal fields. This leads to a broadening of the absorption line.

The relatively high doping level and broadened line around 800 nm ma this material a good choice for a diode pumped Nd laser. Preliminary investigation by Powell[15] confirms the broad absorption bands.

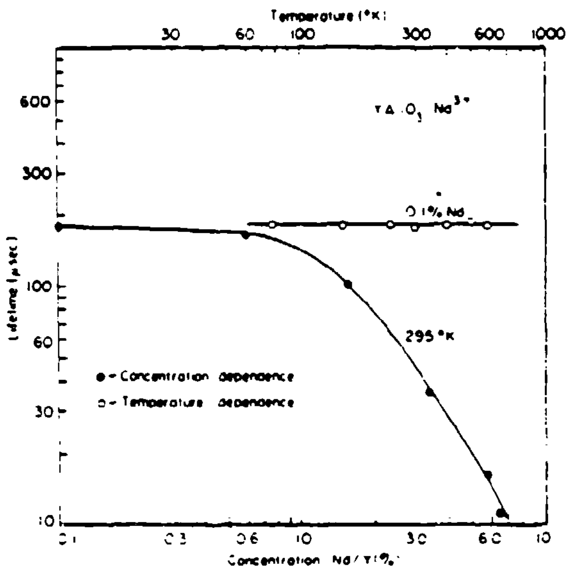


Figure 3.13 Temperature and concentration dependence of the Fluorescence lifetime of $YAlO_3:Nd^{3+}$.

### 3.2.5 Ho:YLF

The extraordinary long fluorescence lifetime of 12 msec for the $^5I_7$-$^5$ transition in multiple doped Ho:YLF ($Er^{3+}$, $Tm^{3+}$) make this material a gooc candidate for laser diode pumping. Unfortunately, we do not have at prese any spectral data on this material to provide further information.

## 3.3 UNSUITABLE LASER MATERIALS

In this section, a few materials will be discussed which are currentl the subject of great interest and activity due to a specific property such tunability, emission of an important wavelength, low manufacturing cost, t due to either a very short upper state lifetime, low gain, or absence of a proper absorption line do not seem to be likely candidates for diode pumpi In this category fall all Cr and Ti doped tunable lasers because their abs tion bands are at much shorter wavelength then can presently be achieved.

Materials we have been looking into more closely but which did not se promising include the following list:

### 3.3.1 Nd:BEL

Nd doped lanthanum beryllate ($Nd^{3+}:La_2Be_2O_5$) or Nd:BEL produced by Al Corporation, is receiving some attention as an intermediate gain solid sta laser medium in flashlamp pumped systems. Considerable development of thi material has recently taken place in the areas of crystal growth, spectros and materials characterization.

For BEL:Nd the lasing transitions in the one micron region occur from lowest level of the $^4F_{3/2}$ multiplet to the $^4I_{11/2}$ multiplet while in YAG:N the transition occurs from the highest level of the $^4F_{3/2}$ multiplet. Ther are two wavelengths for the laser transitions for BEL:Nd, 1.070 and 1.079

The stimulated emission cross-section is one-third that for Nd:YAG. fluorescence lifetime for Nd:BEL was found to be about 150 $\mu$sec at 1 perce Nd doping. At higher concentration the lifetime begins to decrease becau

concentration quenching. The lower gain combined with the much shorter lifetime do not seem to make this material particularly attractive compared to YAG for laser diode pumping.

### 3.3.2 Cr:SrAlF$_5$

Strontium Aluminum Fluoride is very actively pursued by LLNL for possible applications in submarine laser communications. In order to match the cesium absorption in the receiver, the laser emission has to be either 455.5 nm or 459.5 nm.

Cr:SrAlF$_5$ discoverd by Jenssen from IT is tunable from 825 to 1010 nm with a peak emission around 900 nm. Frequency doubling of either the 911 or 919 nm wavelength would meet the wavelength requirements for SLC. For diode pumping, the material poses two problems the upper level lifetime is only 95 $\mu$ sec long and the absorption around 800 nm is very low. Figure 3-14 shows the emission and absorption spectra of SrAlF$_5$ and Figure 3-15 shows the tunable output obtained from this material.

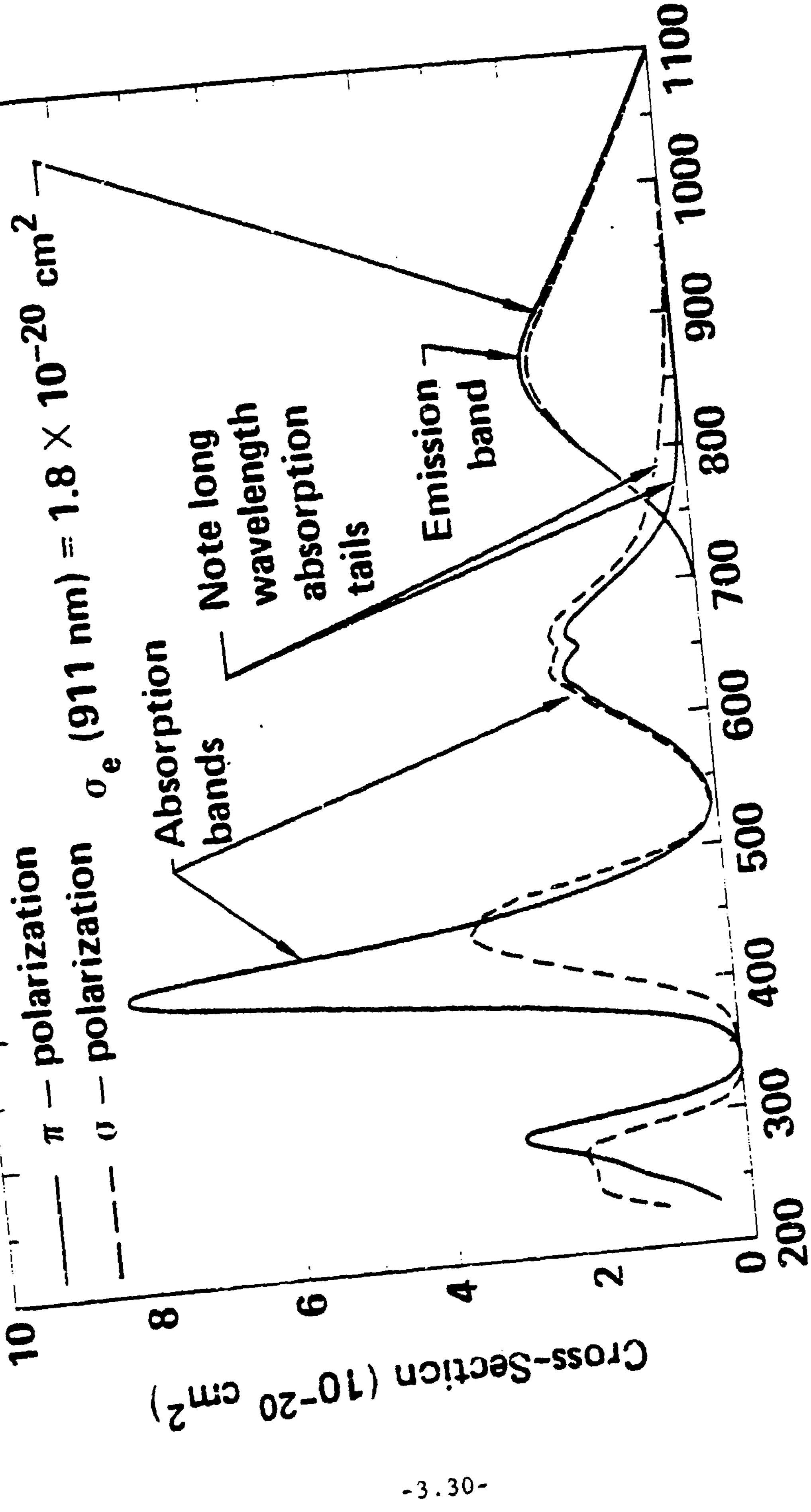
π — polarization
σ — polarization
$\sigma_e$ (911 nm) = 1.8 × $10^{-20}$ cm$^2$
Absorption bands
Note long wavelength absorption tails
Emission band
Cross-Section ($10^{-20}$ cm$^2$)
0
2
4
6
8
10
200
300
400
500
600
700
800
900
1000
1100

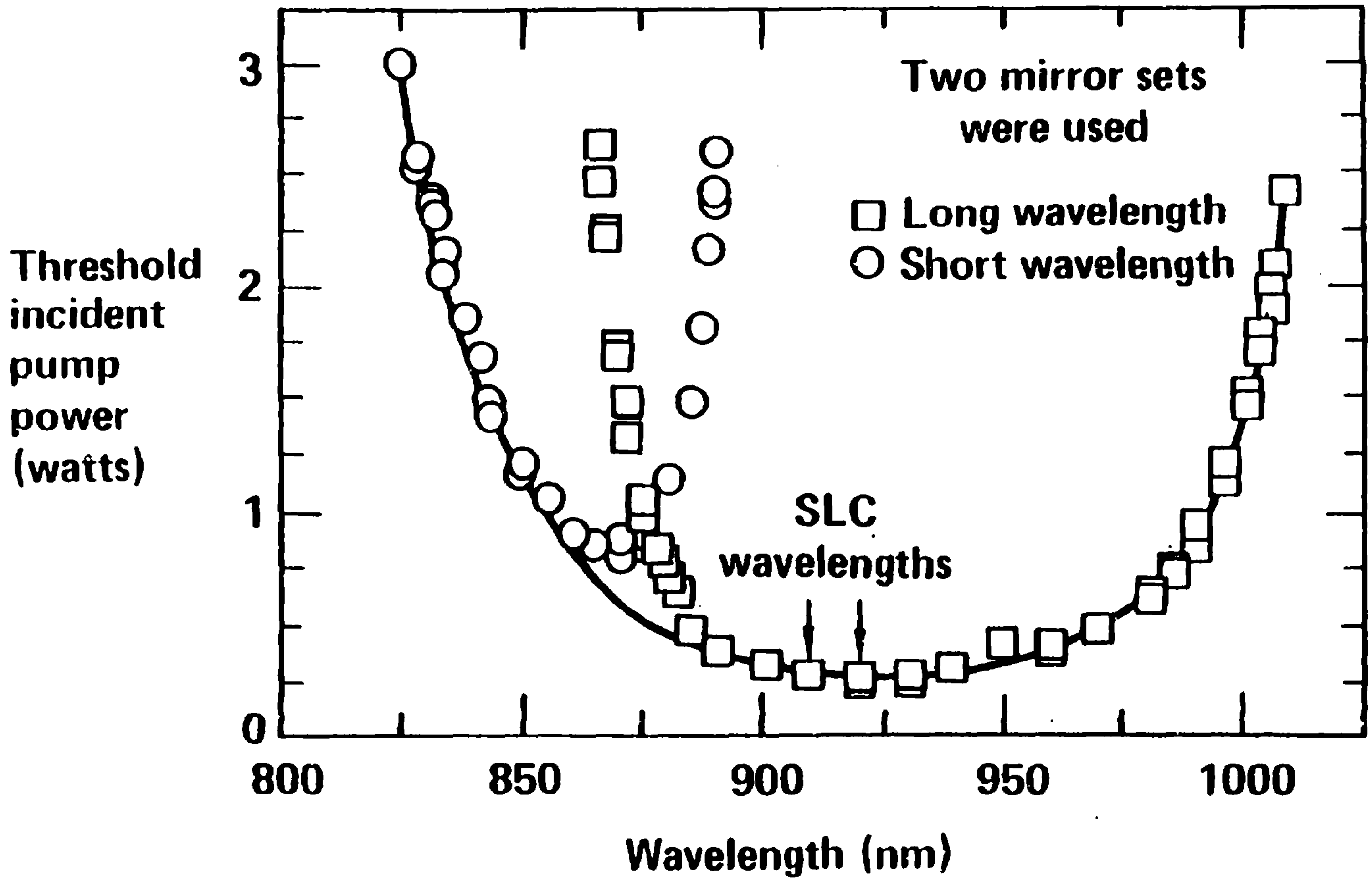


Figure 3.15 Turnability of the $SrAlF_5$:Cr laser
(Ref. Presentation of LLNL on Medium Average Power Solid-State Lasers Oct. 29, 1986)

## References


1. J.L. Nightingal, R.L. Byer, Optics Letter, July 1986, vol. 11, pg. 4

2. S.L. Sipes, Appl. Phys. Letters, 47, 74, 1985.

3. McDonnell Douglas Report N66001-83-C-0072, Final report 1983-1986, prepared for NOSC.

4. T.Y. Fan, G.J. Dixon, R.L. Byer, Optics Letters, Vol. 11, April 1986. 204.

5. W. Kozlovsky, T.Y. Fan, R.L. Byer, CLEO conf. 1986, Paper WG4, pg. 1 Technical Digest.

6. R. Allen, L. Esterovitz, L. Goldberg, J.F. Weller, CLEO 1986, Paper F pg. 390 Technical Digest.

7. E.W. Duczynski, P. Mitzscherlich, G. Huber, CLEO 1986, Paper FC2, pg. Technical Digest.

8. H. Chou, P. Albers, A. Cassanho, H.P. Jenssen, CLEO Conference, Techr Digest, Paper FB6.

9. A.A. Kaminsky, Laser Crystals, New York, Springer-Verlag, 1981.

10. A. Kahn, A.M. Lejus, M. Madsac, J. Thery, D. Vivien, J.C. Bernier, I Appl. Phys., Vol. 52, pg. 6864, 1981.

11. L. Schearer, M. Leduc, D. Vivien, A.M. Lejur, T. Thery, IEEE Quant. Electronics, QE-22, May 1986, pg. 713.

12. G.A. Massey, J.M. Yarborough, Appl. Phys. Letters, Vol. 18, June 197 pg. 576.

13. L Schearer, M. Leduc, IEEE Journal Quantum Electronics, Vol. QE-22, 1986, pg. 756.

14. G. Huber, Private Communication

15. R. Powell, Private Communication

# 4. CRYSTAL GEOMETRY AND DIODE ARRAY PUMP CONFIGURATION (Task 3)

In this chapter endpumping of a laser crystal, and sidepumping of a cylindrical rod and a zig-zag rectangular slab will be discussed.

## 4.1 ENDPUMPING OF A LASER CRYSTAL

In this case, a cylindrical laser rod is pumped through one of the end faces by a single diode diode array. This endpumping concept was the subject of considerable interest during the mid 1970's for use as transmitters for optical fiber communications.

A number of workers have built neodymium lasers end pumped with diodes. Light-emitting diodes have been used to end pump Nd:YAG fibers, superluminescent diodes have end pumped Nd:YAG rods and laser diodes have been used to end pump the stoichiometric neodymium compound $LiNdP_4O_{12}$ with a 1.5 percent electrical-to-optical slope efficiency. Only recently, however, have laser diodes of sufficient output power been available to fully exploit this highly efficient regime of operation.

In particular, Sipes[4.1] from Jet Propulsion Lab, and researchers at Stanford University[4.2] have reported high overall efficiencies with tightly focused end pump geometrics. Since the pump beam from the diode array is collinear with the optical resonator, the overlap between the pumped volume and the $TEM_{00}$ mode can be very good. Also the coupling efficiency into the rod is high and the absorption length can be as long as the crystal. Figure 4-1 shows the experimental set up used by Sipes.

A single Spectra Diode Labs Model SDL-2410-A GaAlAs laser diode array is employed, operating at approximately 200 mW cw output at 810 $\mu$m with approximately 20 percent electrical to optical efficiency. The dual lobed output is then collimated and focused into a 1 cm long x .5 cm diameter 1 percent Nd:YAG sample. The resonator configuration is plano-concave, with the pumped end of the Nd:YAG rod being coated for high reflection at 1.06$\mu$m and output coupler being a 5 cm radius of curvature with a reflectivity at 1.06 $\mu$m of 95 percent.

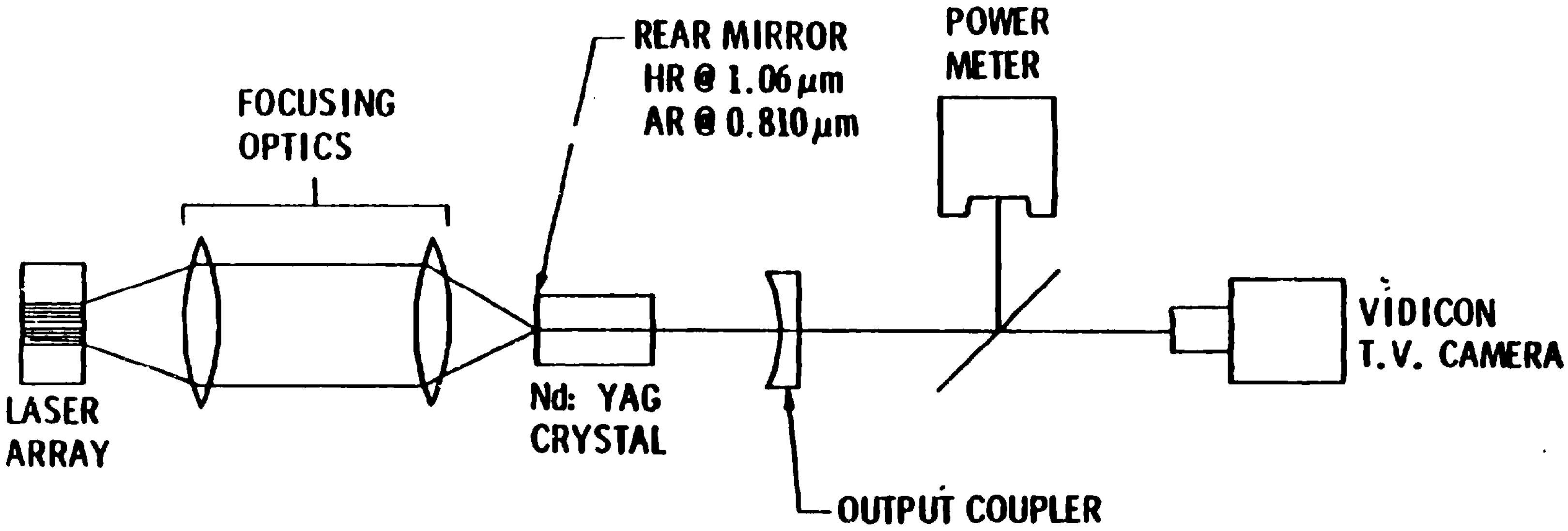


Figure 4.1 Endpumped laser system designed by Sipes (4.1).

The end pump geometry has a number of advantages compared to side pumping. For example, the absorption length can be made as long as necessary to absorb practically all the pump light. Also the pump light can be focused to provide the intensities needed for efficient lasing and the beams can be adjusted to overlap for optimum mode matching.

Figure 4-2 shows input electrical power versus 1.06 $\mu$m output power for the configuration illustrated in Figure 4-1. For approximately 1 watt of electrical input power, 70 mW of Nd:YAG output is measured. This corresponds to a measured laser diode efficiency of approximately 20 percent and an optical conversion efficiency of approximately 35 percent.

Endpumping of a miniature Nd:YAG laser with laser diode arrays is an attractive means of obtaining efficient cw lasers. However, at present, the end pump scheme is useful only for low power lasers because the pump area is very small. In order to achieve a somewhat higher output power, two sources can be polarization coupled together to double the pump power available. Thus by polarization coupling and double ended pumping, 800 mW of pump power and possibly 400 mW of 1.06 $\mu$m power are achievable.

Endpumping from both sides, and using polarization coupling schemes does increase the power output by a factor 2 to 4.

However, should monolithic or stacked 2-D arrays become available at an affordable price the output from a large array could be focused with a condensor arrangement into the end face of a laser rod. Because of the large absorption length in the crystal, spectral output uniformity from the array, and wavelength control is not very critical.

Particularly ideal would be phased arrays. It is conceivable that several hundred watts of average power can be coupled into the end of a 5 or 7 mm Nd:YAG crystal. Compared to using the output from the phased array directly, a solid state laser can be Q-switched, thus high peak powers can be achieved. Figure 4-3 shows the schematics of a high average power endpumped laser.

Figure 4.2 Output vs. input of endpumped laser. (From D.L. Sipes, Appl. Phys. Lett. 47, July 1985, P. 74)

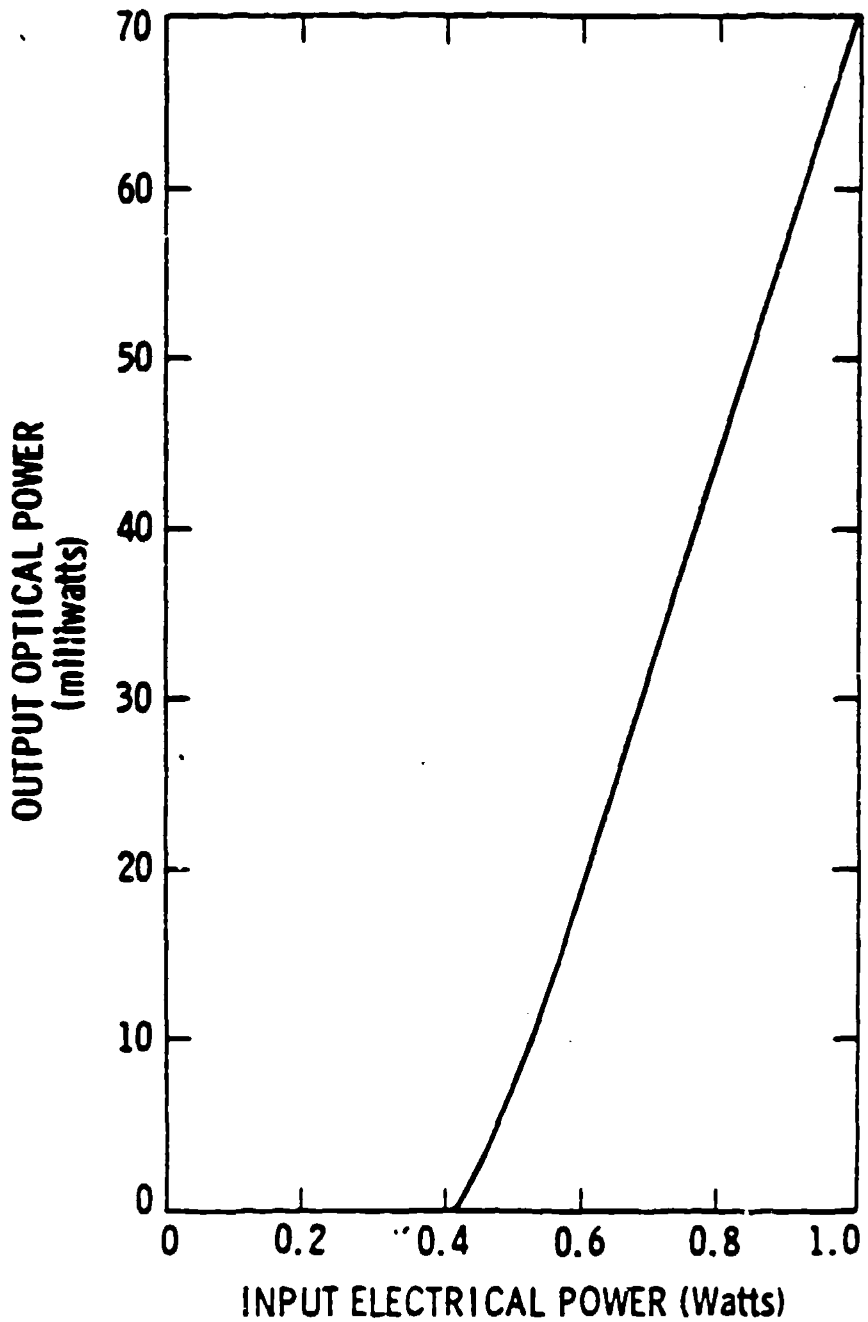

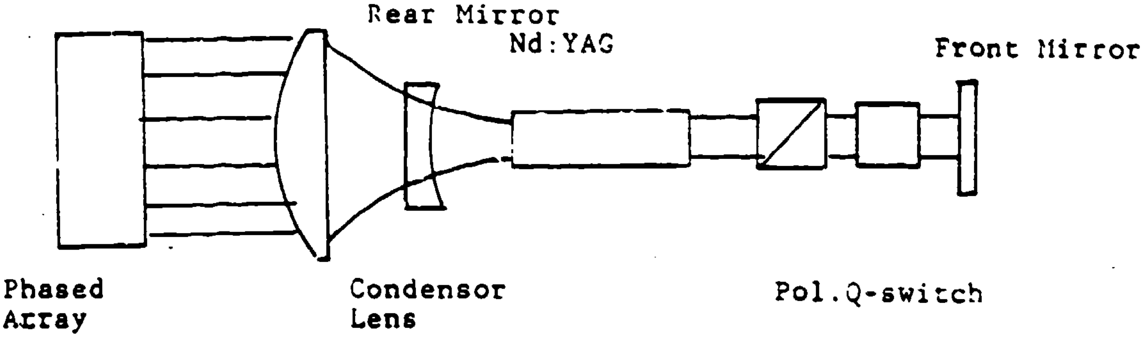


Figure 4.3 Schematic of a high power endpumped laser utilizing coherent arrays.

## 4.2 SIDEPUMPING OF A CYLINDRICAL CRYSTAL

### 4.2.1 Pumping Geometry

Side pumping of a laser rod can be realized by surrounding it with l diode arrays conveniently distributed around the rod to produce the desir pumping profile. There are three practical approaches to couple the radi emitted by the diode lasers to the rod: a) direct coupling; b) with opti between source and absorber; c) fiberoptics coupling. The direct couplir option does not allow for variations other than the placement of the dioc lasers around the rod. Fiberoptics coupling is very impractical for a lar number of diode lasers. Optical coupling can be achieved by using imagir optics such as lenses or elliptical and parabolic mirrors, or by non-imag optics such as reflective or refractive flux concentrators.

Simple considerations regarding the optimum pumping configuration, g high marks to the approach of using intermediate refractive optics. This because, in this case, arrays can be spaced far apart, reducing packaging cooling constraints. Furthermore, by using lenses, the pump distributior be peaked at the center of the rod allowing for a better match with resor modes. In contrast, direct pumping yields a far less optimum pump distr tion and requires dense packaging. Fiberoptics coupling is very lossy, similarly to direct coupling does not allow for an optimum pump distribu although it shares with the optical coupling approach the advantage of relaxing packaging and cooling constraints. Its practical implementatior however, far more complex than for the latter. Figure 4-4 depicts a poss design for the implementation of rod side pumping using linear diode lase arrays and cylindrical lenses.

For the evaluation of the individual merits of these different optic is important to determine how the pumping power is distributed across the and how efficiently the radiation emitted by the diode laser arrays is absorbed in the rod. The determination of these performance characteris requires the use of ray-tracing techniques. For this purpose a computer called CRADLE (computation of rod absorption of diode laser emission) was designed and implemented.

DIODE LASER PUMPED ROD LASER HEAD

Figure 4.4

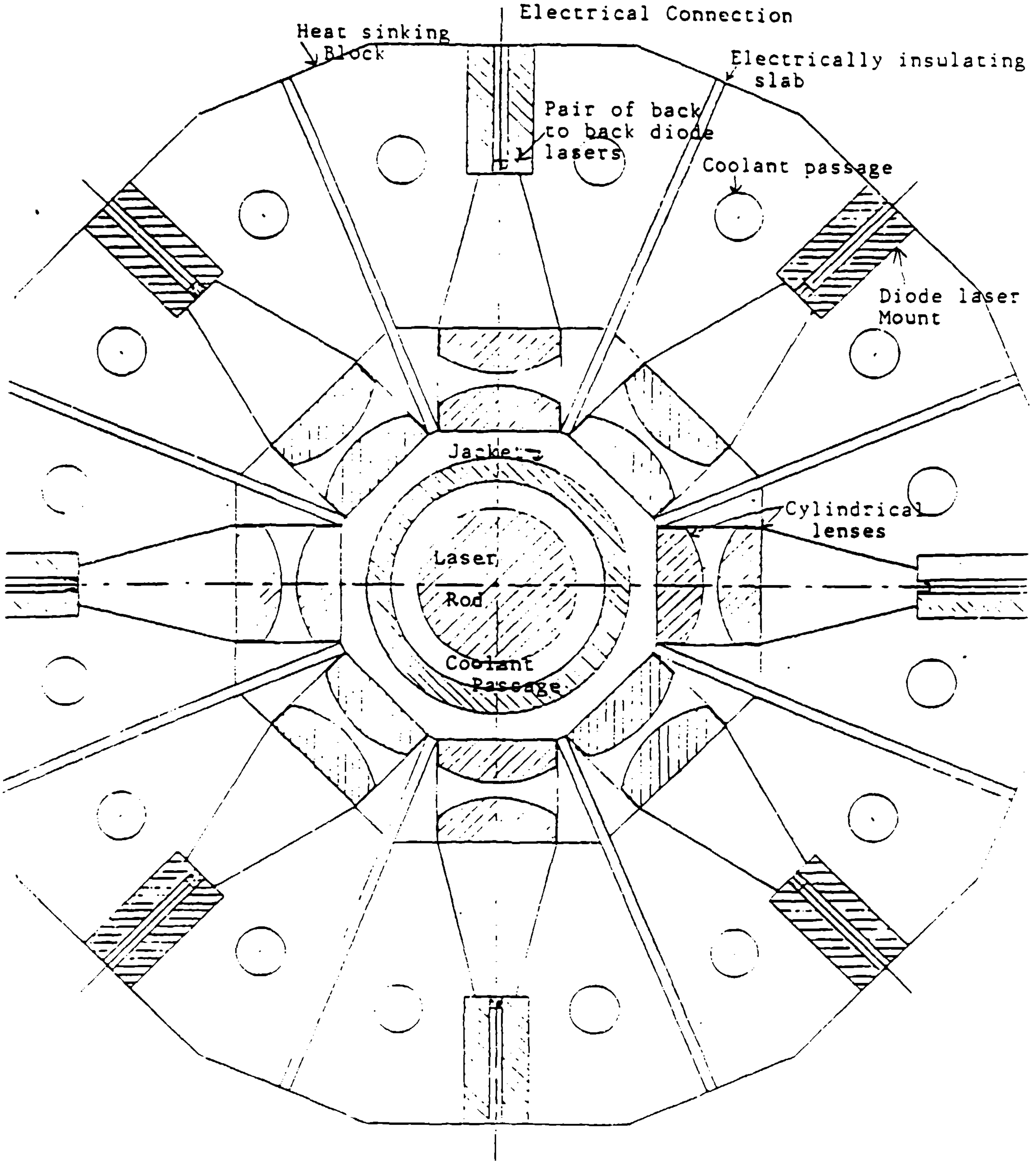

With the exception of the cases involving reflective elements and fiber-optics, all the cases can be analyzed with this code. Details on the algorithm used for this code are given in the following sections. A descr tion of the software configuration and the program listing is given in Appendix A.

### 4.2.2 Ray Trace Analysis

The pumping rate at any particular position inside the rod is directl related to the amount of the amount of pump radiation absorption at that particular point. Certainly the absorption coefficient changes with the change in population of the levels interconnected by the particular pump transition and therefore the time evolution of the absorption should be considered. However, this change in population is only important in three level sysems which will not be considered here. Because the purpose of th analysis will be to determine the relative merits of the different pumping geometries, the pump-rate density will be considered to be directly propor tional to the local pump radiation absorption and therefore only this parameter will be calculated.

The local density $A_D(\overline{r})$ of pump radiation absorption inside the laser is given by the following expression:

$$A_D(\overline{r}) = \sum_{i=1}^{N_a} \iiiint \gamma\,(\lambda) \exp\left[-\,\gamma(\lambda) S(\overline{r}, \overline{ri}, \alpha i)\right]$$
$$\times\ Ii\ (\overline{ri}, \alpha i, \lambda\ , \lambda\ d)\ F(\lambda d, \lambda\, c, \sigma\lambda)$$
$$\times\ d\overline{ri}\ \ d\,\alpha i\ \ d\,\lambda d\,\lambda\, c$$

where $A_D(\overline{r})$ is measured in $W/cm^3$; $N_a$ is the number of arrays around the ro and $r_i$ specify a particular position inside the rod and on the $i^{th}$ linear array respectively, and the other quantities are defined as follows:

$I(r_i, \alpha i, \lambda, \lambda d)$: Diode laser array spectral irradiance in $w/\mu m/rad$. $\lambda_d$ the center wavelength at which the diode laser stripe located at position $r_i$ operates, and $\alpha_i$ specifies a particular emission direction.

$F(\lambda d, \lambda c, \sigma_\lambda)$: Statistical distribution of diode laser center wavelengths ($\lambda d$), centered at the wavelength and having a standard deviation $\sigma_\lambda$. Dimension: $\mu m^{-1}$

$S(r, r_i, \alpha_i)$: Optical path as defined in Figure 4-5 Dimension: cm.

$\gamma(\lambda)$: Spectral absorption coefficient, $cm^{-1}$

The angular distribution of the radiation produced by most of the high power linear arrays is very narrow in the direction parallel to the array. On the other hand, the characteristics of these arrays are very uniform along the length, and a good cavity design will most likely incorporate end mirrors to reduce end effects. Consequently, in order to simplify the analysis, only the two dimensions perpendicular to the rod axis (and also perpendicular to the direction of the array length) will be considered.

Another characteristic of state-of-the-art diode laser arrays is the very narrow output spectral width: typically less than one nanometer. Therefore a further simplification will be to ignore the integral over $\lambda$ in the above expression and substitute $\lambda_d$ for it when evaluating $\gamma(\lambda)$. A further simplification that will be made is to consider the irradiance I to be independent of position and diode laser emission wavelength.

With these simplifications the above expression reduces to:

$$A_D(r,w) = \sum_{x=1}^{N_D} \int_{\lambda 1}^{\lambda_2} \int_{-\alpha a/2}^{\alpha_{a/2}} \left[\gamma(\lambda d) \exp \quad \gamma(\lambda d)\, S(r,w;\alpha i,i)\right]$$
$$\times\ I\,(\alpha i)\, F\,(\lambda d, \lambda c, \sigma_\lambda)\, d\alpha i\, d\lambda d$$

where r is the radial coordinate and w is the aximuth angle about rod axis. $\alpha_a$ is the angular aperture of the optical system and $\lambda_1$ and $\lambda_2$ specify the spectral range of interest, typically and internal centered on $\lambda c$ with a width of about $4\sigma_\lambda$. For practical purposes the distribution $F(\lambda d, \lambda c, \sigma_\lambda)$ will be defined as Gaussian.

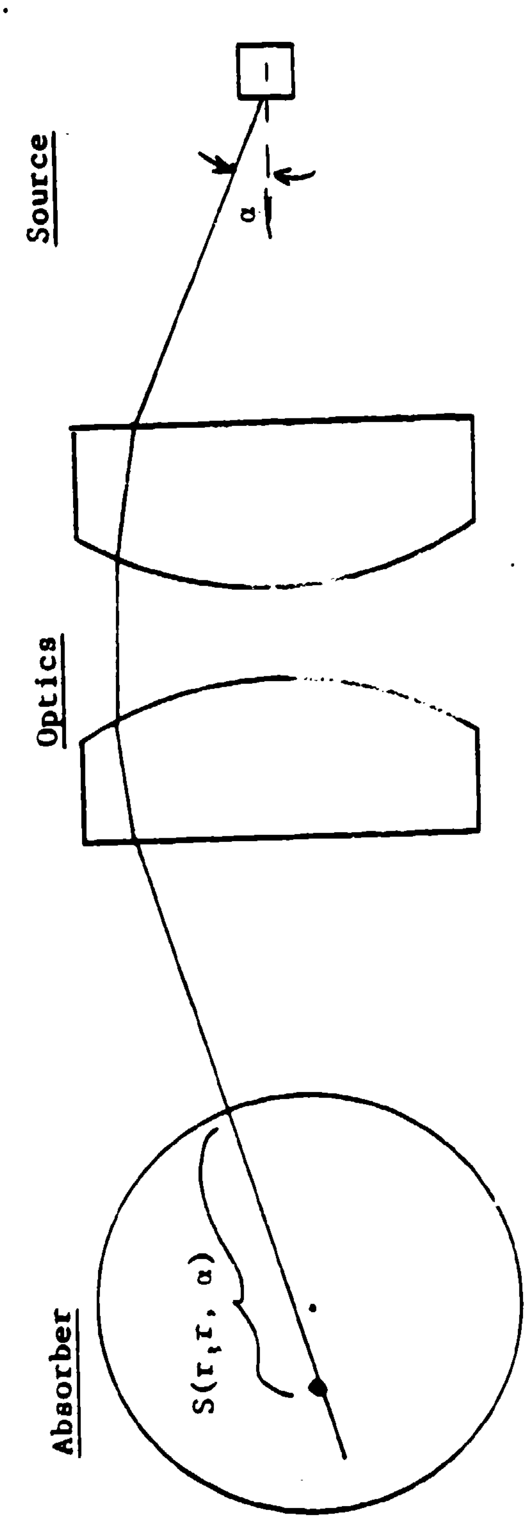
Source
α
Optics
Absorber
S(r,r, α)

$$F(\lambda d, \lambda c, \sigma_\lambda) = \frac{1}{\sqrt{2\pi}\,\sigma_\lambda} \exp\left[-\frac{1}{2}\left(\frac{\lambda d - \lambda c}{\sigma_\lambda}\right)^2\right]$$

The integrals in the last expression for $A_D$ can be solved numerically by converting them to a finite element problem. A large amount of simplification can be accomplished by exploiting the symmetries of the problem. In order to illustrate the method, the pumping geometry shown in Figure 4-4 will be considered for the remainder of this section. In this design there are eight double linear arrays uniformly spaced around the rod. Because of the symmetry of this configuration only the sector of the rod shown in Figure 4-6 needs to be considered. This sector is divided into a total of 200 elements as indicated in the same figure.

The determination of the ray pathlength inside the rod for each individual beamlet has to be made by using ray-tracing techniques. For this purpose, the optical system described in Figure 4-7 will be used. This system includes a total of seven optical surfaces, four of which belong to a symmetrical doublet of cylindrical lenses configurable in all possible ways in terms of radii of curvature.

A computer code called CRADLE (Computation of Rod Absorption of Diode Laser Emission) was implemented for the evaluation of $A_D(r)$. In its present form this code is only applicable to the configuration shown in Figure 4-4. However, it can be adapted to many other configurations. By making the lens index of refraction equal to one, the cylindrical lenses are rendered nonexistent and the configuration of Figure 4-4 reduces to one in which the cooling jacket is the only optical element performing the role of flux concentrator. When the indices of refraction of the lenses, cooling jacket and coolant are all made equal to one the same configuration reduces to the direct coupling case. The other limitation of this code as currently implemented relates to the reflective losses at the various optical surfaces. No provision has been incorporated into the code to account for the losses in the lenses. However, a good optical design should make use of AR coated optics to maximize transmission, and it will therefore be a good approximation

Figure 4.6

CELL DEFINITION USED IN THE PUMP-RADIATION ABSORPTION ANALYSIS

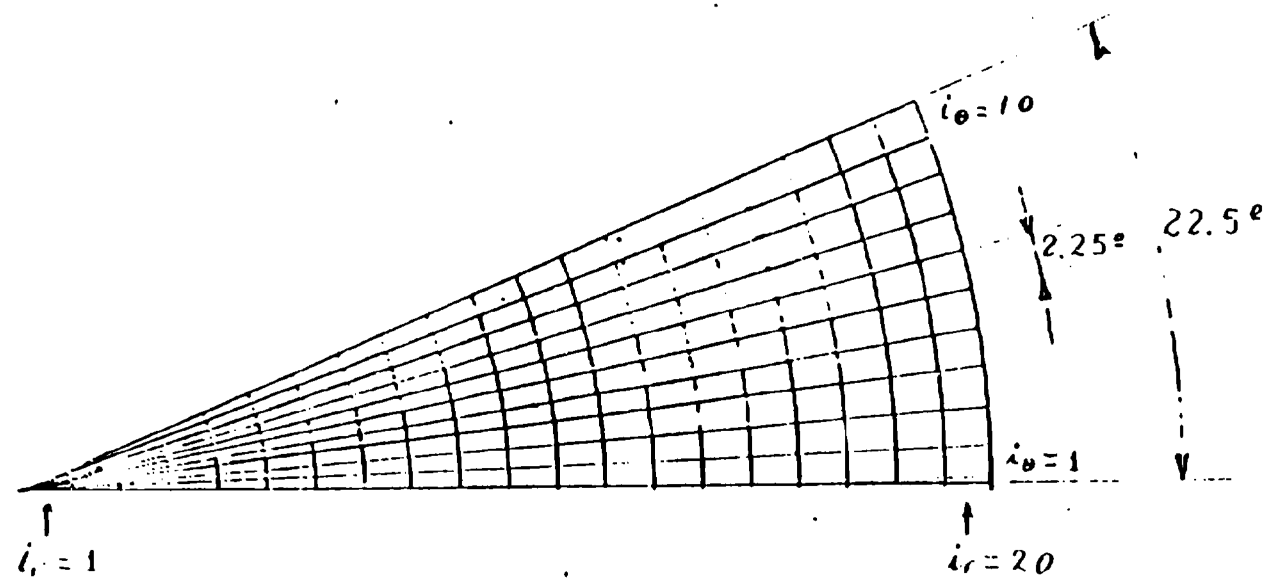

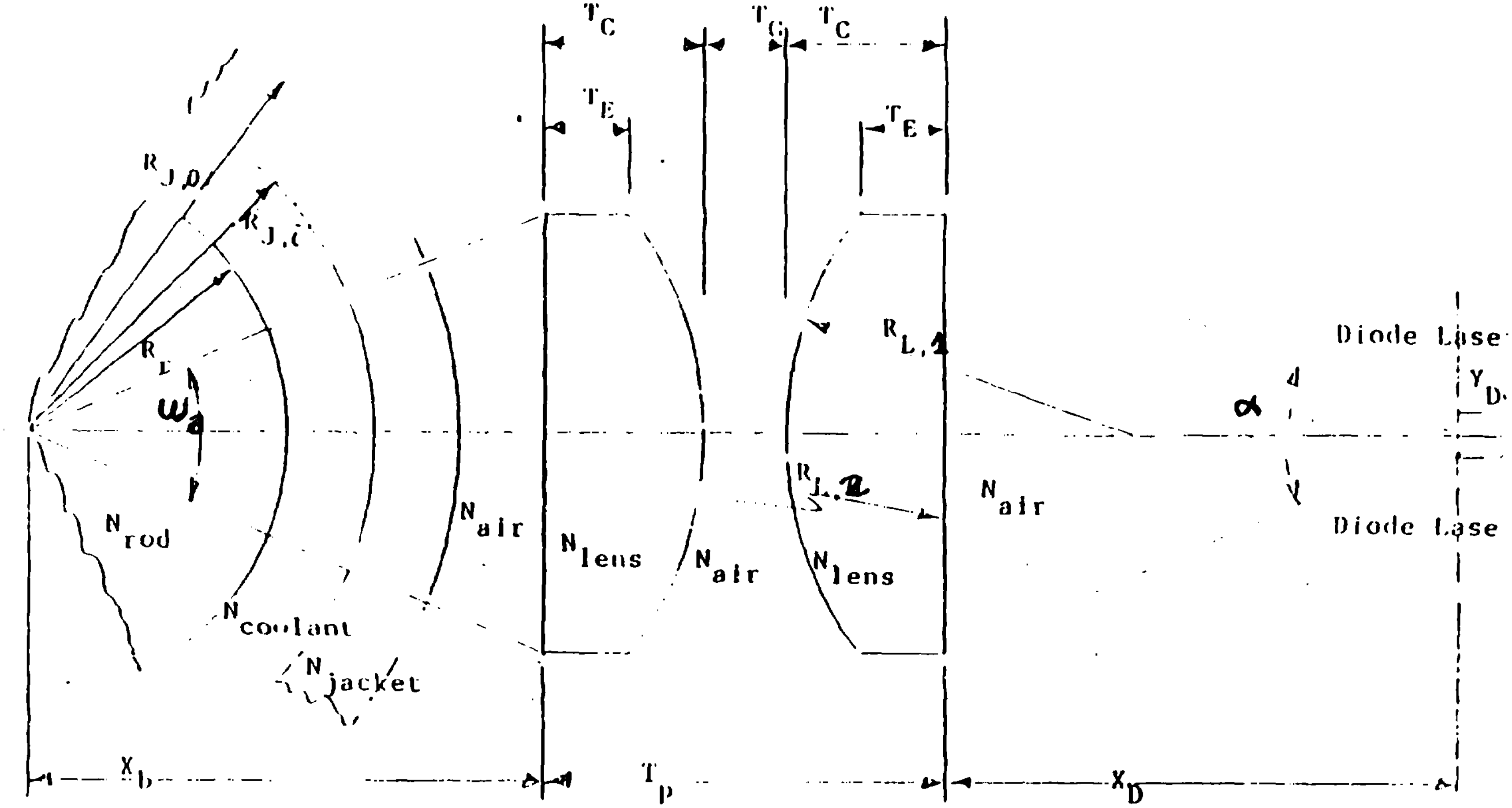


Figure 4.7. Definition of geometetrical and optical parameters.

to evaluate those losses by estimating an average transmission coefficient each surface. The code does provide an option to include the effect of reflection losses at the jacket and laser rod surfaces considering unpolar light and no AR coating.

### 4.2.3 Emitter and Absorber Characterization

In order to evaluate the integral over the angle of emission $\alpha_1$, it necessary to define the irradiance function $I(\alpha_1)$ $I(\alpha)$. For this purpos simple model of the directional dependence of the diode laser irradiance (radiation pattern) will be used. This model is described in detail in Reference 4.3. Assuming that the diode laser cavity resonates at the fundamental transversal mode the radiation pattern is given by:

$$I(\theta,\phi) = C\,(\cos^2\phi\cos^2\theta + \sin^2\theta)$$
$$\times \left\{ \frac{(K_1 - \sin^2\theta)^{1/2} + \beta_{11/ko}}{(K_1 - \sin^2\theta)^{1/2} + (\sin^2\theta\sin^2\theta + \cos^2\theta)/\cos\theta} \right\}^2$$
$$\times \exp\left\{ -\frac{1}{2}\left[ (Xko\cos\phi\sin\theta)^2 + (Yko\sin\phi\sin\theta)^2 \right] \right\}$$

Where $\theta$ and $\phi$ are defined in Figure 4-8. In this expresson C is a coefficient of proportionality. $K_0$ is the free-space wave number given by

$$K_0 = 2\pi/\lambda_c$$

$K_1$ is the peak value of the dielectric constant of the graded index waveg that constitutes the diode laser resonator. It is related to the peak val of the index of refraction by:

$$K_1 = \bar{n}^2$$

Figure 4.8 Radiation pattern from a laser diode.
(M. Ettenberg, Laser Focus, May 1985, P. 86)

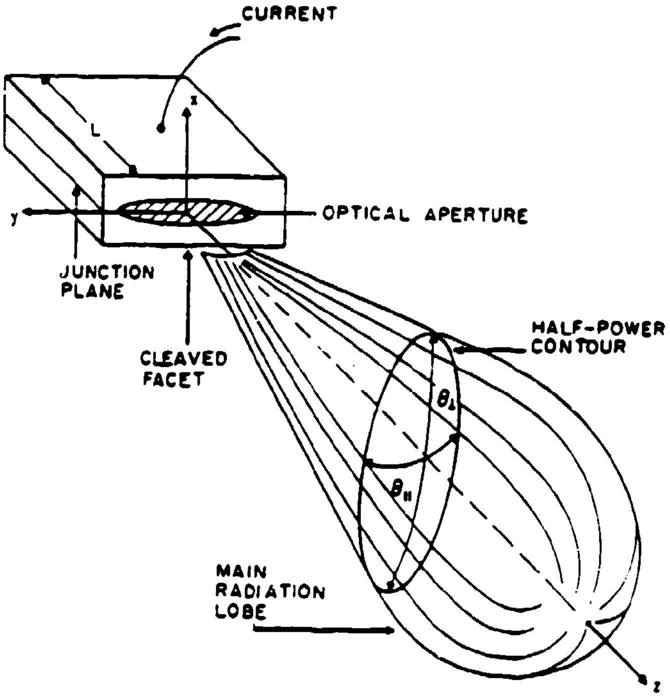

$\beta_{11}$ is the propagation constant for the fundamental transversal mode of t:
waveguide resonator and it is given by:

$$_{11} = Ko\bar{n}\left(1 - \frac{1}{ko\ \bar{n}\ x_o} - \frac{1}{ko\ \bar{n}\ y_o}\right)^{1/2}$$

In the expression $X^o$ and Yo are the parameters that describe the cha of the dielectric constant with position across the waveguide according t following formula:

$$K = K_1\left[1 - \left(\frac{x}{Xo}\right)^2 - \left(\frac{Y}{Yo}\right)^2\right]$$

$\bar{x}$ and $\bar{y}$ are defined in terms of these parameters through the following relationships:

$$\bar{x} = \sqrt{\frac{\lambda c \quad Xo}{\pi \bar{n}}}$$

$$\bar{y} = \sqrt{\frac{\lambda c \quad Yo}{\pi \bar{n}}}$$

and are also linked to the half power full angular widths of the radiatio pattern by the following expressions:

$$\theta_1 = 2 \sin^{-1}\left[0.69 \ \frac{\lambda c}{\pi} \ \bar{Y}\right]$$

$$\theta_{11} = 2 \sin^{-1}\left[0.69 \ \frac{\lambda c}{\pi} \ \bar{X}\right]$$

where $\theta_1$ and $\theta_{11}$ are the FWHPs pependicular and parallel respectively to diode laser output slit (see Figure 4-8).

The irradiance function I ( $\alpha$ ) needed for the two-dimensional analysis can be obtained from I ($\theta,\phi$), by using the angular coordinate $\alpha$ and $\beta$ shown in Figure 4-9. The transformation formulas are:

$$\sin\theta = \sqrt{\sin^2\beta + \cos^2\beta\ \sin^2\alpha} = 1 - \cos^2 \quad \cos^2$$

$$\cos\theta = \cos\alpha\ \cos\beta$$

$$\sin\phi = \sin\beta\ /\sin\theta$$

$$\cos\phi = \sin\alpha\ \cos\beta\ /\sin\theta$$

For the two-dimensional analysis CRADLE performs an average of the irradiance function over the angular coordinate $\beta$ . The integration over $\alpha$ is performed by dividing the angular aperture of the optics in equal intervals. Usually about 100 intervals are used.

The characterization of the laser rod is done in terms of its radius, index of refraction and spectral absorption coefficient $\gamma(\lambda)$. A file containing information of the latter covering the spectral range of interest has to be created for the calculation of the spectral and total absorption of the pump radiation by the rod.

### 4.2.4 Results

In order to arrive at conclusions applicable to practical designs, a pumping cavity with the configuration shown in Figure 4-4 will be taken as a reference design. In this design the laser rod is surrounded by a jacket to allow its cooling by force convection using an axial coolant flow. The pumping cavity consists of eight single or double linear arrays symmetrically located around the rod. The output slits of the diode lasers are imaged near the center of the rod by using a symmetrical doublet of plano-convex cylindrical lenses. Divergence angle for diode lasers in the direction perpendicular to the junction range as high as 60 FWHM (full width at half maximum); typical values for high power diode laser arrays are in the $30^o$ to $40^o$ range. Assuming that the angular dependence of the irradiance follows a gaussian function of the angle, for a collection angle 1.7 times the FWHM

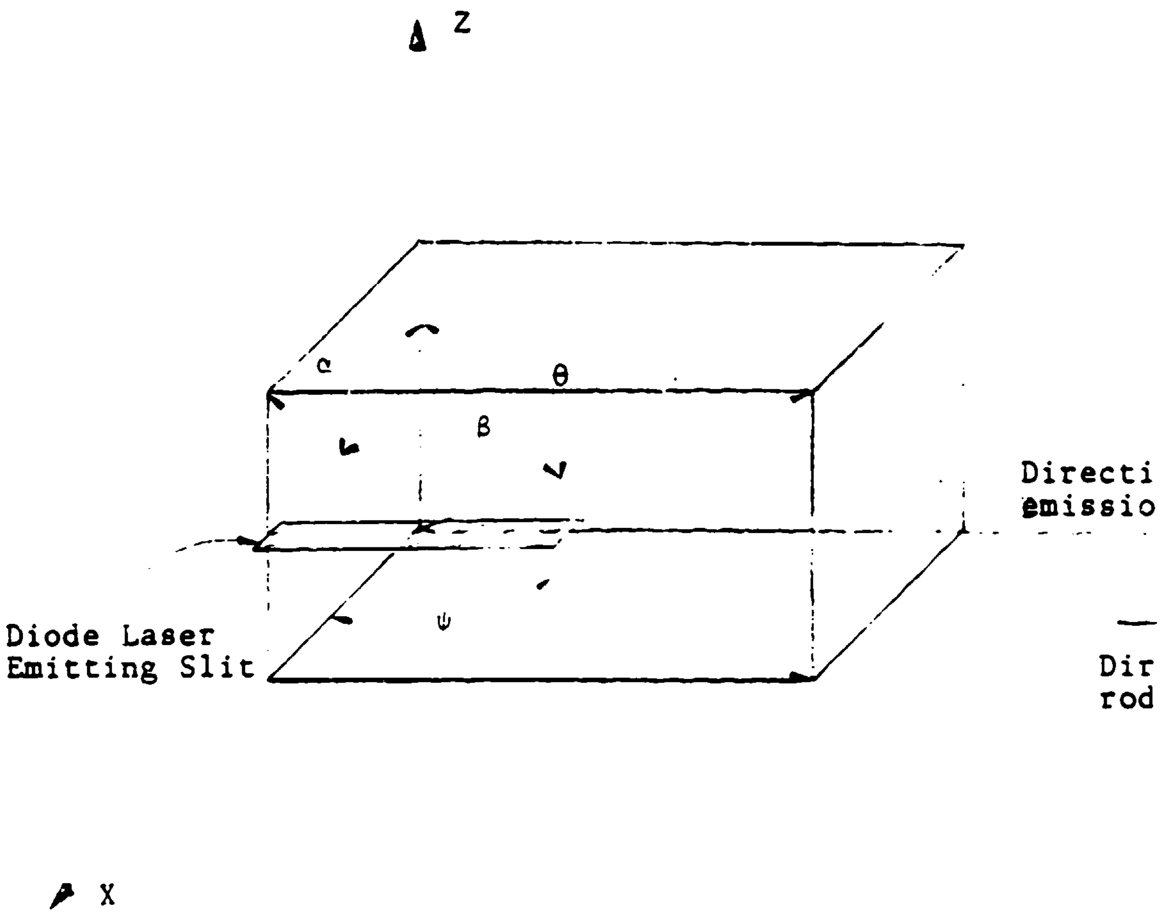


Figure 4.9 Definition of angular coordinates for the radia
pattern model

value the collected radiation will be 95 percent of the total output. However, as can be seen from the irradiance function discussed in Section 4.2.3, the actual irradiance falls off faster than a gaussian and therefore it can be considered that for that collection angle practically all the radiation emitted by the diodes is collected. This means that in most cases, the collection angle required will range between $50^0$ and $70^0$.

The design parameters that have to be defined and entered in the parameter file of CRADLE are shown in Table 4-1. Data on the rod spectral absorption is also required by CRADLE. This information is entered in a file named Spectrum. Table 4-2 lists the value of the spectral absorption of a 1 percent Nd doped YAG crystal around the 808 nm center wavelength in the format required by CRADLE, and Figure 4-10 shows a computer plot of this spectrum. With the data shown in these tables, CRADLE produces an output in table form giving the cross-sectional pump power distribution for a 1/16 sector of the rod as shown in Table 4-3. Figures 4-11 to 4-13 show slices of this distribution cut along the radial direction for different angular positions defined with the index i (see Figure 4-6 for the definition of this index). CRADLE also produces an angular average of the distribution and a radial integration as shown in Figure 4-14 and Figure 4-15. It also gives the fraction of the power emitted by the diode laser array that is absorbed in the rod.

Calculated total absorption for a YAG rod doped with 1 percent of neodymium are shown in Table 4-4 for several rod diameters and for two values of the FWHM of the spectral output of the diode laser array. These values, calculated for the full cavity with the configuration shown in Figure 4-4 are also valid for the half cavity configuration discussed in Section 7. If the rod diameter is taken as half the diameter shown in the table and the reflectivity of the reflective coating applied on the rod is considered to be 100 percent. The advantage of using arrays with a narrow spectral distribution is clearly shown in this Table. State-of-the-art diode laser arrays fabricated using MOCVD technology are already producing outputs with spectral spreads not larger than 4 nm.

Table 4.1 CRADLE parameter file.

Note: Unless otherwise specified, all dimentions are given in cm.
The wavelength is in nanometers and the absorption coeffici-
is in inverse centimeters. Angular apertures are in degrees

Lens parameters

- Rod parameters -

- Jacket and coolant parameters -

Diode LASER parameters -

Table 4.2 Nd:YAG rod absorption spectrum.

Figure 4.10 Nd:YAG ABSORPTION SPECTRUM USED IN THE ANALYSIS OF PUMP RADIATION ABSORPTION

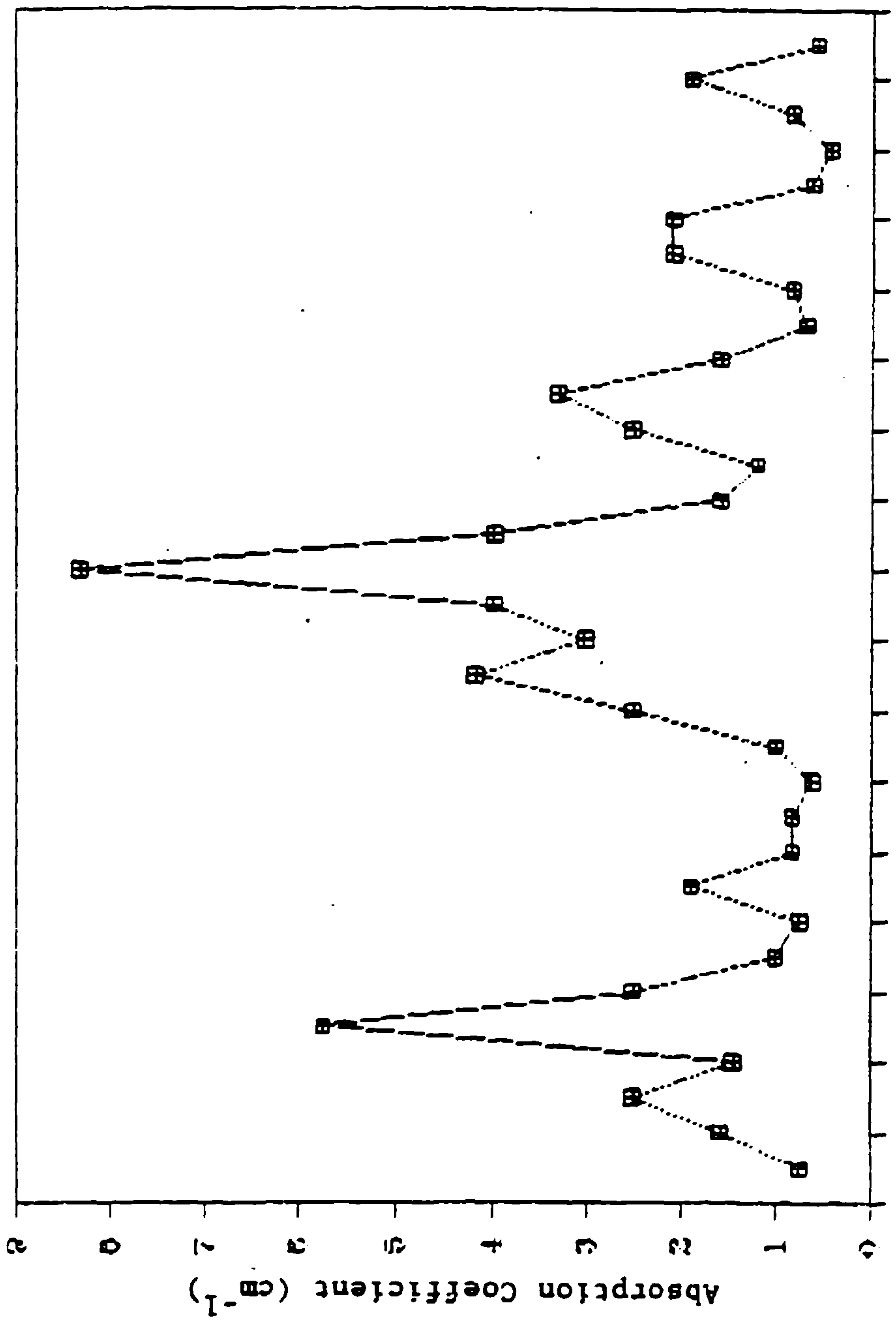

Center wavelength ........... : 807.0 nanometers
Standard deviation .......... : 8.47 nanometers
Half width at half maximum .. : 10.00 nanometers

| Radial Position | i = 1 | ← | — | — | Angular position | — | — | — | → | i = 10 |
|---|---|---|---|---|---|---|---|---|---|---|
| center → | 11.795 | 11.785 | 11.756 | 11.921 | 12.222 | 11.812 | 12.062 | 12.921 | 12.758 | 13.718 |
| | 13.649 | 13.751 | 13.903 | 14.105 | 13.904 | 14.282 | 15.875 | 13.302 | 12.502 | 9.161 |
| | 4.111 | 4.197 | 4.543 | 4.492 | 4.721 | 4.901 | 7.478 | 10.307 | 14.708 | 18.208 |
| | 2.941 | 2.941 | 3.132 | 3.358 | 6.556 | 7.959 | 8.742 | 8.756 | 7.951 | 4.073 |
| | 2.174 | 2.258 | 4.444 | 7.069 | 5.928 | 5.401 | 7.059 | 5.073 | 2.617 | 2.195 |
| | 1.404 | 4.163 | 5.635 | 4.337 | 4.216 | 4.524 | 5.961 | 1.555 | 1.780 | 1.457 |
| | 3.314 | 4.661 | 3.576 | 3.454 | 3.443 | 4.070 | 3.689 | 1.046 | 1.247 | 0.990 |
| | 5.472 | 3.163 | 2.859 | 2.844 | 3.060 | 3.991 | 2.177 | 0.729 | 0.835 | 0.581 |
| | 6.183 | 2.616 | 2.448 | 2.340 | 2.677 | 4.212 | 0.852 | 0.511 | 0.642 | 0.470 |
| | 5.576 | 3.171 | 2.180 | 2.034 | 2.227 | 3.636 | 0.647 | 0.424 | 0.564 | 0.399 |
| | 4.155 | 4.462 | 1.902 | 1.753 | 1.887 | 3.310 | 0.563 | 0.369 | 0.487 | 0.344 |
| | 3.514 | 4.845 | 1.741 | 1.560 | 1.657 | 3.080 | 0.491 | 0.331 | 0.422 | 0.305 |
| | 3.111 | 3.667 | 2.924 | 1.495 | 1.493 | 2.861 | 0.430 | 0.294 | 0.374 | 0.272 |
| | 2.763 | 3.069 | 3.553 | 1.435 | 1.381 | 2.670 | 0.393 | 0.254 | 0.337 | 0.243 |
| | 2.451 | 2.832 | 3.910 | 1.313 | 1.370 | 2.134 | 0.672 | 0.228 | 0.317 | 0.211 |
| | 2.316 | 2.552 | 3.753 | 1.667 | 1.242 | 1.743 | 0.950 | 0.216 | 0.276 | 0.200 |
| | 2.144 | 2.397 | 3.023 | 2.513 | 1.277 | 1.420 | 1.108 | 0.188 | 0.245 | 0.187 |
| | 2.142 | 2.196 | 2.718 | 2.951 | 1.140 | 1.368 | 1.096 | 0.179 | 0.241 | 0.158 |
| | 2.084 | 2.097 | 2.549 | 3.178 | 1.158 | 1.287 | 1.088 | 0.162 | 0.204 | 0.157 |
| Periphery → | 2.035 | 2.062 | 2.321 | 3.534 | 1.086 | 1.201 | 1.082 | 0.149 | 0.204 | 0.138 |

Total absorption ...... : 63.224 %
Total losses .......... : 35.151 %

Table 4.3 Example of pump flux distribution produced by CRADLE

**DISTRIBUTION OF ENERGY DENSITY IN THE LASER ROD DUE TO DIODE PUMP RADIATION**

-- Paraxial Direction ($i_0$=1) --

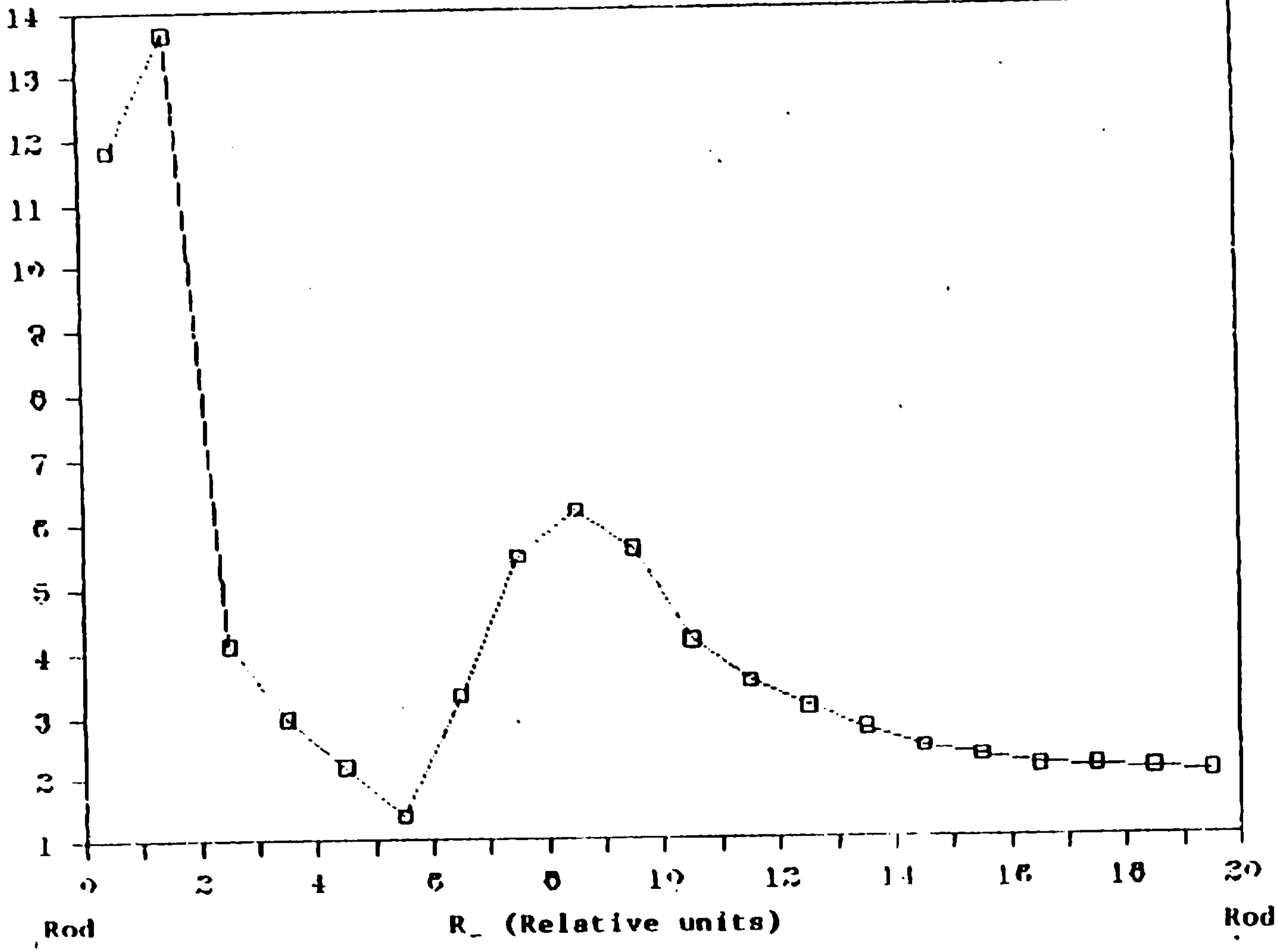

DISTRIBUTION OF ENERGY DENSITY IN THE LASER ROD
DUE TO DIODE PUMP RADIATION

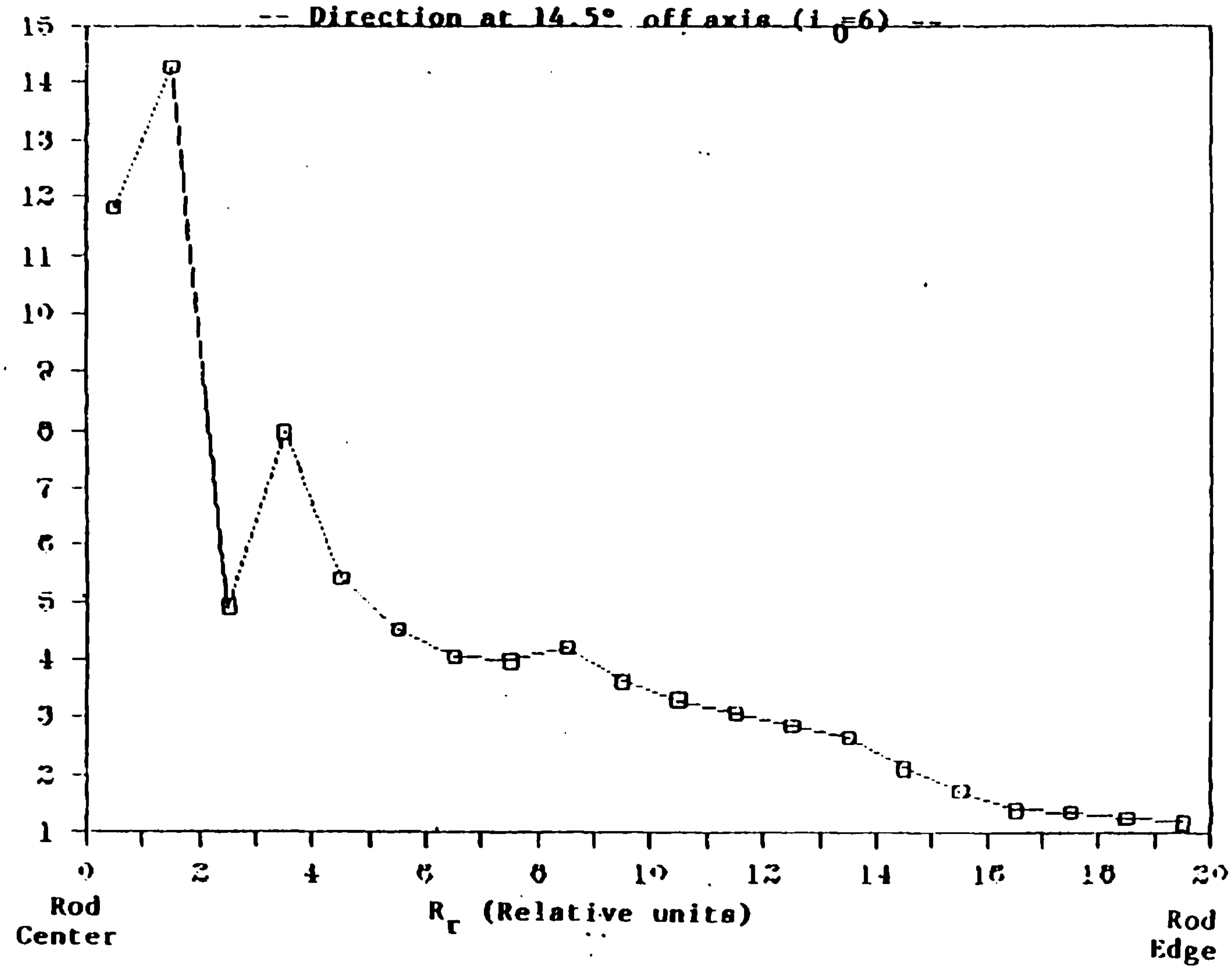


Figure 4.12

DISTRIBUTION OF ENERGY DENSITY IN THE LASER ROD
DUE TO DIODE PUMP RADIATION

-- Direction at 20.9° off axis ($i_0$ =10)

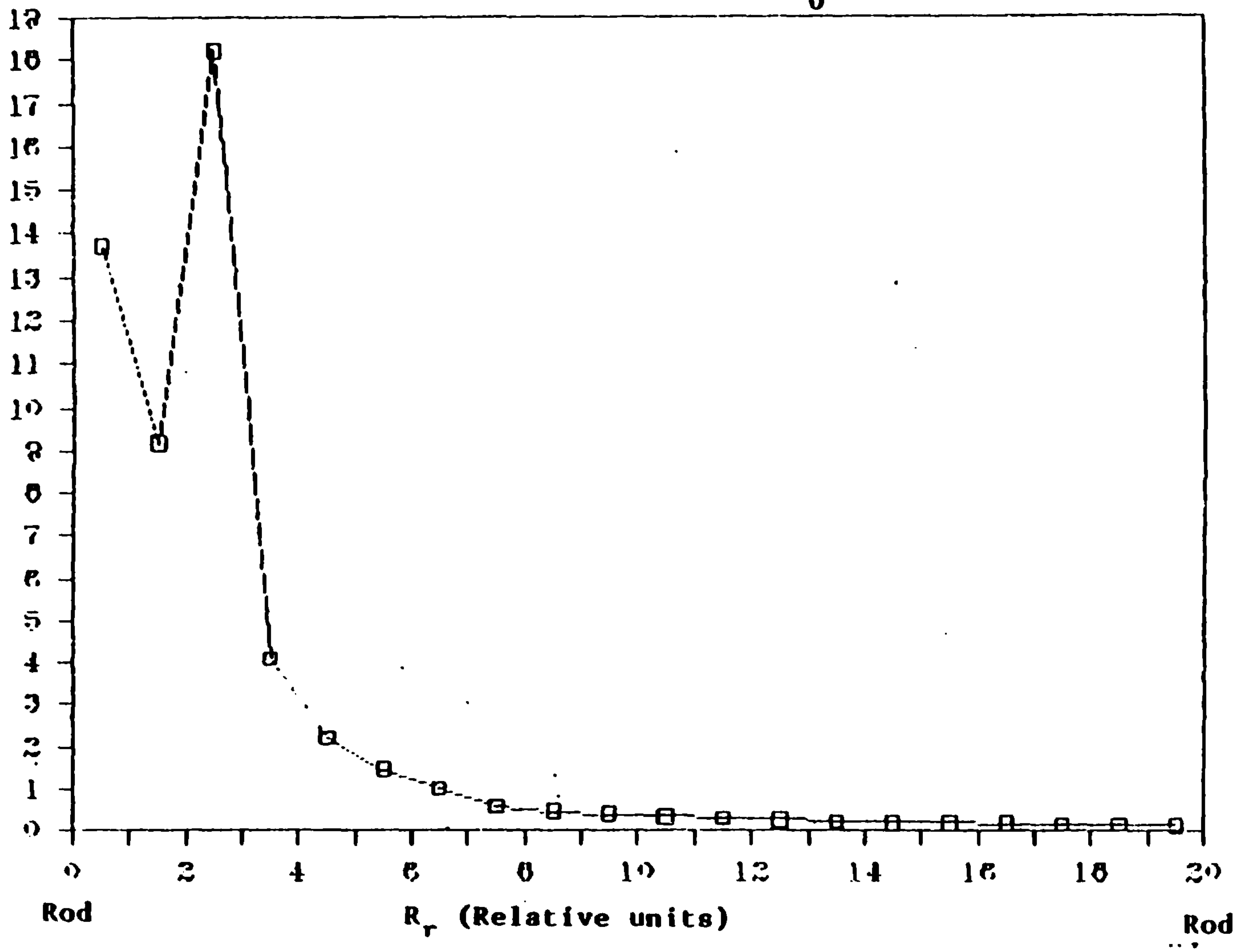

DISTRIBUTION OF ENERGY DENSITY IN THE LASER ROD DUE TO DIODE PUMP RADIATION

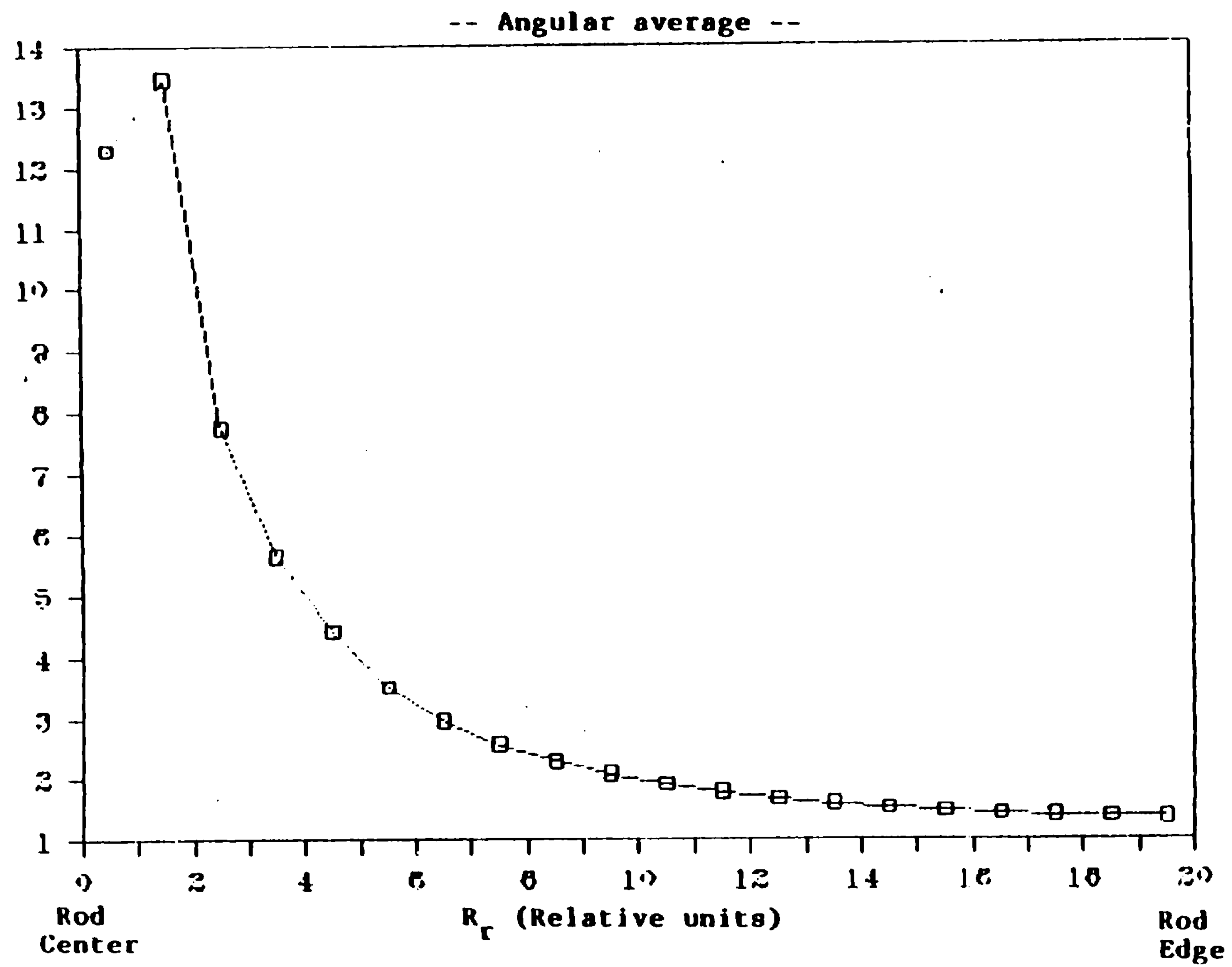


Figure 4.14

Fraction of the Total Pump Energy Absorbed by the Rod
That is Absorbed Inside a Cylinder of Radius $R_r$

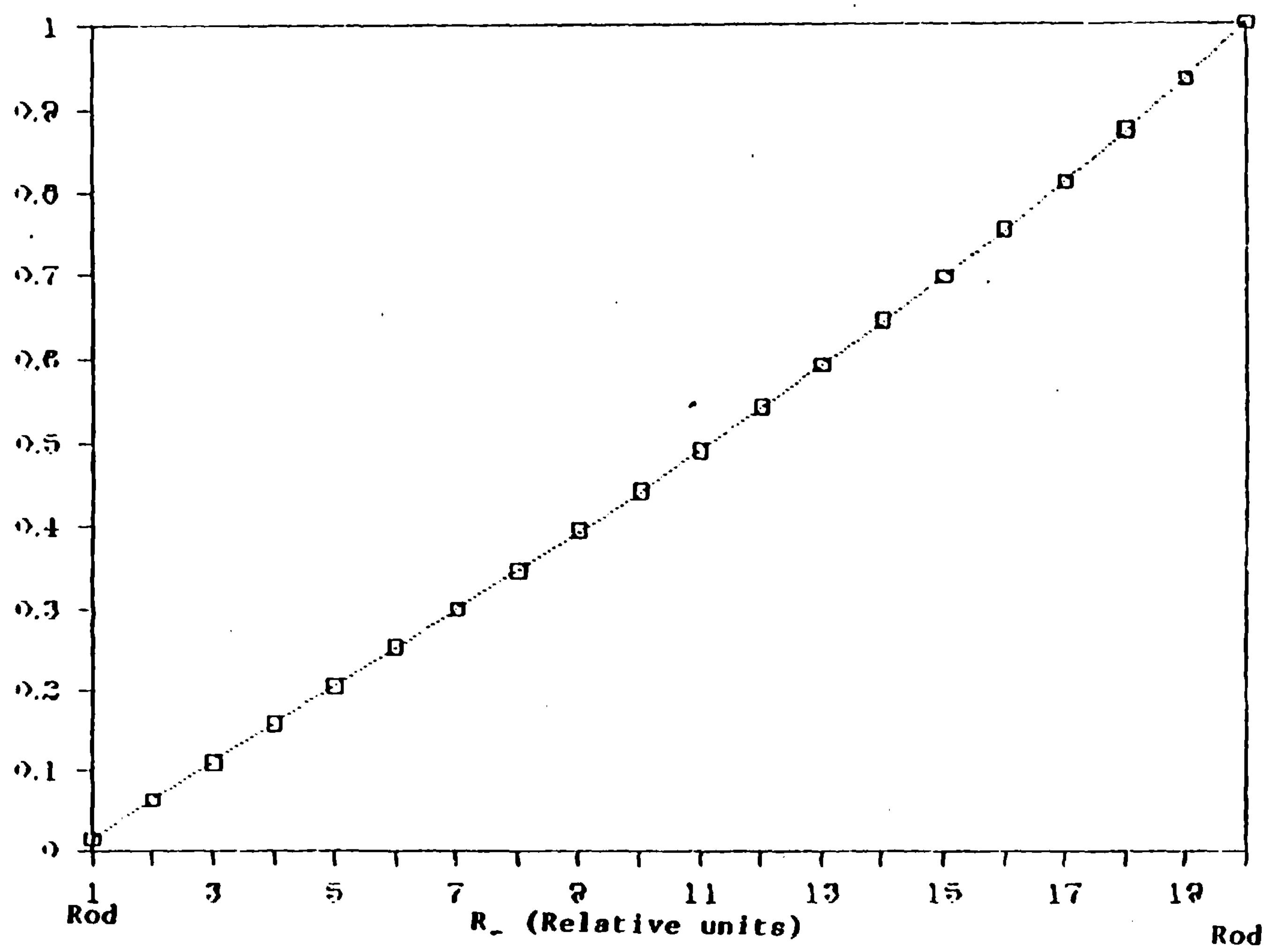

TABLE 4.4

Efficiency of pump radiation absorption as a function of rod diameter and diode laser wavelength distribution width. Distribution center wavelength: $\lambda c = 807$ nm. Reflection losses are neglected.

| Rod Diameter / Bandwidth, A | 6 mm | 8 mm |
|---|---|---|
| 200 | 63% | 79% |
| 40 | 91% | 96% |
| 20 | 93% | 98% |

## 4.3 SIDEPUMPING OF A SLAB

In this subsection we will briefly describe the basic characteristic zig-zag slab lasing and provide a discussion of the key design parameters laser diode pumped slab laser.

A description of the design and performance of a diode pumped slab l developed by McDonnell Douglas, and a discussion of several slab design alternatives will conclude this subsection.

### 4.3.1 Current Status

The concept of a slab laser geometry with a zig-zag optical path cor in the slab by total internal reflection was first proposed by Martin anc Chernoch in 1972[4.4]. Slab geometry development was pursued by General Electric for potential applications to high performance military requiren during the past fourteen years. In this report, we review the recent development in Nd:YAG slab lasers relevant to laser diode pumping.

Solid-state lasers traditionally have been fabricated in a rod geome Under high thermal loading associated with optical pumping, the laser roc manifests radially dependent thermal and stress-induced optical distortic These effects include thermal focusing stress-induced birefringence. The effects severely degrade the performance of rod geometry laser systems a pump power levels. Thermal-optic distortion is the principal problem in obtaining a high quality beam at high average power from a solid state la The distortion can be classified as the sum of that caused by index varia with temperature and that caused by thermal stress birefringence.

In the slab-type laser configuration, the solid host material is in form of a rectangular cross-section slab with plane parallel surfaces or faces. The configuration is shown schematically in Figure 4-16. The sla face-pumped optically, i.e., illuminated through two opposing slab faces obtain the required inversion energy in the active material, and, simulta eously, the same faces are cooled to obtain a one-dimensional, steady, th

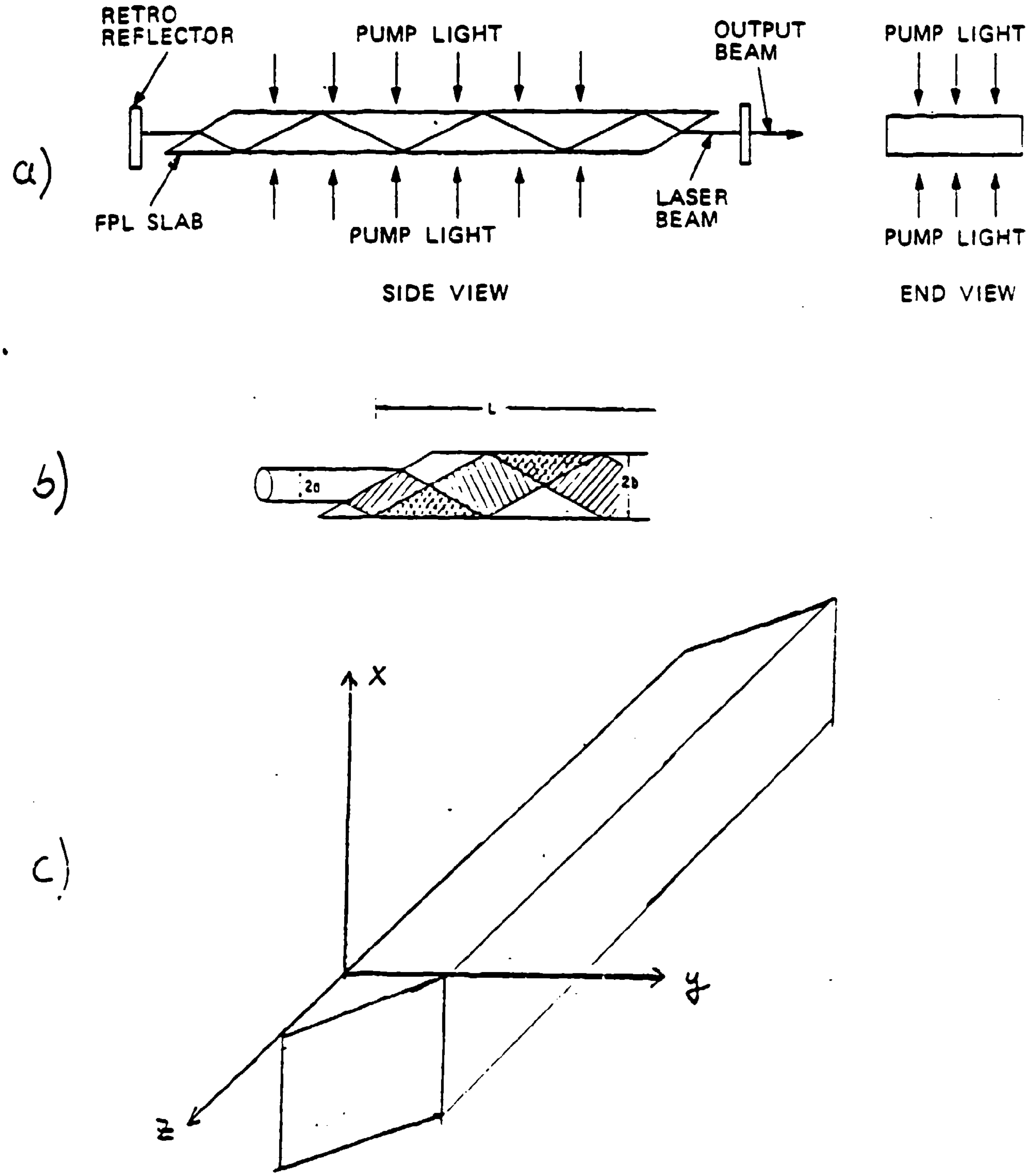


Figure 4.16 Schematic of a zig-zag slab laser a); with Brewster angle entrance face b); and definition of coordinate system c).

state. Thermal stress results in the slab from the heating which is conc( ant with optical pumping and cooling. The volume heating is symmetrical relative to the center plane of the slab, and, therefore, the thermal str( averaged from one slab surface to the other is zero. These conditions le( a high degree of compensation for thermal-optic distortion for a beam pas from one slab face to the other. The laser beam is introduced into the s through suitable entrance optics, usually through a surface at Brewster's angle, as shown in Figure 4-16

In this figure the z-axis is parallel to the long dimension of the s and the x-ray plane represents a cross section of the slab. The x-axis i perpendicular to the major faces of the slab, and the y-axis is parallel those faces.

The slab geometry offers significant advantages compared to the rod geometry laser configuration. The advantages primarily stem from the rectilinear pumping and cooling geometry. In the face pumped and cooled laser, the thermal temperature gradient is assumed to be in the y directi The x faces are assumed to be insulated so that the slab appears to be infinite in the x direction. Under these assumptions, the thermally indu stress is also in the y direction. Furthermore, for light polarized in t or y direction there is no stress induced birefringence.

With the assumption that the edges of the slab are thermally insulat one-dimensional thermal state results in the slab which is symmetrical ab the center plane of the slab. Also, the thermal stress which occurs in t slab is symmetrical about the center plane. Each ray in the laser beam experiences the same index of refraction variations in passing from one s face to the other; thus, no wavefront distortion occurs. The stress-indu birefringence disappears when averaged over a path between faces, and no depolarization results. Further, with uniform face pumping, uniform gain across the optical aperture is assured, so there is no amplitude distorti The zig-zag optical path also has the added advantages of averaging over non-uniform slab pumping in the y direction and proving a longer gain pat the laser medium.

Strictly, however, the absence of distortion results only for a slab of infinite extent, uniformly pumped and cooled. For a slab of finite width and length, edge and end effects give rise to distortion in these regions. Also uniformity of pumping and cooling are important in achieving the low distortion inherent in the configuration. Thus the maximum pumping power which can be used without significant distortion is determined by the deviation from uniformity of pumping/cooling and the edge and end effects.

Pump or cooling induced gradients across the slab width (normal to the plane of reflection), as well as end effects, are often the reason why the slab configuration shows a disappointing optical performance. The slab geometry has the disadvantages of a more expensive optical fabrication and a more complicated mechanical mounting geometry. Also, the internal reflection at the slab surfaces is sensitive to absorption in the coolant and to index of refraction variations of the coolant. Due to the large polished and parallel sides of a zig-zag slab laser, amplified spontaneous emission (ASE) can become a problem in high gain materials such as Nd:YAG.

In the case of diode array pumping, the optical compensation property of the zig-zag slab is not the primary reason for choosing this geometry. Compared to flashlamp pumping, the heat load produced by laser diodes is much reduced; furthermore, arrays are not capable of high average power operations at the present time. The attractive feature of the slab is the large rectangular pump surface which matches the geometry of planar arrays. In addition, the zig-zag slab provides for spatial averaging of the non-uniform pump profile in the plane of reflection, caused by the exponentially decaying pump intensity from the face of the slab. As we noted above, the slab has an intrinsic compensation for non-uniform effects occurring for paraxial rays in a plane of reflection.

The space based submarine laser communications program requires development of efficient, reliable, long lived systems which can deliver 1 J/pulse of 455.5 nm at a pulse repetition rate of 100 Hz. As part of this program, McDonnell Douglas Corporation has embarked on a program aimed at the demonstration of the technical feasibility of laser diode array pumped slab lasers.

The slab geometry was chosen because it offers the advantages of efficient diode coupling, spatial averaging of the nonuniform diode pumpir complete elimination of thermal and stress focusing, linear polarized outp and high quality spatial mode output.

The end result of this development program was the fabrication and de stration of a diode pumped slab laser with 3.85 $cm^2$ of pump area. Develop of diode arrays with the required density, efficiency, wavelength and puls repetition rate was the principal technical challenge of the program. The design and fabrication of the Nd:YAG slab, resonator and Q-switch follow m traditional and established design concepts. Since this design represents state-of-the-art in laser diode pumping we will describe some of the deta design features as well as given details on the performance.

The Nd:YAG slab had a pump length of 8.9 cm, a height of 0.69 cm and thickness of 0.67 cm. (Reference 4.5).

The Nd:YAG slab is pumped from one face only. The opposite face is bonded to a copper heat sink containing a reflective coating to return unu pump radiation back into the slab for a second pass. An anti-reflection coating on the pump face is used to reduce coupling losses (the diode arra not in contact with the YAG). Liquid cooling is employed to remove heat the YAG and diode heat sink.

As shown in Figure 4-17, the slab was pumped by seven planar arrays. Each array was 0.9 cm long and 0.61 cm wide and had an emitting area of 0. cm. On the average each array produced a peak power of 413 W, in a 216 pulse. Electrical input to each array was 58 A and 30 V, which resulted optical output/electrical input efficiency of 24.2 percent. The power der achieved at the arrays corresponds to 750 $W/cm^2$. The total output energy derived by the seven arrays corresponds to 624 mJ.

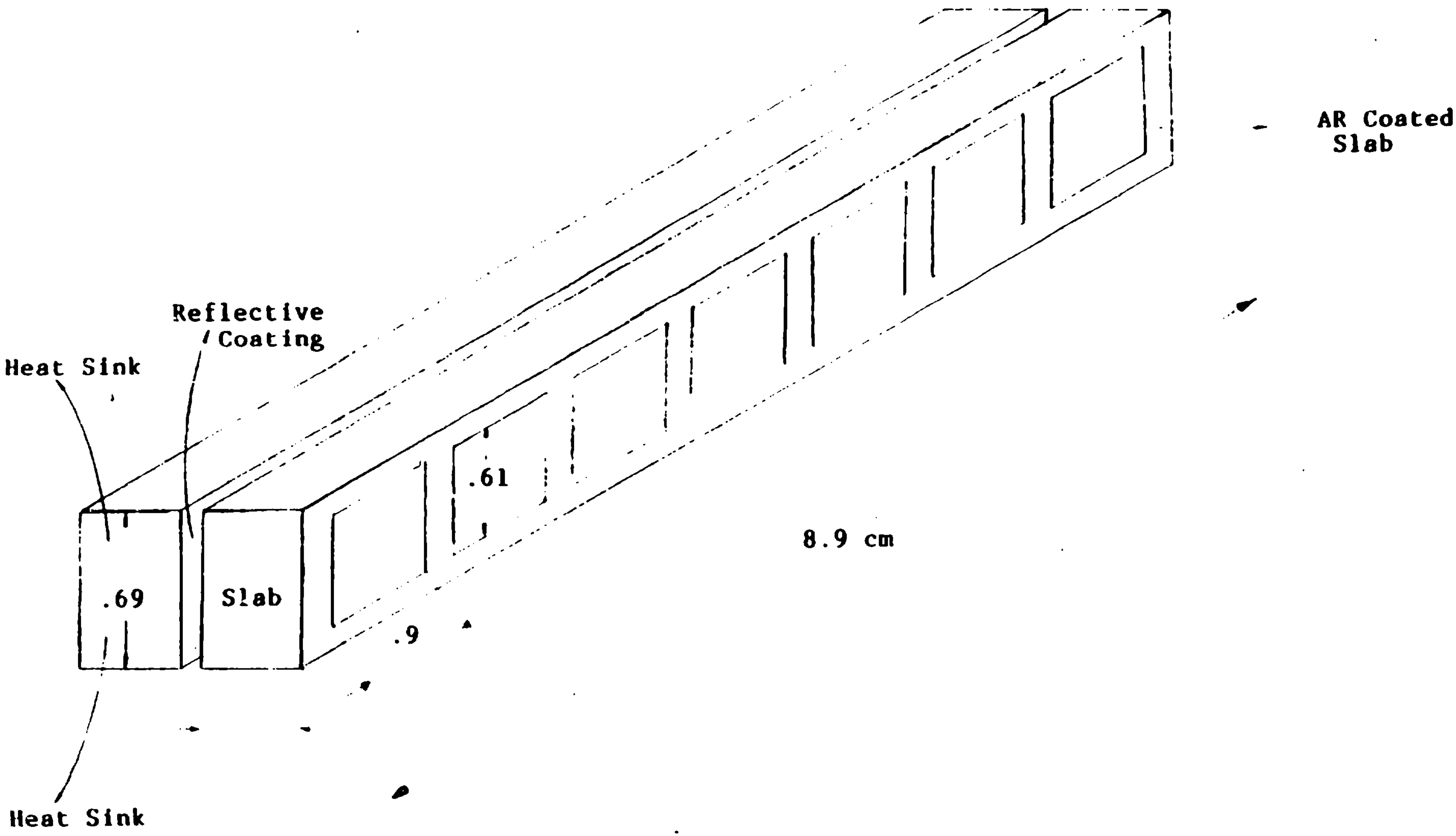


Figure 4.17 Geometry of Slab Laser Built by McDonnell Douglas

Figure 4-18 shows the long pulse output of the laser. The data shown for two different output couplers. The highest slope efficiency of conver: of diode pump energy to laser output was 36.8 percent with the 51.8 percen reflector. The highest absolute efficiency of conversion of diode pump li to laser output ws 26.7 percent.

Figure 4-19 shows the Q-switched performance in addition to the long pulses for comparison. Threshold is higher due to the losses caused by th polarizers and the Q-switches. With a 51.8% reflecting output coupler an output of 105 mJ was obtained. This represents about 18.2 percent convers of pump radiation to Q-switched laser output and a differential conversion efficiency of 33.9 percent. This data was taken with 200 μsec pump pulses With 216 μsec pump pulses and slightly higher pump fluence, 120 mJ Q-switc at 10 Hz was obtained.

### 4.3.2 Alternate Configuration

The output from the emitting surface of the laser diode array has to coupled efficiently to the laser medium. The standard approach is a close coupled pumping scheme whereby the arrays are directly facing the slab or surface. This is optically the most straightforward approach; however, it places severe constraints on the packaging density of the diode array beca the array has to match the size of the slab pump surfaces.

For high average power operation the maximum heat dissipation from th array (50-100 W/cm$^2$) limits the performance of the laser. If the output f the planar array is coupled to the slab via a compound parabolic cylinder, about a factor four in array area can be gained, and the average power of device can be increased by the same factor. An ideal light collector or compound parabolic cylinder (CPC) is a non-imaging device which can take a large array output and geometrically compress it into an area as much as f times smaller than the array (Reference 4.6). Actually the CPC is a non-imaging light funnel as shown in Figure 4-20 that derives its characterist optical properties from the specific shape of the external wall, which is specularly reflecting.

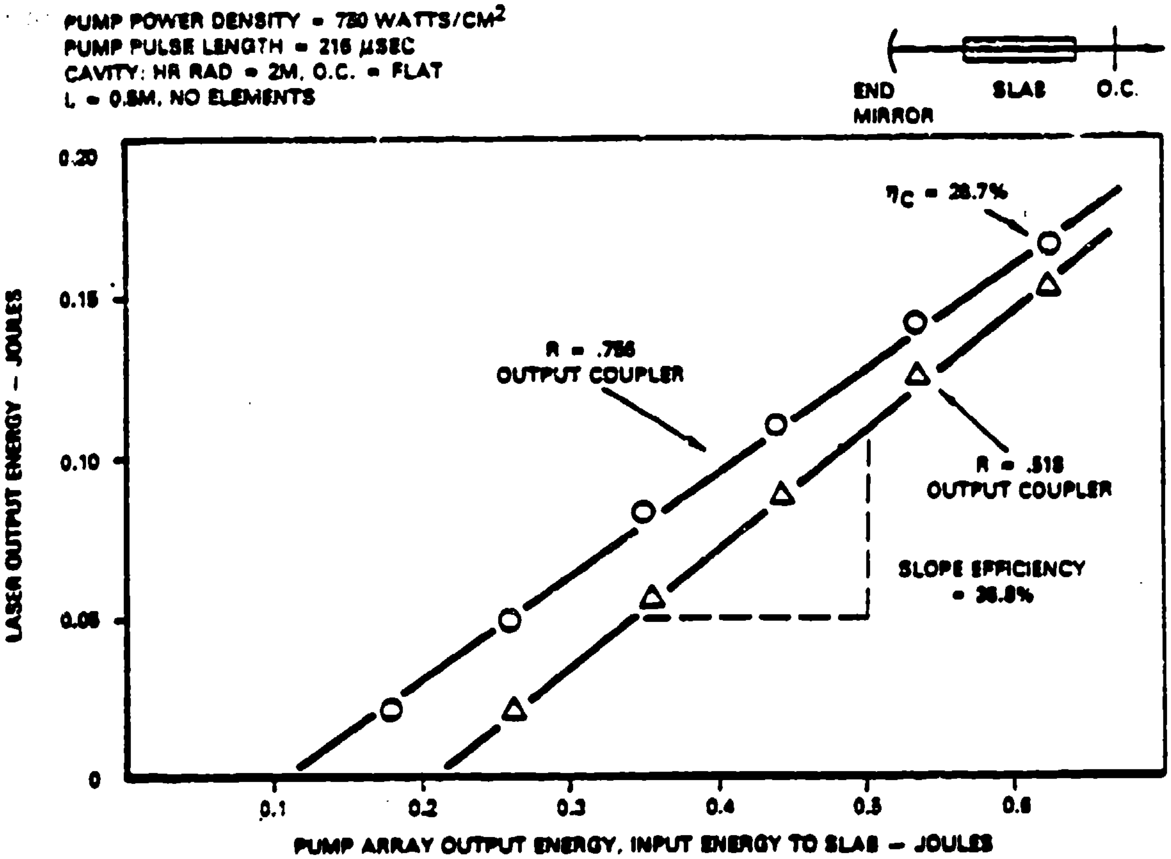


Figure 4.18   Long-pulse slab performance (from Reference 4.5).

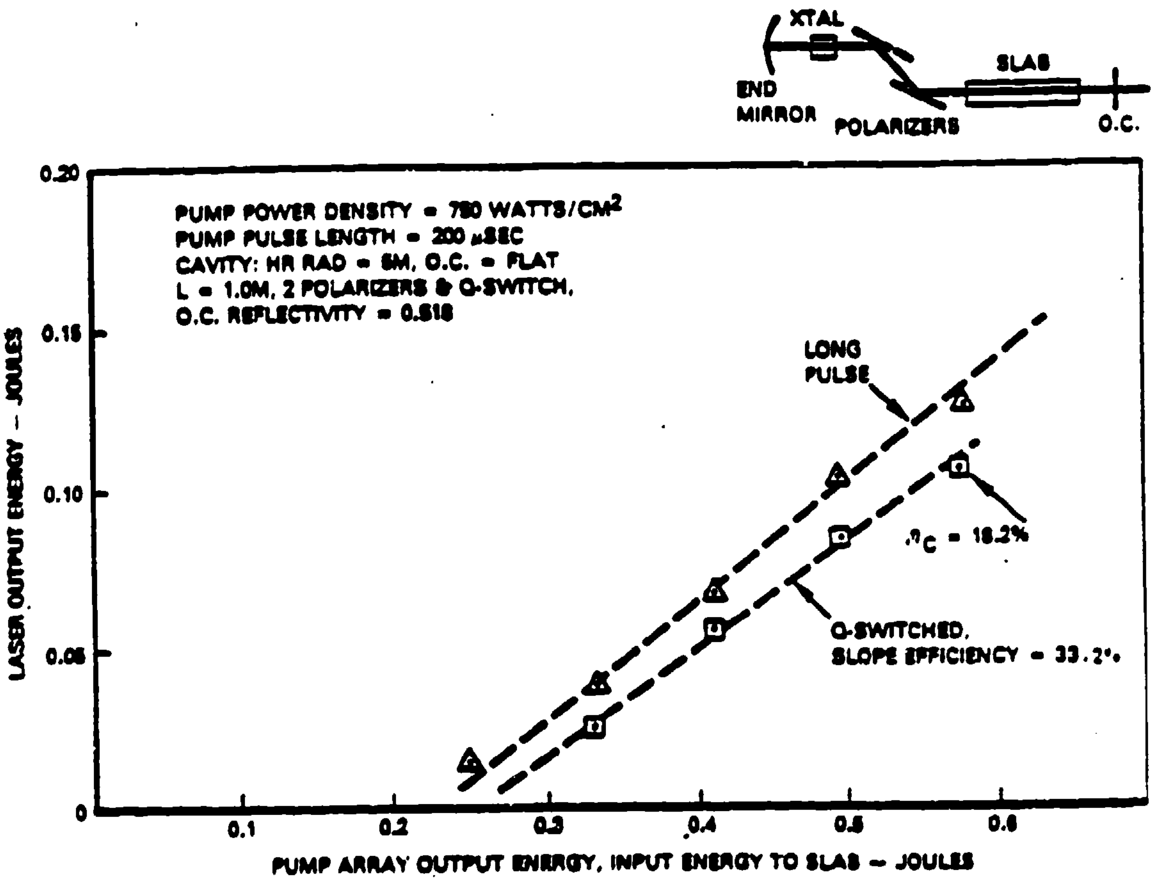


Figure 4.19 Q-switched and long-pulse slab performance (From Reference 4.5)

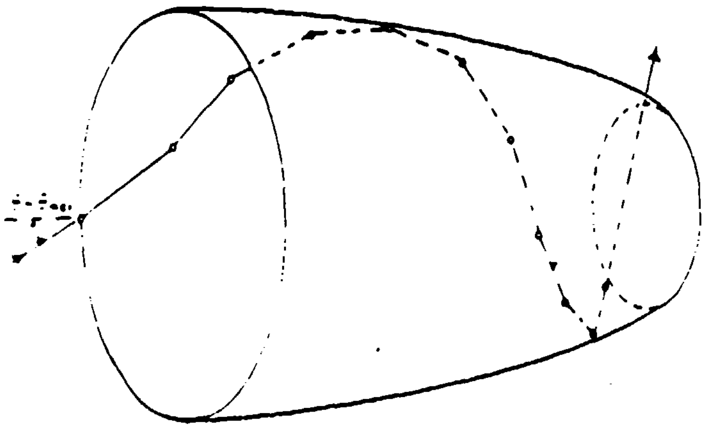

Figure 4.20 Path of a ray striking the surface of a CPC almost tangentially. (Ref. 4.6)

The ideal light collector is a non-imaging reflecting wall light chann that concentrates a divergent beam of light by the maximum amount allowed b physical principles.

Figure 4-21 illustrates the concept with two arrays and two concentrat being used with a single slab.

Compound Parabolic Concentrators (CPC's) in both troughlike and coneli geometries have been built and tested for solar applications. Such devices can achieve a concentration ratio (entrance area/exit area)

$$x = n/\sin\theta_{max} \qquad \text{(trough)}$$

$$x = n^2/\sin^2 e_{max} \qquad \text{(cone)}$$

where $\theta_{max}$ is the angular acceptance (half angle) and n is the index refrac tion of the collector relative to the surrounding medium.

Each CPC has a maximum acceptance angle, i.e., an angle beyond which s or all of the radiation entering the concentrator is multiply reflected and thereby not passed by the CPC. This radiation is returned back to the diod array and doesn't reach the slab.

## 4.4 PERFORMANCE MODELING

In order to determine the power or energy requirements of the laser di array for a desired output, the laser efficiency must be known. In this section, we will define the principal elements of a laser diode pumped soli state laser that contributes to overall efficiency.

Figure 4.21 Slab laser pumped by two diode laser arrays which are coupled to the slab by two CPCs.

(Ref. SAIC proposal "Semiconductor Diode Pumped Solid State Lasers, August 1986)

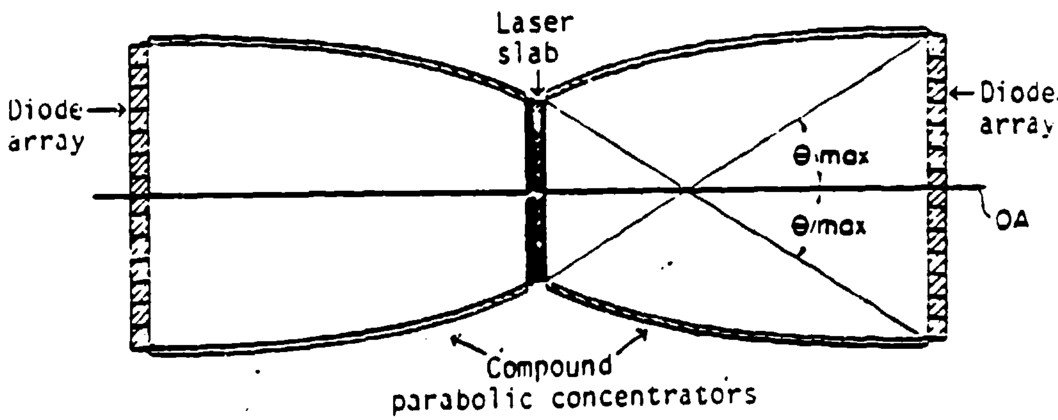

### 4.4.1 Energy Conversion Efficiencies

The energy transfer from electrical input to the laser diodes to laser output from the solid state medium can conveniently be expressed as a three step process:

- o Conversion of electrical input to the laser diode array to pump radiation. This will be expressed as the laser diode efficiency $\eta$
- o Transfer of pump radiation to energy in the upper laser level of th gain medium (upper state efficiency $\eta_u$).
- o Conversion of the stored upper state energy into useful laser outpu (expressed as output efficiency $_{out}$).

With the definitions given above, we can write

$$E_{out} = \eta_o \; \eta_u \eta_{out} E_{EL} \qquad (1)$$

where $E_{out}$ is the laser output and $E_{EL}$ is the electrical input into the di arrays.

Each of the efficiency factors given above include several contributi elements and steps which are involved in the pump and lasing process. The parameters which determine these efficiencies will be discussed below and specific examples will be given.

a) Laser diode efficiency

From the standpoint of the laser designer the parameter $\eta_D$ is a given and depends on the fabrication process of the laser diodes or arrays.

The rate of change of the upper laser level, assuming no stimulated emission, is given by

$$\frac{dN_u}{dt} = N_l W_p - \frac{N_u}{\tau_{sp}} \qquad (2)$$

where $N_u$ and $N_l$ are the population densities of the upper and ground state, $W_p$ is the pumping rate and $\tau_{sp}$ is the spontaneous decay rate of the upper level.

In steady state the upper level population density is given by

$$N_u = N_l W_p \tau_{sp} \tag{3}$$

The stored energy density in the upper laser level is

$$E_s = h\nu_L N_u \tag{4}$$

where $h\nu_L$ is the energy per photon of the solid state laser output.

The upper state population density and pumping rate can be related to the total absorbed pump power $P_{abs}$.

It is $$P_{abs} = N_l W_p h\nu_D V \tag{5}$$

where $h\nu_D$ is the energy per photon of the laser diode pump, and V is the volume of the solid laser medium.

Combining equations (2) and (3) and substituting N $W_p$ from equation (4) yields for the stored energy density

$$E_S = \left(\frac{h\nu L}{h\nu_D}\right)\left(\frac{\tau sp}{V}\right)P_{aBS} \tag{6}$$

The pump power absorbed in the solid state laser is related to the laser diode output power $P_D$ as follows:

$$P_{ABS} = P_D\ (1-e^{-\alpha D l})(1-r) \tag{7}$$

where $\alpha_D$ is the absorption coefficient of the diode wavelength in the solid state medium, $l$ is the path length of the pump radiation in the medium, and r summarizes the reflection losses occurring between the pump source and the solid state medium.

If we introduce equation (7) into (6) and note that

$$P_D = E_D/t_D$$

where $E_D$ and $t_D$ are the laser diode energy per pulse and pulse length, respectively we obtain

$$E_{ST} = \left(\frac{HVL}{HVD}\right)\left(\frac{\tau_{SP}}{t_D}\right)\left(1-e^{-\alpha D t}\right)(1-r)E_D \qquad (9)$$

Instead of the energy density we introduce $E_{ST}$ which is the total ener stored in the upper level

$$E_{ST} = E_S V \qquad (10)$$

We will examine briefly the terms of equation (9). The first term is Stokes efficiency which accounts for the photon energy ratio of the laser a pump emission

$$\eta_V = hV_L/hV_D \qquad (11)$$

The second term expresses the fraction of pump power remaining prior extraction by the Q-switched pulse

$$\eta_P = \tau_{SP}/t_D \qquad (12)$$

For a pump pulse longer than the fluroescence lifetime, gain is reduc because of the depletion of the upper level by spontaneous emission. The two terms in equation (9) determine the transfer efficiency from the pump array into the active medium.

$$\eta_T = (1-\exp(-\alpha_D l)(1-r) \qquad (13)$$

A high efficiency is achieved by making the slab thick enough to absorb the diode radiation, even in the presence of tempertature variations in the array. Reflection losses and spillover losses at the edges of the active medium expressed by the parameter r have to be minimized for efficient transfer of energy. Equation (9) can now be expressed as follows

$$E_{ST} = \eta_V \eta_P \eta_T \eta_Q E_D \qquad (14)$$

or

$$E_{ST} = \eta_u E_D \qquad (15)$$

We did add into the above equation the quantum efficiency $\eta_Q$ which expresses the fraction of pump photons reaching the upper laser level.

b) Output Efficiency

Conversion of the stored upper state energy into useful laser output depends on the following factors:

The spatial overlap of the resonator modes with the upper state inversion density this is usually expressed by the beam fill factor $\eta_B$. Losses due to amplified spontaneous emission (ASE) will reduce the available stored energy. ASE losses can be taken into account by a factor $\eta_F$.

In Q-switched operation, the amount of stored energy extracted by the pulse depends on the inversion above threshold as shown in Figure 4-22. We will express the fraction of energy extracted by $\eta_{EX}$. Optical losses L in the resonator due to scattering, absorption or reflection further diminishes the laser output. It is

$$\eta_R = \frac{1}{1 + L/(1-R_1)} \qquad (16)$$

where $R_1$ is the reflectivity of the output mirror. The efficiency factors discussed above can be grouped together

$$\eta_{OUT} = \eta_B \eta_F \eta_{EX} \eta_R \qquad (17)$$

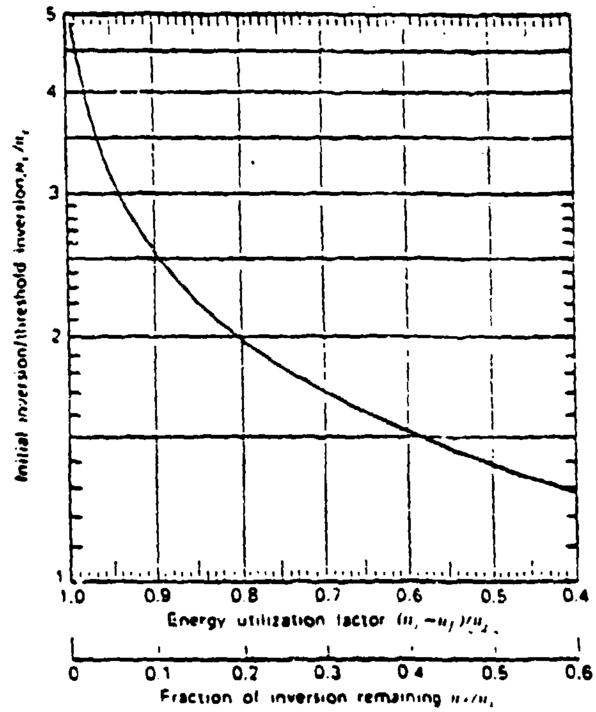


Figure 4.22. Fractional extraction efficiency for a Q-switched laser oscillator vs the number of times above threshold.

Therefore

$$E_{OUT} = \eta_{OUT} \; E_{ST} \tag{18}$$

After having discussed the various steps involved in the pump chain of a laser diode pumped solid state laser, we will give specific examples for Nd:YAG lasers and compare different pump geometries with respect to these factors.

### 4.4.2 Comparison

Table 4-5 lists the individual efficiency factors, discussed in the previous section, for an endpumped, cylindrical and slab Nd:YAG laser. We will first discuss the factors which are independent of the particular pump geometry. The quantum efficiency of 24 percent was chosen, because the arrays incorporated in MDAC's slab laser operate at this efficiency. More recently, linear arrays based on GRIN-SCH technology produced by MDAC's research facility have efficiencies between 45 and 50 percent. Clearly, with the incorporation of these arrays into Nd:YAG lasers, the system overall efficiency listed on the bottom of Table 4-5 will double.

Laser diode pumped solid state lasers with overall efficiencies of 10 percent and above are within reach. The Stokes efficiency $\eta_V = 0.76$ is the energy differrence between the 807 nm pump photon and the 1.064 $\mu$m laser photon. The quantum efficiency $\eta_Q$ for Nd:YAG is between 0.6 and 0.8 according to recent measurements by Shazer (4.7). In the pulsed mode, the diode arrays are switched on the off at a time shorter or equal to the fluorescence lifetime of 230 $\mu$sec, therefore $\eta_p = 1$. In the case of cw or long pulse mode operation, ASE losses are zero and the extraction efficiency is very high as indicated in the table.

The major differences between the three designs, as far as efficiency is concerned, are in the area of beam fill factor, resonator losses and pump transfer efficiency.

Table 4.5 Pump Geometry and Conversion Efficiency Factors For Laser Pumped Nd:YAG Laser

| | | Endpumped Geometry | | | Sidepumped Cylindrical Geo. | | | Long Pulse Side Pumpsed Slab | | | Q-Switched Side Pumped Slab | | |
|---|---|---|---|---|---|---|---|---|---|---|---|---|---|
| Diode Efficiency | $\eta_D$ | .24 | | | .24 | | | .24 | | | .24 | | |
| tokes Efficiency | $\eta_v$ | .76 | Upper State Eff 0.60 | Optical Conversion Eff. 0.36 | 0.76 | Upper State Eff. 0.54 | Optical Conversion Eff. 0.34 | .76 | Upper State Eff. 0.58 | Optical Conversion Eff. 0.27 | .76 | Upper State Eff. .57 | Optical Conversion Eff. .18 |
| uantum Defect | $\eta_Q$ | .80 | | | .80 | | | .80 | | | .80 | | |
| epletion Eff. | $\eta_P$ | 1.0 | | | 1.0 | | | 1.0 | | | 1.0 | | |
| ransfer Eff. | $\eta_t$ | .98 | | | .90 | | | .95 | | | .95 | | |
| eamfill Factor | $\eta_B$ | .90 | Output Eff. 0.60 | | .85 | Output Eff. 0.67 | | .75 | Output Eff. 0.46 | | .75 | Output Eff. .33 | |
| SE losses | $\eta_F$ | 1.0 | | | 1.0 | | | 1.0 | | | .85 | | |
| xtraction Eff. | $\eta_{EX}$ | 0.95 | | | .95 | | | .95 | | | .8 | | |
| esonator Losses | $\eta_R$ | .70 | | | .80 | | | .65 | | | .65 | | |

Clearly the endpumped configuration has the highest beam fill factor due to an almost complete overlap of the collinear pump beam and the resonator modes. Beam fill factor is worse in the slab laser due to pump radiation spill-over, edge effects etc. which are characteristics of a rectangular pump geometry. The value of $\eta_B = .75$ is an estimate, based on the gain profile measurement presented in Reference (4.5). Also the slab design has high optical losses as compared to the other configurations, mainly as a result of scattering losses occurring due to the many bounces at the pump faces.

Introducing a reflectivity of R = 75.6 percent and a measured optical single pass loss of L = 6.3 percent (Reference 4.5) into equation 16 yields $\eta_R = 0.79$. In addition, the report mentioned that substantially higher order mode diffraction losses occurred in the rectangular slab. The value of $\eta_R = .65$ is an estimate adjusted to yield the measured overall efficiency of 6.4 percent. With the exception of reflection losses at optical surfaces such as windows or the laser medium, and spill over of pump radiation, the transfer efficiency is mainly determined by the absorption of pump radiation in the Nd:YAG crystal.

For laser diode pumping of Nd:YAG, the absorption band from the ground state to $^4F_{5/2}$ and $^2H_{9/2}$ manifold states is of interest.

The absorption coefficient of Nd:YAG for the transition from $^4I_{9/2}$ to $^4F_{5/2}$ and $^2H_{9/2}$ is shown in Figure 4-23.

For a spectral width of about 20 Å the absorption coefficient is $\bar{\alpha} \geq 3.8 cm^{-1}$. For a bandwidth of 54 Å, $\alpha$ is at least 2.6 $cm^{-1}$ and the average absorption coefficient is $\alpha = 3.2 cm^{-1}$.

The pump power absorption coefficient for nominally 1 percent doped Nd:YAG at 807 nm can be assumed to be $\bar{\alpha}_D = 3.2\ cm^{-1}$ in a 54 Å wide band.

Figure 4.23   Absorptivity of Nd:YAG near 810 nm
(Ref. B. Zhou et al, Optics Lett. vol. 10, 1985, P. 62)

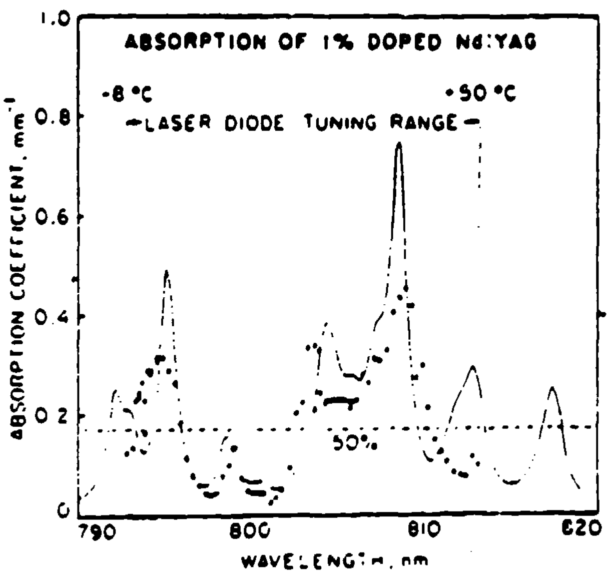

We have chosen this value, because the diode arrays in the MDAC laser had a bandwidth of 40 A FWHM. The fraction of laser diode power absorbed vs. Nd:YAG thickness is listed below:

| $l$/cm | $\eta_T$ |
|---|---|
| 0.4 | 0.72 |
| 0.6 | 0.85 |
| 0.8 | 0.92 |
| 1.0 | 0.96 |

The Nd:YAG slab of the MDAC laser is 0.67 cm thick and has a high reflectance coating on the backface. Therefore virtually all diode laser energy is absorbed. Since the pump face and window are AR coated we think $_t$ = .95 is a good estimate for the transfer efficiency. The 5 percent loss accounts for residual reflections on the window and slab surface, small spill-over losses of radiation not entering the slab, and some radiation absorbed by the back reflector. The endpumped configuration, due to the long path, has excellent transfer efficiency. The sidepumped geometry is not quite as efficient in this respect. In order to obtain the necessary inversion for high output power, the rod should not have a diameter larger than 4 or 5 mm.

If one mounts the Nd:YAG rod in a semicylindrical heat sink with backreflector as shown in Chapter 7, then the path length is doubled and about 90 percent absorption of pump radiation should be possible.

We will now turn our attention to the Q-switched performance of the slab.

The extraction efficiency of the stored energy increases with the number of times about threshold gain as shown in Figure 4-22. For example, at two

times threshold, the extraction efficiency reaches 80 percent. The round gain at threshold is given by

$$1 = R_1 R_2 e^{2gl-2\alpha l}$$

where $l$ is the length of the gain medium and $\alpha$ is the optical loss coefficient, $R_1$ and $R_2$ are the reflectivities of the front and rear mirror. Fro equation follows the threshold gain coefficients:

$$g_{th} = \frac{2l\alpha - \ln R_1 R_2}{2l}$$

Using again the MDAC slab laser as example, we insert the following parameters given in Reference 4.5 into the equation above:

$2l\alpha = 0.126$ round trip absorption and scattering losses

$R_1 = 51.8$ percent

$R_2 = 1.0$

$l = 8.9$ total pump length in the zig-zag path.

With these system parameters one obtains

$g_{th} = 0.044\ cm^{-1}$

From Figure 4-19 follows that the system is pumped 2.4 times above threshold, which yields

$g_{max} = 0.10\ cm^{-1}$

The single pass gain $G_0 = \exp(gl)$ is therefore $G = 2.4$.

This value is in good agreement with the measured data Figure 6-3 of Reference 4.5.

In Nd:YAG a 1 percent gain per cm requires a stored energy density of $E_S = 0.0031$ J/cm$^3$. (Reference 4.8)

Therefore at $G_{max}$ the stored energy density is

$$ES_{max} = 0.031 \text{ J/cm}^3$$

There is an upper limit of the gain coefficient which can be achieved in Nd:YAG before ASE starts to deplete the upper level. This becomes a problem usually if the single pass gluing $G = \exp(gl)$ exceeds about 50, or $gl = 4$. The product of gain coefficient times the path length in the slab for the 100 mJ laser is well below the ASE limit.

We will conclude this section by summarizing the salient performance features for the pump geometries described in this chapter.

The largest payoff for all designs is an increase in diode efficiency. In the case of the slab laser, a higher diode efficiency will not only increase system efficiency but also allow higher average outputs, because planar arrays have a power dissipation problem which limits their average power handling capability.

From a systems point of view, the relatively low beam fill factor and optical losses of the slab laser need improvement. In the sidepumped cylindrical system, absorption of pump power in small rods even in the presence of a back reflector is not as high as in the other systems. Optical losses in an end pumped configuration are important because at the lower power and therefore low gain in these devices, reesidual optical losses are particularly detrimental to laser performance.

From the standpoint of output power and energy the end pumped geometry is limited to about one watt or less of output. For a laser requiring large pulse energies, the high power density afforded by planar arrays is needed.

We will conclude this section by summarizing the salient performance features (besides efficiency) for the three various pump geometries described in this chapter.

In the slab laser the higher beam fill factor and the optical losses are the key areas which need improvement from the design standpoint. The largest payoff in all designs is an increase in diode efficiency.

Due to the small pumping area, the end pumped system is limited to about one watt.

The slab is capable of high energies per pulse. The side pumped cylindrical rod yields high average power at less cost and complexity. For high energy per pulse, the high pump flux afforded by planar arrays is needed.

For cw power operation or high repetition rate operation where not much energy per pulse is required, the side pumped cylindrical rod yields the same or better performance than the slab laser at less cost and complexity.

Figure 4-24 shows the projected power and energy regimes of the pump configuration discussed here.

A side pumped slab laser is clearly the choice for obtaining high pulse energies. Heat dissipation from the planar arrays limits the average power. A slab laser with flux concentrator is capable of higher average power compared to direct pumping, since the concentrator allows to spread the arrays over larger area. Since planar arrays are limited by heat extraction, linear arrays employed in side pumped cylindrical configurations are just as powerful and can even exceed planar arrays. If a sidepumped cylindrical laser is repetitively Q-switched, pulse energies of up to 4 mJ can be obtained with

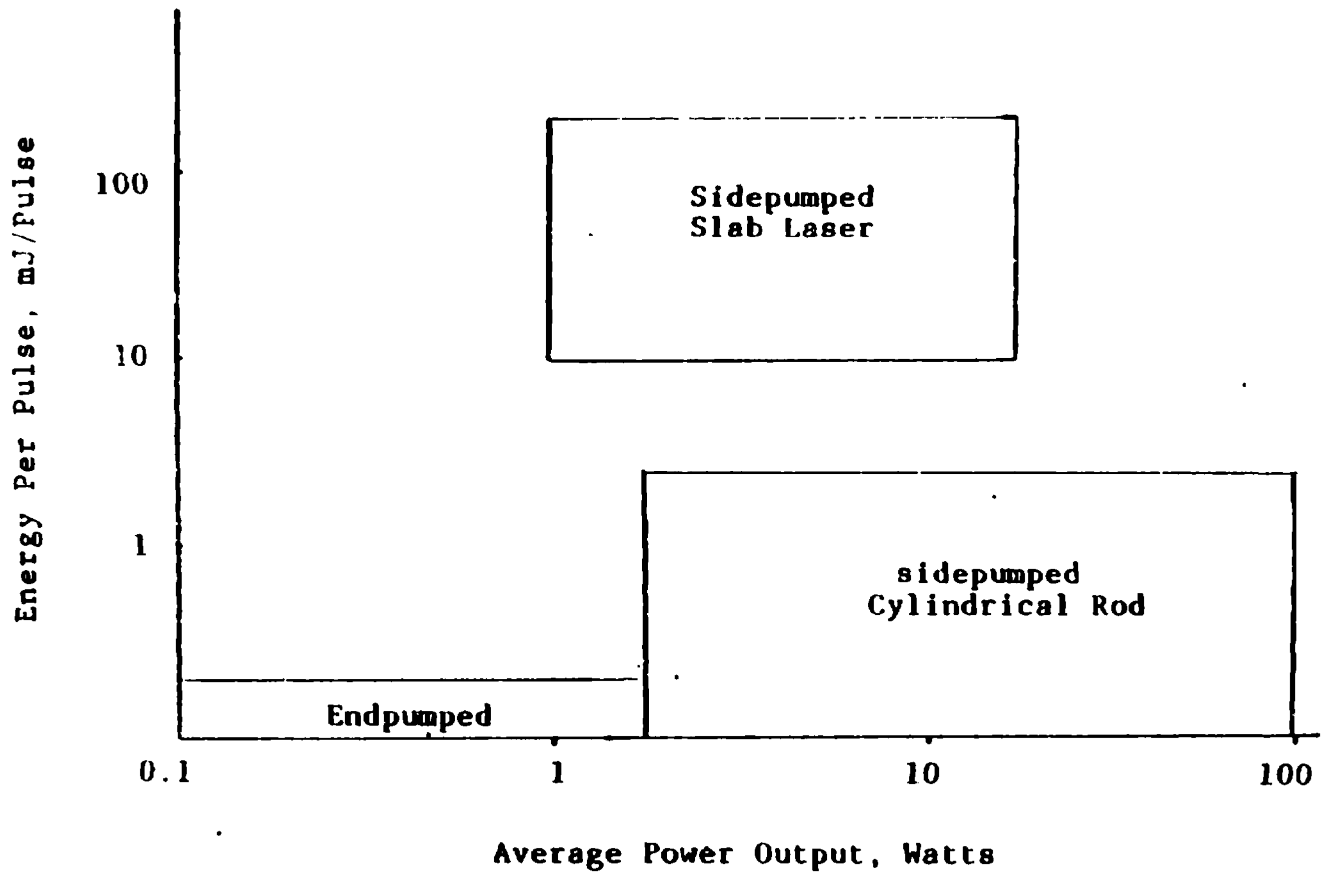


Figure 4.24 Comparison of the current performance of different pump configurations

commercially available linear arrays. This would be for a pump system consisting of 20 linear arrays of 5W output each generating 20W average po· from the laser. At a 5KHz repetition rate, one obtains 4 mJ/pulse.

# References

4.1 D.L. Sipes, Appl. Phys. Lett., Volume 47, July 1985, p. 74

4.2 B. Zhou, T.J. Kane, G.J. Dixon, R.L. Byer, Optics Letters, Vol. 10, February 1985, p. 62.

4.3 Henry Kressel and J.K. Butler, "Semiconductor Lasers and Heterojunction LEDS," Academic Press, 1977.

4.4 Martin, W.S. and Chernoch, J.P., 1972, Patent Number 3,633,126, "Multiple Internal Reflection Face Pumped Laser."

4.5 McDonnell Douglas, Technical Report N66001-83-C-0071, 17 April 1986, prepared for NOSC.

4.6 W.T. Welford, R. Winston, "The Option of Nonimaging Concentrators," Academic Press, 1978.

4.7 L. DeShazer, Private Communication

4.8 W. Koechner, Solid State Laser Engineering, Springer Verlag, 1976.

## 5. COOLING TECHNIQUES (Task 4)

In Section 5.1 we will address the problem of achieving compact, high performance forces liquid cooling of planar and linear arrays. The advent of high-density planar arrays with power densities of $1kW/cm^2$ per pulse implies the requirement for effective and compact heat removal if high repetition rates are to be achieved.

We will show that by scaling liquid-cooled heat exchange technology to microscopic dimensions, an improvement of a factor of five should be feasible, i.e. the thermal impedance can be reduced from about 0.5 $^{o}C/W/cm^2$ characteristic of current design to 0.1 $^{o}C/W/cm^2$.

In Section 5.2 we investigate heat dissipation and cooling of the diode pumped active medium. The thermal load of a diode pumped laser is considerably less than for flashlamp pumping. In order to take advantage of the low heat load, conductive cooling of the active medium is very desirable. Details of efficient heat conduction techniques for laser diode pumped slab or cylindrical solid state materials will be presented.

### 5.1 HIGH PERFORMACNE HEAT SINKS FOR DIODE LASER ARRAYS

Adequate cooling of the crystal laser arrays is required for several reasons. At around room temperature the life of a typical diode laser decreases by a factor of two for every seven to ten Celsuis degrees of increase in temperature. The emission wavelength of the diode lasers changes with temperature, and for some laser materials that have very narrow pumping bands, this may impose strict requirements on the tempeature stabilization function of the cooling system. Temperature also affects the threshold current and efficiency of the arrays.

The thermal design of a diode laser pump system depends very strongly on the kind of opeating mode. Because of power and space limitations, diode laser pump systems opeating in the pulse mode with low duty cycle will always

produce low average heating rates. Under this condition the design is not that critical in terms of reduction of thermal impedances. The situation much more difficult when the system operates in the cw mode. Here the mir zation of thermal impedances is of paramount importance, and it is therefc required to resort to some unconventional designs that will be presented in this section.

In a diode laser the heat source is mainly concentrated in the active layer region and around the intersection of this layer with the facets. ( heating is distributed along the current path through the crystal and over contact areas. In a well designed device this heating source is not the r important and can be ignored. Figure 5-1 shows the different media and components in the path of the heat flow from the active layer to be coolar and Figure 5-2 shows a blow-up of a particular diode laser design, taken Reference 5.1, describing similar details.

From the point of view of the designer the diode laser can be fully characterized by its geometry, thermal impedance and heat dissipation rate Given a particular laser design these parameters can be determined by mea: ments or calculations. An example of the latter method is presented in Reference 5.1 for the determination of the diode thermal impedance. Cons dering the particular design shown in Figure 5.2, the authors calculated the junction-down configuration a thermal impedance of 20.6 K/W, and for junction-up (with the substrate on the heat sink) they determined a value 82.9 K/W. It is reasonable to assume that a stripe of the dimensions show Figure 5-2 could provide an output of about 50 mW with an efficiency of 4( percent. In this case, the power dissipated by the diode would be about and the temperature at the junction would be, for the junction-down mount $20.6 \times 0.075 = 1.54\ ^{o}C$ larger than at the bound layer, which is not very significant. For a pulsed system it may also be important to determine t! relaxation time of the active layer temperature. However, for a typical diode, this is in the order of 10 to 100 ns, and since for the majority o applications the pulse length required is larger than about 100 s, this relaxation time can be ignored.

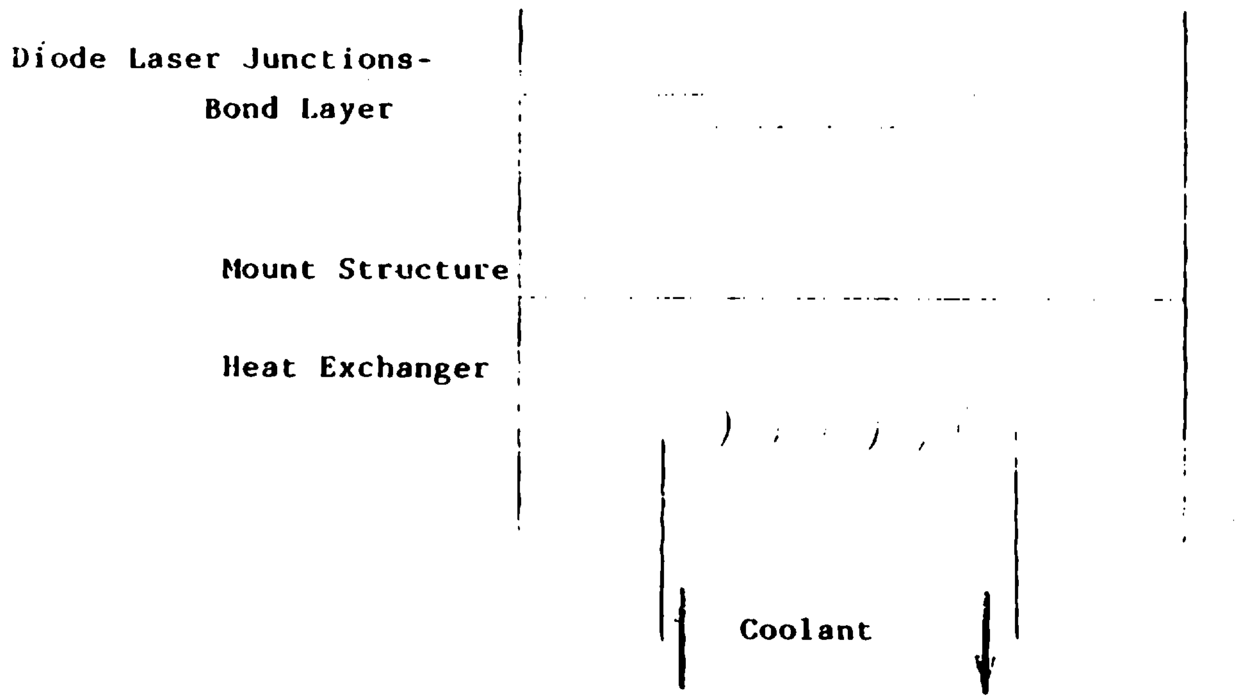


Figure 5.1 Schematic of Heat Sink Structure for Cooling of Laser Diode Arrays

Figure 5.2 Stripe geometry DH laser dimensions and layer conductivities (Reference 5.1)

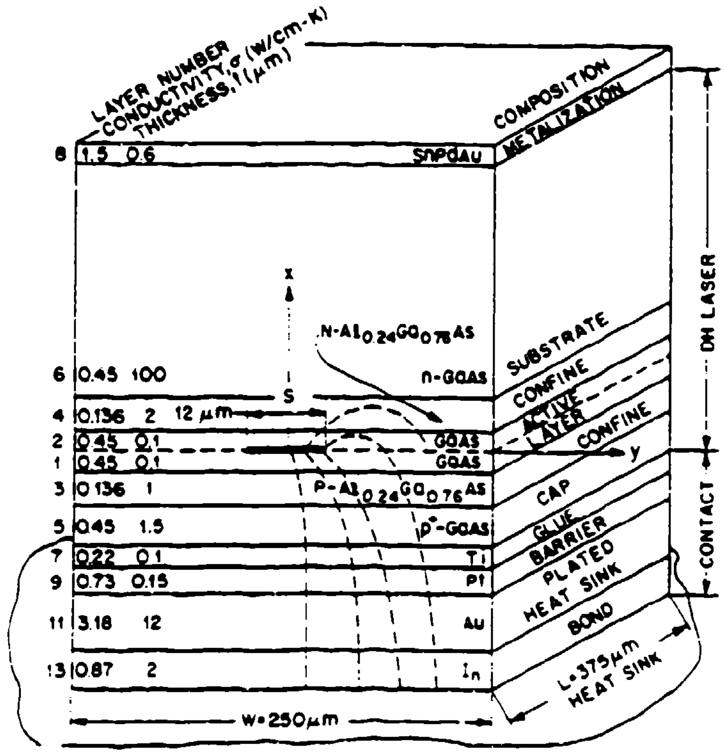

The heat sink design that has been selected most often in the past for several proposed or built systems operating in the pulsed mode involved mounting the diode in metallized BeO slabs that are stacked together and attached to a heat exchanger or are bonded directly to grooves cut on the surface of the heat exchanger (see Figure 5-3). BeO has a high thermal conductivity (half as large as that of copper) and being an electrical insulator has the advantage of simplifying the overall assembly. Furthermore, it has a thermal expansion coefficient not much larger than that of GaAs and therefore it does not generate as much thermal stresses in the diode laser as copper for example. However, for high average power applications, where the need to reduce thermal impedances requires mounting the diodes directly on the heat exchanger, other materials and design concepts are required. The rest of this section will be devoted to a presentation and performance analysis of these other design options.

Most of the diode laser linear arrays currently in the market are mounted directly on copper sinks using a soft bond material such as indium. A soft material is required to limit the thermal stresses produced by the large difference in thermal expansion coefficient between copper and GaAs. Indium also has the advantagte of melting at low temperatures, therefore reducing the possibility of thermally damaging the diode lasers during mounting. These thermal sinks are of large dimensions as compared to the size of the array to reduce the thermal impedance of the assembly. Type II diamond has a thermal conductivity five times as large as that of copper and its use as a heat spreader has been suggested in order to further reduce that impedance (see Reference 5.2). The use of a silicon submount as a buffer layer to absorb the thermal strain differential between the diode and a copper heatsink has also been suggested in the past and a recent study (Reference 5.3) has shown to produce the desired effect when this submount is adequately sized. However, silicon has a low thermal conductivity, and its use can severely degrade the thermal performance of the whole assembly.

Area arrays built by stacking linear arrays mounted on copper slabs, such as illustrated in Figure 5-3, have to be cooled by contact with a heat exchanger. A high performance heat exchanger capable of handling fluxes of up

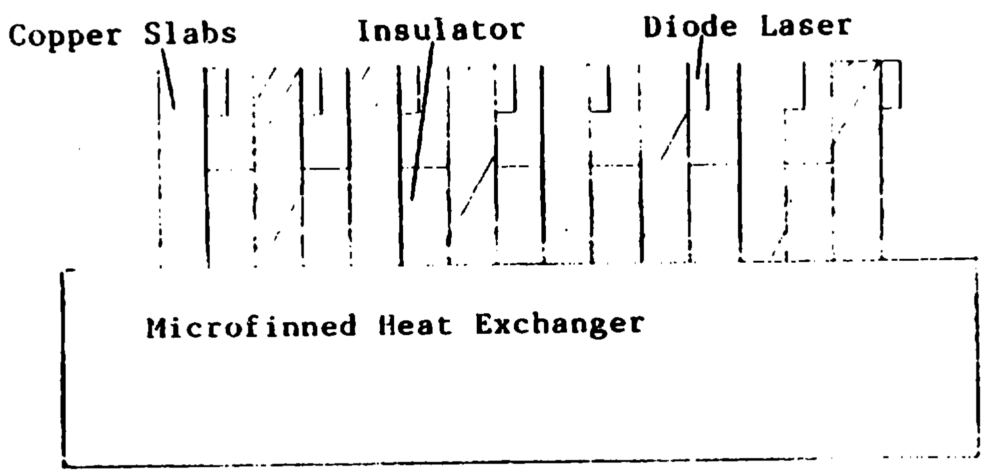


$$\theta_{Slab} = \frac{H}{k_w\ t\ L} = (2.5 - 8.3)\,^{o}C/W$$

$L = 1$ cm

$H = 0.3 - 1$ cm

$\theta_{ex} = 0.1\ ^{o}C/W/cm^2$

$k_w = 4\ W/cm/^{o}C$

For a 20 element/cm stack:

$\theta_{st} = 0.125 - 0.47\ ^{o}C/W.cm^2$

$\theta_{ex} = 0.1\ ^{o}C/W.cm^2$

$\theta_{tot} = 0.225 - 0.57\ ^{o}C/W/cm^2$

to 100 W cm$^2$ and having a thermal impedance of about 0.1 $^{o}$C/W for a 1 cm$^2$ area have been demonstrated (Reference 5.4). Figure 5-4 shows the basic design of this heat exchanger. A cooling configuration as shown in Figure 5-3 could have at best a thermal impedance of about 0.22 $^{o}$C/W for a 1 cm$^2$ area without consideration of the thermal impedance of the diodes and bond layer. If the maximum allowed temperature at the bonding layer is 60$^{o}$C and the water temperature is 20$^{o}$C then the maximum heat dissipation allowed would be 180 W. For diode laser arrays with an efficiency of 40 percent this would correspond to a maximum of 120 W/cm$^2$ of pumping radiation flux in the cw mode. Considering again the design of Figure 5-3 this would correspond to linear arrays producing 6 W/cm. State-of-the-art linear arrays can operate in the cw mode at levels several times that level of output. Current developments point to the feasibility of arrays operating reliably and with acceptable life at cw output levels of 25 W/cm.

Obviously, new concepts for the mounting and cooling of these arrays have to be developed.

The design of Figure 5-3 fails in providing the low thermal impedance required for high flux area arrays because of the long distance between the thermal source and the coolant channels. A considerable reduction of this impedance can be achieved if the coolant channels are placed immediately under the bond layer as illustrated in Figures 5-5 and 5-6. In these designs the diodes are mounted directly on miniature heat exchanger(s) that can be very conveniently stacked. Figure 5-7 shows a constructional detail for the kind of mount that has been proposed here. A simplified thermal analysis for this design are coalesced into a single one occupying the same width as all of them together and having the same opening. The area of contact with the coolant for this larger passage is still about the same as for the original passages taken together. As a simplifying assumption the convective heat-transfer

Figure 5.4 High performance heat exchanger
(Ref. R. Byer, private communication)

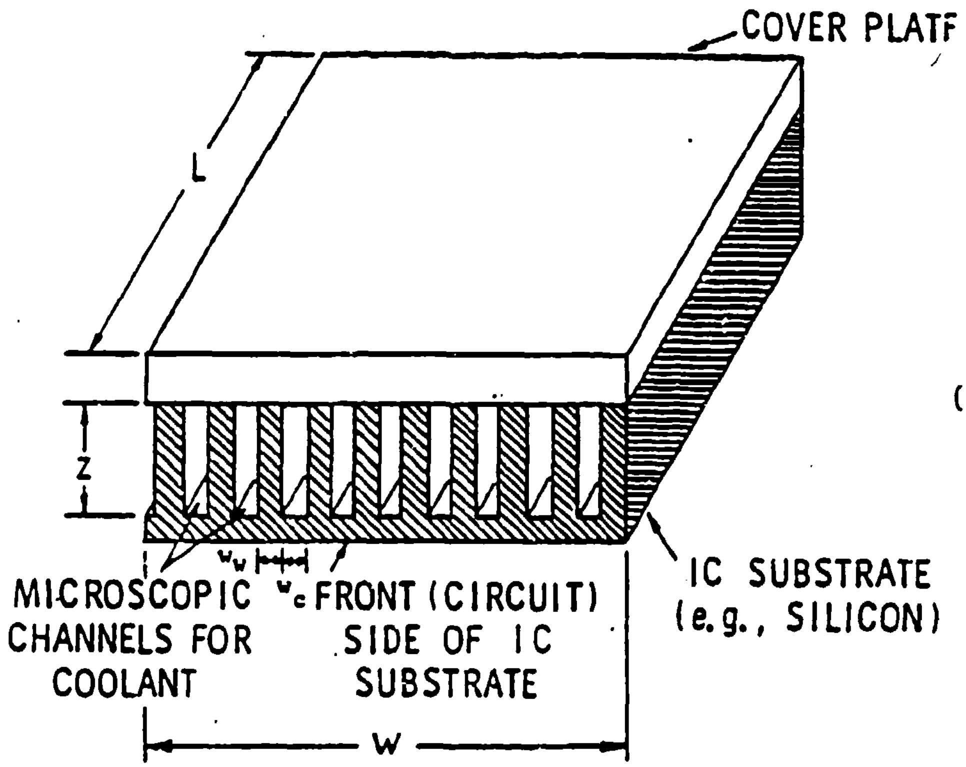


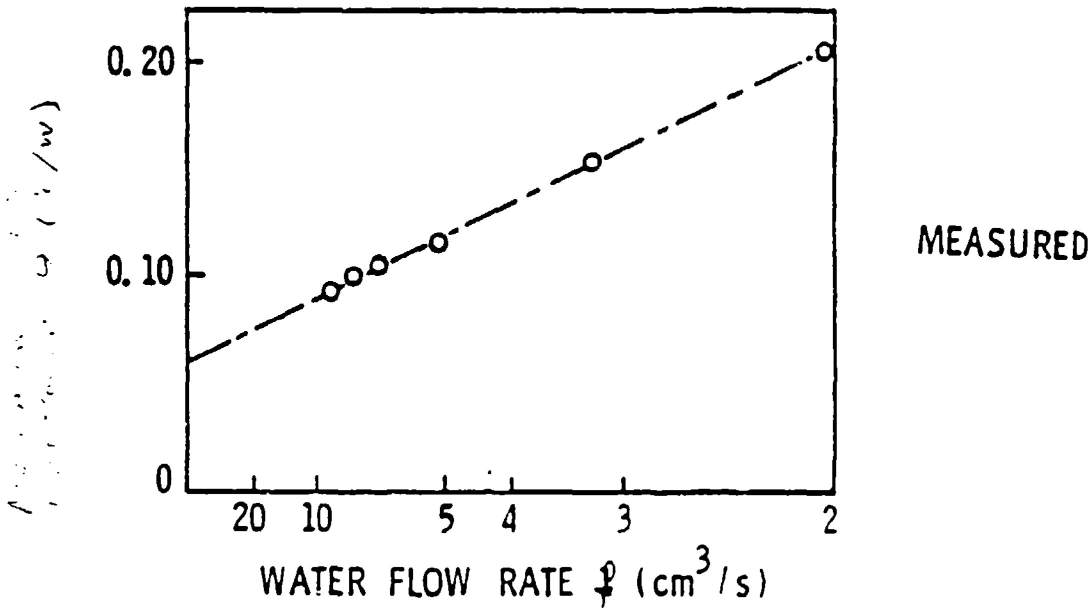

SIDE MOUNTING

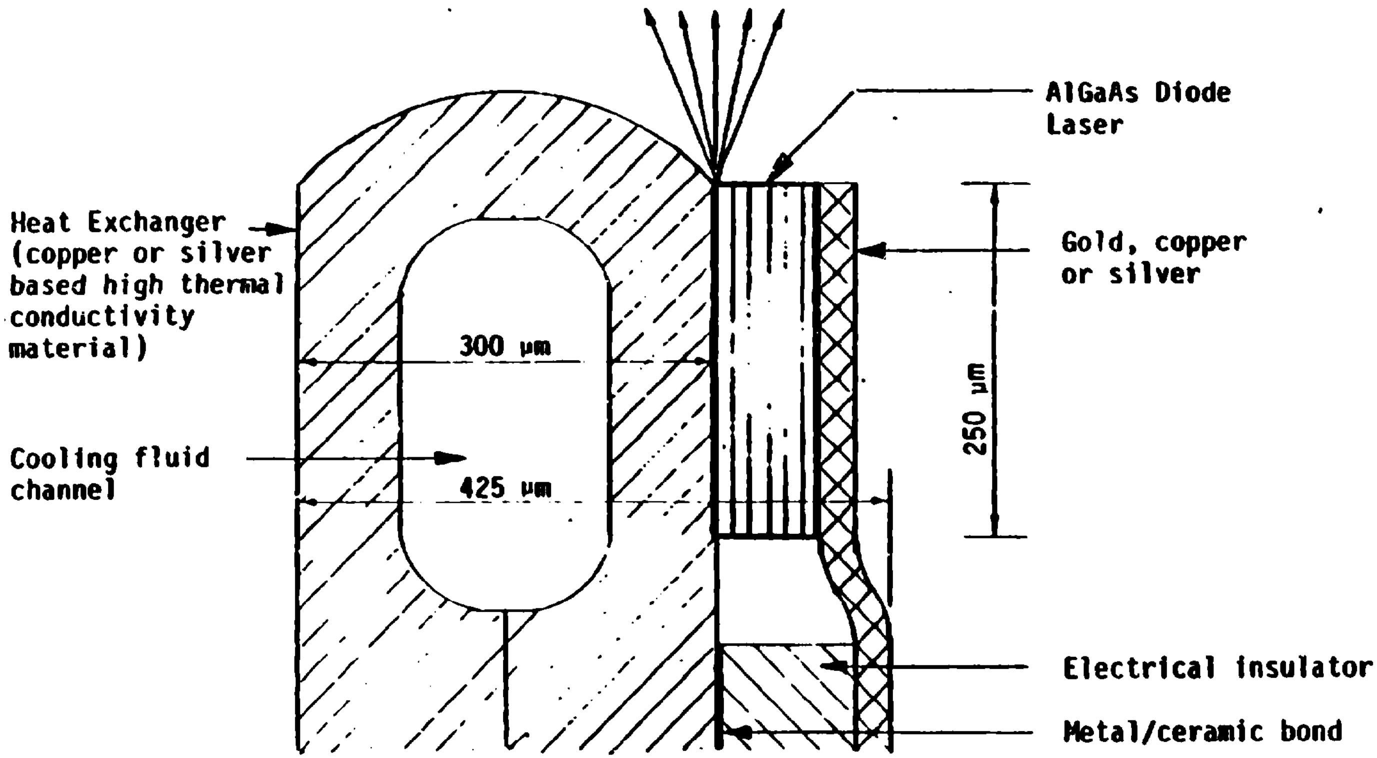


Figure 5.5 Proposed heat sink design

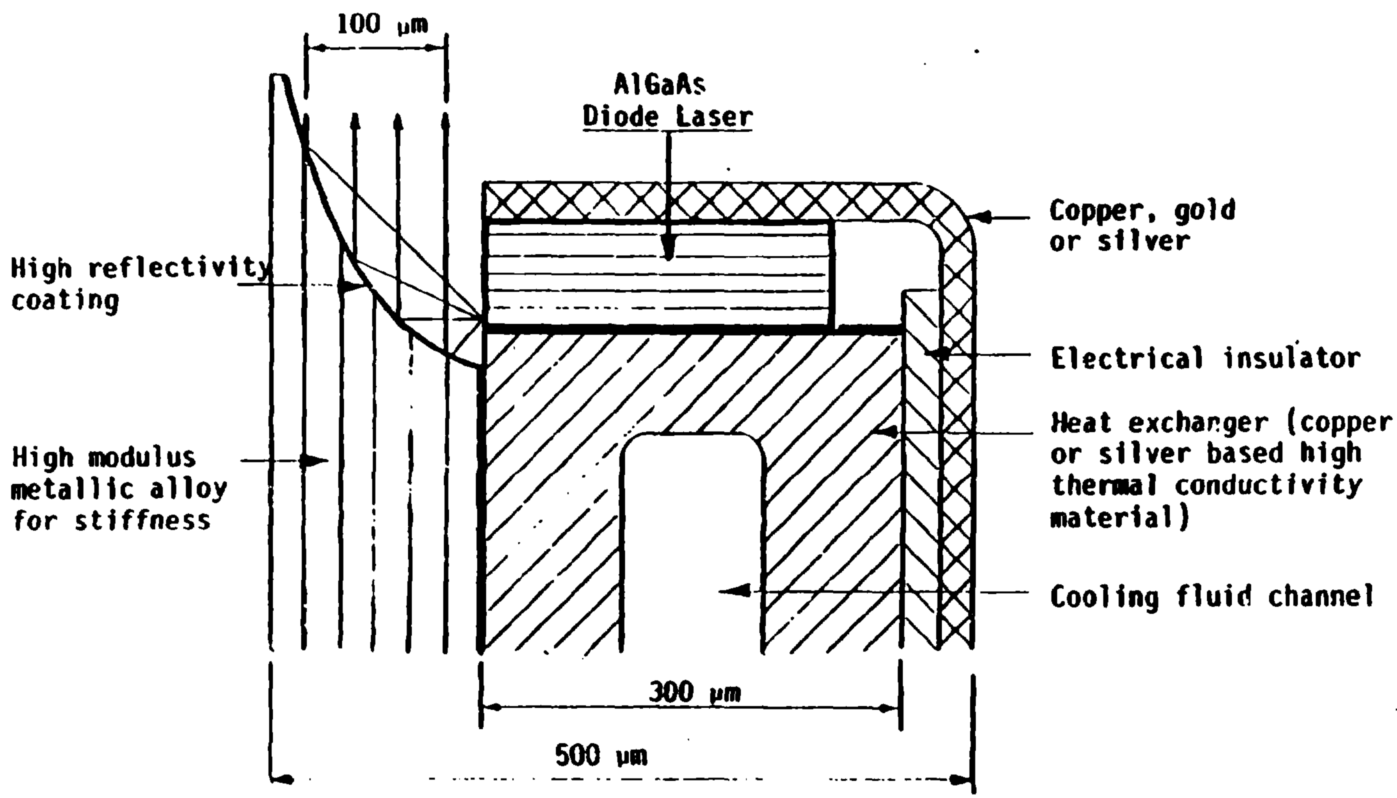


Figure 5.6 Heat sink design with beam deflecting mirror

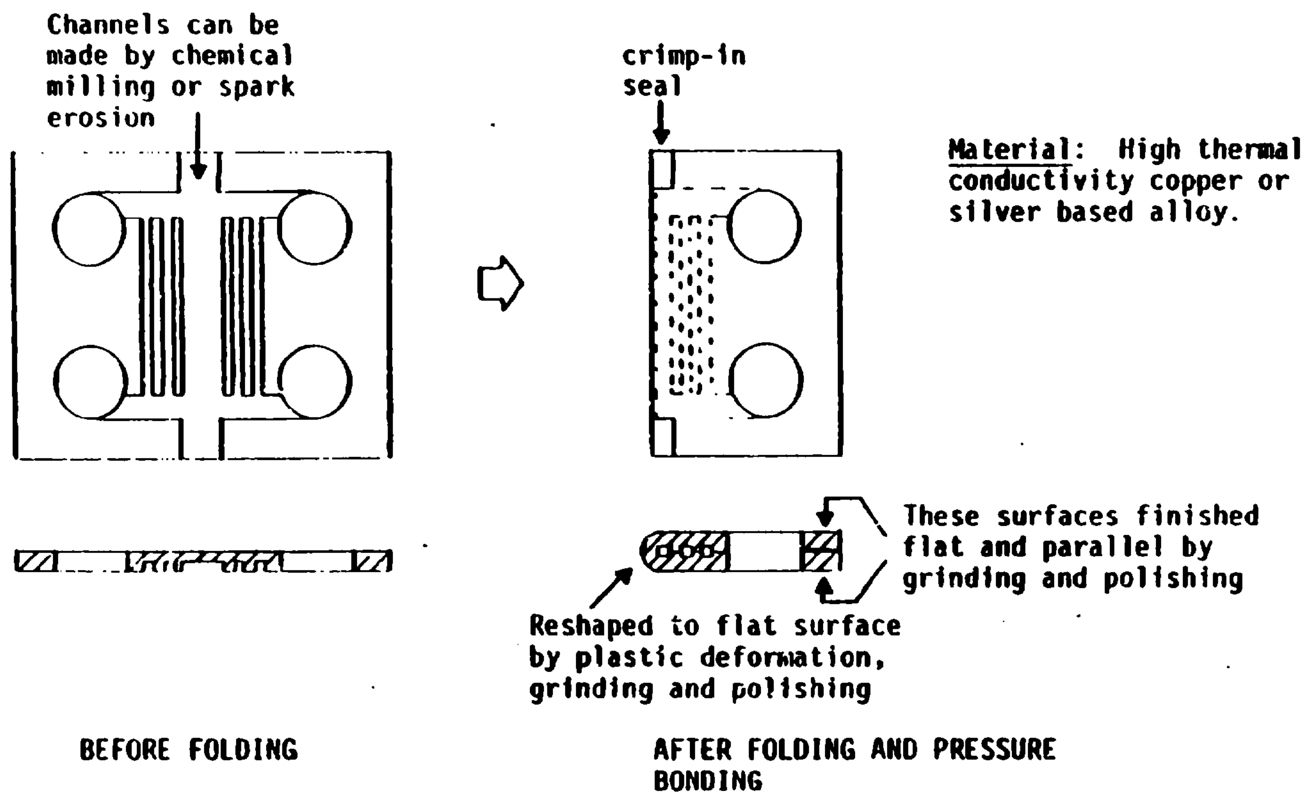


Figure 5.7 Construction of heat exchanger for diode laser mounting and heat sinking

coefficient h is taken as independent of the wall and fluid temperatures a defined as:

$$h = \dot{Q}/npL(T_w - T_f)$$

where $\dot{Q}$ is the heat flow, $T_w$ and $T_f$ are the wall and mean fluid temperatur respectively, p is the cross-sectional perimeter of each channel, L is the channel length and n is the number of channels. Furthermore, the temperat at the cold edge of the channel is assumed to be the coolant fluid tempera (this would actually be the case for an infinitely wide channel).

For a one cm long linear array generating an output of 25 W with an efficiency of 40 percent, the dissipated power is 37.5 W. If the maximum temperature rise allowed for the cooling water is of 5 C, then a flow of 1 $cm^3$ will be needed. The cross-sectional area of the four coolant channels shown in Figure 5-8 is of 0.0012 $cm^2$. Therefore, the coolant fluid mean velocity will be about 1500 cm/s.

The determination of the value of h for the design of Figure 5-8 requ the following definitions:

$Nu = hD_{eff}/k$, the Nusselt number, a dimensionless heat transfer coefficient;

$Pr = \mu C_p/K_f$, the Prandtl number, a property of the fluid ($Pr = 6.4$ for w at 23C);

$Re = v_f D_{eff} P/\mu$ , the Reynolds number.

Here $D_{eff}$ is a "characteristic width" of the channel, defined as $D_{eff}$ (cross-sectional area)/(Perimeter p). The terms $\mu K_f$, P, $C_p$ and $v_f$ denote respectively the viscosity, thermal conductivity, density, specific heat, mean velocity of the coolant fluid. For the design of Figure 5-8 the valu the Reynolds number is 2250, which is just over the transition value of 21

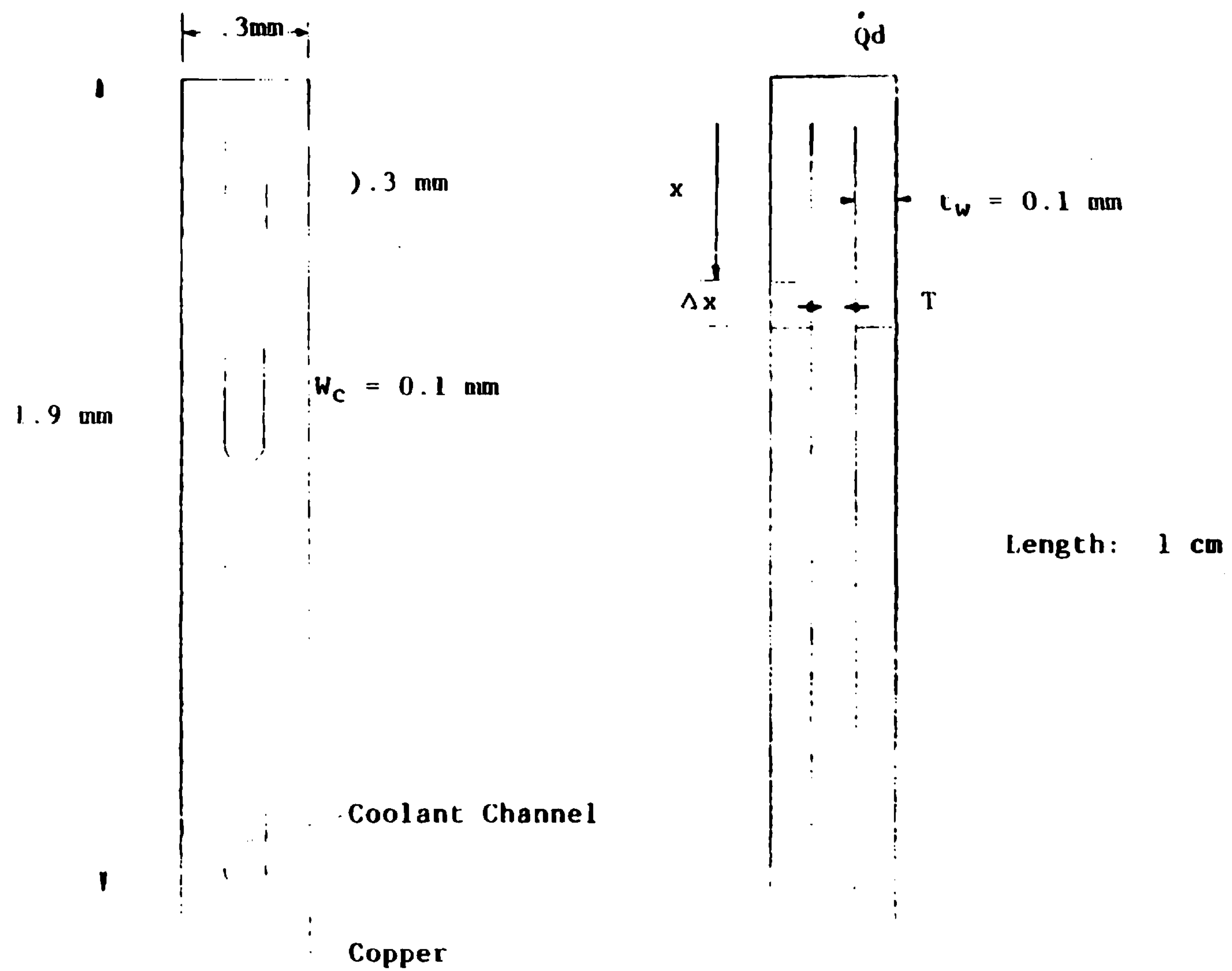


Figure 5.8 Heat sink design for stackable diode laser linear array
Actual design left, and idealized geometry used for analysis (right)

Therefore, a laminar flow will be assumed for the calculation of h. For calculating Nu, we further assume that the flow is "fully developed," i.e invariant along the channel length a good assumption if Pr > 5, a is the for most liquids). Then Nu is a monotonically descreasing function of $x/(D_{eff}$, Re, Pr) where x is the distance from the entrance of the channe (0<x<L). Asymptotic formulas are:

$$Nu \sim \left(\frac{x}{D_{eff}\ Re\ Pr}\right)^{-1/3} \quad \text{for } x/(D_{eff}\ Re\ Pr) << 0.02$$

$Nu \simeq Nu_{oo}$, a constant, for $x/(D_{eff}$ Re Pr) $\geq$ 0.02

"fully-developed temperature profile").

Not knowing a priori which region we are in, we conservatively assu that Nu has the minimum, asymptotic (large x) value $Nu_{oo}$; in any case th dependence of Nu of x is weak. The exact value of $Nu_{oo}$ depends on the s of the channel cross section but is usually between 3 and 9.

Thus we approximate $h=k_f Nu_x/D$, where $Nu_x$ is between three and nine. result is consistent with an intuitive model for convection in which the is conducted through the fluid to the middle of the channel, where it is transported away by the flow. For a given coolant fluid, clearly the on to significantly increase h is to reduce D. Achieving very high values therefore requires channels of microscopic width.

Assuming Nu=9, which is justified for a Reynolds number of 2250, th for the design of Figure 5-8, h = 3.6 $W/cm^{2\,o}C$, and the thermal impedance one cm wide mount results $\theta_{mount}$ = 1.9$^oC/W$. Considering the effect of t coolant fluid temperature raise as equivalent to a thermal resistance $\theta_f$ $(\iota P C_p)^{-1}$, where f is the coolant flow rate through all the channels, th total thermal impedance of the heat sink design of Figure 5-8 results:

$$\theta_{heatsink} = \theta_{mount} + \theta_{fluid} = 2.0^oC/W$$

For a linear array dissipating 37.5 W/cm, this would amount to a temperature differential between the diodes and the cooling water of 75°C.

Assuming a stacking density of 20 linear arrays per cm, the thermal impedance of a one $cm^2$ assembly will be 0.1 °C/W, which is the same value measured for the high-performance heat sinking design of Reference 5.4. It is possible that by careful optimization of the design of Figure 5-8 this thermal resistance could be rendered even lower. However, the estimated value given above is already showing a very acceptable performance level for this kind of design. In fact, if a more realistic value of 40°C for the temperature differential between diodes and cooling water is considered, then, for diode lasers with an efficiency of 40 percent, the cw pumping flux could reach the value of 270 $W/cm^2$.

To complete the analysis of the design of Figure 5-8 it is necessary to evaluate the pressure drop along the channel and the circulation power. For laminar flow, the pressure drop $\Delta P$ across a channel of length L can be calculated using the following expression:

$$\Delta P = \frac{12 \mu L}{W_c^2}$$

which is valid for flow between parallel plates and is only approximately valid for the moderately high aspect ratio channels of Figure 5-8. With the value of $v_f$ estimated earlier, and the design value for $W_c$, 0.01 cm, this pressure drop is about 30 psi, a very reasonable number. The circulation power required for this flow condition is 0.32 W, which is almost negligible compared to the array heat dissipation power.

Copper mounts present the problem of the disparity in thermal expansion coefficient with the material of the diode laser arrays: GaAs ($16.5 \times 10^{-6}$/K for copper vs. $6.8 \times 10^{-6}$/K for the latter). The life of the diode laser arrays is strongly affected by the large thermal strains developed in these assemblies because of the degradation effects generated by fast multiplication

of dislocations through the climb motion. Dislocation slip induced by stra seems to be the primary stage of the degradation.

There is no easily machineable material available that would have a thermal expansion coefficient close to that of GaAs and still show the larg thermal conductivity of copper. There is, however, the possibility of developing metal matrix composite materials such as graphite fiber/copper composites that would allow the tailoring of the expansion coefficient to match that of the diode lasers without seriously deteriorating the high thermal conductivity of copper. Aluminum, magnesium, titanium, lead and nickel alloy matrix fiber reinforced composites have been fabricated at Un Technologies Research Center since 1965. This longstanding, and highly effective, basic metal matrix composite technology has formed the foundati for extensive exploratory fabrication of gas turbine engine components as as other aerospace related hardware items.

In summary, we have shown that by applying liquid cooled heat exchange technology to very small dimensions, the thermal impedance of the heat sink of the laser diode array can be reduced from about 0.5°C/W/cm$^2$ to 0.1°C/W/c This implies that for a given temperature rise allowed in the diode array, average output power can be increased five fold. The complexity of the cooling system for the arrays brought about by a very high packaging densi is greatly reduced if the arrays can stand-off from the Nd:YAG laser. As mentioned before, compound parabolic concentrators or refractive optics ca employed to accomplish this.

Heat dissipation from planar arrays becomes the limitation in high average or cw operation. The problem can be ameliorated by increasing the efficiency of the laser arrays. At present, conversion efficiency of the planar arrays is 24 percent. Therefore, for every watt emitted 3.2 W are dissipated. In the newest GRIN-SHC devices, however, conversion efficienc to 45 percent can be achieved routinely. In this case, only 1.2 watts are dissipated for every watt emitted. Thus, the average emitted power could increased a factor of 2.6 without increasing the total dissipated power by

being able to reproducibly achieve 45 percent conversion efficiency. It is readily apparent that tremendous gains in average output power can be made by increasing the diode efficiency above the current levels. Such improvements would be crucial in applications requiring high repetition rates, high power density or where high conversion ef iciency itself is a primary parameter.

## 5.2 COOLING OF THE SOLID STATE MATERIAL

We will first quantify the heat load that the laser medium must accommodate. In a laser diode pumped solid state medium, as opposed to a flashlamp pumped system, the only sources of heat are due to the quantum defect between the energies of the absorbed pump photon and the laser photon ( n) and the fraction of photons returning from the pump band via non radiative processes to the ground state ( $\eta Q$).

From Section 4.3 we obtain for the stored upper state energy:

$$E_{ST} = \eta_V \eta_P \eta_Q E_{AB}$$

where $E_{AB}$ is the energy absorbed in the gain medium.

The heat dissipated $E_H$ in the laser medium is given by the fraction of diode pump power absorbed but not radiated:

$$E_H = (1 - \eta_V \eta_P \eta_Q) E_{AB}$$

It is customary in flashlamp pumped systems to express the thermal energy as a fraction of the upper state stored energy, i.e.:

$$\frac{E_H}{E_{ST}} = \frac{1 - \eta V \eta P \eta Q}{\eta_V \eta_P \eta_Q}$$

Introducing the values for Nd:YAG given in Section 4.4 $\eta_V = 0.76$, $\eta_P = 1$, $\eta_Q = 0.8$ we obtain:

$$\frac{E_H}{E_{ST}} = 0.64$$

Since the stored energy and laser output energy are related by $E_{OUT} = \eta_{OUT}\, E_{ST}$ and a laser diode pumped Nd:YAG laser has a typical value of 0.46 (see Table 4-5). We obtain also:

$$\frac{E_H}{E_{OUT}} = 1.4$$

It is instructive to compare these ratios with those obtained in flashlamp pumped Nd:YAG lasers.

Mangir et al. (5.4) experimentally determined the energy stored and t heat generated in flashlamp pumped Nd:YAG. They found that the heat depos percent stored energy is 1.5-2 times the value expected from the known spe troscopy of the Nd ions in these hosts and the emission spectrum of xenon flashlamps.

In flashlamps pumping, there are other absorption processes which can heat the laser host without contributing to pumping the $F_{3/2}$ level of the ions. These include UV absorption by the host, absorption of IR from the flashlamp ( $\lambda > 1.1\ \mu m$) by the Nd ion, absorption by impurity ions, which not transfer this energy to Nd ions. The measured value of heat deposited unit stored energy in a flashlamp pumped Nd:YAG laser is:

$$\frac{E_H}{E_{ST}} = 3.25$$

and using the same value for $\eta_{OUT}$ we obtain

$$\frac{E_H}{E_{OUT}} = 7.1$$

In other words, in a flashlamp pumped system, the Nd:YAG crystal has to dissipate five times the heat as compared to a laser diode array pumped laser. For example, only 70 W of heat has to be dissipated in a diode pumped YAG laser with 50 W average output power, as compared to 355 W for the case of a flashlamp pumped system.

$$\frac{E_{H\ DIODE}}{E_{HLAMP}} = 0.2$$

The Nd:YAG slab or rod can be conduction cooled by attaching it to a heat sink, or it can be gas or liquid cooled.

For laser diode pumped Nd:YAG systems, conduction cooling is attractive for a number of reasons: the heat load is considerably lower compared to flashlamp pumping, a cooling jacket and flow passages are eliminated in the pump path thus increasing efficiency, and the design is simplified.

The thermal load of the laser medium is only a fraction of that of the laser diode array. Therefore the heat sink design is not as stressing. The following example will illustrate this difference. We assume that the MDAC slab laser discussed in Section 4.3 is operated at 100 Hz. Since the energy per pulse is 100 mJ and the efficiency is 6.4 percent in long pulse mode, the laser has an average output of 10 W and requires an electrical input power of 156 W. Diode efficiency is 24 percent; therefore, 119 W has to be dissipated by the diode array heat sink. Since the array area is 3.85 cm, we obtain 31 W/cm$^2$. According to our previous calculations a laser diode pumped Nd:YAG system with 10 W output will generate 14 W of heat in the active medium.

For the single side pumped slab laser, bonded to a heat sink on one · this amounts to 3.6 $A/cm^2$.

The heat dissipation in the planar array is 8 times that in the Nd:Y/ slab. A steady state thermal analysis of a conduction cooled slab or rod be partitioned into the following elements:

- Temperature ıradient and profile in the laser medium
- Temperature drop across inter ·ʾ of laser medium and heat sink
- Temperature gradient in the heat sink.

The temperature difference from the cooled edge to the pumped edge o Nd:YAG slab is given by:

$$\Delta T_1 = \frac{P_H d}{kA}$$

where d is the slab thickness, load, A surface area, K thermal conductivi With $P_H = 3.6\ W/cm^2$ from our previous example, and with $A = 3.85\ cm^2$, $k = 0.13\ W/^oKcm$, and $d = 0.67$ cm

we obtain: $\Delta T_1 = 18.5^oC$

In a cylindrical geometry the temperature gradient for the rod cente to the surface for uniform heat generation is given by

$$\Delta T_1 = \frac{P_H}{4\pi kL}$$

where L is the rod length. If the rod is cooled one half of its surface as shown in Figure 7-2, a reasonable approximation is to multiply $\Delta T_1$ by in order to obtain the temperature drop across the rod.

The interface between the Nd:YAG crystal and the heat sink usually consists of a highly reflective gold or silver coating and a solder such as indium or gallium or a silver epoxy between the crystal and the heat rod.

The Nd:YAG crystal is usually bonded or soldered to a copper heat sink by means of silver epoxy, indium or gallium. In addition a highly reflective gold or silver coating is applied to the crystal surface which is in contact with the heat sink. This metal coating reflects the diode laser pump radiation back into the Nd:YAG crystal and provides good thermal contact. In the case of a zig-zag slab laser, a thick dielectric coating of $SiO_2$, $MgF_2$ has to be applied to slab followed by a coating of silver, copper and gold.

The dielectric layer allows total internal reflection without the field penetrating to the silver layer. The silver reflects the diode laser pump light back into the Nd:YAG slab and provides good thermal contact. The copper and gold layers protect the silver and eventually are contacted to the heat sink.

A Nd:YAG rod has to be mounted in a carefully machined saddle of the heat sink as shown in Figure 5-9. The attachment to the heat sink is the same as that outlined above for the slab, although no dielectric coating is needed. The temperature rise across the boundary is given by the equation:

$$\Delta T_2 = P_H \frac{\Delta X}{Ak}$$

where $P_H$ is the heat flow rate, $\Delta X$ is the boundary thickness, A is the surface area, and k is the thermal conductivity.

As an example, for a silver filled epoxy resin with a thermal conductivity $k = 1.6$ W/$^{o}$C cm and a layer thickness of $\Delta X = 0.1$ mm we find $\Delta T_2 = 0.02^{o}$C for the slab laser considered here.

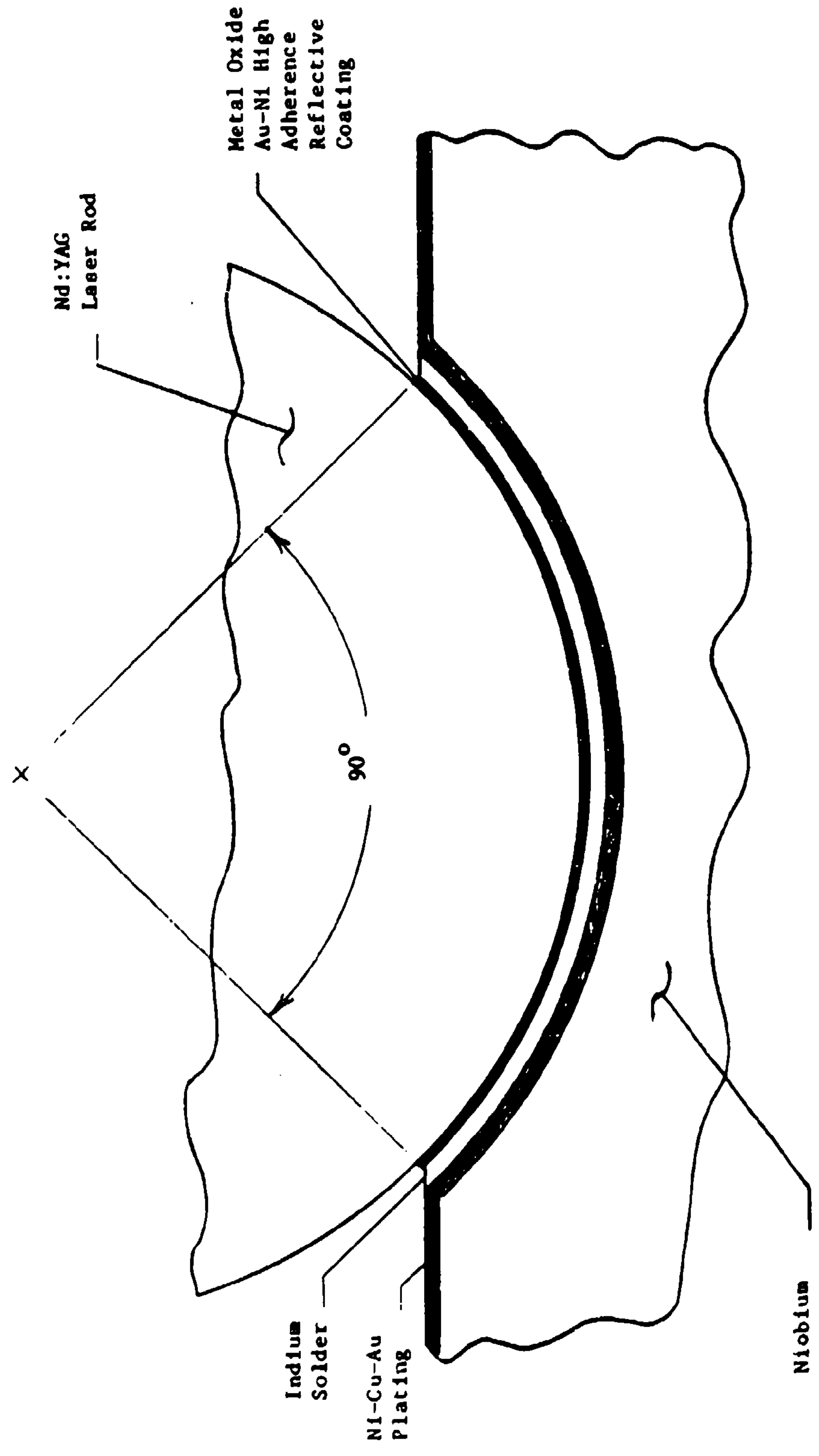
Nd:YAG
Laser Rod
Metal Oxide -
Au-Ni High
Adherence
Reflective
Coating
90°
Indium
Solder
Ni-Cu-Au
Plating
Niobium
Heat Sink

All of the heat input can be assumed to be transferred to the heat sink. The temperature gradient within the heat sink is given by

$$\Delta T_3 = \frac{P_H\, d}{kA}$$

where d is the thickness of the heat sink with d=5 mm, and k=4 w/cm/K for copper and $P_H$ and A as before we obtain

$$\Delta T_3 = 0.45^{\circ}C$$

As illustrated in this example, the largest temperature gradient occurs in the active medium, and the temperature drop across the boundary and within the heat sink can be neglected.

## References

5.1 W.B. Joyce and R.W. Dixon, J. Appl. Phys., Vol. 46, 855 (1975).

5.2 Elsa M. Garmire and Michael T. Tavis, IEEE J. Quantum electron., vol. QE-20, pp 1277-1283 (1984).

5.3 H. Koyama, T. Nichioka, K. Isshiki, H. Namizaki and S. Kawazu, App. Pl Lett., vol. 43, pp 733-735 (1983).

5.4 D.B. Tuckerman and R.F. W. Pease, IEEE Electron., Device Lett., vol. EDL-2, pp 126-129 (1981).

5.5 M.S. Mangir, D.A. Rockwell, IEEE J Quantum. Electronics, vol. QE-22, April 1986, p. 574.

# 6. RESONATOR DESIGNS (Task 4)

A large amount of research has been devoted in the recent past to the design of new optical resonator configurations, which could optimize the efficiency of energy extraction from solid state lasers. In fact, operation with stable cavities in $TEM_{00}$ mode, while producing a beam with a smooth and well-controlled spatial profile, results in a poor filling of the active volume and hence in a large waste of the stored energy. Recent developments can be divided into the following two optical designs: stable telescopic or concave-convex resonators and unstable resonators. Both schemes were extensively studied and experimentally tested and found also commercial exploitations, exhibiting somewhat competing characteristics. (References 1-8)

In stable telescopic resonators a magnifying telescope is added to a conventional stable cavity to expand the mode cross section in the arm of the cavity where the field interacts with the active medium. In the concave-convex resonator, the same effect is achieved by the particular choice of mirror curvature and resonator length. In both cases, the beam quality remains good, but the mode volume is still limited, for the $TEM_{00}$ mode. Furthermore, at the highest intensities, damage problems arise for the optical elements in the resonator section where the beam gets its smaller dimension.

On the other hand, the unstable resonators have become very popular in their confocal positive branch realization and provide the greatest energy extraction, but the field they produce presents a strongly structured spatial shape and the resonator is very unforgiving in terms of alignment tolerances.

In the large number of publications dealing with unstable resonators that followed the pioneering work by Siegman (1), very little attention has been paid, both theoretically and experimentally, to the subject of confocal negative branch configurations.

The main explanation is found in the unattractive presence of a foca point inside the cavity, which can give rise to air breakdown or to damag optical elements in its neighborhood. Actually a few reports have occasi ly appeared describing the operation of negative branch unstable resonato conjunction with dye and solid state lasers but those results did not stimulate further developments in this direction.

On the other hand the negative branch unstable resonator exhibits so unique attracting features: First, they possess an intrinsically higher misalignment tolerance in comparison with equivalent positive branch sche Second, if an aperature stop is located at the focal point a much smoothe output profile can be achieved as compared to a positive branch unstable resonator.

Currently, flashlamp pumped, as well as laser diode pumped slab lase employ confocal positive branch resonators. A description of the main characteristics of this class of resonators is given in subsection 6.1.1. subsection 6.1.2 we will assess the pros and cons of employing confocal negative branch resonators for laser diode pumped slab lasers. For syste having low gain, such as a CW laser diode pumped Nd:YAG laser the stable resonator is a clear choice. The concave-convex and the telescopic reson will be discussed in subsections 6.2.1 and 6.2.2, respectively.

## 6.1 UNSTABLE RESONATORS

The unstable resonator first described by Siegman[1,2] has been studie extensively both theoretically and experimentally. Excellent reviews are found in references 3 and 4. The most useful property of an unstable resonator is the attainment of a large fundamental mode volme and good sp mode selection at high Fresnel numbers. In other words, unstable resonat can produce output beams of low divergence in a short resonator structure which has a large cross-section.

The stable resonator, whose mirror configuration corresponds to a st periodic focusing system, has a long slender Gaussian-profile lowest-orde

mode whose diameter is of the order of a few times $(L\lambda)^{1/2}$. If the diameter of the laser medium is 2a, then the area ratio of the laser medium cross section to the lowest-mode cross section is of the same order as the Fresnel number $N_F=a^2/L\lambda$ characterizing the laser medium. If this Fresnel number is much larger than unity, the lowest-order mode will extract only a fraction $\approx 1/N_F$ of the energy available in the laser medium, and/or the laser must oscillate in a sizable number of higher-order modes to extract all the energy from the laser medium.

Therefore in order to produce a diffraction-limited output beam, the Fresnel number of the laser must be on the order of unity or smaller. This usually limits the diameter of the laser gain medium to a few millimeters.

The lowest-order mode in the unstable resonator, by contrast, since the unstable resonator corresponds to a divergent periodic focusing system, expands on repeated bounces to fill the entire cross section of at least one of the laser mirrors, however large it may be.

An unstable resonator may be used to obtain a nearly diffraction-limited output beam from a large-diameter gain medium which has reasonable high round-trip gain: $2G_0L_g>1.5$, where $G_0$ is the small-signal gain per unit length and $L_g$ is the length of the gain medium. The light rays in an unstable resonator walk outward from the center of the laser.

The laser output is taken as a diffraction-coupled beam passing around rather than through the output mirror. An output beam from an unstable resonator usually has an annular or rectangular-annular intensity pattern in the near field.

Immediately following its invention, the significance of the unstable resonator was recognized for the extraction of diffraction limited energy from large volume gas lasers.[7,8] However, only recently have unstable resonators been applied to solid state laser systems. There are a number of reasons for this slow acceptance. The laser medium must be of high optical quality, for

an unstable resonator to be effective. This requirement has limited appli tions of unstable resonators primarily to gas lasers because the time- and power-dependent thermal distortions occurring in solid state lasers make t type of resonator unattractive.

In addition, the output coupler of an unstable resonator, having the dimensions of a few millimeters in typical solid state lasers, is much mor expensive and difficult to fabricate in comparison to a partially transmit mirror required for a stable resonator.

Furthermore, the alignment tolerance of an unstable resonator is more critical compared to its stable counterpart and the advantage of a large m volume is achieved at a sacrifice of mode quality because of aperture generated Fresnel fringes. The output from a solid state laser is often passed through amplifier stages, or the oscillator may be followed by a harmonic generator. The near field beam pattern of an unstable resonator which consists of a doughnut shaped beam with diffraction rings and a hot in the center is not very attractive in these applications.

As we will discuss later, several new designs have been successful ir circumventing some of these shortcomings.

About 10 years after its discovery, Byer et al.[5,6] applied the unstat resonator concept for the first time to a Q-switched Nd:YAG oscillator/ amplifier system. They did achieve a marked improvement in Nd:YAG output energy in a diffraction limited mode.

Despite these earlier demonstrations of the concept, the limited des flexibility brought about by the somewhat cumbersome output coupling of tl unstable resonator, and its poor tolerance to mirror alignment and optica quality of the laser medium, didnot make it an instant favorite among sol state laser designers. Most commercially available solid state lasers st have stable resonators.

A stimulus for further study and research on employing unstable resonators for solid lasers was provided by the zig-zag slab laser. These structures, having a narrow rectangular cross section and an optical beam with very few distortions, are ideally suited for unstable resonators. Today, most flashlamp pumped and laser diode pumped solid state slab lasers employ unstable resonators. As a result of this activity, several commercially available flashlamp pumped Nd:YAG rod systems also feature an unstable resonator.

The most useful form of unstable resonator is the confocal unstable resonator, introduced by Anan'ev et al.[7] and by Krupke and Sooy[8]. A primary advantage of this configuration is that it automatically produces a collimated output beam. Confocal configurations can be divided into positive and negative branches as shown in Figure 6-1. The negative branch confocal configuration has significant practical advantages in the form of more easily obtainable shorter-radius mirros and considerably easier mirror alignment tolerances. However, the positive-branch resonator seems to be universally employed in practice because the internal focal point in the negative-branch case leads to unacceptable difficulties with optical breakdown.

In analogy to high energy lasers utilizing unstable resonators the output coupling can be accomplished by means of a scraper mirror or edge coupler. Figure 6-2 shows relevant adaptations for solid state lasers.

Figure 6-2a illustrates an unstable resonator with an output scraper mirror. It is inclined at an angle of $45^{\circ}$ to the resonator axis and has a hole in its center which allows light to pass through it and be fed back into the resonator to sustain the lasing. Because the end mirrors and scraper are oversize, this hole determines the size and shape of the beam outcoupled from the resonator.

Figure 6-2b shows the design of a typical positive-branch, confocal unstable resonator. This design usually consists of a concave mirror $M_1$ and a polka-dot convex output mirror $M_2$, both of which are totally reflecting. The polka-dot is a small circular spot of radius d centered on a zero-power lens.

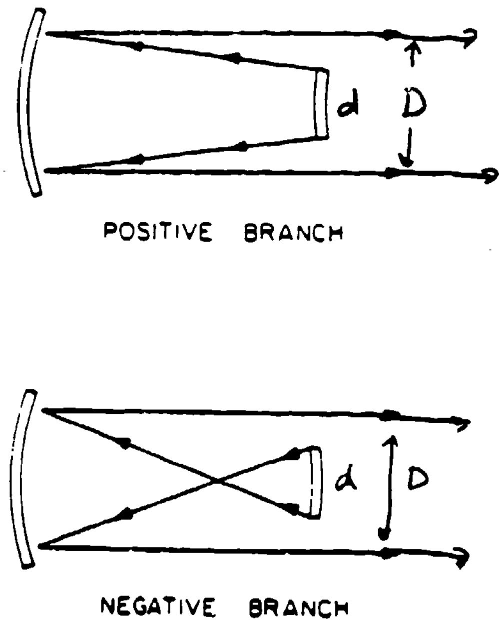


Figure 6.1 Positive- and negative-branch confocal stable resonators

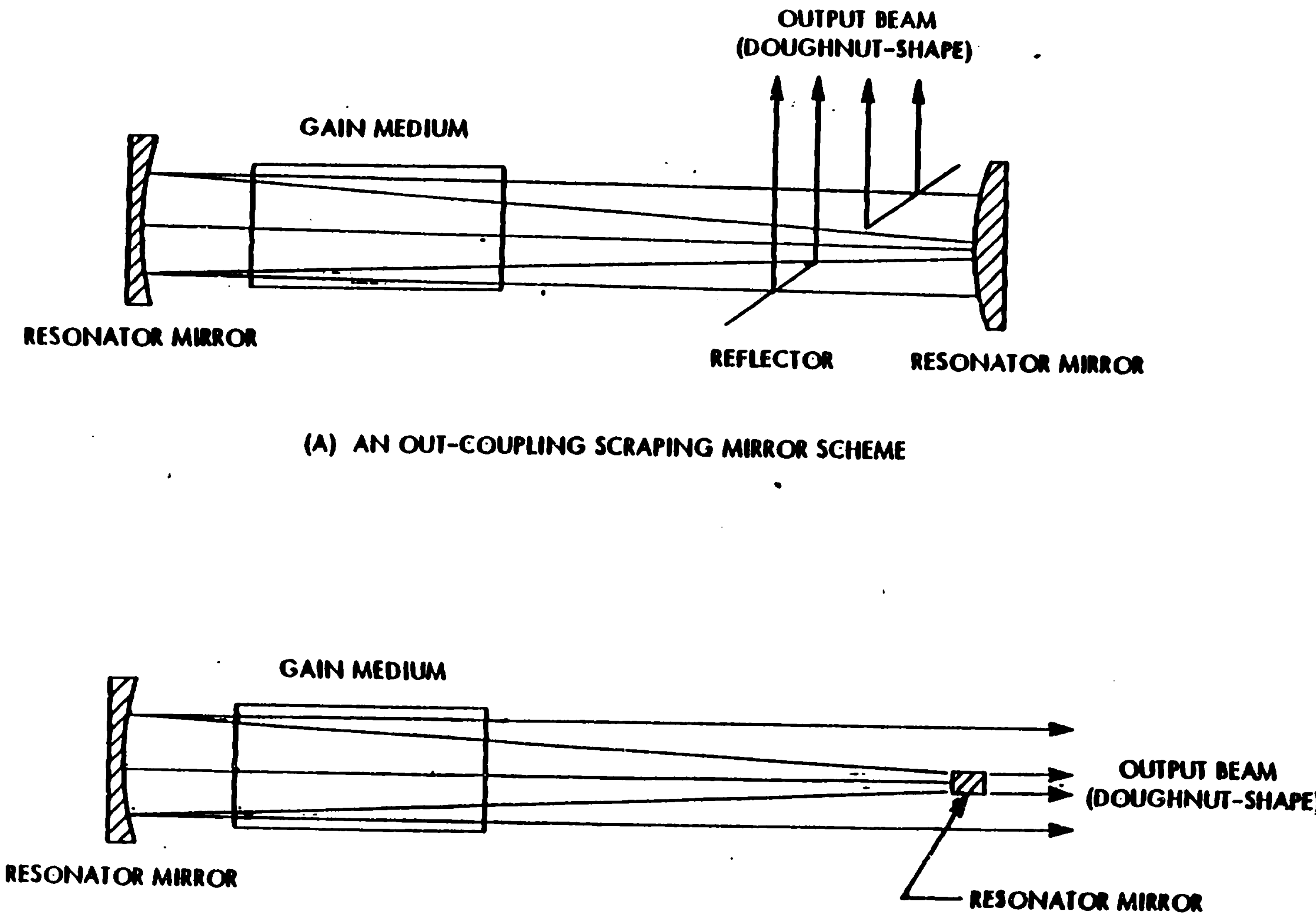


(B) A SMALL MIRROR OUT-COUPLING SCHEME

Figure 6.2 Confocal, positive branch unstable resonators

The output beam is collimated as it exits the resonator around the edges ‹ the polka-dot mirror.

While these two output coupling techniques are borrowed from high en‹ lasers the designs mentioned below are more germane to the design of soli‹ state lasers. In an attempt to eliminate the Fresnel diffraction fringes which can cause damage to optical elements in the output of the laser, th‹ radial birefringent element and apodized or soft aperture designs have be‹ developed.

The radial birefringent element is based on a radial variation of ph‹ retardation in a radial birefringent element, when combined with a polari: form a radial intensity filter, which permits realization of Gaussian-lik‹ reflectance mirrors and soft apertures.

The design of birefringent elements and their incorporation into uns‹ resonators is discussed in detail in References 9-11.

In its simplest form, it is a lens of birefringent material. When a polarized optical beam passes through the lens, the radial variation in thickness of the lens creates a radial variation in the polarization of t‹ optical beam. If the beam then passes through a polarizer, the radial va‹ tion in polarization is converted into a variation in the beam intensity. Thus the combination of a radial birefringent element and a polarizer for‹ radial intensity filter which provides the capability for smoothly modula‹ the intensity profile of an optical beam.

Each radial birefringent element has essentially three parameters th‹ determine the modulation profile of the beam, the center thickness, the r‹ of curvature, and the angle between the principal axis and a polarization axis. The first two parameters are set at the time of fabrication, and t‹ third is varied as the need arises. Although a single-element can be des‹ to generate many useful profiles, multielement radial birefringent elemen‹ can generate a much larger set of modulation profiles.

A schematic of the radial birefringent element resonator is shown in Figure 6-3a. The reflectance profile is shown in Figure 6-3b. As one can see from the curves the resonator has a flat topped intensity profile that is free from Fresnel fringes.

Figure 6-4 shows a design in which the output coupling is accomplished via a Q-switch and polarizer. An apodized aperture eliminates Fresnel diffraction rings. A different output coupler is shown in Figure 6-5. The schematic shows a negative branch unstable resonator featuring an internal aperture which has a diameter designed to remove diffraction rings from the near field beam pattern. A quarter waveplate and a polarizer provide the output coupling.

### 6.1.1 Confocal Positive Branch Unstable Resonator

The confocal positive branch unstable resonator is the most widely used form of the unstable resonator for solid state lasers. It avoids a focal point in the beam and produces a collimated output beam. It has the disadvantages of a hole in the center with resultant Fresnel fringes unless either an apodized aperture or a radial birefringent element is employed as output coupler.

The design of a confocal positive branch unstable resonator which takes into account thermal lensing of the laser rod is discussed in References 6.12.

Referring to Figure 6-1 the annular output beam has an outer diameter of D and inner diameter d, where d is also the diameter of the output coupler.

The resonator magnification

$$M = D/d \qquad (1)$$

is the amount that the feedback beam is magnified when it travels a round trip in the resonator and becomes the output beam.

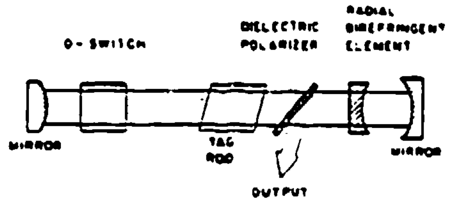


igure 6.3a) Radial birefringent element within an unstabl resonator
(Giuliani et al. Optics Letters, Volume 5, Nov. 1980, P. 491)

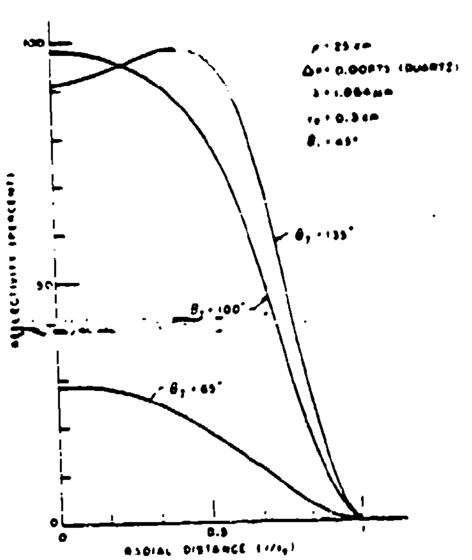


Figure 6.3 b) Reflectance profiles of a 2 element radial birefringent element
(Giuliani et al. Optics Letters, Volume 5, Nov. 1980, P. 491)

o MAGNIFICATION = 1.5

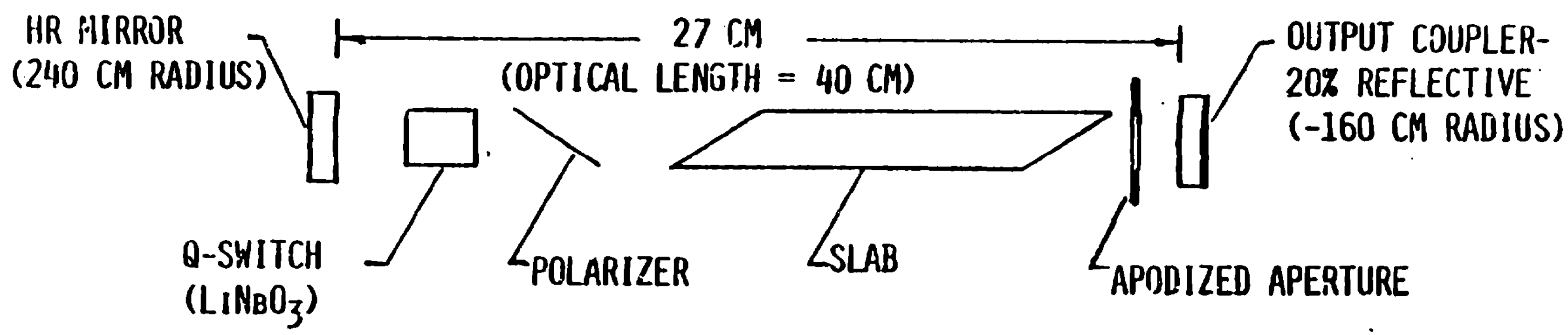


| ELEMENT | EFFICIENCY |
|---|---|
| SLAB | 0.39 |
| HR MIRROR/Q-SQ/POLAR. | 0.95 |
| OUTPUT COUPLER | 0.89 |
| RESONATOR | 0.33 |

RESONATOR PULSE ENERGY OUTPUT = 0.72 J

PULSE LENGTH = 4 NSEC

Figure 6.4 Confocol unstable resonator for slab laser (McDonnell Douglas)

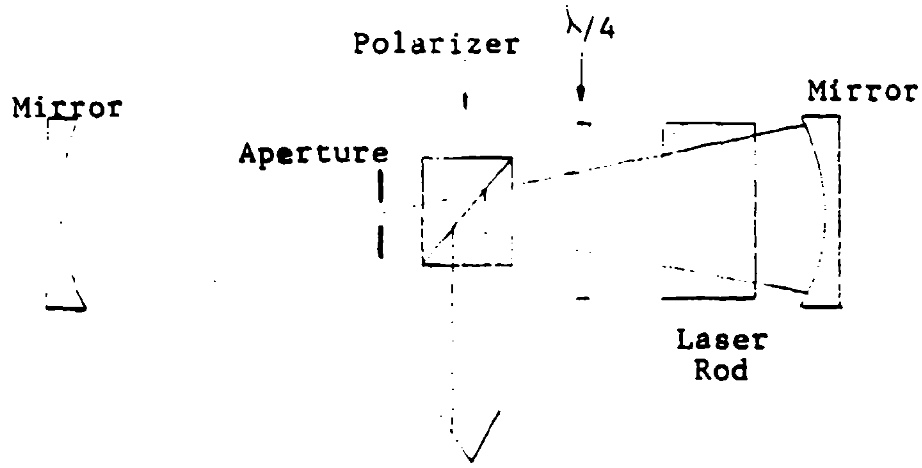


Figure 6.5  Negative Branch Unstable Resonator

The geometrical output coupling is related to the magnification M by

$$\delta_g = 1 - \frac{1}{M^2} \qquad (2)$$

For a confocal resonator, the mirror radii are given by

$$R_1 = \frac{-2L}{M-1} \qquad (3)$$

$$R_2 = \frac{2ML}{M-1} \qquad (4)$$

Where L is the cavity optical length and $R_1$ and $R_2$ are the output and back-cavity mirror curvatures. Note that the output mirror has a negative curvature and thus is convex, while the high-reflection mirror has positive curvature and is concave.

Siegman (3) has investigated the relationship between M and the output coupling $\delta$ for confocal unstable resonators and has shown that $\delta$ is less than geometrically predicted value $(1 - 1/M^2)$. Resonators should be designed to operate at half-integer equivalent Fresnel numbers ($N_{eq}$) to obtain best mode selectivity. Equations relating M and $\delta$ under these conditions lead to the following expressions

$$\left(\frac{M^2 - 1}{M^2}\right)^2 \simeq \begin{cases} 1.44\delta - 0.44\delta^2 & (N_{eq} = 0.5) \\ 1.06\delta - .06\delta^2 & (N_{eq} = 1.5) \\ \delta & (N_{eq} \geq 2.5) \end{cases} \qquad (5)$$

For positive branch confocal unstable resonators:

$$N_{eq} = \frac{M-1}{2M^2} NF \qquad (6)$$

where $N_F$ is the conventional Fresnel number defined by the resonator lengt and mode diameter d by:

$$N_F = D^2/4L\lambda \qquad (7)$$

Physically, the half-integer equivalent Fresnel numbers correspond tc Fresnel diffraction peaks centered on the output coupler, leading to incre feedback into the resonator.

The design of an unstable resonator usually proceeds along the follo lines: The diameter D of the laser rod and the radius $F_1$ of the output coupler are considered as given. The other parameters, cavity length, bac mirror curvature and output coupling, then can be calculated for selected half-integer values of $N_{eq}$. i.e. $N_{eq}$ = 0.5, 1.5, 2.5....

For example, the resonator length is obtained on eliminating M from e 3 and 6. One obtains:

$$L = -1/2|R_1| + 1/4D[|R_1|/(\lambda N_{eq})]^{1/2} \qquad (8)$$

Once L is known M can be calculated from eq. 3, and subsequently $R_2$ a $\delta_g$ can be determined. The actual value $\delta A$ of the output coupling can be obtained from eq. 5.

Since M is the dominant factor, determining the stability and efficie of the system, the procedure described above usually has to be repeated several times until the right value of M is obtained.

The value of M has to be consistent with the gain and loss expected i the system.

As a final step one has to take into account the effect of the laser focal length f as shown schematically in Figure 6-2. One usually chooses available mirror curvature $R_2$ and calculates the rod focal length at the

desired lamp input power required to achieve an effective mirror curvature $R_{2EFF}$. If the mirror to rod distance is less than the rod focal length, then

$$\frac{1}{f} \quad \frac{1}{R_{2EFF}} = \frac{1}{R_2} \tag{9}$$

Essentially the focusing effect of the laser rod is compensated by increasing the radius of curvature of the mirror.

Equation 9 is only a first order approximation, a more rigorous treatment is found in Ref. 12.

### 6.1.2 Negative Branch Unstable Resonators

Due to the presence of an intra-cavity focal point, the negative-branch resonator has been neglected in practical laser applications. Despite the potential problem of air breakdown this resonator merits consideration for laser diode pumped systems due to its unique feature of relatively large misalignment tolerances.

Ewanizky et al. (13) found that their Q-switched Nd:YAG laser featuring negative branch unstable resonator was not signficantly degraded with a mirror misalignment angle of as much as a few milliradians. In a similar system air breakdown was not experienced for Q-switched pulses in the order of 170 ml and 12 nsec. pulse length.

Therefore, for small laser diode pumped solid state lasers, typical of rangefinders and target designators with peak powers not exceeding 5-10 MW, it is conceivable that a negative branch unstable resonator could be employed.

The design parameters for a negative branch resonator of the type shown in Figure 6-6 are:

$$R_1 = 2L/(M+1) \tag{10}$$

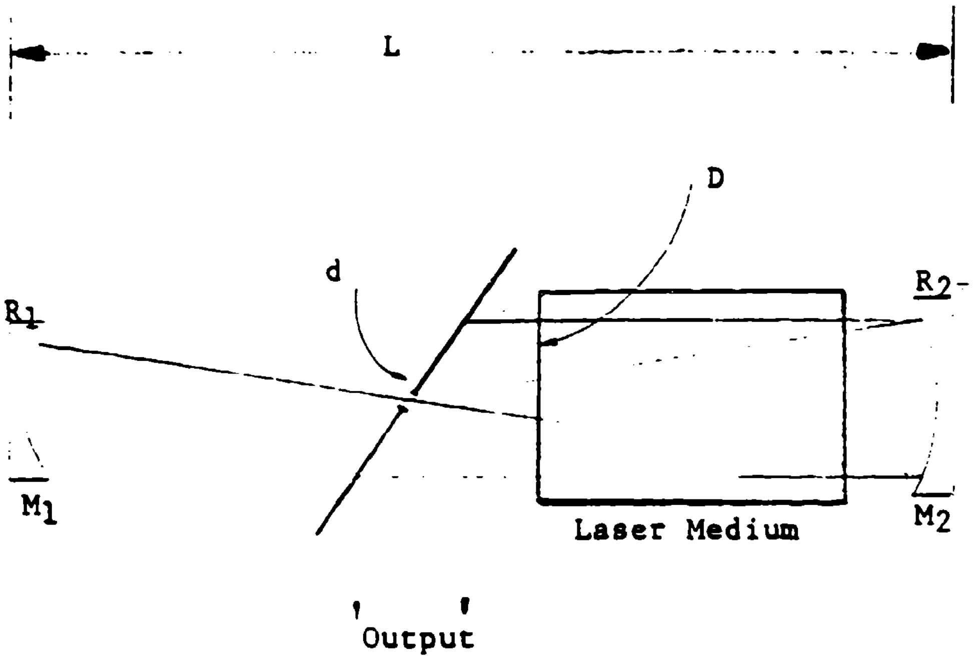


Figure 6.6 Arrangement of a typical negative branch unstal
resonator

$$R_2 = 2ML(M+1) \tag{11}$$

where L is the confocal resonator length

$$L = R_1/2 + R_2/2 \tag{12}$$

and M is the optical magnification

$$M = R_2/R_1 \tag{13}$$

The aperture diameter of the output mirror is

$$d = D/M \tag{14}$$

Recently, a variation of the negative branch unstable resonator was described by Gobbi et al. (14) The design is based on the proper choice for the size of the field limiting aperture d located at the common focal plane of the mirror. If the aperture is chosen such that a plane wave incident on it is focused by mirror $M_1$ to an Airy disk having the same diameter d, then this results in the removal of the hot spot inside the cavity and in a smoothing of the spatial profile.

If the aperture diameter d is chosen such that

$$d = 2(0.61\lambda\ f_1)^{1/2} \tag{15}$$

where $f_1 = F_1/2$, then only the Airy disk is allowed to propagate beyond the aperture, and on reflection from the mirror $M_2$, it is magnified, collimated, and presented Fourier transformed at the aperture plane ready to start another similar cycle.

The radius at which the beam gets zero amplitude is not determined by the geometrical magnification M, but an effective magnification imposed by diffraction.

$$M_{eff} = 1.5M = 1.5\ f_2/f_1 \quad (16)$$

where $f_2 = R_2/2$.

The diameter of the collimated beam passing through the laser crystal

$$D = |M_{eff}|\ d. \quad (17)$$

By adding the constraint on the aperture size that it match the Airy disk, the usual hot spot in the focal plane is completely removed by diffr tion. Actually the combination of aperture d and mirror $M_1$ acts on the resonator field as a low-pass spatial filter. This accounts for the smoothness of the field profile.

The disadvantage of this design is the limited value of D which can t achieved in practical systems. In order to fill a large active volume wit diameter D, such for example a slab laser, either $M_{eff}$ or d has to be larg (See Equation 17). In order for d to be large, it follows from eq. 15 tha has to be large which in turn leads to a long resonator. A large $M_{eff}$ requires a very high gain material, for example a Q-switched Nd:YAG Oscillator. The authors reported a beam diameter of D=4.8 mm inside the laser This required a resonator of 125 cm in length and a magnification of M=4. order to achieve the high gain required for this design the laser was pum 2.5 times above threshold.

Another interesting feature of this design is the beam extraction fr the resonator. Instead of a tilted scraper mirror as shown in Figure 6-6 beam extraction was achieved by means of a polarization coupling scheme, employing a polarizer and a quarter wave plate as shown in Figure 6-5.

## 6.2 STABLE RESONATOR

For solid state lasers with low gain, or for systems where a Gaussiar profile in the near field is required, the stable resonator is the only choice. Almost all laser applications require a small beam divergence, ei

to obtain a small spot size at a large range, or a high power density at the focal plane of a bias. Therefore, the challenge in designing a stable resonator is to maximize low order mode power extraction. More specifically we can establish the following design criteria:

- The diameter of the $TEM_{00}$ mode should be limited by the active material
- The resonator should be dynamically stable, i.e. insensitive to pump-induced fluctuations of the rod focal length.
- The resonator modes should be fairly insensitive to mechanical misalignments.

Lasers operating in the fundamental mode usually require the insertion of an aperture in the resonator to prevent oscillations of higher-order modes. In this case, the efficiency of the laser is generally lower, compared with multimode operation, due to the small volume of active material involved in the laser action. Large-diameter $TEM_{00}$ modes can be obtained using special resonator configurations, but, if proper design criteria are not applied, the resonator becomes quite sensitive to small perturbations in the mirror curvatures and in the alignment. Also, in solid state lasers, thermal focusing of the rod greatly modifies the modes and the pump-induced fluctuations of the focal length may strongly perturb the laser output, even preventing any practical or reliable use of the laser.

For efficient exploitation of the rod of a solid state laser operating in the fundamental mode, two conflicting problems have to be solved. The mode volume in the rod has to be maximized, but the resonator should remain as insensitive as possible to focal length and alignment perturbations. Early solutions proposed compensation of the thermal lens by a convex mirror or by negative lenses ground at the ends of the rod that exactly eliminate the focusing effect of the rod. With these methods high power in a monomode beam can be obtained; the compensation, however, is effective only for one particular value of the focal length. Large fundamental mode volume and good stability against thermal lens fluctuations have been achieved by a particular choice of mirror curvatures or by insertion of a telescope in the resonator.

In the following section we will discuss these two approaches which to the design of convex-concave or telescopic resonators.

### 6.2.1 The Concave-Convex Resonator

The design procedure for resonators known as dynamic stable, in whi fluctuation of the mode volume in the rod is kept under control by an ap priate choice of mirror curvatures, has been developed originally by Ste et al.[15] An expansion of this earlier work was published more recently Kortz[16], Magni[17] and Silverstri[18]. The design approaches are based on a evaluation of stable resonators with an internal focusing element that represents the laser rod under CW or high repetition rate pumping. The criteria applied in these investigations, namely to maximize $TEM_{00}$ mode in the active material, yet maintaining the resonator insensitive to mec cal and optical perturbations leads to a set of equations which allow th calculation of the resonator parameters. Specifically the design criter require that changes in beam diameter are minimized for large variation focal length.

The design resulted in standard convex-concave resonators where the maximum mode volume allowed by diffraction losses imposed by the rod ape has been achieved.

In a stable resonator, the waves which propagate between the two reflectors are refocused, i.e. they bounce back and forth without spreac appreciably.

This fact can be expressed by a stability criterion

$$0 < \left(1 - \frac{L}{R_1}\right)\left(1 - \frac{L}{R_2}\right) < 1. \qquad (18)$$

To show graphically which type of resonator is stable and which is unstable, it is useful to plot a stability diagram on which each particu

resonator geometry is represented by a point. This is shown in Figure 6-7, where the parameters

$$g_1 = 1 - \frac{L}{R_1}$$
$$g_2 = 1 - \frac{L}{R_2} \tag{19}$$

are drawn as the coordinate axes. All configurations are unstable unless they correspond to points lying in the area enclosed by a branch of the hyperbola $g_1 g_2 = 1$ and the coordinate axes.

In any resonator, the $TEM_{00}$ mode spot size at one mirror can be expressed as a function of the resonator parameters

$$w_1^2 = \frac{\lambda L}{\pi} \left[ \frac{g_2}{g_1(1 - g_1 g_2)} \right]^{1/2} \tag{20}$$

The ratio of the spot sizes at the two mirrors is

$$\frac{w_1^2}{w_2^2} = \frac{g_2}{g_1}. \tag{21}$$

The stability condition (e.g. Equation 18) remains unchanged.

Beam properties of resonators containing internal optical elements are described in terms of an equivalent resonator composed of only two mirrors.

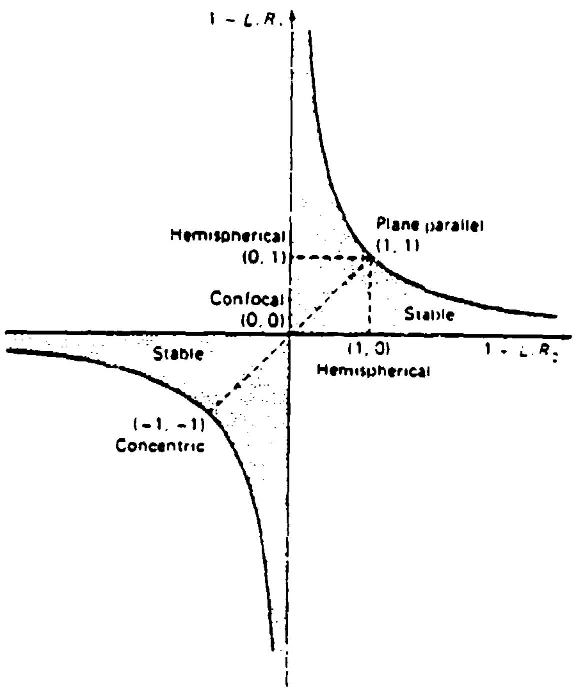


Figure 6.7 Stability diagram for the passive resonator

(Ref. W. Koechner, Solid State Laser Engineering, Spring Verlag, 1976)

The pertinent parameters of a resonator equivalent to one with an internal thin lens are

$$g_1 = \frac{L_2}{f} - \frac{L_o}{R_1}; \quad g_2 = 1 - \frac{L_1}{f} - \frac{L_o}{R_2}, \tag{22a}$$

where: $$L_o = L_1 + L_2 - (L_1 L_2/f) \tag{22b}$$

and f is the focal length of the internal lens; $L_1$ and $L_2$ are the spacings between mirrors $M_1$, $M_2$ and the lens as shown in Figure 6-8.

As an example we will consider a resonator with flat mirrors ($R_1=R_2=00$) and a thin lens in the center ($L_1=L_2=L/2$). From equation 22 we obtain

$$g = g_1 = g_2 \; 1 - \frac{L}{2f}, \tag{23}$$

$$w_1^2 = w_2^2 = \frac{\lambda L}{\pi} (1 - g^2)^{-1/2} \tag{24}$$

For f=00 the resonator configuration is plane-parallel; for f=L/2 we obtain the equivalent of a confocal resonator; and for f=L/4 the resonator corresponds to a spherical configuration.

Figure 6-8 shows the location of a plane-parallel resonator with an internal lens of variable focal length in the stability diagram.

Considering first the resonator's sensitivity to lensing effects, we note that a resonator is insensitive to axial perturbations if the spot size $w_1$ is insensitive to changes of $g_1$ and $g_2$. A calculation of the relative sensitivities of various resonators to small changes in mirror radii is equivalent to the introduction of a lens of some focal length f. In order for the resonator to have a low sensitivity to axial perturbations, i.e. small spot size changes

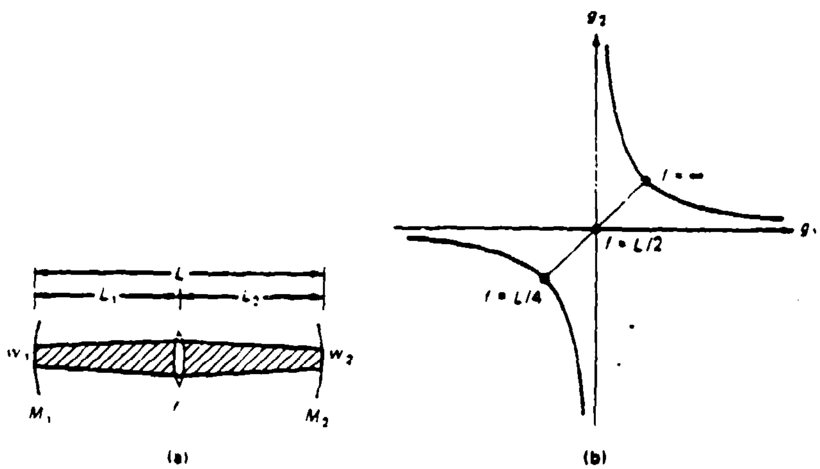


Figure 6.8 Geometry a) and stability diagram of resonator containing a thin positive

(Ref. W. Koechner, Solid State Laser Engineering, Spring Verlag, 1976)

for large changes of $g_1$ and $g_2$, it is necessary that $dw_1/df = 0$. This condition is met for resonator geometries which satisfy the following equation.

$$2g_2g_1 - 1 + \left(\frac{g_1}{g_2}\right)\left(\frac{L_1}{L_2}\right) + \frac{2g_1L_1}{L_2} = 0. \qquad (25)$$

One particular resonator satisfying is determined by

$$g_1g_2 = \frac{1}{2}; \quad L_1 = 0. \qquad (26)$$

In this case the internal lens is either absent or located at the surface of mirror $R_1$. Figure 6-9 shows the resonator stability diagram with curves of constant $TEM_{00}$ mode spot sizes. The curves which are obtained from Equation 25, reveal that the spot size is fairly insensitive to variations of g1 and $g_2$ for resonator configurations which can be represented by points on the hyperbola $g_1g_2 = 0.5$. Note that large spot sizes $w_1$ are obtained for resonators with large $g_2$ values. From Equation 22 follows that in order for $g_2>1$, the radius of curvature of mirror $R_2$ has to become negative, which indicates a convex mirror according to our labeling convention.

As an example, we will calculate the resonator parameters for a dynamically stable concave-convex resonator with a weekly thermally focusing rod. The situation is probably typical for a Nd:YaG crystal side pumped with laser diodes. The following assumptions are made:

$f=6m$, $D=5mm$, $L_1=0.1m$, $L_2=0.7$ m

where f is the thermally induced focal length of the laser rod, D is the diameter of the laser rod and $L_1$ and $L_2$ are the distances to the front and rear mirror.

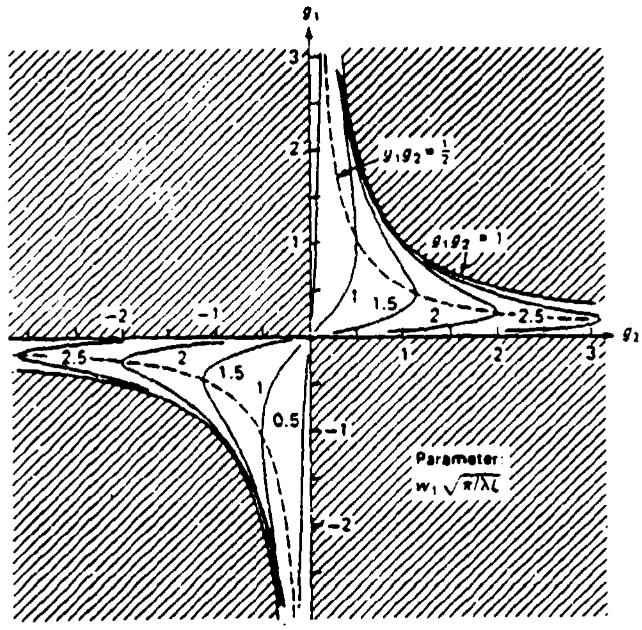


Figure 6.9   Resonator stability diagram with curves for constant mode size

(Ref. J. Steften et al, IEEE J. Quantum Electr. QE-8, 1972, P. 239)

If we want to make the laser rod the limiting aperture for $TEM_{00}$ mode operation, we require about $D=4w_1$. Therefore

$w_1=1.25$ mm

Introducing the stability criterion (Equation 26) into the expression for the spot size (Equation 20) one obtains

$$w1^2 = \lambda L_o / \pi g_1 \qquad (27)$$

from this equation follows

$g_1 = 0.16$

The other parameters follow from Equations 21 and 22.

$g_2=3.12$
$L_o=78.8$cm
$R_1=1.1$m
$R_2=-0.36$ m
$W_2=0.28$ mm

Figure 6-10 shows the schematic of the resonator. As can be seen, the mode size is very small on the convex mirror and expands towards the concave mirror, with the laser rod being the limiting aperture.

Recently resonators with an internal lens representing thermal effects in a pumped laser rod have been thoroughly analyzed in an entirely general way. It has been shown that, as a function of the dioptric power of the lens, two stability zones of the same width exist within which the mode spot size on the lens always presents a minimum in both zones. Corresponding to this minimum, the output power is insensitive to the focal length fluctuations, and the mode volume inside the rod is inversely proportional to the width of the stability zones and hence approximately proportional to the range of input power for which the resonator is stable. (Ref. 17, 18)

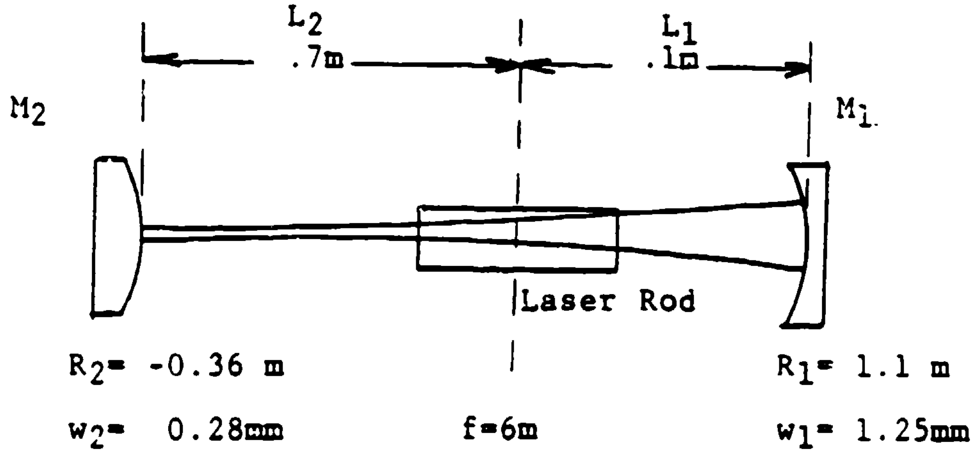


Figure 6.10 Concave-convex resonator for a weakly focuss laser rod.

These design criteria provide equations which allow the calculation of the resonator parameters, namely, the two-mirror radii of curvature ($R_1$, $R_2$) and the two distances of the mirrors from the rod. As an example, Figure 6-11 shows the parameters of optimized resonators for typical CW Nd:YAG lasers. From this figure the values of the curvature radii and the position of the rod can be readily obtained for a given focal length and for a given spot size of the mode in the rod.

The parameters used in these curves are defined as follows: $R_1$, $R_2$ -- radii of curvature of the mirror, positive if concave, $L_1$, $L_2$ distance between the mirrors and the principal plane of the rod; f is the focal length of the rod. The distance from the end of the rod to the principal plane is $H=1/2n_0$.

Figure 6-12 shows a resonator design based on the results presented in Figure 6.11. We assume mode radius of $W_{30}=3$ mm in the active medium. This is the optimum mode radices for a 6 mm diameter rod. The length of resonator is given as 150 cm.

For a focal length of f=17 cm ($1/f = 6\ m^{-1}$) we obtain $R_1=-14$cm, $R_2=55$ cm and $L_1=130$.

## 6.2.2 Telescopic Resonator

Hanns et al.[19,20] and Sarkies[21], reported using a telescope in an Nd:YaG resonator, see Figure 6-13. An attractive feature of the telescope is that it allows easily controllable adjustment to compensate thermal lensing under varied pumping conditions. Also the telescopic resonator avoids the very small spot on the convex mirror of the convex-concave mirror design. This is particularly important at the high power levels typical for Q-switched Nd:YaG lasers.

By introducing a suitably adjusted telescope into a Q-switched Nd:YaG laser resonator, the investigators mentioned above have been able to obtain reliable operation with a large-volume $TEM_{00}$ mode. The basic principle behind the resonator design is that of choosing a telescope adjustment which

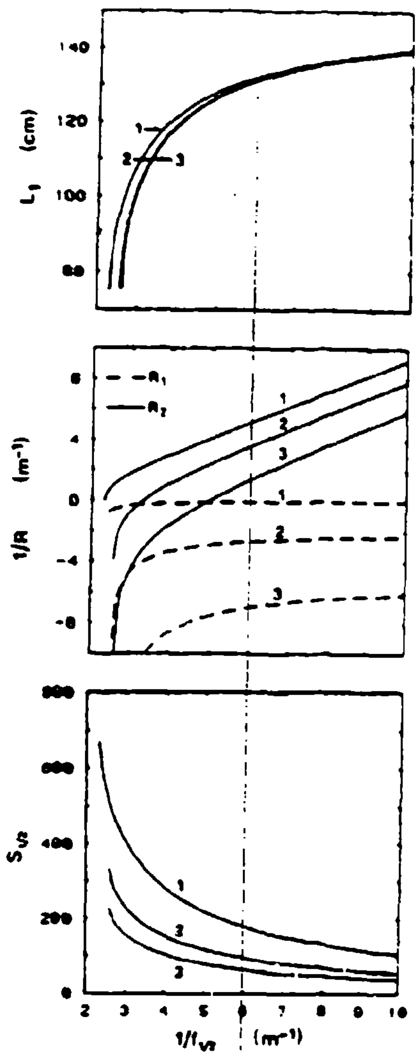


Figure 6.11 Design parameters for concave-convex resonator (From Ref. 17)

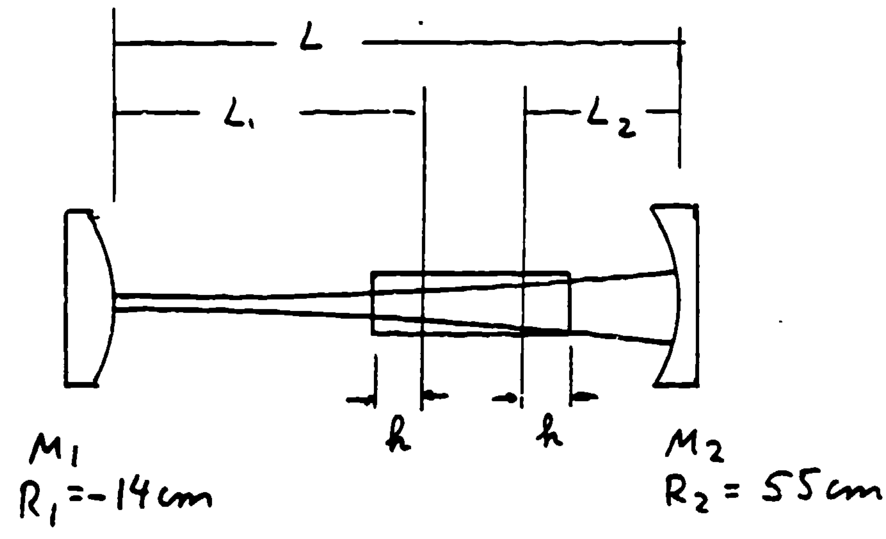


Figure 6.12 Dynamically stable resonator for a strongly focussing rod.

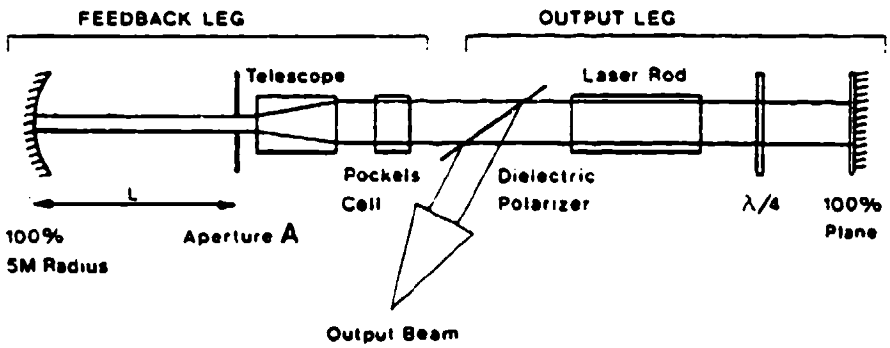


Figure 6.13 Resonator with internal telescope

compensates the thermal lensing in the laser rod (thus permitting a large spot size) and at the same time ensuring that the spot size is insensitive to fluctuations in focal length of the thermal lens.

The telescope performs two distinctly separate functions. Firstly, it reduces the size of the beam to increase the diffraction per unit length. Since the beam size on the input side is always the same as the rod diameter, the diffraction is constant and dependent only on the telescope magnification. Aperture at the telescope output is set to be D/M where D is the rod diameter. Secondly, the telescope is an element of variable focal length. It can therefore be adjusted to place the resonator anywhere on the stability diagram. Because the ratio of the diffraction losses of the higher order modes to the lower order modes increases as the telescope output beam decreases, the telescope can be adjusted to ensure that modes above a certain order do not reach threshold. Thus the mode selection process is controlled by two telescope parameters, the magnification M and the focal length f. Clearly sufficient mode selection can be achieved by either parameter alone, but, on the one hand too high a magnification may result in a very high power density in the feedback beam which could exceed the damage threshold of the components. On the other hand too much bias introduced by the telescope could result in a laser threshold that is very high. Thus the correct balance must be established to ensure optimum operation.

The telescope adjustment is chosen to minimize the effect of focal length variations in the laser rod and at the same time ensures the optimum mode-selection properties of a confocal resonator. Hanna et al. (19) performed a detailed analysis of the telescopic resonator. The analysis yielded simple design equations relating the mode spot sizes, resonator length, telescope magnification and defocusing and diffraction losses. A short summary of the key design parameters is given below.

One can best understand the role of the telescope by considering, for simplicity, a short telescope of magnificatin M (where $f_2 = -Mf_1$) located close to the laser rod. Thus the lens focal lengths are taken to be short

compared to the resonator length. It can be shown that for small defocusi of the telescope, i.e. $\delta << f_1$, the telescope has two main effects: it cha the beam spot size by a factor ~ M and it changes the wavefront curvature though it consisted of a single lens of focal length $f_T = -f_1 f_2 M/\delta$ . Thus telescope can be adjusted to achieve compensation of the thermal lens $f_R$ t making $f_T \approx - f'$ where f' now refers to the focal length resulting from th combination of $f_R$ and $f_m$, i.e. $1/f' = 1/f_r + 1/f_m$. The effect of the magnific tion M is to modify the condition for insensitivity of spot size to varia of fR. This becomes $f/M^2 = L$ where f is the focal length resulting from the combination of fT, $f_R$ and $f_m$ i.e. $1/f = 1/f_T + 1/f'$. The spot size in the laser rod is again given by $W_1 = M(2L\lambda/\pi)^{1/2}$ which can also be written a $= M(2L\lambda/\pi)^{1/2}$. Thus introducing the correctly adjusted telescope allows same large mode volume in the laser rod to be maintained but with a reduct of cavity length by $M^2$. The main limitation of this approach is that it exposes components in the reduced beam to higher intensity and thus greate damage risk.

The authors have presented some of their key findings in graphical f Figure 6-14 shows the results of spot-size versus telescope defocusing corresponding to a particular resonator. The main feature is the broad minimum for spot size in the laser rod (upper curve), implying insensitiv of spot-size $\delta$ . Note that a change of $\delta$ with $f_R$ fixed is equivalent to change of $f_R$ (due to changed pump conditions) with $\delta$ fixed, since both correspond to a change of combined focal length f. Thus Figure 6-14 also represents a plot of spot size versus $f_R$. The minimum of the upper curve therefore implies insensitivity to fluctuations in $f_R$. The desired opera point is at the bottom of this minimum and the telescope must therefore b defocused by the correct amount to ensure this. In arriving at a resonato design the main parameters to be chosen are spot-size $w_1$, in the laser ro resonator length L and magnification M.

These parameters are interrelated as follows:

$$W_1 = M(2L\lambda/\pi)^{1/2} = (\lambda f/\pi)^{1/2}$$

(From Ref. 21)

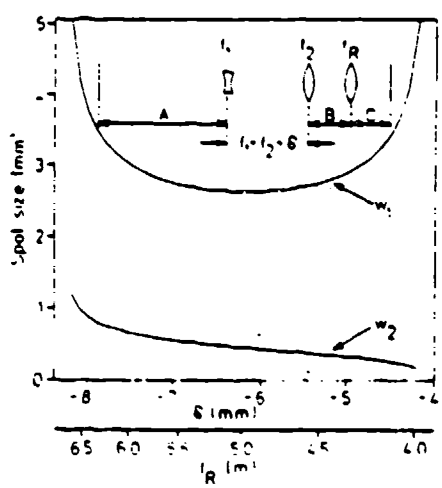


Figure 6.14 Spot size versus defocussing of telescope

$W_1$ is chosen for best utilization of the laser medium. For a 9 mm r diameter, the authors selected $w_1$=2.5 mm to be optimum. With $W_1$ chosen t choice of values for L and M is made to give an acceptable compromise bet a small M and hence an inconveniently large L or small L and hence large which may then lead to excessive intensity in the contracted beam. When L hence M) have been chosen the value of f is fixed ($f=2M^2L$ for the simplif resonator) and this in turn fixes $\delta$ through the relations $1/f = 1/f_T + 1$ $1/f_m$ and $f_T = f_2/\delta$. This assumes $f_R$ to be known, $f_R$ is usually determin passing a HeNe laser beam through the laser rod and measuring the beam wa at the desired pump level.

A circular aperture to select the $TEM_{00}$ mode is inserted and centere In practice we have found that the aperture diameter should be $\sim 15$ time calculated spot diameter at the point of insertion to ensure suppression the $TEM_{01}$ mode.

## 6.3 COMPARISON

The prime resonator configurations for laser diode pumped solid stat lasers are the confocal positive or negative branch unstable resonator an covnex-concave or telescopic stable resonator. The particular choice dep on the gain of the solid state laser material, the beam quality requireme and the particular size and shape of the active material. The positive b unstable resonator has the great advantage that it can be designed to fil large active medium in either a cylindrical or a rectangular geometry. I the most widely used resonator for slab lasers. The disadvantage of this of resonator is the hole in the center and diffraction rings in the beam profile which are typical of polka-dot or scraper mirror designs. At the expense of a more complicated design, apodized aperture and radially bire fringent elements can be used to reduce these effects. Compared to the o configurations mentioned above, the positive branch unstable resonator is design which is most sensitive to mechanical and optical perturbation. T negative branch unstable resonator has a considerably higher stability to misalignment and thermal lensing effects. However, due to the internal f the design is useful only for lasers with peak powers less than 10 MW. A

modified negative branch unstable resonator employs a pinhole at the focal point. The diameter is such that only the Airy disk of the diffraction pattern is transmitted. This design leads to a very smooth output profile in combination with a high alignment tolerance. Both unstable resonator configurations are not suitable when the gain becomes very low. This may be the case in CW pumped solid state lasers, particularly in materials with a lower gain as compared to Nd:YaG. In these cases a stable resonator with a concave-convex mirror configuration or containing a telescope will have to be used. Recent advances in stable resonator design for solid state lasers have been directed at finding regions where the structure is insensitive to change of the focal length of the laser rod. Thermal lensing is a design parameter in these dynamic stable resonators. The choice between the convex-concave and the telescopic resonator is not easy to make. The former has the advantage that it uses no additional optical elements on the other hand, the telescope required in the latter design provides a convenient way of optimizing the resonator for different operating conditions.

## References


1. A.E. Siegman, Proc. IEEE, vol. 53, Pg. 227, 1965.

2. A.E. Siegman, R. Arrathoon, IEEE, International Quantum Electronics, QE-3, Pg. 156, 1967.

3. A.E. Siegman, Applied Optics, Volume 13, Pg. 353, 1974.

4. W.H. Steier, Unstable Resonator Laser Handbook, 1979, ed. M. Stitch.

5. R.L. Byer, R.L. Herbst, Laser Focus, July 1978, pp. 48-57.

6. R.L. Herbst, M. Komine, R.L. Byer, Optical Comments, Volume 21, Pg. 1977.

7. Yu, A. Ananev, G.N. Vinokurov, L.V. Kovalchuk, N.A. Sventsitskaya, V Sherstobitov, Sov. Physics, JETP, Volume 31, pg. 420, 1970.

8. W.F. Krupke, W.R. Sooy, IEEE Journal of Quantum Electronics, QES, December 1969.

9. G. Giuliani, Y.K. Park, and R.L. Byer, "The radial birefringent elem and its application to laser resonator design," presented at the Ele International Quantum Electronics Conference, Boston, Mass., June 19

10. G. Giuliani, Y.K. Park, and R.L. Byer, "The radial birefrngent eleme and its application to a Nd:YaG resonator," Opt. Lett., 5, 491-493 (1980).

11. J.M. Eggleston, G. Giuliani, R.L. Byer, J. Opt. Soc. Am., volume 71, October 1981, p. 1264.

12. D. Andreou, Review of Scientific Instruments, Volume 49, May 1978, F 586-590.

13. T.F. Ewanizky, J.M. Craig, Applied Optics, Volume 15, P. 1465, 1976.

14. P.G. Gobbi, S. Morosi, G.C. Reali, A.S. Zarkasi, Applied Optics, Vol 24, P. 26, 1985.

15. J. Steffers, J.P. Lortscher, G. Herziger, IEEE Quantum Electronics, Feb. 1972, Pg. 239.

16. H.P. Kortz, R. Ifflander, H. Weber, Applied Optics, Volume 20, Decem 1981, Pg. 4124.

17. V. Magni, Applied Optics, Volume 25, January 1986, Pg. 107.

18. S. De Silverstri, P. Laporta, V. Magni, Optics Com. April 1986, volume 57, pg. 339.

19. D.C. Hanna, C.G. Sawyers, M.A. Yuratick, Optical and Quantum Electronics, volume 13, 1981, pg. 493-507.

20. D.C. Hanna, C.G. Sawyers, M.A. Yuratick, Optics Comm., Volume 37, June 1981, pg. 359.

21. P.H. Sarkies, Optics Comm. Volume 31, November 1979, pg. 189.

# 7. SPECIFIC CW LASER DESIGN

In this section we will bring together the various system elements discussed in the report in order to design a highly efficient solid state laser for underwater illumination. Our design goal is an average output power of three watts in the green, and a wall plug efficiency of at least 1.5%.

The performance of a diode laser pumped Nd:YAG laser system with second harmonic conversion to the green depends upon detailed design choices for each sub-system.

## 7.1 SYSTEM CONFIGURATION

Several critical design choices have to be made with regard to the diode array pump configuration, resonator design and harmonic generation.

The power regime of this laser made the side pumped cylindrical rod a clear choice. A diode laser array configuration and performance is identified that is within current capabilities of several vendors. One of the key technical issues to be resolved is the selection of an efficient doubling method. We considered the following approaches for the CW pumped laser:

- Intracavity doubling
- Repetitively Q-switched plus intracavity doubling
- Modelocked with internal or external doubling

The intracavity power density is low in a CW laser; therefore, the beam has to be tightly focused into the nonlinear crystal for efficient conversion. In addition, the doubling crystal must have a high nonlinearity. Most often used with CW lasers is barium sodium niobate, $Ba_2NaNb_5O_{15}$.

The low gain of a CW laser, combined with the critical adjustment of focusing the beam to a small area inside the doubling crystal, make this approach not very attractive for a fieldable military system. The same can be

said for modelocking, which is also very critical to operate and requires feedback loop for stabilization. In addition, there is a deleterious interaction between modelocking and intracavity harmonic generation (7.1

The design we selected is the CW pumped repetitively Q-switched Nd:' laser with internal frequency doubling. Since the peak power of a continuously pumped, Q-switched Nd:YAG laser is in the kW range, a much h power density is achieved compared to CW operation, and therefore less focusing into the doubling crystal is needed.

As for continuous lasers, output of a CW pumped, Q-switched laser is frequency doubled most efficiently with an intracavity crystal. Typical average harmonic output from such a laser can be as large as the fundamer output. Such lasers typically emit pulses lasting several hundred nanose at repetition rates of several kilohertz; average powers are normally a watts, although average power has reached ten watts in one device (7.2).

A back-up to the repetitively Q-switched laser with internal doublir the externally doubled repetitively Q-switched laser. It has the advant that the function of the oscillator and doubler are separated and oscill performance is not affected due to heating of the doubling crystal. How even with Q-switching the power density is still low and an external foc arrangement has to be employed.

The next critical issue is the selection of the doubling crystal. selection of a nonlinear optical material for this application is limite the average power and peak power densities that a crystal can tolerate. Thermally induced phase mismatch, resulting from beam power absorption, the average power capability. The damage threshold limits the peak powe density capability. There are only a few optical crystals materials ava that satisfy these requirements. These are: KD*P, CD*A, and the most recently developed KTP crystals. Each of these crystals has properties are unique for certain applications. Table 7-1a lists the nonlinear coefficients and damage threshold of these crystals. Some of the unique

| CRYSTAL | NONLINEAR COEFFICIENT ($10^{-9}$ cm dyne$^{-1/2}$) | DAMAGE THRESHOLD ($GW/cm^2$) |
|---|---|---|
| Deuterated Potassium Dihydrogen Phosphate $KD_2PO_4$ (KD*P) | $d_{36}$=.96x | .23 (.2 ns) |
| Deuterated Cesium Dihydrogen Arsenate $C_2D_2A_sO_4$ (CD*A) | $d_{36}$=.96 | > .26 (12 ns) |
| Lithium Iodate $LiIO_3$ | $d_{15}$=13.2 | .06 (20 ns) |
| Lithium Niobate $LiNbO_3$ | $d_{15}$=13 | > 10 (.006 ns) |
| Potassium Titanium Penta-Phosphate $KTiOPO_4$ (KTP) | $d_{33}$=29.5 | 0.16 (20 ns) |
| Barium Sodium Niobate $Ba_2NaNb_5O_{15}$ | $d_{33}$=43 | .04 |

a)

| | KD*P | | CD*A | | KTP |
|---|---|---|---|---|---|
| Type of Phase Matching and Temperature | Type I @22 °C | Type II @22 °C | Type I @22 °C | 90° @105 °C | Type II @25 °C |
| Spectral Bandwidth $L\,\Delta\lambda$ (FWHM) (A-cm) | 72.5 | 55.7 | 22.5 | 22.5 | 5.7 |
| Angular Bandwidth $L\,\Delta\theta$ (FWHM) (mrad-cm) | 2.4 | 5 | 9 | > 50 | 15 |
| Temperature Bandwidth $L\,\Delta T$ (FWHM) (°C-cm) | 6† | 6. | 6† | 6 | 15 |
| Phase-matching angle @ 1.06 μm | 41° | 53.5° | 82° | 90° | 26° |
| Walk-off angle (mrad) | 27 | 18 | 31 | 0 | 1 |

b)

Table 7.1 Properties of nonlinear crystals. Nonlinear coefficient a) and phase matching properties b).
(Milek et. al. Report AD704556, Hughes Aircraft Co. 1970)

properties of these crystals and the results obtained with them are revie below.

KD*P (Deuterated $KH_2PO_4$). KD*P is the most highly developed of the nonlinear crystals discussed. The deuterated material is required to rec absorption at 1.06 $\mu$m and thus minimize the thermally induced phase mismε Crystals are available in large sizes with excellent optical quality.

The KD*P crystal has a low absorption constant (<0.01 $cm^{-1}$) and a hi power-density damage threshold at 1.06 $\mu$m. Effects due to thermally indu phase mismatching are negligibly small at an incident average power level to about 25 W, with peak power density of 250 $MW/cm^2$ and a 35 ns pulse du tion. Nonlinear absorption due to two-photon processes is also insignifi under these conditions.

CD*A (Deuterated $CsH_2AsO_4$). CD*A is isomorphic with KD*P and is usu found to be a more efficient harmonic converter than KD*. The temperatur tuned, $90^{o}$ phase-matched CD*A is a preferred configuration. However, the phase-matching temperature of the crystal at 1.06 $\mu$m is $110^{o}C$. This temp ture is sufficiently high that the crystal is susceptible to damage due dehydration, which occurs at about $150^{o}C$. The damage level for a temper tuned CD*A was less than 10W at an energy density of about 2 $J\text{-}cm^{-2}$ (35 r This property has severely limited the usefulness of $90^{o}$ phase matched CI for high-power harmonic conversion.

KTP ($KTiOPO_4$). KTP is a new type of nonlinear crystal which is curr under development. The crystal exhibits several unique properties, inclu a high nonlinear coefficient comparable to that of $Ba_aNaNb_5O_{15}$, a high da threshold, and a low degree of sensitivity to thermally induced phase mis match. These combined properties make KTP the most attractive crystal fo high-power frequency conversion (Ref. 7.3, 7.4).

The spectral, angular, and temperature phase-matching characteristi second harmonic generation at 1.06 $\mu$m in KTP are shown in Table 7-16. Th

large temperature bandwidth observed is a unique characteristic of this nonlinear material. Because of its large nonlinear coefficient, this further reduces the length of crystal required for high conversion efficiency. As a result, a second harmonic generation efficiency near 50% can be readily obtained in a 3.5 mm crystal length at an incident power intensity of about 100 $MW/cm^2$.

The best performance from our system can be achieved with KTP; therefore, we will select this material as the doubling crystal.

Based on the foregoing discussion, the system configuration shown in Figure 7-5 was selected. A Nd:YAG rod is pumped by linear laser diode arrays. The system is Q-switched by an acoustic-optic resonator and contains the doubling crystal in the resonator. A concave-convex design was chosen for good mode selection, and for a small beam waist at the location of the doubling crystal. The cavity is folded in order to recover both harmonic beams.

## 7.2 SOLID STATE GAIN MEDIUM AND DIODE ARRAY CONFIGURATION

Due to its high gain and good mechanical and physical properties, Nd:YAG is our first choice for this laser. However, ND:YLF is a close contender. For CW pumping, the gain depends on the product of cross section $\delta$ and population inversion, which in turn is proportional to the product of absorbed pump light and upper state lifetime $\tau f$. In Nd:YLF, the $\delta \tau_f$ product is 1.5 times larger as compared to ND:YAG. Since CW threshold is inversely proportional to this product, all other factors being equal, Nd:YLF should be a better material compared to Nd:YAG. It also has the advantage of producing a polarized beam. Whether one can take advantage of the better properties of Nd:YLF in a diode pumped system depends on other factors such as crystal quality, optical losses in the material, etc.

Assuming a Nd:YAG for the gain medium we will design the laser array pump such that the system can generate 15 W of CW output, multimode, unpolarized in an empty resonator at 1.064 $\mu$m. As we will discuss below, this is our estimate of what is needed to produce three watts average power in the green.

Insertion of an acousto-optic Q-switch into the resonator and operation
$TEM_{00}$ mode will reduce the average power to about seven watts. Optical
associated with the doubling crystal and polarization losses will further
reduce the power to about 4W. Intracavity doubling will recover most of
radiation.

An acousto-optic Q-switch has a slow opening time. As discussed in Reference 7.5, the transient effects associated with slow Q-switching hel mode selection. With a low optical distortion medium, the diffraction lo difference between the lowest and higher-order modes so that the lowest-o mode dominates in the Q-switched mode.

The diode array has to be designed to produce 15 watts of output fro basic laser. In Section 4.4.2 we determined the optical efficiency of a pumped cylindrical rod to be about $\eta = 0.35$. Therefore a diode output o 43 watts is needed to produce the desired output. Assuming a laser array conversion efficiency of 25% and an efficiency of 95% for the power condi- tioning unit, the system requires 182 W of electrical input.

Linear arrays with five watt CW output are commercially available fr Siemens and Spectra Diode Labs. In our design of a conduction cooled roo four linear arrays are mounted around the semicylindrical area, i.e. 20 W of pump power. With a three cm long Nd:YAG rod, a maximum of 60 W of pum power would be available. Reducing the power level to 45W or 3.75 w from array will increase lifetime. The detailed optical design of the condens lenses and the pump distribution can be obtained from the computer progra developed by FIBERTEK, Inc. The input parameters for this analysis are:

- Radii of lenses (focal length)
- Diode to lens separation
- Lens to rod center separation
- Lens spacing
- Refractive indices
- Diameter of Nd:YAG rod

- Absorption spectrum
- Diode center wavelength
- Diode output spread (FWHM of statistical spread)

The small signal gain of the Nd:YAG rod can be calculated from the pumped volume and the projected stored energy in the rod. For a 30 mm long crystal of 3 mm diameter we obtain $V = 0.21\ cm^3$.

Taking the value of $\eta = 0.54$ for the fraction of pump radiation reaching the upper state level, then $P = 24.3$ W and $E_s = 26.6 \times 10^{-3} J/cm^3$ or $G_0 = 0.08\ cm^{-1}$.

Figure 7-1 shows a cross-section of the semi-cylindrical pump geometry. The rod support structure provides a heat sink for removal of waste heat from the crystal, and it also reflects back pump radiation for a second path in the rod.

A summary of the salient features of the oscillator is provided in Table 7-2.

## 7.3 Q-SWITCH

In an acousto-optic Q-switch, an ultrasonic wave is launched into a block of fused silica, which acts as an optical phase grating when an ultrasonic wave passes through it. The high optical quality of fused silica combined with a very high damage threshold makes an acousto-optic Q-switch the universal choice for CW lasers.

The low-gain characteristics of CW-pumped solid state lasers do not require a very high extinction ratio for Q-switching but do demand exceptionally low insertion loss. Since the best optical quality fused silica with antireflection coatings can be used as the active medium, the overall insertion loss of the Q-switch can be reduced to less than 0.5% per pass.

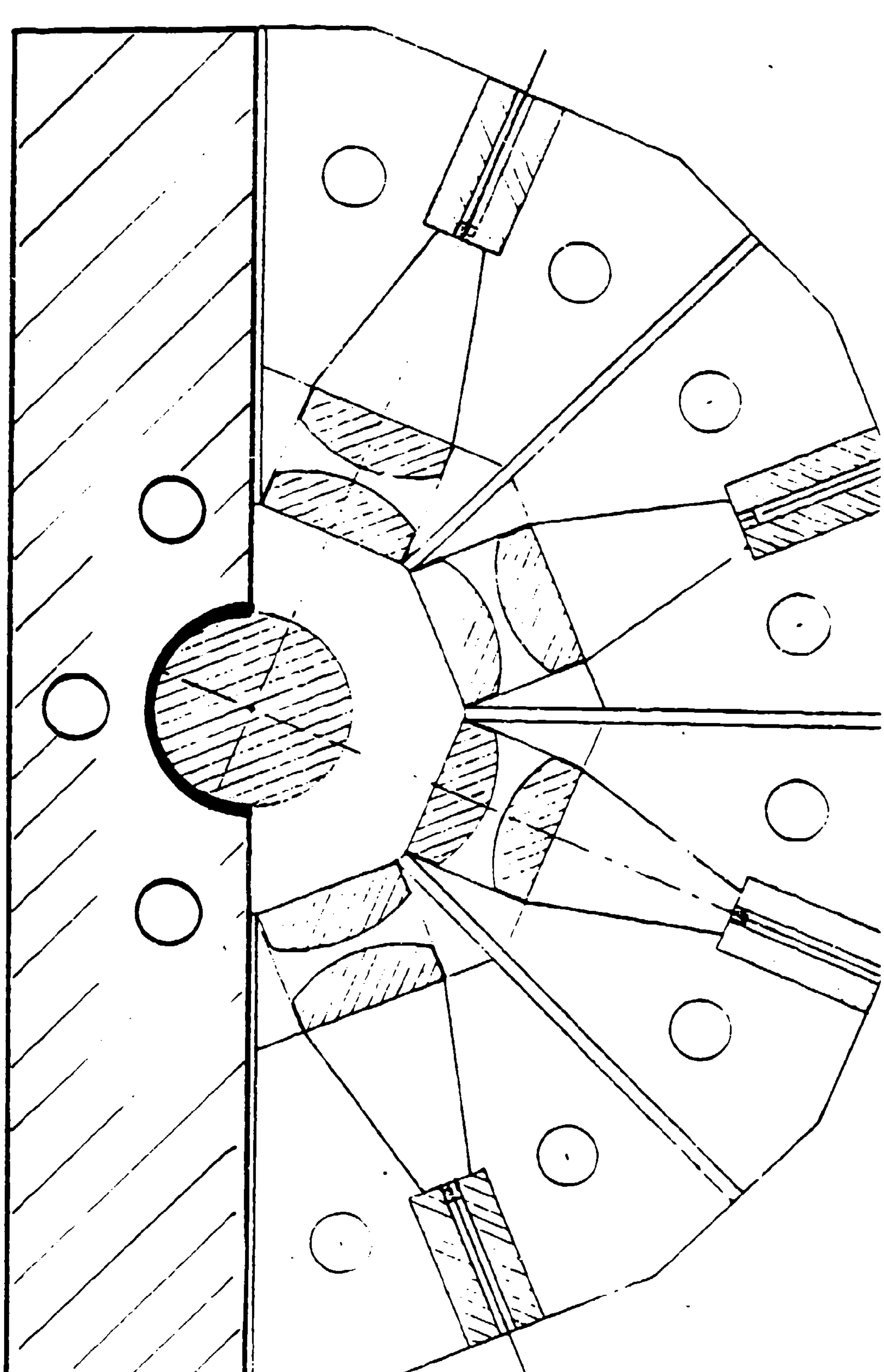

Table 7.2.

Summary of system parameters for cw laser diode pumped, repetitively Q-switched, intracavity doubled Nd:YAG laser.

| | |
|---|---|
| Laser material length, cm: | 3 |
| Resonator length, m: | .35 |
| Inversion volume, $cm^3$: | .21 |
| Average output power, w: | 3 |
| Energy per pulse, mj: | 0.5 |
| Repetition rate, Hz: | 6,000 |
| Pulse width, nsec: | 100 |
| Output wavelength, nm: | 532 |
| Peak power, kW: | 5 |

The performance data of an acousto-optic Q-switched Nd:YAG laser wit[h] output comparable to the system under consideration is shown in Figure 7-[2]. For repetition rates below approximately 800 Hz the peak power is indepen[dent] of repetition rate. At these low repetition rates there is sufficient ti[me] between pulses for the inversion to reach the maximum value. In the tran[si]tion region between 0.8 and 3kHz, peak power starts to decrease as the repetition rate is increased. Above 3kHz, the peak power decreases very rapidly for higher repetition rates. The optimum repetition rate for a frequency doubled is between four and eight kHz. The lower repetition ra[te] yields higher peak power which produces higher harmonic output, whereas t[he] higher repetition rate yields a higher average power.

We assume a repetition rate of 5kHz. According to Figure 7-2 peak p[ower] on the order of 15 kW can be expected from the laser. Typically these la[sers] operate with an 80% reflective output mirror. The circulating power is therefore 75 kW. Efficient frequency doubling in KTP requires about 25-3[0] $MW/cm^2$. This power density can be achieved if the beam diameter is reduc[ed] 0.5 mm in the resonator. The particular concave-convex resonator discuss[ed] the next section will accomplish the desired beam compression.

## 7.4 OPTICAL RESONATOR

In our opinion, the dynamic-stable concave-convex resonator treated Section 6.2.1 is the best choice for the CW pumped, repetitively Q-switch[ed] and intracavity doubled Nd:YAG laser. The resonator maximizes $TEM_{00}$ mode volume in the active material, and it provides a small beam waist at the convex mirror, which is necessary for efficient doubling. We assume a we[ak] focusing rod with f=6 meters, a diameter of 3 mm, and a separation of the from the concave and convex mirror of $L_1$ = 0.05 m and $L_2$ = 0.3 m.

The mode size at the Nd:YAG rods is $W_1$=D/4 = 0.75 mm. If we follow design procedure outlined in Section 6.2.1 we obtain

$L_o$ = 35 cm (from eq. 22b)

$g_1$ = 0.2 (from eq. 27)

Figure 7.2 Performance of a repetitively Q-switched, cw pumped Nd:YAG laser system.
(W. Koechner, Solid State Laser Engineering, Springer Verlag, 1976)

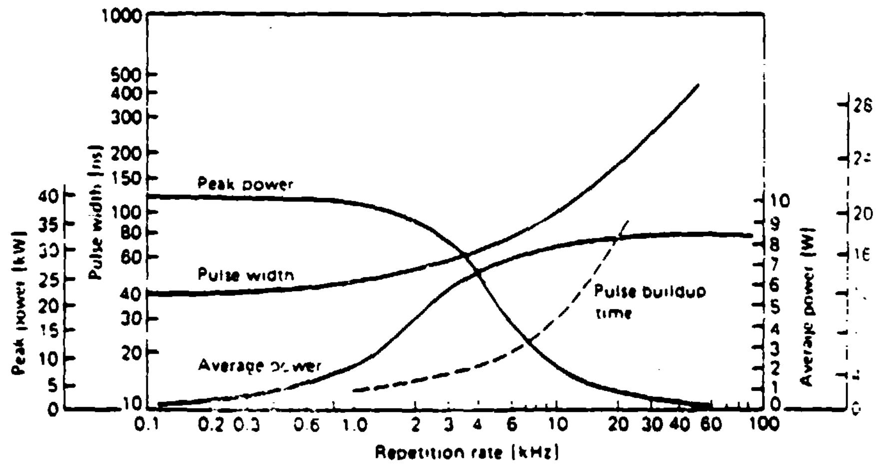

$g_2 = 2.5$ (from eq. 26)

$w_2 = 0.2$ mm (from eq. 21)

$R_2 = 23$ cm (from eq. 22a)

$R_1 = 47$ cm (from eq. 22a)

Figure 7-3 shows a schematic of the resonator. The mode size is ver small at the location of the doubling crystal and expands towards the con mirror, with the Nd:YAG rod being the limiting aperture.

### 7.3.3 Harmonic Generator

The second harmonic generation efficiency depends on incident intens crystal type and length, and on laser beam spatial mode quality.

KTP is a relatively new nonlinear optical material that is increasin being used commercially for second harmonic generation of the 1.06 m Nd: laser. KTP ($KTiOPO_4$) has been shown to have particularly favorable prope for use in second harmonic generation of 1.06 $\mu$m Nd:YAG lasers. The lar nonlinear optical d coefficient combined with a high optical damage thres make this material presently one of the most useful for nonlinear optical devices.

The supply of commercially available KTP is limited, furthermore onl small crystals can be grown. Crystals are currently only available in si up to 5 mm cubes. For the laser designed in this section, only a very sm crystal is needed. A 3 mm cube is sufficient to obtain the desired conve efficiency. Also there are clear indications that KTP crystals of suffici quantities and quality will become available in the near future.

Several companies such as Inrad, Airtron, Virgo Optics, and Ferroxcu are now exploring the fabrication of this material either by hydrothermal flux growth methods. In addition, the next development in this technolog be epitaxially grown KTP presently explored at Bell Laboratories.

The energy conversion efficiency of one DTP crystal (3.5 mm length) function of input power density is shown in Figure 7-4.

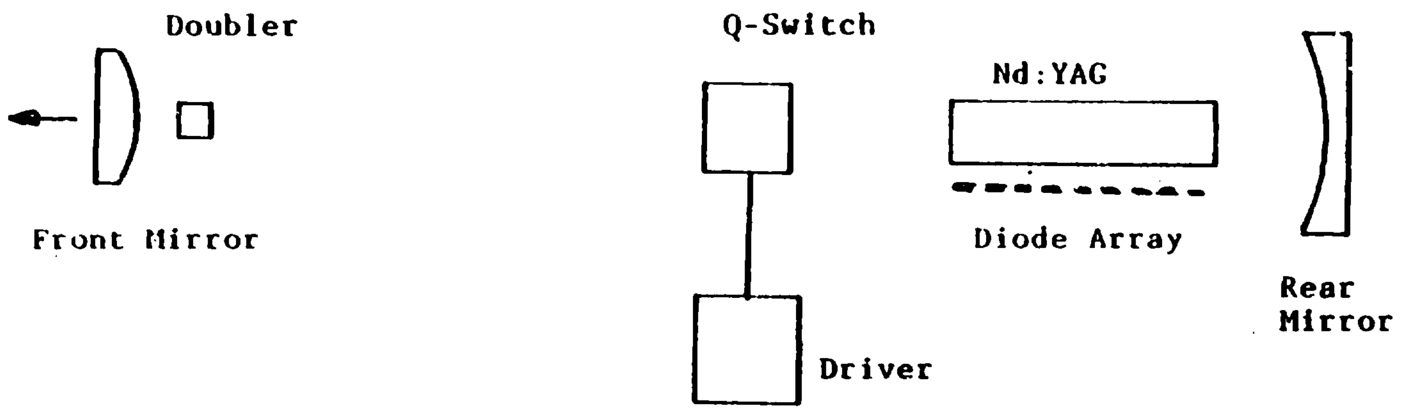


Figure 7.3 Simplified block diagram of the cw pumped, repetitively Q-switched, intracavity doubled Nd:YAG laser.

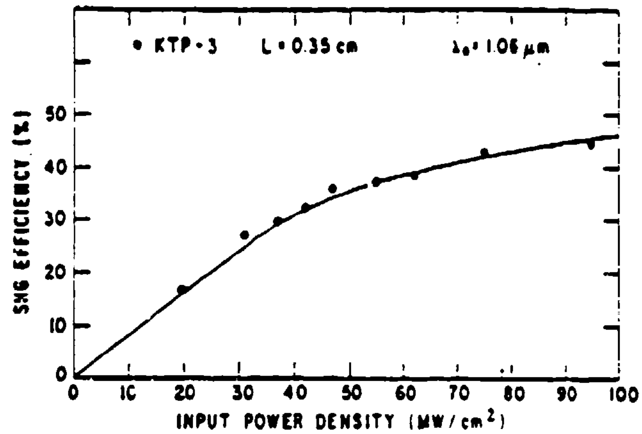


Figure 7.4 Conversion efficiency of KTP at 1.06 μ

The intracavity frequency doubled Nd:YAG laser can be significantly affected by thermo-optical effects in the frequency doubling crystal. The slight absorption of the circulating 1.064 $\mu$m power, as well as the 532 nm power produced by frequency doubling, can modify the laser parameters through complex interdependent relationships. As a result, the laser performance may degrade and become unstable.

At the level of 4 watts average power, in combination with the low absorption KTP material, no thermal instabilities are expected.

Extraction of power only in one direction simplifies the design; however, at the expense of 50% reduction in output power. Combining the two oppositely directed second harmonic beams together for higher efficiency output has been tried in the past; however, interference effects caused large output fluctuations.

The two frequency doubled beams are phase locked via the fundamental beam. However, dispersion in the air of the green beam reflected off the rear mirror and directed a second time through the harmonic generator will cause a time varying phase difference of the combined beams. Introduction of a quarter wave plate at the harmonic, inserted between the doubling crystal and the rear mirror, will combine the two green beams orthogonally polarized and no interference effects will take place. In order to leave the fundamental beam unaffected, the phase retarder must be half wave for 1.064 $\mu$m. The final design of the optical resonator containing the harmonic generator is shown in Figure 7-5.

## 7.4 POWER BUDGET AND EFFICIENCY SUMMARY

The energy flow of the underwater illuminator system is illustrated in Figure 7-6. A summary of the system efficiency available with today's technology and projected performance available in a three to five year time frame is shown in Table 7-3.

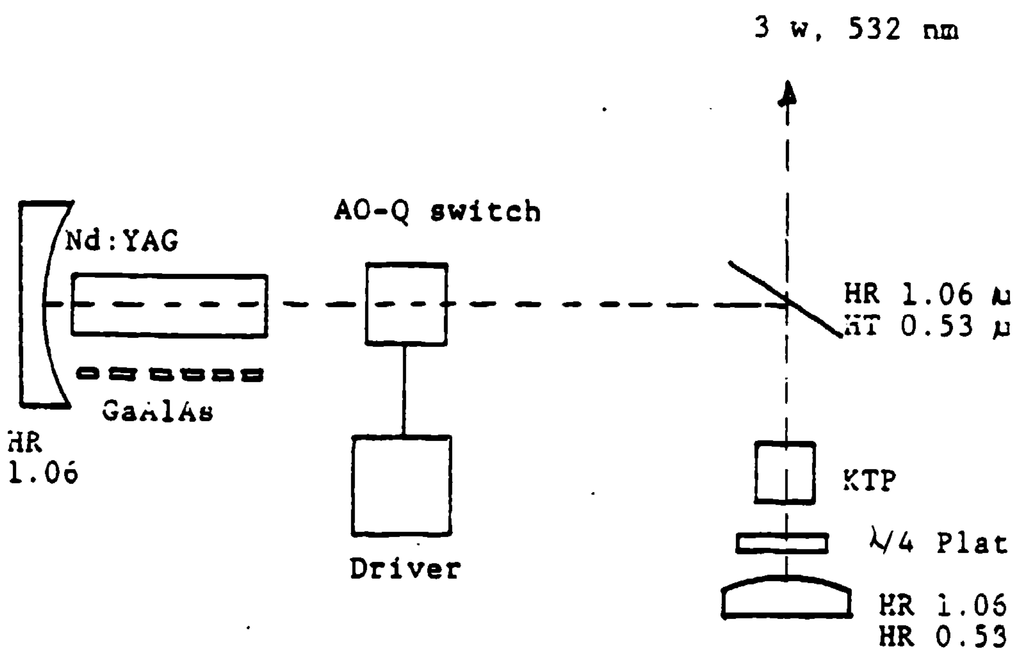


Figure 7.5 Conceptual design of a cw laser diode pumped, repetitively Q-switched and intracavity doubl Nd:YAG laser.

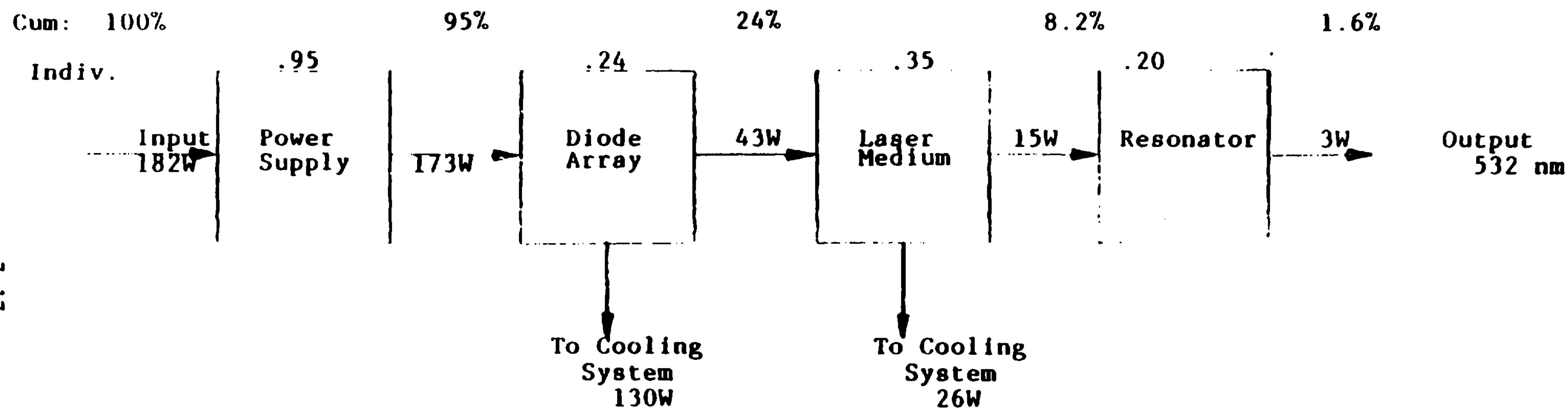


Figure 7.6 Energy flow of diode pumped Nd:YAG laser.

Table 7.3 - Projected Efficiency

| | Near Term | Long Ter |
|---|---|---|
| Power Conversion | .95 | .95 |
| Diode Arrays | .25 | .50 |
| Upper State Transfer | .54 | .54 |
| Output Efficiency | .64 | .64 |
| Doubling Efficiency | .20 | .30 |
| TOTAL | 1.6% | 4.9% |

## References

7.1 J. Falk, IEEE J. Quant. Electronics, QE-10, vol. 1, 1974, pg. 21.

7.2 J.M. Yarborough, E.O. Ammarum, IEEE J. Quant. Electronics, QE-9, Vol. 6, 1973, pg. 702.

7.3 Liu, Y.S., 1977, "Spectral Phase-Matching Properties for Second Harmonic Generation in Nonlinear Crystals," Appl. Phys. Lett. 31, 187.

7.4 Liu, Y.S. Drafall, L., Dentz, D., and Belt, R. 1980, "Properties in Second Harmonic Generation in KTP,", Proc. of the Third International Conference Lasers '80

7.5 W. Koechner, Solid State Laser Engineering, Springer Verlag 1976, Chapter 5.2

# 8. CONCLUSION

During the 1970's and early 1980's, solid state laser technology went through a process of evolutionary changes, characterized by incremental improvements in system performance and reliability.

However, during the last several years rather dramatic possibilities have appeared on the horizon which could bring about a revolutionary change in solid state laser technology. The most important developments are:

- Laser diode array pumping of solid state lasers
- Tunable lasers
- Phase conjugated and Raman shifted lasers
- High performance nonlinear materials such as KTU and organic crystals.

We are just on the verge of seeing these technologies emerge, but none has yet reached the maturity needed for large commercial or military applications.

This report is concerned with the most far reaching new technology, namely laser diode pumping of solid state lasers. The report provides an assessment of the technological and economic issues surrounding the use of diode arrays for pumping solid state lasers.

Laser diode pumping requires a different engineering approach to the design of solid state lasers. The pertinent characteristics of the pump sources, laser materials, crystal geometry and diode pump configuration, cooling cycle and resonator design are covered in this report, together with a specific laser design. Economic issues and manufacturing processes for mass producing diode arrays are treated also.

Just as vacuum tubes have been replaced by the transistor and later by integrated circuits, we envision gas filled arc lamps being replaced by linear and planar laser diode arrays.

The development and commercialization last year of these arrays have opened up the possibility of creating practical all-solid state lasers, w potential advantages of compactness, high efficiency and long lifetime.

Solid state lasers with wall plug efficiencies of 10% and higher wil possible in the future.

Laser diode pumping always looked attractive but was not practical c such technological barriers as low efficiency, low power, and short lifet The significant progress made in diode laser technology coupled with the emerging technology of linear and planar diode arrays has removed these former technological barriers. In the newer devices, efficiencies of up 50 percent can be achieved, and lifetimes of 10,000 hours have been built employed at pump sources for solid state lasers.

Feasibility of such arrays has now been demonstrated, but manufactur costs are prohibitive and must be reduced sharply before widespread appli tions will emerge.

The future of laser diode pumping seems to be assured at least for s specialized military applications, but widespread commercial uses will be slowed by their relatively high cost. High costs are not inherent as rec cost studies by SDL and MDAC have shown. With production of laser diode arrays increasing, cost can reach a very attractive level.

Technology is available, and it is mainly an economic issue to find applications which will drive costs down and stimulate further use of the systems.

Appendix A

CRADLE Source Code Listing

Page A1 to A37

```
1   calact%=0      '$DYNAMIC
5   DEFDBL A-Z:VERSION$="9.29":ON ERROR GOTO 40000: NUMLINES% = 1
6   DIM WINDOWX%(3), WINDOWY%(3), WINDOWW%(3), WINDOWH%(3), S$(50), PROG$(49
7   DIM LAMBDA(40), AABS(40), ABSO(20,160), VOL(20), LL(40), ATTRIBUTE%(3)
8   DIM SUM(20,10), SUMM(2,20,10), FIRST(20,10), LAST(20,10)
9   DIM ABSORB(2), LOSS(2), INTABSORB(20), ABSDENS(20)
10  FOR I%=1 TO 10:KEY I%,"":NEXT
201 EDIT.CALL%=0:SCREEN 0,0,0,0:WIDTH 80:COLOR 15,0,0:CLS:KEY OFF:MENU$="CDWREXS
LV"+CHR$(27)
210 GOSUB 9910                               ' —— Read Configureation file ——
220 EXT%=0:GOSUB 9000                        ' —— Main Menu ——
221 if len(a$)=2 then b$=right$(a$,1):if b$=chr$(31) Then 220
222 if len(a$)=2 then b$=right$(a$,1):if b$=chr$(18) Then error 201
225 IF INSTR(MENU$,A$) =1 THEN MESSAGE$="":locate csrlin,pos(0)-1:print a$::GOTO
 230 ELSE MESSAGE$="Enter only the letter(s) beteween the [] to make a selectio
n.":GOTO 398
230 IF A$="X" THEN EXT%=EXT%+1:MESSAGE$="Press X/Esc again if you wish to termin
ate program, or enter a new selection":IF EXT%=2 THEN 600 ELSE 399
240 IF A$=CHR$(27) THEN A$="X":GOTO 230
260 IF A$="E" THEN GOSUB 400:GOTO 510
270 IF A$="D" THEN OPEN"RETURN.BAT" FOR OUTPUT AS#1:PRINT#1,"CRADLE.EXE":CLOSE#1
:CHAIN"CDLINSTL.EXE"
280 IF A$="L" THEN GOSUB 400:GOTO 420
290 IF A$="S" THEN GOSUB 400:GOTO 450
300 IF A$="V" THEN GOSUB 400:GOTO 480
310 IF A$="R" THEN GOSUB 400:GOTO 530
320 IF A$="C" THEN 17000
340 IF A$="W" THEN gosub 7000:goto 220
398 EXT%=0
399 GOSUB 9100:GOTO 221
400 '┌──────────────────────────────────────────────────────────┐
401 '│  Get second part of menu selection                        │
402 '└──────────────────────────────────────────────────────────┘
410 GOSUB 11090:IF A$="S" OR A$="C" THEN print a$::RETURN ELSE RETURN 399
420 '┌──────────────────────────────────────────────────────────┐
421 '│  Load from disk                                           │
422 '└──────────────────────────────────────────────────────────┘
430 IF A$="S" THEN FILACT%=1 ELSE FILACT%=3
440 GOSUB 4000:GOTO 398
450 '┌──────────────────────────────────────────────────────────┐
451 '│  Save to disk                                             │
452 '└──────────────────────────────────────────────────────────┘
460 IF A$="S" THEN FILACT%=2 ELSE FILACT%=4
470 GOSUB 4000:GOTO 398
480 '┌──────────────────────────────────────────────────────────┐
481 '│  View parameters                                          │
482 '└──────────────────────────────────────────────────────────┘
490 IF A$="S" THEN VWACT%=1 ELSE VWACT%=2
500 GOSUB 5000:GOTO 398
510 '┌──────────────────────────────────────────────────────────┐
511 '│  Edit Files                                               │
512 '└──────────────────────────────────────────────────────────┘
513 IF A$="S" THEN EDITACT%=1 ELSE EDITACT%=2
520 GOSUB 6000:GOTO 398
530 '┌──────────────────────────────────────────────────────────
```

CRADLE.BAS   Source code listing.

```
5?1 '|  Print parameters                                              |
5?2 '└───────────────────────────────────────────────────────────────┘
540 IF A$="S" THEN VWACT%=? ELSE VWACT%=4
550 GOSUB 5000:GOTO ?98
600 '┌───────────────────────────────────────────────────────────────┐
601 '|  Exit guard routine                                            |
602 '└───────────────────────────────────────────────────────────────┘
610 if edit.call% then 630 else end
630 b%=1?:a$="Have you saved all of your data file(s) to disk?":loca
 clreol:attr%=158:gosub 11000:gosub 9996
640 a$=inkey$:if a$="" then 640 else gosub 11020:if a$="Y" then end
8
4000 '┌──────────────────────────────────────────────────────────────────
4001 '| ────── Write and Read file operations                          ──
4002 '└──────────────────────────────────────────────────────────────────
4010 '┌───────────────────────────────────────────────────────────────┐
4020 '|  Routine to open standard window                               |
4030 '└───────────────────────────────────────────────────────────────┘
4031 IF PRNT% THEN LPRINT "FILACT% =";FILACT%
4040 f$="":WWIDTH%=40:WHEIGHT%=1:X%=19:Y%=17:f.fg%=15:f.bg%=1:color
attr%=(f.bg% and 7)*16+f.fg%:gosub ?1000
4041 IF FILACT%<? THEN FILDO$="Spectrum" else f:ldo$="Cradle"
4050 ON FILACT% GOSUB 4100,4200,4400,4500
4060 IF EDITACT%=0 THEN 4065 ELSE SCRNACT%=4:GOSUB 11110
4065 GOSUB ?1270:RETURN
4100 '┌───────────────────────────────────────────────────────────────┐
4101 '|  Read Spectrum file                                 FILACT%=1 |
4102 '└───────────────────────────────────────────────────────────────┘
4110 T$="Load "+SPCDEF$+"."+EXT1$+" into memory ?":X%=1:Y%=1:color f
OSUB ?2750
4120 GOSUB 11090:if a$=chr$(27) then 4190 else IF A$="Y" THEN ARCHIV
OTO 4131 ELSE IF A$<>"N" THEN 4120
4130 gosub ?2890:EXT$=EXT1$:FILE$=SPCDEF$:PURPOSE$="Loading":GOSUB 5
IVO$="NULL" THEN GOTO 4190
4131 A$=ARCHIVO$:GOSUB 11020:ARCHIVO$=A$:color f.fg%,f.bg% :X%=1:Y%=
OWS%:GOSUB ?2890:T$="Reading "+DRIVE$+ARCHIVO$+"."+EXT1$:GOSUB ?1580
4140 A$=DRIVE$+PATH$+ARCHIVO$+"."+EXT1$:GOSUB 11020:F$=A$:i%=0
4150 CLOSE#1:OPEN F$ FOR INPUT AS#1
4160 I%=I%+1:INPUT#1,LAMBDA(I%),AABS(I%)
4170 IF EOF(1) THEN 4180 ELSE 4160
4180 SCPDEF$=ARCHIVO$:SPCLINES%=I%:MESSAGE$="Read "+STR$(SPCLINES%)+
 data from file "+SPCDEF$+".":RETURN
4190 f$="NULL":MESSAGE$="Load routine aborted. Current Spectrum file
emains unchanged.":RETURN
4200 '┌───────────────────────────────────────────────────────────────┐
4201 '|  Write Spectrum file                                FILACT%=2 |
4202 '└───────────────────────────────────────────────────────────────┘
4210 T$="Save "+SPCDEF$+"."+EXT1$+" to Disk ?":X%=1:Y%=1:color f.fg%
B ?2750
4220 GOSUB 11090:if a$=chr$(27) then 4290 else IF A$="Y" THEN ARCHI
OTO 4231 ELSE IF A$ "N" THEN 4220
4230 gosub ?2890:EXT$=EXT1$:FILE$=SPCDEF$:PURPOSE$="Saving":GOSUB 50
VO$="NULL" THEN GOTO 4290
4231 A$=ARCHIVO$:GOSUB 11020:ARCHIVO$=A$:color f.fg%,f.bg% :X%=1:Y%=
0:T$="Writing "+DRIVE$+ARCHIVO$+"."+EXT1$:GOSUB ?1580
```

```
4340 A$=DRIVE$+PATH$+ARCHIVO$+"."+EXT1$:GOSUB 11020:F$=A$:i%=0
4345 gosub 16100:if spclines%=0 then goto 4380
4350 CLOSE#1:OPEN F$ FOR OUTPUT AS#1
4351 FOR I%=1 TO SPCLINES%
4360 PRINT#1,LAMBDA(I%),AABS(I%)
4370 NEXT
4380 spcdef$=archivo$:MESSAGE$="Saved"+STR$(SPCLINES%)+" pair(s) of data to file
 "+spcdef$+".":RETURN
4390 F$="NULL":MESSAGE$="Save routine aborted. Current Spectrum file on disk rem
ains unchanged.":RETURN
4400 '┌──────────────────────────────────────────────────────────┐
4401 '|  Read Cradle   file                           FILACT%=3  |
4402 '└──────────────────────────────────────────────────────────┘
4410 T$="Load "+CDLDEF$+"."+EXT2$+" into memory ?":X%=1:Y%=1:color f.fg%,f.bg% :
GOSUB 32750
4420 GOSUB 11090:if a$=chr$(27) then 4490 else IF A$="Y" THEN ARCHIVO$=CDLDEF$:G
OTO 4431 ELSE IF A$<>"N" THEN 4420
4430 gosub 32890:EXT$=EXT2$:FILE$=CDLDEF$:PURPOSE$="Loading":GOSUB 50000:IF ARCH
IVO$="NULL" THEN GOTO 4490
4431 A$=ARCHIVO$:GOSUB 11020:ARCHIVO$=A$:color f.fg%,f.bg% :X%=1:Y%=1:W%=NUMWIND
OWS%:GOSUB 32890:T$="Reading "+DRIVE$+ARCHIVO$+"."+EXT2$:GOSUB 31580
4440 A$=DRIVE$+PATH$+ARCHIVO$+"."+EXT2$:GOSUB 11020:F$=A$
4450 CLOSE#1:OPEN F$ FOR INPUT AS#1
4460 INPUT#1,RI, RO, XL, APANGLE, TE, TG, INDEX, RROD, NROD
4461 INPUT#1,RWATER, RJACKET, NJACKET, NWATER, N, XD, YD, TPP, TPR, LAMBDAO, SIG
4470 CLOSE#1
4480 CDLDEF$=ARCHIVO$:MESSAGE$="File "+cdldef$+" Successfully loaded.":RETURN
4490 F$="NULL":MESSAGE$="Load routine aborted. Current Cradle file in memory rem
ains unchanged.":RETURN
4500 '┌──────────────────────────────────────────────────────────┐
4501 '|  Write Cradle   file                          FILACT%=4  |
4502 '└──────────────────────────────────────────────────────────┘
4510 T$="Save "+CDLDEF$+"."+EXT2$+" to Disk ?":X%=1:Y%=1:color f.fg%,f.bg% :GOSU
B 32750
4520 GOSUB 11090:if a$=chr$(27) then 4590 else IF A$="Y" THEN ARCHIVO$=CDLDEF$:G
OTO 4531 ELSE IF A$<>"N" THEN 4520
4530 gosub 32890:EXT$=EXT2$:FILE$=CDLDEF$:PURPOSE$="Saving":GOSUB 50000:IF ARCHI
VO$="NULL" THEN GOTO 4590
4531 A$=ARCHIVO$:GOSUB 11020:ARCHIVO$=A$:color f.fg%,f.bg% :X%=1:Y%=1:W%=NUMWIND
OWS%:GOSUB 32890:T$="Writing "+DRIVE$+ARCHIVO$+"."+EXT2$:GOSUB 31580
4540 A$=DRIVE$+PATH$+ARCHIVO$+"."+EXT2$:GOSUB 11020:F$=A$
4550 CLOSE#1:OPEN F$ FOR OUTPUT AS#1
4560 PRINT#1,RI, RO, XL, APANGLE, TE, TG, INDEX, RROD, NROD
4561 PRINT#1,RWATER, RJACKET, NJACKET, NWATER, N, XD, YD, TPP, TPR, LAMBDAO, SIG
4570 CLOSE#1
4580 cdldef$=archivo$:MESSAGE$="File "+cdldef$+" Successfully Written.":RETURN
4590 F$="NULL":MESSAGE$="Save routine aborted. Current Cradle file on disk remai
ns unchanged.":RETURN
5000 '┌──────────────────────────────────────────────────────────────────────────┐
5001 '| ──────  View a parameter routine                                  ────── |
5002 '└──────────────────────────────────────────────────────────────────────────┘
5005 IF VWACT% 3 THEN 5010 ELSE SCRNACT%=3:GOSUB 11110:color 2,0:CLS:attr%=2
5010 ON VWACT% GOSUB 5020,5220,5520,5720
5011 SCRNACT%=1:GOSUB 11110:RETURN
5020 '────────────────────────────────────────────────────────────────────────────
```

```
5021 '| View a Spectrum file                                              V
5022 '└────────────────────────────────────────────────────────────────────
5025 if spcdef$="NULL" then message$="No Spectrum file in memory.":re
5026 gosub 16100:if spclines%=0 then spclines%=1
5030 LEFT%=INT(SPCLINES%/2):RIGHT%=SPCLINES%-LEFT%
5031 IF LEFT% < RIGHT% THEN LEFT%=LEFT%+1:RIGHT%=RIGHT%-1
5040 '
5050 b%=1:a%=1:A$="Wavelength":gosub 9996:a%=40:gosub 9996
5051 a%=15:A$="Absorption coefficient":gosub 9996:a%=55:gosub 999
5052 b%=2:a%=4:A$="(nm)":gosub 9996:a%=43:gosub 9996
5053 a%=22:A$="(cm^-1)":gosub 9996:a%=62:gosub 9996
5060 OFFSET%=0:COL%=1
5063 a%=1:b%=3:a$=STRING$(80,196):gosub 9996:attr%=113:A$=STRING$(1
=4 TO 22 STEP 2:gosub 9996:NEXT:attr%=2:b%=24:a$=STRING$(79,196):gos
r 1,7
5070 FOR A%=4 TO LEFT%+3
5080 LOCATE A%,COL%:COLOR 2,7:PRINT USING "##":(OFFSET%+(A%-3))::COL
 USING "####.#";LAMBDA(OFFSET%+(A%-3)):LOCATE A%,(COL%+20):PRINT USI
:AABS(OFFSET%+(A%-3));
5090 NEXT A%
5100 IF OFFSET% <> 0 THEN 5110 ELSE OFFSET%=LEFT%:LEFT%=RIGHT%:COL%=40:
5110 SCRNACT%=3:GOSUB 11110:attr%=7:A$="Press any key when ready to r
in menu":GOSUB 11000:b%=25:gosub 9996:GOSUB 11090
5120 IF A$="" THEN 5110 ELSE MESSAGE$="Viewing of Spectrum file "+SP
T1$+" terminated":RETURN
5220 '┌────────────────────────────────────────────────────────────────────
5221 '| View a Cradle file                                                 V
5222 '└────────────────────────────────────────────────────────────────────
5225 if cdldef$="NULL" then message$="No Cradle in memory.":return
5230 attr%=2:B%=1:A$="Viewing of Cradle file "+DRIVE$+PATH$+CDLDEF$+'
SUB 11000:gosub 9996:FORM$="##.###^^^^ "
5240 b%=2: a%=2: A$="── Lens parameters ──":gosub 9996
5250 b%=3: a%=7: A$="Lens radii of curvature (First and Second)──────
 b%,57:print USING FORM$;RI,RO;:gosub 9996
5260 B%=4:          A$="Position of the lens surface closest to the rod·
 b%,57:PRINT USING FORM$;XL;:gosub 9996
5270 B%=5:          A$="Full aperture of the lens pair system in degree
 b%,57:PRINT USING FORM$;APANGLE;:gosub 9996
5280 B%=6:          A$="Edge thickness────────────────────────────────
 b%,57:PRINT USING FORM$,TE;:gosub 9996
5290 B%=7:          A$="Gap between lenses────────────────────────────
 b%,57:PRINT USING FORM$;TG;:gosub 9996
5300 B%=8:          A$="Lens glass index of refraction────────────────
 b%,57:PRINT USING FORM$;INDEX;:gosub 9996
5310 B%=9: a%=2: A$="── Rod parameters ──":gosub 9996
5320 B%=10:a%=7: A$="LASER rod radius─────────────────────────────────
 b%,57:PRINT USING FORM$;RROD;:gosub 9996
5330 B%=11:         A$="Rod index of refraction───────────────────────
 b%,57:PRINT USING FORM$;NROD;:gosub 9996
5340 B%=12:a%=2: A$="── Jacket and coolant parameters ──":gosub 999
5350 B%=13:a%=7: A$="Jacket inner radius──────────────────────────────
 b%,57:PRINT USING FORM$;RWATER;:gosub 9996
5360 B%=14:         A$="Jacket outer radius───────────────────────────
 b%,57:PRINT USING FORM$;RJACKET;:gosub 9996
5370 B%=15:         A$="Jacket index of refraction────────────────────
 b%,57:PRINT USING FORM$;NJACKET;:gosub 9996
```

```
5380 B%=16:        A$="Coolant index of refraction------------------------":locate
 b%,57:PRINT USING FORM$;NWATER;:gosub 9996
5390 B%=17:a%=2: A$="-- Diode LASER parameters --":gosub 9996
5400 B%=18:a%=7: A$="LASER medium index of refraction-----------------":locate
 b%,57:print USING FORM$;N;:gosub 9996
5410 B%=19:        A$="Diode LASER output slit coordinates--------------":locate
 b%,57:PRINT USING FORM$;XD,YD;:gosub 9996
5420 B%=20:        A$="Beam angular width :":gosub 9996
5430 B%=21:a%=10:A$="perpendicular to the active layer---------------":locate b%
,57:PRINT USING FORM$;TPP;:gosub 9996
5440 B%=22:        A$="parallel to the active layer--------------------":locate b%
,57:PRINT USING FORM$;TPR;:gosub 9996
5450 B%=23:a%=7: A$="Center wavelength--------------------------------":locate
 b%,57:PRINT USING FORM$;LAMBDA0;:gosub 9996
5460 B%=24:        A$="Standard deviation-------------------------------":locate
 b%,57:PRINT USING FORM$;SIG;:gosub 9996
5470 SCRNACT%=3:GOSUB 11110:COLOR 7,0:A$="Press any key when ready to return to
main menu":GOSUB 11000:LOCATE 25,A%:PRINT A$;:GOSUB 11090
5480 IF A$="" THEN 5470 ELSE MESSAGE$="Viewing of Cradle file "+CDLDEF$+"."+EXT2
$+" terminated":RETURN
5520 '┌──────────────────────────────────────────────────────────────────────┐
5521 '| Print a Spectrum file                                        VWACT%=3 |
5522 '└──────────────────────────────────────────────────────────────────────┘
5525 if spcdef$="NULL" then message$="No Spectrum in memory.":return
5526 PRNACT%=1:GOSUB 11190:B%=13:A$="":GOSUB 11170:LOCATE B%,1:COLOR 2,0:attr%=2
:PRINT "Enter Title ";:FIG%=67:GOSUB 10320:TITLE$=IP$
5527 A$="Printing Spectrum file "+SPCDEF$+"."+EXT1$:GOSUB 11170
5528 LPRINT TAB(11);"Time:";TIME$;:LPRINT TAB(57);"Date:";DATE$
5529 A$="Rod Absorption Spectrum":GOSUB 11000:LPRINT TAB(A%);A$:LPRINT
5530 PRNACT%=2:GOSUB 11190:LPRINT TAB(11);TITLE$:GOSUB 11190:LPRINT
5545 LPRINT TAB(15);STRING$(50,196):LPRINT
5550 LPRINT TAB(20);"Reference      Wavelength      Absorption"
5552 LPRINT TAB(20);" Number           (nm)         Coefficient"
5553 LPRINT TAB(20);"                                 (cm^-1)"
5554 LPRINT TAB(15);STRING$(50,196);
5570 FOR A%=1 TO SPCLINES%
5580 LPRINT TAB(22);:LPRINT USING "##";(A%);:LPRINT TAB(35);:LPRINT USING "####.
#";LAMBDA(A%);:LPRINT TAB(52);:LPRINT USING "##.####";AABS(A%)
5590 NEXT A%
5591 LPRINT TAB(15);STRING$(50,196)
5592 A$="                "+DRIVE$+PATH$+SPCDEF$+"."+EXT1$:FOR I%=1 TO 40-SPCLINES%+2:
LPRINT:NEXT:LPRINT A$:LPRINT CHR$(12)
5600 MESSAGE$="Printing of Spectrum file "+SPCDEF$+"."+EXT1$+" complete":RETURN
5720 '┌──────────────────────────────────────────────────────────────────────┐
5721 '| Hard copy of a Cradle file                                   VWACT%=4 |
5722 '└──────────────────────────────────────────────────────────────────────┘
5724 if cdldef$="NULL" then message$="No Cradle file in memory.":return
5725 PRNACT%=1:GOSUB 11190:B%=13:A$="":GOSUB 11170:LOCATE B%,1:COLOR 2,0:attr%=2
:PRINT "Enter Title ";:mooo%=0:FIG%=67:GOSUB 10320:TITLE$=IP$
5726 LPRINT TAB(11);"Time:";TIME$;:LPRINT TAB(64);"Date:";DATE$
5727 A$="Cradle PARAMETER FILE":GOSUB 11000:LPRINT TAB(A%);A$:LPRINT
5728 PRNACT%=2:GOSUB 11190:LPRINT TAB(6);TITLE$:GOSUB 11190
5729 A$="Printing Cradle file "+CDLDEF$+"."+EXT2$:GOSUB 11170
5730 FORM$="##.###     "
5731 LPRINT :LPRINT TAB(4);STRING$(71,196);LPRINT
```

```
5732 GOSUB 11190
5733 LPRINT "    Note: Unless otherwise specified, all dimentions ar
m.";
5734 LPRINT "          The wavelength is in nanometers and the absor
cient";
5735 LPRINT "          is in inverse centimeters. Angular apertures
es."::GOSUB 11190
5736 LPRINT TAB(4):STRING$(71,196)::LPRINT
5740 LPRINT :LPRINT :PRNACT%=2:GOSUB 11190:LPRINT "    - Lens paramet
 11190
5750 LPRINT "        Lens radii of curvature (First and Second)-------
ING FORM$;RI,RO
5760 LPRINT "        Position of the lens surface closest to the rod--
ING FORM$;XL
5770 LPRINT "        Full aperture of the lens pair system in degrees-
ING FORM$;APANGLE
5780 LPRINT "        Edge thickness-----------------------------------
ING FORM$;TE
5790 LPRINT "        Gap between lenses-------------------------------
ING FORM$;TG
5800 LPRINT "        Lens glass index of refraction-------------------
ING FORM$;INDEX
5810 LPRINT :LPRINT :GOSUB 11190:LPRINT "    - Rod parameters -":GOSU
5820 LPRINT "        LASER rod radius---------------------------------
ING FORM$;RROD
5830 LPRINT "        Rod index of refraction--------------------------
ING FORM$;NROD
5840 LPRINT :LPRINT :GOSUB 11190:LPRINT "    - Jacket and coolant par
OSUB 11190
5850 LPRINT "        Jacket inner radius------------------------------
ING FORM$;RWATER
5860 LPRINT "        Jacket outer radius------------------------------
ING FORM$;RJACKET
5870 LPRINT "        Jacket index of refraction-----------------------
ING FORM$;NJACKET
5880 LPRINT "        Coolant index of refraction----------------------
ING FORM$;NWATER
5890 LPRINT :LPRINT :GOSUB 11190:LPRINT "    - Diode LASER parameters
190
5900 LPRINT "        LASER medium index of refraction-----------------
ING FORM$;N
5910 LPRINT "        Diode LASER output slit coordinates--------------
ING FORM$;XD,YD
5920 LPRINT "        Beam angular width :"
5930 LPRINT "           perpendicular to the active layer-------------
ING FORM$;TPP
5940 LPRINT "           parallel to the active layer------------------
ING FORM$;TPR
5950 LPRINT "        Center wavelength--------------------------------
ING FORM$;LAMBDA0
5960 LPRINT "        Standard deviation-------------------------------
ING FORM$;SIG
5980 A$="       "+DRIVE$+PATH$+CDLDEF$+"."+EXT2$:FOR I%=1 TO 15:LPRIN
T A$:LPRINT CHR$(12)
5990 MESSAGE$="Printing of Cradle file "+CDLDEF$+"."+EXT2$+" complet
```

```
6000 '┌────────────────────────────────────────────────────────────────────┐
6001 '| ——— Edit routines Cradle and Spectrum                          ——— |
6002 '└────────────────────────────────────────────────────────────────────┘
6003 DEF SEG=0:POKE &H418,PEEK(&H417) AND 223 'SET CURSOR KEYS ON
6004 DEF SEG=0:POKE &H41A,PEEK(&H41C):DEF SEG 'CLEAR THE KEY BOARD
6005 edit.call%=-1:SCRNACT%=4:GOSUB 11110:COLOR 2,0:CLS  'Open editor screen in
page 2
6010 ON EDITACT% GOSUB 6130,6020
6011 EDITACT%=0:SCRNACT%=1:GOSUB 11110:MESSAGE$="Be sure to save your "+EDT$+" f
ilè before you exit this program":RETURN
6020 '┌────────────────────────────────────────────────────────────────────┐
6021 '| ——— Edit Cradle files                                  EDITACT%=2  |
6022 '└────────────────────────────────────────────────────────────────────┘
6030 GOSUB 12000                    'Generate screen
6032 'ON KEY(3) GOSUB 12650
6033 'ON KEY(4) GOSUB 12670
6034 'KEY(3) ON:KEY(4) ON
6035 Cradle.ROT%=1:GOSUB 12750
6040 '┌──────────────────────────────────────────────────┐
6051 '|  Expect key for editing Cradle                   |
6052 '└──────────────────────────────────────────────────┘
6060 GOSUB 12630:if modo% then a$=in$ else 6060
6070 IF LEN(A$)=2 THEN A$=RIGHT$(A$,1)
6080 IF A$=CHR$(27) THEN EDT$="Cradle":KEY(2) OFF:KEY(3) OFF:KEY(4) OFF:RETURN
6090 IF A$=CHR$(13) THEN GOSUB 12695
6091 IF A$=CHR$(61) THEN GOSUB 12650
6092 IF A$=CHR$(62) THEN GOSUB 12670
6100 IF A$=CHR$(72) OR A$=CHR$(75) THEN GOSUB 12690
6110 IF A$=CHR$(77) OR A$=CHR$(80) THEN GOSUB 12695
6111 if a$=chr$(71) then cradle.rot.new%=1:gosub 12700                'home
6112 if a$=chr$(79) then cradle.rot.new%=20:gosub 12700               'end
6113 if a$=chr$(31) then gosub 12000:GOTO 6035                        'redraw
6114 if a$=chr$(73) then 6115 else 6117                               'pageup
6115 cradle.rot.new%=cradle.rot%-4
6116 if cradle.rot.new%<1  then cradle.rot.new%=1: gosub 12700 else gosub 12700
6117 if a$=chr$(81) then 6118 else 6120                               'pagedw
6118 cradle.rot.new%=cradle.rot%+4
6119 if cradle.rot.new%>20 then cradle.rot.new%=20:gosub 12700 else gosub 12700
6120 GOTO 6060
6130 '┌──────────────────────────────────────────────────┐
6131 '|  Edit Spectrum files                              |
6132 '└──────────────────────────────────────────────────┘
6140 GOSUB 15000                    'Generate screen
6162 'ON KEY(3) GOSUB 15520
6173 'ON KEY(4) GOSUB 15540
6184 'KEY(3) ON:KEY(4) ON
6195 Spectrum.ROT%=0:GOSUB 15310
6200 '┌──────────────────────────────────────────────────┐
6201 '|  Expect input conrtol                             |
6202 '└──────────────────────────────────────────────────┘
6210 GOSUB 15430:if modo% then a$=in$ else 6210
6220 IF LEN(A$)=2 THEN A$=RIGHT$(A$,1)
6230 IF A$=CHR$(27) THEN EDT$="Spectrum":KEY(2) OFF:KEY(3) OFF:KEY(4) OFF:GOSUB
11500:RETURN
6240 IF A$=CHR$(13) THEN GOSUB 15150:goto 6270
```

```
6241 IF A$=CHR$(61) THEN GOSUB 15520:goto 6270
6242 IF A$=CHR$(62) THEN GOSUB 15540:goto 6270
6250 IF A$=CHR$(72) then gosub 15670:goto 6270
6251 if A$=CHR$(75) THEN GOSUB 15210:GOTO 6270
6260 IF A$=CHR$(77) then gosub 15150:GOTO 6270
6261 if A$=CHR$(80) THEN GOSUB 15560:GOTO 6270
6262 if a$=chr$(71) then gosub 15730:GOTO 6270
6263 if a$=chr$(79) then gosub 15780:GOTO 6270
6264 if a$=chr$(73) then gosub 15830:GOTO 6270
6265 if a$=chr$(81) then gosub 15860:GOTO 6270
6266 if a$=chr$(46) then gosub 16000:GOTO 6270
6267 if a$=chr$(31) then gosub 15000:gosub 15310:GOTO 6270
6270 GOTO 6210
7000 '┌──────────────────────────────────────────────────────────
7001 '| ─────   Show program diagram of Cradle                   ─
7002 '└──────────────────────────────────────────────────────────
7010 screen 2
7015 def seg=&hb800
7020 bload "Cradle.PIC" ,0
7030 a$=inkey$:if a$="" then 7030
7035 screen 0,0,0,0:Message$="Displaying of parameter diagram was cc
essfully":return
7040 screen 0,0,0,0:Message$="Displaying of parameter diagram was at
aly"+str$(temp):return
9000 '┌──────────────────────────────────────────────────────────
9001 '| ─────   MAIN MENU OF CRADLE PROGRAM                      ─
9002 '└──────────────────────────────────────────────────────────
9010 TITLE$="CRADLE":T$="Main Menu":GOSUB 9900
9020 attr%=95:b%=2:a%=1
9021 a$=STRING$(80,205):gosub 9996
9022 FOR b%=3 TO 9:a$=STRING$(80,32):gosub 9996:NEXT
9023 b%=10:a$=STRING$(80,205):gosub 9996
9030 B%=3:a%=1:a$="[EC]....Edit  Cradle parameters":gosub 9996
9031 B%=4:a$="[LC]....Load  Cradle parameters":gosub 9996
9032 B%=5:a$="[SC]....Save  Cradle parameters":gosub 9996
9033 B%=6:a$="[VC]....View  Cradle parameters":gosub 9996
9034 B%=7:a$="[PC]....Print Cradle parameters":gosub 9996
9035 B%=8:a$="[W].....parameter definitions diagram":gosub 9996
9036 B%=9:a$="[C].....Calculate Total Absorption":gosub 9996
9040 B%=3:a%=40:a$="[ES]....Edit  Spectrum parameters":gosub 9996
9041 B%=4:a$="[LS]....Load  Spectrum parameters":gosub 9996
9042 B%=5:a$="[SS]....Save  Spectrum parameters":gosub 9996
9043 B%=6:a$="[VS]....View  Spectrum parameters":gosub 9996
9044 B%=7:a$="[PS]....Print Spectrum parameters":gosub 9996
9045 B%=8:a$="[D].....change/view program Defaults":gosub 9996
9046 B%=9:a$="[X/Esc].eXit program (press either twice)":gosub 9996
9050 locate 15,1:color 15,0:gosub 9991         'Show note'
9100 A$=MESSAGE$:B%=13:GOSUB 11170
9110 gosub 11400:locate 11,1:CALL CLREOL:A%=7:B%=11:ATTR%=14:A$="Ent
ce —» ":GOSUB 9996:LOCATE B%,29:COLOR 14,0:attr%=14:FIG%=1:GOSUB 10
GOSUB 11020:RETURN
9900
9901 '     Display Top line
9902
9904 COLOR 7,0:CLS:attr%=94:a$=TITLE$:a%=1:b%=a%:gosub 9996:attr%=2:
:a$="       Version  "+VERSION$:gosub 9996
```

```
9905 A%=81-LEN(T$):attr%=95:a$=T$:gosub 9996:attr%=2:GOSUB 10000:a%=40:a$=day$:go
sub 9996
9906 RETURN
9910 '
9911 '      Read program configurations
9912 '
9913 on error goto 9914:goto 9920
9914 if err=53 OR ERR=62 then message$="Please Configure your CRADLE program. (O
ption [D] from the MAIN MENU.)":spcdef$="NULL":cdldef$="NULL":resume 9971 ELSE 4
0000
9920 CLOSE#1:OPEN "config.cdl" FOR INPUT AS 1
9930 INPUT#1,DRIVE$,PATH$,EXT1$,EXT2$,SPCDEF$,CDLDEF$
9931 CLOSE#1
9932 on error goto 40000
9940 A$=COMMAND$:CALL UPCASE(A$):IF INSTR(A$,"MASK")<>0 THEN prnt%=1:lprint "  Pr
inter Active at "+time$+" on "+date$+"  " ELSE PRNT%=0
9942 on error goto 9980
9945 IF SPCDEF$="NULL" THEN f%=0:goto 9960: else f%=1
9950 ARCHIVO$=SPCDEF$:gosUB 4140
9960 if cdldef$="NULL" then 9970 else f%=f%+1
9965 archivo$=cdldef$:gosub 4440
9970 message$="Program configured. "+str$(f%)+" File(s) loaded"
9971 on error goto 40000:return
9980 if err=53 then f%=f%-1:goto 40171 else 40000
9990 RETURN
9991 A%=5:B%=CSRLIN:ATTR%=15:A$="NOTE: Unless otherwise specified, all dimension
s should be given in cm.":GOSUB 9996:a%=a%+6
9992 B%=B%+1:A$="The wavelength should be given in nanometers and the absorption
":GOSUB 9996
9993 B%=B%+1:A$="coefficient in inverse centimeters. Angular apertures should be
":GOSUB 9996
9994 B%=B%+1:A$="given in degrees.":GOSUB 9996
9995 return
9996 DEF SEG=0:PAGE%=PEEK(1122):DEF SEG:CALL XOPRINT(A$,B%,A%,ATTR%,PAGE%):RETUR
N
10000 ' ┌──────────────────────────────────────────────────────────────┐
10010 ' │ — This routine sets Day$ to the current day of week and returns — │
10020 ' └──────────────────────────────────────────────────────────────┘
10030 DAY%=0:CALL WEEKDAY(DAY%):DLEN%=VAL(MID$("3346535",DAY%,1))
10040 DLOC%=ASC(MID$("ADGKOVY",DAY%))-64:DAY$=MID$("SunMonTuesWednesThursFriSatu
r",dloc%,dlen%)+"day"
10050 MONTH%=VAL(LEFT$(DATE$,2)):DAY%=VAL(MID$(DATE$,4,2)):YEAR$=(RIGHT$(DATE$,4
))
10060 '  —— Get the Month name ——
10070 dlen%=val(mid$("785534469783",month%,1))
10080 dloc%=asc(mid$("07?DILPTZcjr",month%,1))-47
10090 mon$=mid$("JanuaryFebruaryMarchAprilMayJuneJulyAugustSeptemberOctoberNovem
berDecember",dloc%,dlen%)
10100 '          1      8       16    21    26 29   33   37     43       52      59
   67
10230 '  —— LOCATE 1,18:PRINT DAY$;", ";MON$;" ";DAY;",";YEAR
10290 '  —— Set DAY$ to the print variable
10300 DAY$    = DAY$+", "+MON$+STR$(DAY%)+", "+year$
10310 RETURN
10320 ' ──────────────────────────────────────────────────────────────
```

```
10321 '|  ---- This routine prints a frame and inputs characters to
10322 '└──────────────────────────────────────────────────────────
10330   IP$ = line input string
10340 ' IN$ = input string (i.e. current letter being proccesed)
10350 ' FIG = maximum length of IP$
10355 b%=CSRLIN:A%=POS(0)
10360 IF MODO%=1 THEN ch$=chr$(32):Ln%=0:call strip(ip$,ch$,Ln%):ip
n%):modo%=0:goto 10400
10370 IF MODO%=2 THEN 10400
10380 if modo%=3 then 10390 else 10420
10390 ch$=chr$(32):Ln%=0:call strip(ip$,ch$,Ln%):ip$=left$(ip$,Ln%)
10400 i%=len(ip$):a$=ip$+string$(fig%-len(ip$),177):gosub 9996:loca
ip$):goto 10430
10420 IP$="":IN$="":i%=0:b%=CSRLIN:A%=POS(0):a$=STRING$(FIG%,177):g
10430 IF FIG% = 1 THEN 10440 ELSE 10450  'To determine which counte
10440 I%=I%+1:IF I% = FIG% + 1 THEN RETURN ELSE 10460 'Read charcte
rd
10450 I%=I%+1:IF I% = FIG% + 1 THEN 10590  'make user hit return or
10460 IN$=INKEY$:IF IN$="" THEN 10460                       'Read nex
10470                     'proccess character
10480 IF MODO%=2 AND LEN(IN$)=2 THEN MODO%=1:RETURN
10490 IF MODO%=2 AND IN$=CHR$(27) THEN MODO%=1:RETURN
10500 IF MODO%=2 AND IN$=CHR$(13) THEN MODO%=0:RETURN
10510 'IF IN$=" " AND FIG%=1 THEN GOTO 10460 'no space character if
10520  iF IN$="." THEN GOTO 64480                              'no pe
10530 IF IN$=CHR$(13) THEN IF FIG%=1 THEN 10460 ELSE RETURN 'Tests
10540 IF IN$=CHR$(8) THEN X%=LEN(IP$):IF X%=0 THEN GOTO 10460 ELSE
,X%-1):R%=CSRLIN:C%=POS(0):LOCATE R%,C%-1:i%=I%-1:PRINT "":LOCATE
 10460
10550 PRINT IN$;    display character entered
10560 IP$=IP$+IN$  'add character to line input string
10570 GOTO 10430   'get inc I + get next character
10580                     'Once reached FIG limit
10590 IN$=INKEY$:IF IN$="" THEN 10590
10600 IF MODO%=2 AND LEN(IN$)=2 THEN MODO%=1:RETURN
10610 IF MODO%=2 AND IN$=CHR$(27) THEN MODO%=1:RETURN
10620 IF MODO%=2 AND IN$=CHR$(13) THEN MODO%=0:RETURN
10630 IF IN$=CHR$(8) THEN 10540              'allow only back space or r
10640 IF IN$=CHR$(13) THEN RETURN ELSE GOTO 10590
11000 '┌──────────────────────────────────────────────────────────
11001 '|  ----      Routine to center a string (a$) on the screen
11002 '└──────────────────────────────────────────────────────────
11010 A%=INT(41-(LEN(A$)/2)):RETURN
11020 '┌──────────────────────────────────────────────────────────
11021 '|  ----      Routine to convert a string (a$) to upper case
11022 '└──────────────────────────────────────────────────────────
11030 CALL UPCASE(A$)
11080 RETURN
11090 '┌──────────────────────────────────────────────────────────
11091 '|  ---- Routine to accept one key from the keyboard (upper ca
11092 '└──────────────────────────────────────────────────────────
11100 time.out%=0:on timer(1) gosub 11104:timer on
11101 A$=INKEY$:IF A$="" THEN 11102 ELSE 11103
11102 if time.out% =5 THEN MESSAGE$="Selection time-out":A$="":RETU
11103 GOSUB 11020:timer off:RETURN
```

```
11104 TIME.OUT%=time.out%+1:return
11110 '┌──────────────────────────────────────────────────────────────┐
11111 '|  ── Routine to record and change screen pages            ── |
11112 '└──────────────────────────────────────────────────────────────┘
11120 ON SCRNACT% GOTO 11130,11140,11150,11160,11161
11130 SCREEN 0,0,0,0:RETURN
11140 SCREEN 0,0,1,0:RETURN
11150 SCREEN 0,0,1,1:RETURN
11160 SCREEN 0,0,2,2:RETURN
11161 SCREEN 0,0,1,2:RETURN
11170 '┌──────────────────────────────────────────────────────────────┐
11171 '|  ── Routine to display a message at line B% of the screen  ── |
11172 '└──────────────────────────────────────────────────────────────┘
11180 LOCATE B%,1:CALL CLREOL
11181 ATTR%=15:GOSUB 11000:gosub 9996:RETURN
11190 '┌──────────────────────────────────────────────────────────────┐
11191 '|  ── Routine program the printer  (EPSON/IBM complatibles)  ── |
11192 '└──────────────────────────────────────────────────────────────┘
11200 ON PRNACT% GOTO 11210,11220,11230,11240,11250
11210 LPRINT CHR$(27);"@";:RETURN
11220 LPRINT CHR$(27);"E";:PRNACT%=3:RETURN
11230 LPRINT CHR$(27);"F";:PRNACT%=2:RETURN
11240 LPRINT CHR$(27);"E";:RETURN
11250 LPRINT CHR$(27);"E";:RETURN
11300 '┌──────────────────────────────────────────────────────────────┐
11301 '|  ── Routine to display screen in rapid secuence.           ── |
11302 '└──────────────────────────────────────────────────────────────┘
11331 DEF SEG=0:PAGE%=PEEK(1122):DEF SEG
11332 CALL XDPRINT(A$,B%,A%,ATTR%,PAGE%):RETURN
11400 '
11401 '      Show defaults
11402
11410 b%=20:attr%=6:if spcdef$="" then spcdef$="NULL"
11411 if cdldef$="" then cdldef$="NULL"
11420 LOCATE B%,1:CALL CLREOL:a$="Data Drive & Path ──────────> "+drive$+pa
th$:GOSUB 11000:gosub 9996:b%=b%+1
11430 locate b%,1:call clreol:a$="Current Spectrum file in memory -> "+spcdef$+"
."+ext1$:gosub 9996:b%=b%+1
11440 locate b%,1:call clreol:a$="Current Cradle   file in memory -> "+cdldef$+
."+ext2$:gosub 9996:b%=b%+1
11450 locate b%,1:call clreol:if prnt% then a$="PRINTER ACTIVE FOR DEBUGING":gos
ub 9996
11499 return
11500 '┌──────────────────────────────────────────────────────────────┐
11501 '| ──── ODD CHECK ROUTINE                                  ──── |
11502 '└──────────────────────────────────────────────────────────────┘
11510 GOSUB 16100:IF SPCLINES%/2=INT(SPCLINES%/2) THEN GOTO 11520 else return
11520 a$="Warning, you can't have an even nuber of data pairs  Press 'Esc' to q
it editing"
11530 b%=25:a%=1:attr%=11:gosub 9996
11540 gosub 11090:if a$="" then sound 100,5:goto 11540
11550 if a$=chr$(27) then return else return 6210
12000 '┌──────────────────────────────────────────────────────────────┐
12001 '| ──── Editor routines                                    ──── |
12002 '└──────────────────────────────────────────────────────────────┘
```

```
12005 COLOR 7,0:XX%=1:YY%=3:FORM$="##.###    "
12010 b%=1:a%=1:a$="Cradle Editor       Editing File :"+CDLDEF$:attr%
00
12020 b%=2:a$=STRING$(80,196):gosub 11700:attr%=3
12030 b%=3 :a$="╒═ Lens Parameters ═══════════════════════════ For
══════════════ ":gosub 11300
12040 B%=4 :a$="|─Lens radii of curvature First                  |─LASE
              |":gosub 11300
12050 B%=5 :a$="|                          Second                |─Ref
raction       |":gosub 11300
12060 B%=6 :a$="|─Position of the lens surface                   |
              |":gosub 11300
12070 B%=7 :a$="|   closest to the rod                           ╞═ Jac
ant parameters ╡":gosub 11300
12080 B%=8 :a$="|─Full aperture of the lens                      |─Jac
ius           |":gosub 11300
12090 B%=9 :a$="|   pair system in degrees                       |─Jac
ius           |":gosub 11300
12100 B%=10:a$="|─Edge thickness                                 |
efraction     |":gosub 11300
12110 B%=11:a$="|─Gap between lenses                             |─Jac
              |":gosub 11300
12120 B%=12:a$="|─Lens glass index of refraction                 |─Cool
              |":gosub 11300
12130 B%=13:a$="╘══════════════════════════════════════════════════
══════════════ ":gosub 11300
12140 B%=14:a$="╒═ Diode LASER parameters ═══════════════════════
══════════════ ":gosub 11300
12150 B%=15:a$="|─LASER medium index of refraction
              |":gosub 11300
12160 B%=16:a$="|─Diode LASER output slit coordinates
              |":gosub 11300
12170 B%=17:a$="|─Beam angular width                                  ┌
══════════════ ":gosub 11300
12180 B%=18:a$="|   ─Perpendicular to the active layer                 |
f Commands    |":gosub 11300
12190 B%=19:a$="|   ─Parallel to the active layer                      |
raw the screen |":gosub 11300
12200 B%=20:a$="|─Center wavelength                                    |
  F4 Save file |":gosub 11300
12210 B%=21:a$="|─Standard deviation                                   |
to Quit editor |":gosub 11300
12220 B%=22:a$="╘══════════════════════════════════════════════════
══════════════ ":gosub 11300
12230    ┌──────────────────────────────────────────┐
12240    |  print variables                          |
12250    └──────────────────────────────────────────┘
12260 FOR Cradle.ROT% =1 TO 20:CLR%=0:COLOR 5,1:GOSUB 12400:NEXT:RE
12270    ┌──────────────────────────────────────────┐
12280    |  locate data  py% px%                     |
12290    └──────────────────────────────────────────┘
12291 GOSUB 12300:LOCATE PY%,PX%:RETURN
12300 IF Cradle.ROT% =7 THEN PX%=35+XX% ELSE 12320
12301 ON Cradle.ROT% GOTO 12302,12303,12304,12305,12306,12307,12309
12302 PY%=YY%+1:RETURN
```

```
12703 FY%=YY%+3:RETURN
12704 FY%=YY%+4:RETURN
12705 FY%=YY%+6:RETURN
12706 FY%=YY%+7:RETURN
12707 FY%=YY%+8:RETURN
12708 FY%=YY%+9:RETURN
12730 IF Cradle.ROT%=9 THEN FX%=51+XX%:FY%=YY%+3:RETURN
12740 IF Cradle.ROT% <=13 THEN FX%=69+XX% ELSE 12765
12750 ON Cradle.ROT%-7 GOTO 12760,12730,12761,12762,12763,12764
12760 FY%=YY%+1:RETURN
12761 FY%=YY%+5:RETURN
12762 FY%=YY%+5:RETURN
12763 FY%=YY%+8:RETURN
12764 FY%=YY%+9:RETURN
12765 IF Cradle.ROT%=16 THEN FX%=51+XX%:FY%=YY%+13:RETURN
12766 FX%=39+XX%
12767 ON Cradle.ROT%-13 GOTO 12768,12769,12765,12770,12771,12772,12773
12768 FY%=YY%+12:RETURN
12769 FY%=YY%+13:RETURN
12770 FY%=YY%+15:RETURN
12771 FY%=YY%+16:RETURN
12772 FY%=YY%+17:RETURN
12773 FY%=YY%+18:RETURN
12400 ' ________________________________________________
12401 ' |  Display Data  in window                      |
12402 ' |________________________________________________|
12403 GOSUB 12270:CLR$=STRING$(10,32):IF CLR% THEN PRINT CLR$::RETURN
12410 ON Cradle.ROT% GOTO 12420,12430,12440,12450,12460,12470,12480,12490,12500,
12510,12520,12525,12530,12540,12550,12560,12570,12580,12590,12600
12420 PRINT USING FORM$:RI:RETURN
12430 PRINT USING FORM$:RO:RETURN
12440 PRINT USING FORM$:XL:RETURN
12450 PRINT USING FORM$:AFANGLE:RETURN
12460 PRINT USING FORM$:TE:RETURN
12470 PRINT USING FORM$:TG:RETURN
12480 PRINT USING FORM$:INDEX:RETURN
12490 PRINT USING FORM$:RROD:RETURN
12500 PRINT USING FORM$:NROD:RETURN
12510 PRINT USING FORM$:RWATER:RETURN
12520 PRINT USING FORM$:RJACKET:RETURN
12525 PRINT USING FORM$:NJACKET:RETURN
12530 PRINT USING FORM$:NWATER:RETURN
12540 PRINT USING FORM$:N:RETURN
12550 PRINT USING FORM$:XD:RETURN
12560 PRINT USING FORM$:YD:RETURN
12570 PRINT USING FORM$:TFF:RETURN
12580 PRINT USING FORM$:TFR:RETURN
12590 PRINT USING FORM$:LAMBDA0:RETURN
12600 PRINT USING FORM$:SIG:RETURN
12610 ' ________________________________________________
12611 ' |  Clear Cradle.ROT% and set cursor             |
12612 ' |________________________________________________|
12620 COLOR 5,1:CLR%=1:GOSUB 12400:GOSUB 12270:CLR%=0:RETURN
12670 ' ________________________________________________
12671 ' |  Get input from keyboard                      |
```

```
12632 '└──────────────────────────────────────────────┘
12633 locate 23,1:call clreol
12634 attr%=7:modo%=3:a$="Enter new datum":b%=23:a%=1:gosub 9996:ip$
12635 locate b%,len(a$)+1:color 31,0:print ":";:fig%=35:COLOR 7,0
12636 gosub 10320                    'gosub 12770 Set ip$ & Get String
12637 if modo% then return else IF VAL(IP$)=0 THEN IN$=CHR$(13):MODC
12638 GOSUB 12990:GOSUB 12750                'Set var w/ip$ & Hi color wr
12639 gosub 12695
12649 return
12650 '┌──────────────────────────────────────────────┐
12651 '│  F3 function key call   (Load)               │
12652 '└──────────────────────────────────────────────┘
12660 FILACT%=3:GOSUB 4000:B%=25:A$=MESSAGE$:B%=25:GOSUB 11000:GOSUE
 12230:Cradle.ROT%=1:GOSUB 12750:LOCATE 1,34:CALL CLREOL:COLOR 2,0:F
:GOSUB 11170:RETURN
12670 '┌──────────────────────────────────────────────┐
12671 '│  F4 function kev call   (Save)               │
12672 '└──────────────────────────────────────────────┘
12680 FILACT%=4:GOSUB 4000:A$=MESSAGE$:B%=25:GOSUB 11000:GOSUB 1117(
12690 '┌──────────────────────────────────────────────┐
12691 '│  Left - up key scroll                        │
12692 '└──────────────────────────────────────────────┘
12693 Cradle.ROT.NEW%=Cradle.ROT%-1:IF Cradle.ROT.NEW%=0 THEN Cradle
12694 GOSUB  12700:RETURN
12695 '┌──────────────────────────────────────────────┐
12696 '│  right - down key scroll                     │
12697 '└──────────────────────────────────────────────┘
12698 Cradle.ROT.NEW%=Cradle.ROT%+1:IF Cradle.ROT.NEW%=21 THEN Crad)
12699 GOSUB 12700:RETURN
12700 '┌──────────────────────────────────────────────┐
12701 '│  Clear old write new - up key scroll         │
12702 '└──────────────────────────────────────────────┘
12703 GOSUB 12740:Cradle.ROT%=Cradle.ROT.NEW%
12710 GOSUB 12750   'Hilighted color
12720 RETURN
12730 '┌──────────────────────────────────────────────┐
12731 '│  Normal color write                          │
12732 '└──────────────────────────────────────────────┘
12740 GOSUB 12610:COLOR 5,1:GOSUB 12400:RETURN
12750 '┌──────────────────────────────────────────────┐
12751 '│  Highlight color write                       │
12752 '└──────────────────────────────────────────────┘
12760 GOSUB 12610:COLOR 14,1:GOSUB 12400:RETURN
12770 '┌──────────────────────────────────────────────┐
12771 '│  Set ip$                                     │
12772 '└──────────────────────────────────────────────┘
12780 'ON Cradle.ROT% GOTO 12790,12800,12810,12820,12830,12840,1285(
,12880,12890,12900,12910,12920,12930,12940,12950,12960,12970,12980
12790 'IP$=STR$(R1):RETURN
12800 'IP$=STR$(R0):RETURN
12810 'IP$=STR$(L):RETURN
12820 'IP$=STR$(ARANGLE):RETURN
12830 'IP$=STR$(T5):RETURN
12840 'IP$=STR$(T6):RETURN
12850 'IP$=STR$(INDEX):RETURN
```

```
12860 'IP$=STR$(RROD):RETURN
12870 'IP$=STR$(NROD):RETURN
12880 'IP$=STR$(RWATER):RETURN
12890 'IP$=STR$(RJACKET):RETURN
12900 'IP$=STR$(NJACKET):RETURN
12910 'IP$=STR$(NWATER):RETURN
12920 'IP$=STR$(N):RETURN
12930 'IP$=STR$(XD):RETURN
12940 'IP$=STR$(YD):RETURN
12950 'IP$=STR$(TFF):RETURN
12960  IP$=STR$(TFR):RETURN
12970 'IP$=STR$(LAMBDA0):RETURN
12980 'IP$=STR$(SIG):RETURN
12990 ' ┌─────────────────────────────────────────────────────┐
12991 ' |  Set var with ip$                                   |
12992 ' └─────────────────────────────────────────────────────┘
12995 ON Cradle.ROT% GOTO 14000,14005,14010,14020,14030,14040,14050,14060,14070,
14080,14090,14100,14110,14120,14130,14140,14150,14160,14170,14180
14000 RI=VAL(IP$):RETURN
14005 RO=VAL(IP$):RETURN
14010 XL=VAL(IP$):RETURN
14020 APANGLE=VAL(IP$):RETURN
14030 TE=VAL(IP$):RETURN
14040 TG=VAL(IP$):RETURN
14050 INDEX=VAL(IP$):RETURN
14060 RROD=VAL(IP$):RETURN
14070 NROD=VAL(IP$):RETURN
14080 RWATER=VAL(IP$):RETURN
14090 RJACKET=VAL(IP$):RETURN
14100 NJACKET=VAL(IP$):RETURN
14110 NWATER=VAL(IP$):RETURN
14120 N=VAL(IP$):RETURN
14130 XD=VAL(IP$):RETURN
14140 YD=VAL(IP$):RETURN
14150 TFF=VAL(IP$):RETURN
14160 TFR=VAL(IP$):RETURN
14170 LAMBDA0=VAL(IP$):RETURN
14180 SIG=VAL(IP$):RETURN
15000 ' ┌─────────────────────────────────────────────────────┐
15010 ' |  Spectrum  input routines (Generate display)        |
15020 ' └─────────────────────────────────────────────────────┘
15021 SPC.COLOR.HI%=14:SPC.COLOR.LOW%=2:SPC.COLOR.BG%=0:CLR$=STRING$(10,32)
15030 COLOR SPC.COLOR.LOW%,SPC.COLOR.BG%:CLS:b%=1:a%=1:attr%=2:a$="Spectrum Edit
or":gosub 9996
15031 b%=1:a%=20:a$="Current File "+SPCDEF$:gosub 9996  'Display current file
15050 b%=3:a%=1:A$="Wavelength":gosub 9996:a%=40:gosub 9996
15051 a%=15:A$="Absorption coefficient":gosub 9996:a%=55:gosub 9996
15052 b%=4:a%=4:A$="(nm)":gosub 9996:a%=43:gosub 9996
15053 a%=22:A$="(cm^-1)":gosub 9996:a%=62:gosub 9996
15054 a%=1:b%=2:a$=STRING$(80,196):gosub 9996
15055 a$=" Alt-C clears all entries to zero —— F3 load from disk —— F4 Save to
 disk "
15056 attr%=15:gosub 11000:gosub 9996
15070 offset%=0:FOR A% = 1 TO 20
15080 LOCATE (A%+4),1 :PRINT USING "##";A%;
```

```
15090 LOCATE (A%+4),4 :PRINT USING "####.#":LAMBDA(A%);
15100 LOCATE (A%+4),20:PRINT USING "##.####":AABS(A%);
15110 LOCATE (A%+4),41:PRINT USING "##";20+A%;
15120 LOCATE (A%+4),44:PRINT USING "####.#":LAMBDA(20+A%);
15130 LOCATE (A%+4),60:PRINT USING "##.####":AABS(20+A%);
15140 NEXT A%
15142 RETURN
15150 '┌──────────────────────────────────────────────────────────┐
15151 '|  Right Scroll                                            |
15152 '└──────────────────────────────────────────────────────────┘
15160 GOSUB 15270        'clear old
15170 Spectrum.ROT%=Spectrum.ROT%+1
15180 IF Spectrum.ROT%>=80 THEN Spectrum.ROT%=0
15190 GOSUB 15310        'set new
15200 RETURN
15210 '┌──────────────────────────────────────────────────────────┐
15211 '|  Left  Scroll                                            |
15212 '└──────────────────────────────────────────────────────────┘
15220 GOSUB 15270        'clear old
15230 Spectrum.ROT%=Spectrum.ROT%-1
15240 IF Spectrum.ROT%<=-1 THEN Spectrum.ROT%=79
15250 GOSUB 15310        'set new
15260 RETURN
15270 '┌──────────────────────────────────────────────────────────┐
15271 '|  Clear old                                               |
15272 '└──────────────────────────────────────────────────────────┘
15280 COLOR SPC.COLOR.LOW%,SPC.COLOR.BG%
15290 GOSUB 15350        'set address
15300 RETURN
15310 '┌──────────────────────────────────────────────────────────┐
15311 '|  Set  New                                                |
15312 '└──────────────────────────────────────────────────────────┘
15320 COLOR SPC.COLOR.HI%,SPC.COLOR.BG%
15330 GOSUB 15350        'set address
15340 RETURN
15350 '┌──────────────────────────────────────────────────────────┐
15351 '|  Set address                                             |
15352 '└──────────────────────────────────────────────────────────┘
15355 Spectrum.KEY%=0:Spectrum.WORD%=0
15360 IF Spectrum.ROT%/2=INT(Spectrum.ROT%/2) THEN COL%=4:FORM$="###
L%=20:FORM$="##.####":Spectrum.KEY%=1
15370 IF Spectrum.ROT%>39 THEN COL%=COL%+40:ROW%=Spectrum.ROT%-40:Sc
=20 ELSE ROW%=Spectrum.ROT%
15380 ROW%=INT(ROW%/2)
15390 Spectrum.WORD%=Spectrum.WORD%+ROW%
15400 LOCATE ROW%+5,COL%:PRINT CLR$;
15410 LOCATE ROW%+5,COL%
15415 IF Spectrum.KEY% THEN PRINT USING FORM$;AABS(Spectrum.WORD%+1
 USING FORM$;LAMBDA(Spectrum.WORD%+1);
15420 RETURN
15430 '┌──────────────────────────────────────────────────────────┐
15431 '|  Edit routine                                            |
15432 '└──────────────────────────────────────────────────────────┘
15433 locate 25,1:call clreol
15434 ATTR%=7:modo%=3:a$="Enter new datum":b%=25:a%=1:gosub 999
```

```
15435 locate b%,len(a$)+1:color 31,0:print ":";:fig%=35:COLOR 7,0
15440 'COLOR SPC.COLOR.LOW%,SPC.COLOR.BG%
15450 'GOSUB 15350        'set address
15460 'LOCATE ROW%+5,COL%:PRINT CLR$;:LOCATE ROW%+5,COL%
15470 'IF Spectrum.KEY% THEN IP$=STR$(AABS(Spectrum.WORD%+1)) ELSE IP$=STR$(LAMB
DA(Spectrum.WORD%+1))
15480 GOSUB 10320:if modo% then return ELSE IF VAL(IP$)=0 THEN IN$=CHR$(13):MODO
%=1:RETURN
15490 IF Spectrum.KEY% THEN AABS(Spectrum.WORD%+1)=VAL(IP$) ELSE LAMBDA(Spectrum
.WORD%+1)=VAL(IP$)
15500 GOSUB 15310:gosub 15150  Reset variable & Scroll right
15510 RETURN
15520 '┌──────────────────────────────────────────────────┐
15521 '|  F3 functiom key call   (Load)                  |
15522 '└──────────────────────────────────────────────────┘
15530 FILACT%=1:GOSUB 4000:IF F$="NULL" THEN a$="Load routine aborted" ELSE GOSU
B 15000:Spectrum.ROT%=0:GOSUB 15310:a$="Load OK,"+str$(spclines%)+" pair(s) of d
ata."
15531 a%=50:locate 1,a%:call clreol:attr%=11:B%=1:GOSUB 9996:RETURN
15540 '┌──────────────────────────────────────────────────┐
15541 '|  F4 function key call   (Save)                  |
15542 '└──────────────────────────────────────────────────┘
15550 FILACT%=2:GOSUB 4000:IF F$="NULL" THEN a$="Save routine aborted" else a$="
Save OK,"+STR$(SPCLINES%)+" pairs(s) of data."
15551 a%=50:locate 1,a%:call clreol:attr%=11:B%=1:GOSUB 9996:RETURN
15560 '┌──────────────────────────────────────────────────┐
15561 '|  Key down                                        |
15562 '└──────────────────────────────────────────────────┘
15570 GOSUB 15270       'clear old
15580 Spectrum.ROT%=Spectrum.ROT%+2
15590 IF Spect  m.ROT%=80 THEN Spectrum.ROT%=0
15591 if spectrum.rot%=81 then spectrum.rot%=1
15600 GOSUB 15310       'set new
15660 RETURN
15670 '┌──────────────────────────────────────────────────┐
15671 '|  scroll key up                                   |
15672 '└──────────────────────────────────────────────────┘
15680 GOSUB 15270       'clear old
15690 Spectrum.ROT%=Spectrum.ROT%-2
15700 IF Spectrum.ROT%=-1 THEN Spectrum.ROT%=79
15701 if spectrum.rot%=-2 then spectrum.rot%=78
15710 GOSUB 15310        set new
15720 RETURN
15730 '┌──────────────────────────────────────────────────┐
15731 '|  Home scroll                                     |
15732 '└──────────────────────────────────────────────────┘
15740 gosub 15270       'clear old
15750 spectrum.rot%=0
15760 gosub 15310        set new
15770 return
15780 '┌──────────────────────────────────────────────────┐
15781 '|  End scroll                                      |
15782 '└──────────────────────────────────────────────────┘
15790 gosub 15270       'clear old
15800 spectrum.rot%=79
```

```
15810 gosub 15310        'set new
15820 return
15830 '┌──────────────────────────────────────────────┐
15831 '|  Page up                                      |
15832 '└──────────────────────────────────────────────┘
15840 gosub 15270        'clear old
15850 spectrum.rot%=spectrum.rot%-6
15860 if spectrum.rot%<0 then spectrum.rot%=0
15870 gosub 15310        'set new
15871 RETURN
15880 '┌──────────────────────────────────────────────┐
15881 '|  Page down                                    |
15882 '└──────────────────────────────────────────────┘
15890 gosub 15270        'clear old
15910 spectrum.rot%=spectrum.rot%+6
15920 if spectrum.rot%>79 then spectrum.rot%=79
15930 gosub 15310        'set new
15940 RETURN
16000 '┌──────────────────────────────────────────────┐
16001 '|  Clear all entries                            |
16002 '└──────────────────────────────────────────────┘
16003 LOCATE 25,1:COLOR 15,0:PRINT STRING$(79,32);
16004 a$="Clear all entries to zero? ":locate 25,5:color 15,0:print
16005 a$=inkey$:if a$="" then 16004 else gosub 11020:if a$="Y" then
ocate 25,1:print string$(79,32)::return
16010 for i%=1 to 40
16020 lambda(i%)=0:aabs(i%)=0
16030 next
16035 'KEY(1) STOP:KEY(2) STOP:KEY(3) STOP: KEY(4) STOP
16040 gosub 15000
16045 'KEY(1) ON:KEY(2) ON:KEY(3) ON: KEY(4) ON
16050 return 6195
16100 '┌──────────────────────────────────────────────┐
16101 '|  Find first Zero                              |
16102 '└──────────────────────────────────────────────┘
16110 for i%=1 to 40
16120 if lambda(i%)=0 and aabs(i%)=0 then i%=i%-1:goto 16140
16130 next:IF I%=41 THEN I%=40
16140 spclines%=i%:if prnt% then lprint "SPCLINES% =";spclines%
16141 return
17000 '┌──────────────────────────────────────────────┐
17001 '|  Calculate Spectral and/or Total absorption   |
17002 '└──────────────────────────────────────────────┘
17003 ext3$="CDL":TOTAB$="FRN":calact%=1
17010 a$="Sub Menu:    S .....calculate Spectrum    T .....calculate
tion":b%=13:gosub 11170
17020 a$=inkey$:if a$="" then 17020
17025 temp$="ST"+chr$(27):gosub 11020:if instr(temp$,a$)=0 then 1702
17030 if a$="T" then 24000
17040 if a$=chr$(27) then 220
20000 'Ray tracing program for the calculation of the energy deposit
20010  density in a cylindrical rod  when pumped by eight linear arr
20020 'of  laser diodes  arranged  around  the  rod  in  a  symmetr
20030 'configuration.
20040  Calulate spectral absorption
```

```
20060 cls
20070 '
20071 title$="Cradle":T$="Spectral Absorption":gosub 27000
20100 AFANGLE=3.14159265#*AFANGLE/180'/2'
20110 A=2!*XL*SIN(AFANGLE): A=A+.1: SAGO=RO-SQR(RO*RO-A*A/4!)
20120 SAGI=RI-SQR(RI*RI-A*A/4!): TC=TE+SAGO+SAGI: TF=2!*TC+TG
20130 locate 4,1:PRINT "A = ";: PRINT USING "##.####      ";A
20140 locate 5,1:PRINT "TC = ";: PRINT USING "##.####      ";TC
20150 locate 6,1:PRINT "TF = ";: PRINT USING "##.####      ";TF
20180 '
20190 'N=3.6:                     ' GaAs index of refraction
20200  INDEX=1.5168               ' Lens glass index of refration
20210  NJACKET=1.4525              Quartz jacket index of refraction
20220  NWATER=1.33                 Coolant index of refraction
20230 '
20240 locate 8,5:PRINT "Enter range of run numbers you want (from 1 to ";SPCLINE
S%;"): ":print
20260 PRINT TAB(45);:CX=POS(0):CY=CSRLIN: INPUT "From :  ",RRUN1%:IF RRUN1%=0 TH
EN 23564
20270 IF (RRUN1%<0) OR (RRUN1%>spclines%) THEN LOCATE CY,CX: PRINT STRING$(30,""
): LOCATE CY,CX: GOTO 20260
20280
20290 PRINT TAB(45);: CX=POS(0): CY=CSRLIN: INPUT"to   :  ",RRUN2%
20300 IF (RRUN2%<RRUN1%) OR (RRUN2%>spclines%) THEN LOCATE CY,CX: PRINT STRING$(
30,""): LOCATE CY,CX: GOTO 20290
20310 '
20330 LOCATE 13,1:call clreol:COLOR 2,0:attr%=2:PRINT "Enter Title ";:MODO%=0:FI
G%=67:GOSUB 10320:TITLE$=IF$
20340 '
20341 ' Dimentions!!!!!
20342 '
20360 REDIM ABSO(20,160)
20370 NR%=20: NSECT%=10: NTHETA%=16*NSECT%
20380 '
20390 for i%=1 to spclines%:LL(i%)=lambda(i%):next
20400 erase lambda
20460 '
20470 FOR RRUN%=RRUN1% TO RRUN2%: WAVEL=LL(RRUN%): ABCOEFF=AABS(RRUN%)
20480 '
20490 FOR KK%=0 TO 20: FOR LL%=0 TO 160
20500 ABSO(KK%,LL%)=0': NEXT LL%: VOL(KK%)=0': NEXT KK%
20510 cls:color 2,0
20530 LPRINT: LPRINT
20540 PRINT"                   Date: ";DATE$;"          TIME: ";TIME$
20550 LPRINT"                   Date: ";DATE$;"          TIME: ";TIME$
20560 LPRINT: LPRINT: LPRINT TITLE$: LPRINT: LPRINT: LPRINT
20570 LPRINT "Diode laser wavelength : ";: LPRINT USING "####.#";WAVEL;
20580 LPRINT " nanometers": LPRINT
20590 LPRINT "Absorption coefficient : ";: LPRINT USING "###.##";ABCOEFF;
20600 LPRINT " inverse centimeters"
20610 LPRINT : LPRINT: LPRINT: LPRINT
20620 '
20640 L=WAVEL/1000'
20650
20670 PRINT: PRINT
```

```
20680 LPRINT: LPRINT: LPRINT: LPRINT
20690 '
20700 '1) Determine entry point and calculate several combinations
20710 '    parameters that are needed for later calculations.
20720 '
20730 PI=3.14159265358979#
20740 '
20750 HALF%=NTHETA%/2: DR=RROD/NR%: DTHETA=2!*PI/NTHETA%
20760 K1=N^2: K0=2*PI/L: C1=K0*N:
20770 TX=TPP*PI/180!: TY=TPR*PI/180!: XB=.693*L/(PI*SIN(TX/2!))
20780 YB=.693*L/(PI*SIN(TY/2!)): X0=N*PI*XB^2/L: Y0=N*PI*YB^2/L
20790 B11=C1*(1!-(1!/X0-1!/Y0)/C1)^.5
20800 '
20810 RL1=RO: RL2=RI: RL3=RI: RL4=RO
20820 XC1=XL+TP-RL1: XC2=XL+TC+TG+RL2: XC3=XL+TC-RL3: XC4=XL+RL4
20830 XDD=XL+TP+XD
20840 '
20850 RADINP=0!: LOSSES=0!: ABSORPT=0!
20860 FOR III%=1 TO 100: ALFA=(20!-(III%-.5)*.4)*PI/180!
20870 SA=SIN(ALFA): CA=COS(ALFA): INTEN=0!
20880 FOR JJJ%=1 TO 10: BETA=(JJJ%-.5)*2!*PI/180!
20890 SB=SIN(BETA): CB=COS(BETA)
20900 CST=CA*CB: P2=CST*CST: SNT=SQR(1!-P2)
20910 IF SNT=0! THEN SNP=0!: CSP=1!: GOTO 20930
20920 SNP=SB/SNT: CSP=SA*CB/SNT
20930 I1=(CST*CSP)^2+SNP^2: I2=(K1-SNT^2)^.5: I=(I2+B11/K0)
20940 I=I/(I2+I1/CST)
20950 KX=K0*CSP*SNT: KY=K0*SNP*SNT: PSI11=EXP(-.25*((XB*KX)^2+(YB*K
20960 I=CB*I*PSI11                        'LPRINT USING "###.###
20970 INTEN=INTEN+I: NEXT JJJ%: RADINP=RADINP+INTEN
20980 DELTA=-ALFA: YI=YD: XI=XDD: ' PRINT ALFA: PRINT
20990 '
21000 XC=XC1: RL=RL1: S$="1": GOSUB 21080
21010 XC=XC2: RL=RL2: S$="2": GOSUB 21170
21020 XC=XC3: RL=RL3: S$="3": GOSUB 21080
21030 XC=XC4: RL=RL4: S$="4": GOSUB 21170
21040 G=DELTA: X=XL: Y=YI
21050 GOTO 21270
21060 '
21070 '
21080 SND=SIN(DELTA): CSD=COS(DELTA): X1=XI-XC
21090 P1=X1*CSD+YI*SND: P1SQ=P1*P1: P2=X1*X1+YI*YI-RL*RL
21100 P3=SQR(P1SQ-P2): P=P1-P3: XI=XI-CSD*P: YI=YI-SND*P
21110 IF YI>A/2! THEN PRINT "WARNING: RAY GOES BEYOND LENS APERTURE
; S$
21120 X1=XI-XC: THETAN=ATN(YI/X1): MU=THETAN-DELTA: SNM=SIN(MU)
21130 NU=SNM/SQR(INDEX*INDEX-SNM*SNM): NU=ATN(NU): DELTA=THETAN-NU
21140 RETURN
21150 '
21160
21170 SND=SIN(DELTA): CSD=COS(DELTA): X1=XI-XC
21180 P1=X1*CSD+YI*SND: P1SQ=P1*P1: P2=X1*X1+YI*YI-RL*RL
21190 P3=SQR(P1SQ-P2): P=P1+P3: XI=XI-CSD*P: YI=YI-SND*P
21200 IF YI>A/2! THEN PRINT "WARNING: RAY GOES BEYOND LENS APERTURE
; S$
```

```
21210 X1=XI-XC: THETAN=ATN(-YI/X1): MU=THETAN+DELTA: SNM=SIN(MU)
21220 SNM=SNM*INDEX: NU=SNM/SQR(1'-SNM*SNM): NU=ATN(NU): DELTA=NU-THETAN
21230 RETURN
21240 '
21250 '
21260 '
21270 NREF=NJACKET: R=RJACKET: GOSUB 21320
21280 NREF=NWATER/NJACKET: R=RWATER: GOSUB 21320
21290 NREF=NROD/NWATER: R=RROD: GOSUB 21320
21300 GOTO 21420
21310 '
21320 CSG=COS(G): SNG=SIN(G)
21330 DIST=ABS(X*SNG-Y*CSG): IF DIST =R GOTO 23100
21340 S1=X*CSG+Y*SNG: S1SQ=S1*S1: S2=X*X+Y*Y: S3=SQR(S1SQ-S2+R*R)
21350 S=S1-S3: SO=S1+S3
21360 YI=Y-SNG*S: XI=X-CSG*S: THETAN=ATN(YI/XI): X=XI: Y=YI
21370 MU=THETAN-G: SNM=SIN(MU)
21380 NU=SNM/SQR(NREF*NREF-SNM*SNM): NU=ATN(NU): G=THETAN-NU: RETURN
21390 '
21400
21410 '
21420 CSG=COS(G): SNG=SIN(G): S1=X*CSG+Y*SNG: S1SQ=S1*S1: S2=R*R: S=0'
21430 ANGLE=G*180'/PI: XO=X-Y/TAN(G): PRINT XO,Y,ANGLE: PRINT
21440 'LPRINT XO,Y,ANGLE
21460 '
21470 '2) Determine entry cell.
21480
21490 THETA=THETAN
21500 I%=NR%: J%=1+INT(THETA/DTHETA): IF THETA 0' THEN J%=NTHETA%+J%-1
21510 SIDE%=3: T4=J%*DTHETA: T2=T4-DTHETA: R1=R-DR: R3=R
21520 '
21530 '3) Determine next cell.
21540 '
21550 IF SIDE%=1 THEN GOSUB 21650
21560 IF SIDE%=2 THEN GOSUB 22000
21570 IF SIDE%=3 THEN GOSUB 22320
21580 IF SIDE%=4 THEN GOSUB 22750
21590 NEXT III%: GOTO 23140
21600 '
21610 '
21620 'Determine exit face and energy deposition when the ray enters the cell
21630 'trough face 1.
21640 '
21650 SN2=SIN(T2): CS2=COS(T2): TAN2=TAN(T2): D=SNG-TAN2*CSG: SS2=(Y-TAN2*X)/D
21660 IF SS2 S GOTO 21710
21670 XI=X-SS2*CSG: YI=Y-SS2*SNG
21680 SIGN=1': IF (XI*CS2) 0 THEN SIGN=-1'
21690 IF ABS(XI) 1E-08 THEN IF (YI*SN2) 0 THEN SIGN=-1' ELSE SIGN=1'
21700 RR=SIGN*SQR(XI*XI+YI*YI): IF RR R3 THEN IF RR R1 GOTO 21850
21710 SN4=SIN(T4): CS4=COS(T4): TAN4=TAN(T4): D=SNG-TAN4*CSG: SS4=(Y-TAN4*X)/D
21720 IF SS4 S GOTO 21790
21730 XI=X-SS4*CSG: YI=Y-SS4*SNG
21740 SIGN=1': IF (XI*CS4) 0 THEN SIGN=-1'
21750 IF ABS(XI) 1E-08 THEN IF (YI*SN4) 0 THEN SIGN=-1' ELSE SIGN=1'
21760 RR=SIGN*SQR(XI*XI+YI*YI): IF RR R3 THEN IF RR R1 GOTO 21900
```

```
21770 '
21780 S3=S1+SQR(S1SQ-S2+R3*R3)
21790 '
21800 INTEN1=INTEN*EXP(-ABCOEFF*(S3-S)): ABSORP=INTEN-INTEN1
21810 ABSO(I%,J%)=ABSO(I%,J%)+ABSORP: INTEN=INTEN1
21820 S=S3: SIDE%=1: I%=I%+1: R3=I%*DR: R1=R3-DR
21830 IF I%>NR% GOTO 23040 ELSE GOTO 21950
21840 '
21850 INTEN1=INTEN*EXP(-ABCOEFF*(SS2-S)): ABSORP=INTEN-INTEN1
21860 ABSO(I%,J%)=ABSO(I%,J%)+ABSORP: INTEN=INTEN1
21870 S=SS2: SIDE%=4: IF J%=1 THEN J%=NTHETA% ELSE J%=J%-1
21880 T4=J%*DTHETA: T2=T4-DTHETA: GOTO 21950
21890
21900 INTEN1=INTEN*EXP(-ABCOEFF*(SS4-S)): ABSORP=INTEN-INTEN1
21910 ABSO(I%,J%)=ABSO(I%,J%)+ABSORP: INTEN=INTEN1
21920 S=SS4: SIDE%=2: IF J%=NTHETA% THEN J%=1 ELSE J%=J%+1
21930 T4=J%*DTHETA: T2=T4-DTHETA: GOTO 21950
21940 '
21950 RETURN 21550
21960
21970 'Determine exit face and energy deposition when the ray enters
21980 'through face 2.
21990 '
22000 SN4=SIN(T4): CS4=COS(T4): TAN4=TAN(T4): D=SNG-TAN4*CSG: SS4=(Y
22010 IF SS4<S THEN GOTO 22130
22020 XI=X-SS4*CSG: YI=Y-SS4*SNG
22030 SIGN=1!: IF (XI*CS4)<0 THEN SIGN=-1!
22040 IF ABS(XI)<1E-08 THEN IF (YI*SN4)<0 THEN SIGN=-1! ELSE SIGN=1!
22050 RR=SIGN*SQR(XI*XI+YI*YI): IF RR>R3 GOTO 22130
22060 IF RR<R1 GOTO 22190
22070 '
22080 INTEN1=INTEN*EXP(-ABCOEFF*(SS4-S)): ABSORP=INTEN-INTEN1
22090 ABSO(I%,J%)=ABSO(I%,J%)+ABSORP: INTEN=INTEN1
22100 S=SS4: SIDE%=2: IF J%=NTHETA% THEN J%=1 ELSE J%=J%+1
22110 T4=J%*DTHETA: T2=T4-DTHETA: GOTO 22270
22120 '
22130 S3=S1+SQR(S1SQ-S2+R3*R3)
22140 INTEN1=INTEN*EXP(-ABCOEFF*(S3-S)): ABSORP=INTEN-INTEN1
22150 ABSO(I%,J%)=ABSO(I%,J%)+ABSORP: INTEN=INTEN1
22160 S=S3: SIDE%=1: I%=I%+1: R3=I%*DR: R1=R3-DR
22170 IF I%>NR% GOTO 23040 ELSE GOTO 22270
22180
22190 S3=S1-SQR(S1SQ-S2+R1*R1)
22200 INTEN1=INTEN*EXP(-ABCOEFF*(S3-S)): ABSORP=INTEN-INTEN1
22210 ABSO(I%,J%)=ABSO(I%,J%)+ABSORP: INTEN=INTEN-ABSORP
22220 S=S3: IF I%=1 GOTO 22240
22230 SIDE%=3: I%=I%-1: R3=I%*DR: R1=R3-DR: GOTO 22270
22240 SIDE%=1: IF J%<=HALF% THEN J%=J%+HALF% ELSE J%=J%-HALF%
22250 T4=J%*DTHETA: T2=T4-DTHETA: R3=I%*DR: R1=R3-DR: GOTO 22270
22260
22270 RETURN 21550
22280
22290 'Determine exit face and energy deposition when the ray enters
22300 'through face 3.
22310 '
```

```
22320 SN2=SIN(T2): CS2=COS(T2): TAN2=TAN(T2): D=SNG-TAN2*CSG: SS2=(Y-TAN2*X)/D
22330 IF SS2<S GOTO 22390
22340 XI=X-SS2*CSG: YI=Y-SS2*SNG
22350 SIGN=1': IF (XI*CS2)<0 THEN SIGN=-1'
22360 IF ABS(XI)<1E-09 THEN IF (YI*SN2)<0 THEN SIGN=-1! ELSE SIGN=1'
22370 RR=SIGN*SQR(XI*XI+YI*YI): IF RR>R3 GOTO 22640 ELSE IF RR<R1 GOTO 22540
22380
22390 SN4=SIN(T4): CS4=COS(T4): TAN4=TAN(T4): D=SNG-TAN4*CSG: SS4=(Y-TAN4*X)/D
22400 IF SS4<S GOTO 22460
22410 XI=X-SS4*CSG:YI=Y-SS4*SNG
22420 SIGN=1': IF (XI*CS4)<0 THEN SIGN=-1'
22430 IF ABS(XI)<1E-08 THEN IF (YI*SN4)<0 THEN SIGN=-1! ELSE SIGN=1'
22440 RR=SIGN*SQR(XI*XI+YI*YI): IF RR>R3 GOTO 22640 ELSE IF RR<R1 GOTO 22590
22450 '
22460 S3=S1-SQR(S1SQ-S2+R1*R1)
22470 INTEN1=INTEN*EXP(-ABCOEFF*(S3-S)): ABSORP=INTEN-INTEN1
22480 ABSO(I%,J%)=ABSO(I%,J%)+ABSORP: INTEN=INTEN1
22490 S=S3: IF I%=1 GOTO 22510
22500 SIDE%=3: I%=I%-1: R3=I%*DR: R1=R3-DR: GOTO 22700
22510 SIDE%=1: IF J%>HALF% THEN J%=J%+HALF% ELSE J%=J%-HALF%
22520 T4=J%*DTHETA: T2=T4-DTHETA: R3=I%*DR: R1=R3-DR: GOTO 22700
22530 '
22540 INTEN1=INTEN*EXP(-ABCOEFF*(SS2-S)): ABSORP=INTEN-INTEN1
22550 ABSO(I%,J%)=ABSO(I%,J%)+ABSORP: INTEN=INTEN1
22560 S=SS2: SIDE%=4: IF J%=1 THEN J%=NTHETA% ELSE J%=J%-1
22570 T4=J%*DTHETA: T2=T4-DTHETA: GOTO 22700
22580 '
22590 INTEN1=INTEN*EXP(-ABCOEFF*(SS4-S)): ABSORP=INTEN-INTEN1
22600 ABSO(I%,J%)=ABSO(I%,J%)+ABSORP: INTEN=INTEN1
22610 S=SS4: SIDE%=2: IF J%=NTHETA% THEN J%=1 ELSE J%=J%+1
22620 T4=J%*DTHETA: T2=T4-DTHETA: GOTO 22700
22630 '
22640 S3=S1+SQR(S1SQ-S2+R3*R3)
22650 INTEN1=INTEN*EXP(-ABCOEFF*(S3-S)): ABSORP=INTEN-INTEN1
22660 ABSO(I%,J%)=ABSO(I%,J%)+ABSORP: INTEN=INTEN1
22670 S=S3: SIDE%=1: I%=I%+1: R1=R3: R3=R1+DR
22680 IF I%<NR% GOTO 22040
22690 '
22700 RETURN 21550
22710 '
22720 'Determine exit face and energy deposition when the ray enters the cell
22730 'through face 4.
22740 '
22750 SN2=SIN(T2): CS2=COS(T2): TAN2=TAN(T2): D=SNG-TAN2*CSG: SS2=(Y-TAN2*X)/D
22760 IF SS2<S GOTO 22870
22770 XI=X-SS2*CSG: YI=Y-SS2*SNG
22780 SIGN=1': IF (XI*CS2)<0 THEN SIGN=-1'
22790 IF ABS(XI)<1E-08 THEN IF (YI*SN2)<0 THEN SIGN=-1' ELSE SIGN=1
22800 RR=SIGN*SQR(XI*XI+YI*YI): IF RR>R3 GOTO 22870 ELSE IF RR<R1 GOTO 22970
22810 '
22820 INTEN1=INTEN*EXP(-ABCOEFF*(SS2-S)): ABSORP=INTEN-INTEN1
22830 ABSO(I%,J%)=ABSO(I%,J%)+ABSORP: INTEN=INTEN1
22840 S=SS2: SIDE%=4: IF J%=1 THEN J%=NTHETA% ELSE J%=J%-1
22850 T4=J%*DTHETA: T2=T4-DTHETA: GOTO 23010
22860 '
```

CRADLE.BAS    Source code listing.

```
22870 S3=S1+SQR(S1SQ-S2+R3*R3)
22880 INTEN1=INTEN*EXP(-ABCOEFF*(S3-S)): ABSORP=INTEN-INTEN1
22890 ABSO(I%,J%)=ABSO(I%,J%)+ABSORP: INTEN=INTEN1
22900 S=S3: SIDE%=1: I%=I%+1: R1=R3: R3=R1+DR
22910 IF I%>NR% GOTO 23040 ELSE GOTO 23010
22920 '
22930 S3=S1-SQR(S1SQ-S2+R1*R1)
22940 INTEN1=INTEN*EXP(-ABCOEFF*(S3-S)): ABSORP=INTEN-INTEN1
22950 ABSO(I%,J%)=ABSO(I%,J%)+ABSORP: INTEN=INTEN1
22960 S=S3: IF I%=1 GOTO 22980
22970 SIDE%=3: I%=I%-1: R3=I%*DR: R1=R3-DR: GOTO 23010
22980 SIDE%=1: IF J%<=HALF% THEN J%=J%+HALF% ELSE J%=J%-HALF%
22990 T4=J%*DTHETA: T2=T4-DTHETA: R3=I%*DR: R1=R3-DR
23000 '
23010 RETURN 21550
23020 '
23030 '
23040 PRINT: PRINT "Ray ";: PRINT USING "###";III%;: PRINT " has e
23050 LOSSES=LOSSES+INTEN
23060 RETURN 21590
23070 '
23080 PRINT I%,J%,SIDE%,INTEN: PRINT T2,T4,R1,R3,S: RETURN
23090 '
23100 PRINT "RAY DOES NOT INTERSECT THE ROD": STOP
23110 PRINT "ERROR": STOP
23120 '
23130 '
23140 FOR KK%=1 TO NR%: FOR LL%=1 TO HALF%
23150 ABSO(KK%,LL%)=ABSO(KK%,LL%)+ABSO(KK%,NTHETA%+1-LL%)
23160 ABSO(KK%,NTHETA%+1-LL%)=ABSO(KK%,LL%)
23170 NEXT LL%: NEXT KK%
23180 '
23190 '
23200 DD=DR*DR*DTHETA/2': FOR KK%=1 TO NR%
23210 VOL(KK%)=(2!*KK%-1)*DD*10000'
23220 FOR LL%=1 TO NSECT%: FOR MM%=1 TO 7
23230 ABSO(KK%,LL%)=ABSO(KK%,LL%)+ABSO(KK%,LL%+2*NSECT%*MM%)
23240 NEXT MM%: ABSORPT=ABSORPT+ABSO(KK%,LL%)
23250 ABSO(KK%,LL%)=ABSO(KK%,LL%)/VOL(KK%)
23260 NEXT LL%: NEXT KK%
23270 PRINT: PRINT: LPRINT: LPRINT
23280 FOR P%=1 TO NR%: FOR Q%=1 TO NSECT%
23290 PRINT USING "###.### "; ABSO(P%,Q%);
23300 LPRINT USING "###.### "; ABSO(P%,Q%);
23310 NEXT Q%: NEXT P%
23320 '
23330 ABSFRAC=100'*ABSORPT/RADINP
23340 LOSSFRAC=100'*LOSSES/RADINP
23350
23360 PRINT: PRINT: LPRINT: LPRINT
23370 PRINT "Absorbed energy  :  ";: PRINT USING "###.###_ _%";ABSFR
23380 LPRINT "Absorbed energy  :  ";: LPRINT USING "###.###_ _%";ABS
23390 PRINT "Losses ........  :  ";: PRINT USING "###.###_ _%";LOSSF
23400 LPRINT "Losses ........  :  ";: LPRINT USING "###.###_ _%";LO
23410
```

```
23420 WAVEL%=CINT(WAVEL): A$=STR$(WAVEL%): B$=LEFT$(A$,4): A$=RIGHT$(B$,3)
23430 FILES$=DRIVE$+PATH$+TOTAB$+A$+"."+ext3$
23440 OPEN FILES$ FOR OUTPUT AS 1
23450 '
23460 PRINT #1, WAVEL,ABCOEFF
23470 FOR P%=1 TO NR%: FOR Q%=1 TO NSECT%
23480 PRINT #1, ABSO(P%,Q%);
23490 NEXT Q%: PRINT #1,: NEXT P%
23500 PRINT #1,ABSFRAC,LOSSFRAC
23510 '
23520 CLOSE #1
23530 '
23540 LPRINT: LPRINT: LPRINT "FILE NAME: " FILES$: LPRINT CHR$(12)
23550 '
23560 a$=inkey$:if a$="" then 23561 else if a$=chr$(27) then 23562
23561 NEXT RRUN%:goto 23570
23562 print "Do you wish to stop calculations of spectral absorption permanently
 ?"
23563 a$=inkey$:if a$="" then 23563 else gosub 11020:if a$="Y" then 23564 else 2
3561
23564 message$="Calculation of spectral absorption has been discontinued":goto 2
20
23570 message$="Calculation of Spectral absorption complete":goto 220
24000 'Ray tracing program for the calculation of the energy deposition
24010 'density in a cylindrical rod  when pumped by eight linear arrays
24020 'of  laser diodes  arranged  around  the  rod  in  a  symmetrical
24030 'configuration.
24040 '
24060 CLS
24061 title$="Cradle":T$="Total Absorption":gosub 27000
24062 GOSUB 16100:IF SPCLINES%/2=INT(SPCLINES%/2) THEN GOTO 27060
24080 '
24090 LOCATE 16,1:call clreol:COLOR 2,0:attr%=2:PRINT "Enter Title "::MODE%=0:FI
G%=67:GOSUB 10320:TITLE$=IF$
24110 REDIM ABSO(20,10)  ', SUM(20,10), SUMM(2,20,10), FIRST(20,10), LAST(20,10)
24130 'DIM ABSORP(2), LOSS(2), VOL(20), INTABSORP(20), ABSDENS(20)
24150 '
24160 NR%=20: NSECT%=10: NTHETA%=16*NSECT%: HWHM=10'
24170 SIGMA=2'*SIG*SIG: SIGMA=1'/SIGMA
24180 PI=3.141592653589793#
24190 DR=RROD/NR%: DTHETA=2'*PI/NTHETA%
24260 'CLEAR ALL VARIABLES
24270 'FOR P%=1 TO NR%: FOR Q%=1 TO NSECT%
24280 'ABSO(P%,Q%)=0': SUM(P%,Q%)=0': SUMM(1,P%,Q%)=0': SUMM(2,P%,Q%)=0'
24290  FIRST(P%,Q%)=0': LAST(P%,Q%)=0'
24300 'NEXT Q%: VOL(P%)=0': INTABSORP(P%)=0': ABSDENS(P%)=0': NEXT P%
24310 '
24320 'W=0': ABSORP(1)=0': ABSORP(2)=0': LOSS(1)=0': LOSS(2)=0'
24330 'INTABSORPTION=0'
24340 '
24360 PRINT: PRINT: LPRINT: LPRINT
24370 PRINT"                    Date: ";DATE$;"          TIME: ";TIME$
24380 LPRINT"                    Date: ";DATE$;"          TIME: ";TIME$
24390 PRINT: PRINT
24400 LPRINT : LPRINT: LPRINT: LPRINT TITLE$: LPRINT: LPRINT: LPRINT
```

```
24410 LPRINT "Center wavelength ........... :  ";: LPRINT USING "###-
A0: LPRINT "nanometers"
24420 LPRINT "Standard deviation .......... :  ";: LPRINT USING "###.
 LPRINT "nanometers"
24430 HWHM=1.18*SIG:LPRINT "Half width at half maximum .. :  ";: LPR
##.##  ";HWHM;: LPRINT "nanometers"
24440 LPRINT: LPRINT: LPRINT
24450 '
24460 '
24470 '
24480 DLAMBDA=LAMBDA(1)-LAMBDA0: DLS=DLAMBDA*DLAMBDA
24490 WAVEL=LAMBDA(1)
24500 '
24510 WAVEL%=CINT(WAVEL): A$=STR$(WAVEL%): B$=LEFT$(A$,4): A$=RIGHT$
24520 FFILES$=DRIVE$+PATH$+TOTAB$+A$+"."+EXT$$
24530 OPEN FFILES$ FOR INPUT AS 1
24540 '
24550 INPUT #1, WAVEL,ABCOEFF
24560 FOR P%=1 TO NR%: FOR Q%=1 TO NSECT%
24570 INPUT #1, ABSO(P%,Q%)
24580 NEXT Q%: NEXT P%
24590 INPUT #1,ABSFRAC,LOSSFRAC
24600 '
24610 CLOSE #1
24620 '
24630 PRINT "PROCESSING DATA FILE # ";: PRINT USING "###";1
24640 '
24650 WEIGHT=EXP(-SIGMA*DLS): W=W+WEIGHT
24660 PRINT WAVEL,DLAMBDA,WEIGHT
24670 '
24680 FOR P%=1 TO NR%: FOR Q%=1 TO NSECT%
24690 FIRST(P%,Q%)=WEIGHT*ABSO(P%,Q%)
24700 NEXT Q%: NEXT P%
24710 '
24720 AFIRST=WEIGHT*ABSFRAC
24730 LFIRST=WEIGHT*LOSSFRAC
24740 '
24750 ILAST%=(SPCLINES%-1)/2
24760 FOR I%=1 TO ILAST%
24770 '
24780 FOR J%=1 TO 2:IRUN%=2*I%-(2-J%)
24790 '
24800 DLAMBDA=LAMBDA(IRUN%)-LAMBDA0: DLS=DLAMBDA*DLAMBDA
24810 WAVEL=LAMBDA(IRUN%)
24820 '
24830 WAVEL%=CINT(WAVEL): A$=STR$(WAVEL%): B$=LEFT$(A$,4): A$=RIGHT$
24840 FFILES$=DRIVE$+PATH$+TOTAB$+A$+"."+EXT$$
24850 OPEN FFILES$ FOR INPUT AS 1
24860 '
24870 INPUT #1, WAVEL,ABCOEFF
24880 FOR P%=1 TO NR%: FOR Q%=1 TO NSECT%
24890 INPUT #1, ABSO(P%,Q%)
24900 NEXT Q%: NEXT P%
24910 INPUT #1,ABSFRAC,LOSSFRAC
24920
```

```
24930 CLOSE #1
24940
24950 PRINT "PROCESSING DATA FILE # ";: PRINT USING "###";IRUN%
24960 '
24970 WEIGHT=EXP(-SIGMA*DLS): W=W+WEIGHT
24980 PRINT WAVEL,DLAMBDA,WEIGHT
24990 '
25000 FOR P%=1 TO NR%: FOR Q%=1 TO NSECT%
25010 SUMM(J%,P%,Q%)=SUMM(J%,P%,Q%)+WEIGHT*ABSO(P%,Q%)
25020 NEXT Q%: NEXT P%
25030
25040 ABSORP(J%)=ABSORP(J%)+WEIGHT*ABSFRAC
25050 LOSS(J%)= LOSS(J%)+WEIGHT*LOSSFRAC
25060 '
25070 NEXT J%: NEXT I%
25080
25090 '
25100 DLAMBDA=LAMBDA(spclines%)-LAMBDA0: DLS=DLAMBDA*DLAMBDA
25110 WAVEL=LAMBDA(spclines%)
25120 '
25130 WAVEL%=CINT(WAVEL): A$=STR$(WAVEL%): B$=LEFT$(A$,4): A$=RIGHT$(B$,3)
25140 PFILES$=DRIVE$+PATH$+TOTAB$+A$+"."+EXT3$
25150 OPEN PFILES$ FOR INPUT AS 1
25160 '
25170 INPUT #1, WAVEL,ABCOEFF
25180 FOR P%=1 TO NR%: FOR Q%=1 TO NSECT%
25190 INPUT #1, ABSO(P%,Q%)
25200 NEXT Q%: NEXT P%
25210 INPUT #1,ABSFRAC,LOSSFRAC
25220 '
25230 CLOSE #1
25240 '
25250 PRINT "PROCESSING DATA FILE # ";: PRINT USING "###";spclines%
25260 '
25270 WEIGHT=EXP(-SIGMA*DLS): W=W+WEIGHT
25280 PRINT WAVEL,DLAMBDA,WEIGHT
25290 '
25300 FOR P%=1 TO NR%: FOR Q%=1 TO NSECT%
25310 LAST(P%,Q%)=WEIGHT*ABSO(P%,Q%)
25320 NEXT Q%: NEXT P%
25330
25340 ALAST=WEIGHT*ABSFRAC
25350 LLAST=WEIGHT*LOSSFRAC
25360
25370
25380 WW=3!*W
25390 FOR P%=1 TO NR%: FOR Q%=1 TO NSECT%
25400 SUM(P%,Q%)=(2!*SUMM(1,P%,Q%)+4!*SUMM(2,P%,Q%)-FIRST(P%,Q%)+LAST(P%,Q%))/WW
25410 NEXT Q%: NEXT P%
25420
25430 ABSORPTION=(2!*ABSORP(1)+4!*ABSORP(2)-AFIRST+ALAST)/WW
25440 LOSSES=(2!*LOSS(1)+4!*LOSS(2)-LFIRST+LLAST)/WW
25450
25460 PRINT: PRINT
25470 FOR P%=1 TO NR%: FOR Q%=1 TO NSECT%
```

```
25480 PRINT USING "###.### ";SUM(R%,O%);
25490 LPRINT USING "###.### ";SUM(R%,O%);
25500 NEXT O%: NEXT R%
25510 '
25520 PRINT: PRINT: LPRINT: LPRINT: LPRINT: LPRINT
25530 PRINT "Total absorption ...... :  ";: PRINT USING "###.###_
25540 LPRINT "Total absorption ...... :  ";: LPRINT USING "###.###_
ON
25550 PRINT "Total losses .......... :  ";:PRINT USING "###.###_ _
25560 LPRINT "Total losses .......... :  ";: LPRINT USING "###.###_
25570 '
25580 FFILES$=DRIVE$+PATH$+"ABSO."+EXT$: FFILES$="A:ABSO.PRN"
25590 OPEN FFILES$ FOR OUTPUT AS 1
25600 '
25610 PRINT #1,W,PROD
25620 FOR R%=1 TO NR%: FOR O%=1 TO NSECT%
25630 PRINT #1, SUM(R%,O%);
25640 NEXT O%: PRINT #1,: NEXT R%
25650 PRINT #1,ABSORPTION,LOSSES
25660 '
25670 CLOSE #1
25680 '
25690 LPRINT: LPRINT: LPRINT: LPRINT "FILE NAME: " FFILES$: LPRINT
25700 '
25710
25720 PRINT: PRINT: LPRINT: LPRINT
25730 PRINT"                     Date: ";DATE$;"          TIME: ";TIME$
25740 LPRINT"                     Date: ";DATE$;"          TIME: ";TIME$
25750 PRINT: PRINT
25760 LPRINT : LPRINT: LPRINT: LPRINT TITLE$: LPRINT: LPRINT: LPRIN
25770 LPRINT "Center wavelength .......... :  ";: LPRINT USING "##
A0;: LPRINT "nanometers"
25780 LPRINT "Standard deviation .......... :  ";: LPRINT USING "##
 LPRINT "nanometers"
25790 LPRINT "Half width at half maximum .. :  ";: LPRINT USING "##
: LPRINT "nanometers"
25800 LPRINT "Rod diameter ............... :  ";: LPRINT USING "##
: LPRINT "centimeters"
25810 LPRINT: LPRINT: LPRINT
25820 '
25830 '
25840 '
25850 DD=DR*DR*DTHETA/2'
25860 FOR R%=1 TO NR%: VOL(R%)=(2*R%-1)*DD*10000'
25870 FOR O%=1 TO NSECT%
25880 ABSDENS(R%)=ABSDENS(R%)+SUM(R%,O%)
25890 NEXT O%: INTABSORP(R%)=INTABSORPTION+VOL(R%)*ABSDENS(R%)
25900 INTABSORPTION=INTABSORP(R%): ABSDENS(R%)=ABSDENS(R%)/NSECT%
25910 NEXT R%
25920
25930 '
25940 FOR R%=1 TO NR%
25950 INTABSORP(R%)=INTABSORP(R%)/INTABSORP(20)
25960 NEXT R%
25970 '
```

```
25980 '
25990 PRINT: PRINT
26000 FOR P%=1 TO NP%: X=P%-.5: P=P%
26010 PRINT TAB(10);: PRINT USING "###.###  ";X;
26020 PRINT TAB(25);: PRINT USING "###.###  ";ABSDENS(P%);
26030 PRINT TAB(50);: PRINT USING "###.###  ";P;
26040 PRINT TAB(65);: PRINT USING "##.####  ";INTABSORP(P%)
26050 LPRINT TAB(10);: LPRINT USING "###.###  ";X;
26060 LPRINT TAB(25);: LPRINT USING "###.###  ";ABSDENS(P%);
26070 LPRINT TAB(50);: LPRINT USING "###.###  ";P;
26080 LPRINT TAB(65);: LPRINT USING "##.####  ";INTABSORP(P%)
26090 NEXT P%
26100
26110 PRINT: PRINT: LPRINT: LPRINT: LPRINT: LPRINT
26120 PRINT "Total absorption ...... :  ";: PRINT USING "###.###_ _%";ABSORPTION
26130 LPRINT "Total absorption ...... :  ";: LPRINT USING "###.###_ _%";ABSORPTI
ON
26140 PRINT "Total losses .......... :  ";:PRINT USING "###.###_ _%";LOSSES
26150 LPRINT "Total losses .......... :  ";: LPRINT USING "###.###_ _%";LOSSES
26160 '
26170 '
26180 '
26190 FFILES$=DRIVE$+PATH$+"INTABS."+EXT3$ 'FFILES$="A:INTABS.PRN"
26200 OPEN FFILES$ FOR OUTPUT AS 1
26210 '
26220 PRINT #1,W,PROD
26230 FOR P%=1 TO NP%
26240 X=P%-.5: P=P%: PRINT #1, X,ABSDENS(P%), P, INTABSORP(P%)
26250 NEXT P%
26260 PRINT #1,ABSORPTION,LOSSES
26270 '
26280 CLOSE #1
26290 '
26300 LPRINT: LPRINT: LPRINT: LPRINT "FILE NAME: " FFILES$: LPRINT CHR$(12
26310 '
26320 message$="Calcualtion of total absorption completed":goto 220
27000 '┌──────────────────────────────────────────────┐
27001 '│  Title Calculations Screen                   │
27002 '└──────────────────────────────────────────────┘
27010 COLOR 7,0:CLS:attr%=94:a$=title$:a%=1:b%=a%:gosub 9996:GOSUB 10000:a%=len(
a$)+1:a$="   "+dav$:gosub 9996
27020 t$="Spectral Absorption":A%=80-LEN(T$):attr%=95:a$=T$:gosub 9996
27030 a$=string$(80,196):attr%=2:a%=1:b%=2:gosub 9996
27050 return
27060 '┌──────────────────────────────────────────────┐
27061 '│Print error message due to even number of spc's│
27062 '└──────────────────────────────────────────────┘
27070 message$="You need to have an odd number of spectrum data pairs":goto 220
31000 '┌──────────────────────────────────────────────┐
31010 '│  Window Display routines                     │
31020 '└──────────────────────────────────────────────┘
31050 '  ADD WINDOW AT (X,Y) WITH WWIDTH% AND WHEIGHT%
31060 WWIDTH%=WWIDTH%+2                          'Add 2 chars. for border
31070 WHEIGHT%=WHEIGHT%+2
31090 NUMWINDOWS%=NUMWINDOWS%+1
```

```
31090 WINDOWX%(NUMWINDOWS%)     =  X%
31100 WINDOWY%(NUMWINDOWS%)     =  Y%
31110 WINDOWW%(NUMWINDOWS%)     =  WWIDTH%
31120 WINDOWH%(NUMWINDOWS%)     =  WHEIGHT%
31125 ATTRIBUTE%(NUMWINDOWS%) =  ATTR%
31126 W%=NUMWINDOWS%
31130 GOSUB 31180                                    'Save text within w
31140 GOSUB 31480                                    'Draw the window
31150 RETURN
31160 ' ┌──────────────────────────────────────────────────────────┐
31170 ' |  Save TEXT in window at (X,Y) of WWIDTH% and WHEIGHT%   |
31180 ' └──────────────────────────────────────────────────────────┘
31191 DEF SEG=0:PAGE%=PEEK(1122):PAGE.OFFSET%=PAGE%*4096:DEF SEG=&HB
31190 FOR IY% = Y% TO Y%+WHEIGHT%-1
31200   S$(NUMLINES%)= ""
31201   ADDRESS%=PAGE.OFFSET%+((IY%-1)*160)+((X%-1)*2)
31210   FOR IX% = 1 TO  WWIDTH%                      'Copy% each char. to
31211     S$(NUMLINES%)=S$(NUMLINES%)+CHR$(PEEK  (ADDRESS%))+CHR$(PEE
1))
31221     ADDRESS%=ADDRESS%+2
31230   NEXT IX%
31240   NUMLINES%=NUMLINES%+1
31250 NEXT IY%
31255 DEF SEG
31260 RETURN
31270 ' ┌──────────────────────────────────────────────────────────┐
31280 ' |  Remove window                                           |
31290 ' └──────────────────────────────────────────────────────────┘
31300 X% = WINDOWX%(NUMWINDOWS%)                           'Let (X,Y) 
eft
31310 Y% = WINDOWY%(NUMWINDOWS%)                           'of window 
31320 WWIDTH%=WINDOWW%(NUMWINDOWS%)                  window's width
31330 WHEIGHT%=WINDOWH%(NUMWINDOWS%)                 window's height
31340 NUMWINDOWS%=NUMWINDOWS%-1                      remove one window
31345 W%=NUMWINDOWS%
31350 GOSUB 31390                                    restore the text
31360 RETURN
31370 ' ┌──────────────────────────────────────────────────────────┐
31380 ' |  Restore text                                            |
31390 ' └──────────────────────────────────────────────────────────┘
31395 DEF SEG=0:PAGE%=PEEK(1122):PAGE.OFFSET%=PAGE%*4096:DEF SEG=&HB
31400 FOR IY% = Y% + WHEIGHT% - 1 TO Y% STEP - 1
31410   NUMLINES% = NUMLINES% - 1
31415   ADDRESS% = PAGE.OFFSET%+((IY%-1)*160)+((X%-1)*2)
31420   FOR IX% = 1 TO (WWIDTH%*2) STEP 2
31430
31433   POKE ADDRESS%,ASC(MID$(S$(NUMLINES%),IX%,1))
31435   POKE ADDRESS%+1,ASC(MID$(S$(NUMLINES%),IX%+1,1))
31436   ADDRESS% = ADDRESS% +2
31437   NEXT IX%
31440 NEXT IY%
31445 DEF SEG
31450 RETURN
31460 ' ──────────────────────────────────────────────────────────
31470      DRAW WINDOW at (X,Y%) of WWIDTH% and WHEIGHT%
31480   ──────────────────────────────────────────────────────────
```

```
31490 B%=Y%:A%=X%:TEMP$=A$:ATTR%=ATTRIBUTE%(W%)
31500 A$=CHR$(213)+STRING$(WWIDTH%-2,205)+CHR$(184):GOSUB 9996
31510 FOR IY%=Y%+1 TO Y%+WHEIGHT%-2
31520   B%=IY%
31530   A$=CHR$(179)+SPACE$(WWIDTH%-2)+CHR$(179):GOSUB 9996
31540 NEXT IY%
31550 B%=Y%+WHEIGHT%-1:
31560 A$=CHR$(212)+STRING$(WWIDTH%-2,205)+CHR$(190):GOSUB 9996
31570 A$=TEMP$:RETURN
31580 '
31590 '|  WRITE TEXT T$ at relative (X,Y)  within window W     |
31600 '
31610 TEMP$=A$:IF LEN(T$) (WINDOWW%(W%)-2 -X%+1 THEN SIZE%=(WINDOWW%(W%)-2 -X%+
 ELSE SIZE%=LEN(T$)+1
31620 B%=WINDOWY%(W%)+Y%:A%=WINDOWX%(W%)+X%:ATTR%=ATTRIBUTE%(W%)
31630 A$=LEFT$(T$,SIZE%):GOSUB 9996                     'truncate the text
31640 A$=TEMP$:RETURN                                    'if too big to
it
31650 '
31660 '|  GOTOXY% (W,X,Y%)                                       |
31670 '
31680 LOCATE Y% + WINDOWY%(W%),X% + WINDOWX%(W%)        'goto X,Y% within
31690 RETURN                                             'the window
32750 '
32751 '|  CENTER TEXT in window(W%) at Y%                        |
32752 '
32760 CENTER% = INT(((WINDOWW%(W%)-2)-LEN(T$))/2)
32770 T$=STRING$(CENTER%,32)+T$
32780 X%=1:GOSUB 31600:RETURN
32790 '
32791 '|  CENTERS window and opens it WHEIGHT% & WWIDTH%          |
32792 '
32800 X% = INT(40-(WWIDTH%+2)/2)::if X% =0 then X%=1
32801 if X% 80 then X%=80
32810 Y% = INT(12-(WHEIGHT%+2)/2)::if Y% =0 then Y%=1
32811 if Y% 25 then Y%=25
32820 GOSUB 31050
32830 RETURN
32850 '
32851 '|  Title line writes a title at the center of the window |
32852 '
32860 TEMP$=A$:X% = WINDOWX%(W%)+INT((WINDOWW%(W%)-LEN(T$))/2)
32870 B%=WINDOWY%(W%):A%=X%:A$=T$:ATTR%=ATTRIBUTE%(W%):GOSUB 9996
32880 A$=TEMP$:RETURN
32890 '
32891 '|  Clears the current line (Y%) of the window              |
32892 '
32900 T$=STRING$(WINDOWW%(W%)-2,32):GOSUB 31590:RETURN
40000 '
40010 '| -- Error Handler routine
40020 '
40030 if prnt% then LPRINT "Error number " [illegible] ";ERR
40060 '
40070    Error [illegible]
40080 '
40090 if ERR [illegible]
```

```
40090 IF ERR=53 AND ERL=50051 THEN RESUME NEXT ELSE 40091
40091 if err=53 and erl=50260 then 40100 else 40160
40095 '-----
40100 GOSUB 51540:A$="No Files available for loading in directory '
40130 GOSUB 45050:GOSUB 45000:RESUME 40140                   ---- Return
40140 GOSUB 51540:ARCHIVO$="NULL":RETURN
40160 ' ---- This next error only occurs when actualy READING a file
40161 IF ERR=53 THEN A$="File not found in drive "+F$ ELSE 40180
40170 GOSUB 45050:GOSUB 45000:if esc% then 40171 else resume
 0171 IF ERL=4150 OR ERL=4160 THEN RESUME 4190
40172 IF ERL=4450 OR ERL=4460 THEN RESUME 4490 ELSE BEEP:goto 44990
40175 '-----Disk not ready Error 71
40180 IF ERR=71 THEN A$="Insert diskette for drive "+DRIVE$+" and
oor" ELSE 40200
40190 GOSUB 45050:GOSUB 45000:RESUME

40200  -----Device Error 57
40201 IF ERR=57 THEN A$=" DEVICE ERROR (Unrecoverable) while "+BUFF
m drive "+DRIVE$ ELSE 40220
40210 GOSUB 45050:GOSUB 45000:RESUME 220
40220  -----Disk full Error 61
40221 IF ERR=61 THEN A$=" Disk full, please insert a new disk in dr
" Press 'Esc' to abort" ELSE 40240
40222 GOSUB 45050:GOSUB 45000
40230 IF ERL=4340 OR ERL=4350 then IF ESC% THEN GOTO 47000 ELSE RES
40240  -----Disk Write protected Error 70
40241 IF ERR=70 THEN A$="File Write Protected, please remove write
sert a new disk in "+DRIVE$ ELSE 40300
40242 GOSUB 45050:GOSUB 45000:IF ESC% THEN GOTO 47000 ELSE RESUME
40300 '-----Disk media Error 72 [This should very rarely occur (Fat
dware or Media is at fault)
40301 IF ERR=72 THEN A$="Fatal Disk Media Error -- Please insert a
 in drive "+DRIVE$ ELSE 40320
40310 GOSUB 45050:GOSUB 45000:IF ESC% THEN GOTO 47000 ELSE RESUME
40320 IF ERR=52 then message$="Bad File Number Error in line :"+str
tle to proceed' else 40340
40330 GOSUB 45050:GOSUB 45000:close:reset:RESUME 220
40340 if err=76 then a$="Path not found in drive "+drive$+" Please
nfiguration file" else 40360
40350 gosub 45050:gosub 45000:close:reset:resume 270
40360 if err=4 then end else 40370
40370 if err=200 then 40375 else 40410
40375 a$="A file name of 'NULL' is not permited. Please enter a new
40380 error.f note$=" Soft Error ":gosub 45000
40390 if esc% then prot=0:resume 51380 else resume 40400
40400 LOCATE SIRL%+FIN%+7,19:PRINT STRING$(3,32)::PROT=1:GOTO 51400
40410      ----------------- next possible error should go here

44990 errpost%=1:gosub 11110:A$="Fatal Error number :"+STR$(ERR)+"
+STR$ ERL)+" in CRADLE.BAS":message$=a$
44991 error.f note$=" Unrecoverable Error ":a1$="Press any key to r
Menu or press 'Esc' to return to DOS":GOSUB 45000
44992 if esc% then end else SCRNACT%=1:GOSUB 11110:on error goto 40
00
44993 goto 220
```

```
45000 '┌──────────────────────────────────────────────────────┐
45001 '│ Opens the ERROR window and displays the message...    │
45002 '└──────────────────────────────────────────────────────┘
45010 WWIDTH%=75:WHEIGHT%=3:COLOR 15,13:ATTR%=79:GOSUB 32900
45020 X%=1:Y%=1:T$=ERROR.TYPE$:GOSUB 32250
45021 DEF SEG=0:POKE &H418,PEEK(&H417) AND 223 'SET CURSOR KEYS ON
45022 DEF SEG=0:POKE &H41A,PEEK(&H41C):DEF SEG 'CLEAR THE KEY BOARD
45030 T$=A$:GOSUB 32750:Y%=Y%+1:T$="Press any key or 'Esc' to abort current rout
ine"::if len(a1$)>0 then t$=a1$
45031 GOSUB 32750:a1$="":if prnt% then lprint a$
45040 GOSUB 11090:IF A$="" THEN 45040 ELSE IF A$=CHR$(27) THEN ESC%=1 ELSE ESC%=
2
45041 GOSUB 31270:RETURN
45050 '┌──────────────────────────────────────────────────────┐
45051 '│ Set Error.TYPE$                                       │
45052 '└──────────────────────────────────────────────────────┘
45060 ERROR.TYPE$="[ Disk Error ]":RETURN
47000 '┌──────────────────────────────────────────────────────┐
47001 '│ Esc key pressed                                       │
47002 '└──────────────────────────────────────────────────────┘
47010 IF ERL=4150 OR ERL=4160 THEN RESUME 4190
47020 IF ERL=4350 OR ERL=4360 THEN RESUME 4390
50000 '┌─────────────────────────────────────────────────────┐
50010 '│ ───────────────── Variables ─────────────────────── │
50020 '├─────────────────────────────────────────────────────┤
50030 '│ DIMENTION   PROG$(64)                                │
50040 '│ DIRL........Line where dir frame starts              │
50050 '│ DR..........Contains current row pointer             │
50060 '│ DC..........Contains current col pointer             │
50070 '│ AR..........Pointer/Max files found                  │
50080 '│ L...........For loop to load 8 chars dir             │
50090 '│ modo........'mode  of 'GET' routine use              │
50100 '│ archivo$....returns file name or 'NULL' for no choice │
50110 '│ drot........current rotation of prog$(drot)          │
50120 '│ dirx........row coordinate                           │
50130 '│ diry........col coordinate                           │
50140 '│ drot.new....next drot to be                          │
50150 '│ a$..........dummy variable                           │
50160 '│ offset......offset                                   │
50170 '│ filedo$.....file type i.e. Spectrum                  │
50180 '│ ***you must specify purpose$ to "Loading" or "Saving" │
50190 '│    before calling this routine                       │
50200 '│                                                      │
50210 '│                                                      │
50220 '└─────────────────────────────────────────────────────┘
50230 DEF SEG=0:POKE &H417,PEEK(&H417) OR 64    'set capslock on
50231 DEF SEG=0:POKE &H418,PEEK(&H417) AND 223 'SET CURSOR KEYS ON
50232 DEF SEG=0:POKE &H41A,PEEK(&H41C):DEF SEG 'CLEAR THE KEY BOARD
50234 fildo$=purpose$+" "+fildo$+" files"
50235 T$="Reading Directory ":GOSUB 31580:IF EDITACT%>0 THEN SCRNACT%=2 ELSE SCRN
ACT%=1
50241 GOSUB 11110
50250 DIRL%=3:FILL$=[illegible]:FOR I%=1 TO 64:[illegible]
$(I%):NEXT I%
50251 color 2,0:[illegible]:ATTR%=0:[illegible]
```

```
50260   CALL FINDFIRSTF(DIR$,ATTR%,ERCD%)
50265 IF ERCD%=-1 AND PURPOSE$="Saving" then nofiles$="No other sele
able":nofiles%=1:fin%=1:goto 50440
50266 if ercd% and purpose$="Loading" then error 53
50270 DEL$=".":A%=0:FOR AR% =1 TO 99
50280   CALL GETNAMEF(PROG$(AR%),FLEN%)
50290   PROG$(AR%)=LEFT$(PROG$(AR%),FLEN%)+DEL$
50291   if prnt% then LPRINT "File Name :":prog$(ar%);" Number :":ar
50298   A%=INSTR(PROG$(AR%),DEL$)
50299   PROG$(AR%)=LEFT$(PROG$(AR%),A%-1)
50300   ERCD%=0
50310   CALL FINDNEXTF(ERCD%)
50320   IF ERCD% THEN 50380
50330 NEXT AR%
50380 WIDTH 80
50390 CLS:COLOR 7,0:scrnact%=3:gosub 11110:DIR$=LEFT$(DIR$,LEN(DIR$)
50391 b%=0:c%=0:d%=0:call drvspace(drive$,b%,c%,d%):free$="["+str$(c
(c%)*csng(d%))+" Bytes free ]"
50392 MAJ%=0:MIN%=0:CALL GETDOSV(MAJ%,MIN%):DOS$=STR$(MAJ%)+"."+STR$
50393 CH$=CHR$(32):LN%=0:CALL STRIP(DOS$,CH$,LN%):DOS$="[ DOS Versio
S$,LN%)+" ]"
50400 '┌──────────────────────────────────────────────────────┐
50410 '│  Draw Directory Box                                   │
50420 '└──────────────────────────────────────────────────────┘
50430 FIN%=int(AR%/8):IF ar% mod 8<>0 then fin%=fin%+1
50431 'lprint "Fin = ";fin%
50432 if fin%=0 then fin%=1:if prnt% then lprint "Fin (after 0 check
50440 colOR 7,0:CLS:attr%=14:b%=DIRL%:a%=1:a$="╒":gosub 9996:a$="╕":
9996
50441 attr%=78:a$=space$(78):a%=2:gosub 9996
50450 FOR L%=1 TO FIN%:ATTR%=14
50460 B%=DIRL%+L%:A%=1:A$="|"+STRING$(78,32)+"|":GOSUB 9996:NEXT L%
50470 B%=DIRL%+FIN%+1:A$="╘"+STRING$(78,205)+"╛"
50471 b$="["+str$(ar%)+" File(s) ]":mid$(a$,3,len(b$))=b$
50472 mid$(a$,(79-len(free$)),len(free$))=free$:gosub 9996
50480 A$=FILDO$:GOSUB 11000:B%=1:GOSUB 9996
50490 IF nofiles% THEN ATTR%=7:B%=FIN%+DIRL%:A$=nofiles$:GOSUB 11000
GOTO 50580
50500 I%=0:FOR DR%=DIRL%+1 TO DIRL%+FIN%      'from screen row  to
50510 FOR DC%=2 TO 65 STEP 9        'Display file names in 3 columns
50520 I%=I%+1                        ' Go to next row in Array
50530 IF PROG$(I%)=SPACE$(12) THEN 50570  ELSE B%=DR%:A%=DC%
50540 ATTR%=7:A$=" "+PROG$(I%):GOSUB 9996      Stop when Array is emp
50550 NEXT DC%
50560 NEXT DR%
50570
50580 '┌──────────────────────────────────────────────────────┐
50590 '│  Set-up Control routine                               │
50600 '└──────────────────────────────────────────────────────┘
50610 ATTR%=7:B%=2:A%=1:A$=STRING$(80,196):B$="Filer Version 1.0":mi
(b$),len(b$))=b$:GOSUB 9996
50620 B%=DIRL%-2:A%=1:ATTR%=14:A$="╒"+STRING$(78,205)+"╕":b$="[ Dire
ir$+" ]"
50621 mid$(a$,3,len(b$))=b$:mid$(a$,(79-len(dos$)),len(dos$))=dos$:[illegible]
50630 B%=DIRL%-1:A%=1:A$="|"+STRING$(78,32)+"|":GOSUB 9996
```

```
51070 DROT.NEW%=DROT%-1
51080 IF DROT.NEW%  1 THEN DROT.NEW%=AR%
51090 GOSUB 51170:RETURN 'gosub clr old drot % mark new
51100 ' ┌──────────────────────────────────────────────────────┐
51110 '|  Scroll Drot right                                     |
51120 ' └──────────────────────────────────────────────────────┘
51121 IF NOFILES% THEN RETURN
51130 IF DROT%=0 THEN DROT%=1:DROT.NEW%=1:GOSUB 51500:GOTO 50930
51140 DROT.NEW%=DROT%+1
51150 IF DROT.NEW%  AR% THEN DROT.NEW%=1
51160 GOSUB 51170:RETURN  gosub clr old drot % mark new
51170 ┌──────────────────────────────────────────────────────┐
51180 '|  Clear old drot and mark new drot                     |
51190 └──────────────────────────────────────────────────────┘
51200 ATTR%=7:gosub 51210:DROT%=DROT.NEW%:ATTR%=112:gosub 51210:ret
51210 y%=int(DROT%/8):IF DROT% mod 8 0 then y%=y%+1
51220 DIRX%=DIRL%+y%
51230 x%=int(DROT% mod 8):if DROT% mod 8 = 0 then x%=8
51240 diry%=x%*9-5
51250 B%=dirx%:A%=diry%:A$=prog$(DROT%):GOSUB 9996
51290 RETURN
51300 ' ┌──────────────────────────────────────────────────────┐
51310 '|  Hanlde return                                     .  |
51320 ' └──────────────────────────────────────────────────────┘
51330 IF DROT%=0 THEN ARCHIVO$=FILE$:GOSUB 51540:RETURN
51340 IF PURPOSE$="Saving" THEN 51341 ELSE 51350
51341 T1$="WARNING - File on disk will be replaced":T2$="Save data
og$(DROT%)+"."+ext$+"?":T3$="":where$="to":GOTO 51360
51350 T1$="WARNING - Loading a file will replace ":T2$="current mem
3$="Load parameters from file "+PROG$(DROT%)+"."+EXT$+"?":where$="f
51360 ATTR%=47:WWIDTH%=41:WHEIGHT%=3:X%=19:Y%=9:GOSUB 31000:T$=" "+
where$+" disk ":GOSUB 32850
51370 X%=1:Y%=1:T$=T1$:GOSUB 32750
51371 T$=T2$:Y%=2:GOSUB 32750:T$=T3$:Y%=3:GOSUB 32750
51372 GOSUB 11090:IF A$="" THEN 51372 ELSE GOSUB 31270
51373 IF A$="Y" THEN ARCHIVO$=PROG$(DROT%):GOSUB 51540:RETURN
51374 GOTO 50730
51380 ┌──────────────────────────────────────────────────────┐
51390 '|  Handle 'Esc'                                         |
51400 ' └──────────────────────────────────────────────────────┘
51410 IF DROT%=0 THEN ARCHIVO$="NULL":GOSUB 51540:RETURN
51420 DROT.NEW%=0:GOSUB 51170:b%=DIRL%-1:a%=2:a$=space$(78):attr%=1
A$="Press 'Esc' to exit without "+PURPOSE$:gosub 11000:gosub 9996:g
o 51570:DROT%=0:GOTO 50730
51430 ' ┌──────────────────────────────────────────────────────┐
51440 '|  Create a new file                                    |
51450 ' └──────────────────────────────────────────────────────┘
51460 temp$=a$:IF DROT%=0 THEN attr%=7:gosub 51570:DROT%=1
51470 DROT.NEW%=0:GOSUB 51170:DROT%=0:LOCATE DIRL%+FIN%+3,19:ip$=te
IO%=G:COLOR 7,0:attr%=7:GOSUB 10320:IF MODO% THEN 51480 ELSE 51490
51480 LOCATE DIRL%+FIN%+3,19:PRINT space$(8)::A$=IN$:IF A$=CHR$(27
:GOTO 51420 ELSE GOTO  50731
51490 ARCHIVO$=IP$:call upcase(archivo$)::if archivo$="NULL" then ar
GOSUB 51540:RETURN
51500 ────────────────────────────────────────────────────────
```

```
50640 ATTR%=15:A$="Use Cursor keys "+CHR$(24)+" "+CHR$(25)+" "+CHR$(27)+" "+CHR$
(26)+" Home & End to point to the desired file.":gosub 11000:B%=3:GOSUB 9996
50641 ATTR%=15:A$="Press the ENTER key to sellect the highlighted file.":GOSUB 1
1000:B%=4:GOSUB 9996
50642 ATTR%=15:A$="Or just type in a new file name and press the ENTER key.":GOS
UB 11000:B%=5:GOSUB 9996
50650 B%=DIRL%:A%=2:ATTR%=78:A$=" Drive --» "+DRIVE$:GOSUB 9996
50651 B%=DIRL%:A%=16:A$=" Ext. --» ."+EXT$:GOSUB 9996
50652 B%=DIRL%:A%=33:A$=" Path --» "+PATH$:GOSUB 9996
50660 B%=DIRL%+FIN%+3:A%=4:A$="File Name --»":GOSUB 9996
50661 B%=DIRL%+FIN%+3:A%=40:A$="Default Selection --»":GOSUB 9996
50670 DROT%=1:SCRNACT%=3:GOSUB 11110:GOTO 51420
50690 '┌──────────────────────────────────────────────────────┐
50700 '│  Process input                                       │
50710 '└──────────────────────────────────────────────────────┘
50720 SCRNACT%=3:GOSUB 11110:DROT%=0
50730 A$=INKEY$:IF A$="" THEN 50730
50731 if len(a$)=2 then B$=right$(a$,1) else b$="":goto 50827
50790 IF b$=CHR$(72) THEN GOSUB 50860:GOTO 50730
50800 IF b$=CHR$(80) THEN GOSUB 50940:GOTO 50730
50810 IF b$=CHR$(75) THEN GOSUB 51030:GOTO 50730
50820 IF b$=CHR$(77) THEN GOSUB 51100:GOTO 50730
50821 IF b$=CHR$(71) THEN DROT.NEW%=1:GOSUB 51170:GOTO 50730
50822 IF b$=CHR$(79) THEN DROT.NEW%=AR%:GOSUB 51170:GOTO 50730
50825 IF b$=CHR$(31) THEN GOTO 50400
50826 goto 50730
50827 IF A$=CHR$(13) THEN 51300       'ELSE ARCHIVO$=PROG$(DROT%)
50828 IF A$=CHR$(27) THEN 51380       'ELSE ARCHIVO$=FILE$
50830 FOR I%=65 TO 90:IF A$=CHR$(I%) THEN GOTO 51430 ELSE NEXT
50840 FOR I%=97 TO 122:IF A$=CHR$(I%) THEN GOTO 51430 ELSE NEXT
50841 FOR I%=48 TO 57:IF A$=CHR$(I%) THEN GOTO 51430 ELSE NEXT
50850 GOTO 50730
50860 '┌──────────────────────────────────────────────────────┐
50870 '│  Scroll Drot up                                      │
50880 '└──────────────────────────────────────────────────────┘
50881 IF NOFILES% THEN RETURN
50890 IF DROT%=0 THEN DROT%=1:DROT.NEW%=1:GOSUB 51500:GOTO 50930
50900 DROT.NEW%=DROT%-8
50910 IF DROT.NEW%   1 THEN DROT.NEW%=DROT%+((FIN%-1)*8) ELSE 50930
50920 IF DROT.NEW%   AR% THEN DROT.NEW%=DROT.NEW%-8
50930 GOSUB 51170:RETURN 'gosub clr old DROT% & mark new
50940 '┌──────────────────────────────────────────────────────┐
50950 '│  Scroll Drot down                                    │
50960 '└──────────────────────────────────────────────────────┘
50961 IF NOFILES% THEN RETURN
50970 IF DROT%=0 THEN DROT%=1:DROT.NEW%=1:GOSUB 51500:GOTO 50930
50980 DROT.NEW%=DROT%+8
50990 IF DROT.NEW%   AR% then DROT.NEW%=DROT% mod 8:IF DROT.NEW%=0 THEN DROT.NEW
%=8
51020 GOSUB 51170:RETURN 'gosub clr old drot & mark new
51030 '┌──────────────────────────────────────────────────────┐
51040 '│  Scroll Drot left                                    │
51050 '└──────────────────────────────────────────────────────┘
51051 IF NOFILES% THEN RETURN
51060 IF DROT%=0 THEN DROT%=1:DROT.NEW%=1:GOSUB 51500:GOTO 50930
```

```
51510 '|  Change escape status                                          |
51520 '└────────────────────────────────────────────────────────────────┘
51530 b%=DIRL%-1:a%=2:attr%=12:a$=space$(78):gosub 9996:A$="Press  Esc  to retur
n to default selection":gosub 11000:gosub 9996:attr%=7:gosub 51570:RETURN
51540  ┌────────────────────────────────────────────────────────────────┐
51541 '|  GET CORRECT SCREEN TO RETURN TO                                |
51542 '└────────────────────────────────────────────────────────────────┘
51550 IF EDITACT%>0 THEN SCRNACT%=4 ELSE SCRNACT%=1
51560 GOSUB 11110:RETURN
51570 '┌────────────────────────────────────────────────────────────────┐
51571 '|  resets default file to color attr%                            |
51572 '└────────────────────────────────────────────────────────────────┘
51580 b%=DIRL%+FIN%+3:a%=63:a$=FILE$:gosub 9996:RETURN
```

## Appendix B

### Floppy Disk of CRADLE Code

This appendix contains the floppy disk and user instructions of the CRADLE code.

CRADLE is a menu driven code with editing capability for the calculation of pump flux distribution and absorption efficiency of a linear laser diode array pumped solid state laser.

CRADLE (Computation of Rod Absorption of Diode Laser Radiation) is a computer code written in the IBM PC advance BASIC language. To use this program it is necessary to have at least the following system:

- An IBM PC, PC XT, PC AT, or compatible that runs IBM BASIC Compiler.
- An 8087 math coprocessor chip installed in the motherboard.
- Two floppy disk drives, or one hard disk and one floppy disk drive. IF the system has a large memory, and software for an electronic disk, it may also be useful to use the electronic disk. If the user decides for this configuration, the configuration file and the batch file provide in the diskette named CRADLE will have to be modified to include the appropriate commands.
- Enough free disk storage space to accommodate a few intermediate files created by the software (about one kilobyte).
- A color/graphics adapter installed in the system.
- A color monitor.
- PC-DOS 2.00, 2.10, or 3.00
- The IBM BASIC Compiler, version 2.00 (not the Microsoft BASIC Compiler nor MicroWay's 87BASIC Compiler).
- The MicroWay's 87BASIC Compiler, version 4.02 or later.

Two diskettes are attached to this report. One named CRA: contains executable CRADLE files, a batch file, a configu: file, and a binary file for the screen presentation of a figure containing the definition of several parameters. other, named YSG.TAD, contains a parameter file and a spe file for easy start-up. The batch file has been configur for a system with two floppy disk drives. To use CRADLE, the user will have to setup its own CRADLE diskette. Thi should include at least the files contained in the disket named CRADLE as delivered plus COMMAND. COM, BASRUN.EXE, and 87BRUN.EXE. The diskette CRADLE should be installed in drive A, and the diskette YAG.TAD in drive B. To run CRADLE simply enter CDL from DOS.